UNIVERSITY OF SOUTHAMPTON

FACULTY OF LAW, ARTS & SOCIAL SCIENCES

School of Art

Reducing the Risk of Open Display: Optimising the Preventive Conservation of Historic Silks

by

Naomi Luxford

Thesis for the degree of Doctor of Philosophy

December 2009

UNIVERSITY OF SOUTHAMPTON

ABSTRACT

FACULTY OF LAW, ARTS & SOCIAL SCIENCES
TEXTILE CONSERVATION CENTRE

Doctor of Philosophy

REDUCING THE RISK OF OPEN DISPLAY: OPTIMISING THE PREVENTIVE CONSERVATION OF HISTORIC SILKS

by Naomi Luxford

English Heritage properties contain a wealth of textiles on open display, however these are ephemeral objects. Amongst the natural fibres found in historic houses, silk is reported to be the most vulnerable to damage, especially from light. The critical deterioration factors for silk deterioration have been reassessed highlighting the important role of humidity, which has previously been overlooked. Monitoring behind a number of tapestries has recorded the formation of high humidity microclimates. This is a possible reason for the similar condition of brightly coloured samples taken from the reverse of a tapestry and the same thread which had faded on the displayed side.

Kinetics experiments studied the rate of silk deterioration and suggest the activation energy is approximately 50 kJ mol^{-1}, although this may vary for other types of silk, such as weighted materials. However as elemental analysis demonstrated around 10% of the 100 samples, taken from over 1000 objects containing silk in the English Heritage collection, were from tin-weighted silks, plain silks were the study's focus. Year long accelerated ageing experiments have demonstrated that although the inclusion of UV radiation during light ageing increased the rate of deterioration, light ageing caused small changes to silk. Thermal ageing with different humidity levels demonstrated increasing the relative humidity (RH), increased the rate of silk deterioration significantly. Further degradation of silk was observed when samples had been contaminated by the saturated salt solution used to create the RH environment during ageing. During ageing increased RH and increased temperatures led to greater yellowing of silk samples.

Experimental results have been used to make preventive conservation recommendations including lowering the RH below 50%, reducing the temperature and the continued exclusion of UV radiation. A theoretical silk deterioration curve for unweighted silk has been drawn, from which initial isoperms have been plotted. The analytical results have been compared with near-infrared (NIR) spectroscopy using multivariate analysis (MVA). This developed a predictive model for the tensile strength of silk using the NIR spectra. The potential of this non-invasive, non-destructive technique to monitor silk condition *in situ* has been tested at Brodsworth Hall and shown to rank the condition of samples successfully.

Contents

List of Figures

Chapter 1

Chapter 2

Chapter 3

Chapter 4

Chapter 5

Chapter 6

Chapter 7

Chapter 8

Chapter 9

Chapter 10

Chapter 11

Chapter 12

Appendix 1

Appendix 3

Appendix 5

Appendix 6

List of Tables

Chapter 7

Chapter 11

Appendix 7

Appendix 8

Declaration of Authorship

I, Naomi Luxford, declare that the thesis entitled, *Reducing the Risk of Open Display: Optimising the Preventive Conservation of Historic Silks* and the work presented in the thesis are both my own, and have been generated by me as the result of my own original research. I confirm that:

- this work was done wholly or mainly while in candidature for a research degree at this University;
- where any part of this thesis has previously been submitted for a degree or any other qualification at this University or any other institution, this has been clearly stated;
- where I have consulted the published work of others, this is always clearly attributed;
- where I have quoted from the work of others, the source is always given. With the exception of such quotations, this thesis is entirely my own work;
- I have acknowledged all main sources of help;
- where the thesis is based on work done by myself jointly with others, I have made clear exactly what was done by others and what I have contributed myself;
- none of this work has been published before submission.

Signed: ……..

Date:…….

Acknowledgements

Over the last three years I have regularly felt like I have been locked in my own personal room 101. At the points of complete frustration, annoyance and when I have felt like walking away there has been my supervisor Dave Thickett, who has supported my decisions, discussed ideas and listened patiently before making incisive suggestions that have helped this project endlessly. For his guidance and wisdom I am eternally grateful.

Within English Heritage the assistance, information and suggestions of the collections curators and conservators, particularly for the five selected properties (Apsley House – Susan Jenkins and Sally Johnson, Audley End House – Gareth Hughes and Phillippa Mapes, Brodsworth Hall – Crosby Stevens, Caroline Carr-Whitworth, Caroline Rawson and Bethan Stanley, Osborne House – Michael Hunter and Ranger's House – Annie Kemkaran-Smith) is acknowledged. Special mention should also go to Soki Rhee for sending environmental data and undertaking *in situ* XRF at Audley End House, Sarah Lambarth for regularly changing my English Heritage password and Trevor Reynolds for providing training and access to HOMS.

Special thanks for permission to sample their collections on display at Osborne House and for permission to include images go to The Royal Collection, particularly Jonathan Marsden and at Ranger's House, the Wernher Foundation Trustees. Finally thanks to all the staff at Brodsworth Hall for their assistance during the *in situ* visit.

I would like to thank the staff and students at the Textile Conservation Centre (TCC). Particular thanks go to my academic supervisor Paul Wyeth especially for his assistance during the *in situ* visit to Brodsworth Hall and helping organise my trip to New Zealand, which has helped me realise what should be important in life (even if I am still to prioritise it). I would also like to acknowledge the help of

Jeong-jin Kim in getting to grips with the HPSEC, all the lab technicians during my time at the TCC (Carol, Karen, Sally and Jenny), Karen Thompson for help understanding the language of textile conservation and silk condition reports, Nell Hoare for her help with additional funding and all in admin (Heloise, Christine, Sharon, Lee and Nickie). Thanks also to the TCC Foundation trustees for additional financial support which has been so important while writing up.

The biggest thanks have to go to Emma (just in case) Richardson for her endless enthusiasm for life, support during difficult (and great) periods, getting me addicted to jiving and general life support – I could not have done it without you. The biggest lesson of my PhD has been that life and work have equal importance, that and that for all the calculated experimental errors there is one you can never account for – human error! Xx

I would also like to thank Harry Cobbold for his sterling IT support as well as Beth Harland and the other WSA PhD students for providing information, support and sharing the experience.

For their information and assistance with analysis I would like to acknowledge Roger Wilkes and David Dungworth (SEM-EDS), Kathryn Hallett, James Parker and Simon Mitchell (HPSEC), Mike Dobby (XRF), Birmingham Museums and Art Gallery (BMAG) for loan of their XRF, Sonia O'Connor for answering questions on X-ray radiography work, Marianne Odlyha and Frank Barretto (AAS) and Darryl Green (ICP-OES).

For their support, interest, permission to sample and include images, I would like to thank all those at Glasgow Museums, especially Helen Hughes and Jane Rowlands. I would also like to acknowledge the help of Jane Thompson-Webb and Simon Cane at BMAG for their assistance and arranging my visit to their store and Aston Hall. Thanks go to William Lindsay at the Royal College of Art, for his continued support including allowing me to begin teaching, long after he ceased to

be my personal tutor. For providing a copy of her article, I would like to thank Anne-Laurence Dupont and to Virginia Costa for her interest in my work. For suggesting suitable National Trust collections for reference and to increase my understanding of silk in historic houses I would like to acknowledge Helen Lloyd and Kysnia Marko. Finally thanks to Jim Reilly and Doug Nishimura at the Image Permanence Institute for their assistance, particular Doug's ever patient and simplification of the kinetics calculations and various methodologies.

For their assistance collecting references and providing copies thanks to the staff at the Science Museum Store in Imperial College library. Also thanks to Ann Wise at the Warner Archive and Richard Humphries for his knowledge, enthusiasm and honesty with regards to reproduction silks.

I am grateful for funding provided by the Pasold Research Fund and the University of Southampton Postgraduate Conference Attendance Fund, which enabled me to present my research at the Natural Fibres conference in New Zealand. The final thanks go to the AHRC, for funding travel to the conference and this research.

Abbreviations

A	pre-exponential factor
Å	angstrom (1 x 10^{-10} m)
AAS	Atomic Absorption Spectroscopy
AEH	Audley End House
AFM	Atomic Force Microscopy
Ala	alanine
ATR	attenuated total reflectance
B.C.	before Christ
BS	British Standard
C	carbon
°C	degrees Celsius
cm	centimetre
cm^{-1}	wavenumber, expressed as inverse centimetres
Cp	insoluble precipitate after treatment of fibroin with chymotrypsin
Cs	soluble precipitate after treatment of fibroin with chymotrypsin
Da	daltons
DLS	Dynamic Light Scattering
DP	degree of polymerisation
DSC	Differential Scanning Calorimetry
DTA	Differential Thermal Analysis
e	extension at maximum load
E_a	activation energy
EDS	Energy Dispersive X-ray Spectrometry (also known as EDX)
FTIR	Fourier Transform Infrared Spectroscopy
FT-NIR	Fourier Transform Near-Infrared Spectroscopy
FT-Raman	Fourier Transform Raman Spectroscopy
g	gram
GFAAS	Graphite Furnace Atomic Absorption Spectrometry

Gly	glycine
gm^{-3}	grams per cubic metres
GnHCl	guanidine hydrochloride
H	hydrogen
H-chain	heavy component of silk fibroin
HCl	hydrochloride
HOMS	Historic Object Management System
HPLC	High Performance Liquid Chromatography
HPSEC	High Performance Size Exclusion Chromatography
Hz	hertz
ICP-AES	Inductively Coupled Plasma-Atomic Emission Spectroscopy
ICP-MS	Inductively Coupled Plasma-Mass Spectrometry
ICP-OES	Inductively Coupled Plasma-Optical Emission Spectroscopy
IE-HPLC	Ion-Exchange High Performance Liquid Chromatography
J	joules
k	rate constant
K	kelvin, unit of temperature
K_α	X-ray emission occurring when an electron transitions to the innermost K shell from the L shell
kDa	kilodaltons
kg	kilogram
KI	potassium iodide
kJ	kilojoules
kJ mol^{-1}	kilojoules per mole
keV	kiloelectron volts
kV	kilovolts
l	litre
L_α	X-ray emission occurring when an electron transitions to the L shell from the M shell
L_β	X-ray emission occurring when an electron transitions to the L shell from the N shell

L-chain	light component of silk fibroin
$Lmin^{-1}$	litre per minute
LiSCN	lithium thiocyanate
lux	unit of illuminance
m	metre
M	molar
MAA	methacrylic acid
mAU	milliabsorbance units
MDa	megadaltons
mg	milligram
mg/L	milligram per litre
$MgCl_2.6H_2O$	magnesium chloride
min	minute
MIR	mid-infrared
ml	millilitre
µm	micrometre
µW/lumen	microwatts per lumen
mm	millimetre
MODHT	Monitoring of Damage to Historic Tapestries, European Research Project (EVK4-2001-00048)
mol	moles
M_n	number-averaged molecular weight
M_p	peak molecular weight
M_w	weight-averaged molecular weight
MRF	mould risk factor
MSC	multiplicative scatter correction
MVA	multivariate analysis
N	newtons
N	nitrogen
nA	nanoamps
NAA	Neutron Activation Analysis

NaBr	sodium bromide
NaCl	sodium chloride
NIR	near-infrared
nm	nanometres
NMR	Nuclear Magnetic Resonance
O	oxygen
%	percent
%DC	percentage maximum dimensional change
P25	glycoprotein of ~ 30 kDa which associates with the H-L chain complex in silk fibroin
PC	principal component
PCA	Principal Component Analysis
PDA	personal digital assistant (used with portable XRF)
PDA	Photodiode Array (detector used with HPSEC)
PIXE	Particle Induced X-ray Emission
PLS	Partial Least Squares
Pol	polarised
ppb	parts per billion
ppm	parts per million
PTFE	polytetrafluoroethylene
R	gas constant (8.314 J K^{-1} mol^{-1})
R^2	coefficient of determination
Rh	rhodium
RH	relative humidity
RMSEC	Root Mean Square Error of Calibration
RMSEP	Root Mean Square Error of Prediction
rpm	revolutions per minute
s	second
SAXD	Small Angle X-ray Diffraction
SAXS	Small Angle X-ray Scattering
SDS	sodium dodecyl sulfate

SEC	Size Exclusion Chromatography
SEM	Scanning Electron Microscopy
ser	serine
Sn	tin
SNV	standard normal variate
t	time
T	temperature
TED	time to equivalent damage
TEM	Transmission Electron Microscopy
T_g	glass transition temperature
TG	Thermogravimetry, also known as Thermogravimetry Analysis (TGA)
TG-DTA	Thermogravimetry, differential thermal analysis
Ti	titanium
Tnd	fibroin dissolved in lithium thiocyanate digested with trypsin
Tp	fibroin dissolved in water digested with trypsin
tris-HCl	trizma hydrochloride
TTSP	Time-Temperature Superposition
TWPI	Time Weighted Preservation Index
Tyr	tyrosine
UV	ultra-violet light
Vis	visible light
λ	wavelength (nm)
WAXS	Wide Angle X-ray Scattering
XRD	X-ray Diffraction
XRF	X-ray Fluorescence
Zn	zinc

Introduction

Silk has been revered for millennia for its lustre, beauty, handle and drape. Coupled with its easy dyeability which makes bright and fast colours possible, it has been reported as the queen of textiles.[1] Textiles reveal social, commercial and political histories to share with current and future generations. However textiles, and especially silk, are ephemeral organic objects. Silk degradation leads to brittle fabrics which split and eventually become powdery, disintegrating at the slightest touch. Consolidation of silk objects alters both the handle and appearance of the silk forming stiff and flat textiles. Alternative conservation treatments prevent the loss of silk by covering with a layer of net, however neither option prevents the deterioration.

Within English Heritage there is a wealth of textile artefacts. Textiles in historic houses are commonly on open display, increasing the risk to the objects from fluctuating humidity, dust, airborne pollutants and light. As silk deterioration cannot be prevented and the treatment of silk objects has limited success, an alternative approach is desirable. Reducing the rate of silk deterioration by optimising the preventive conservation would increase the display lifetime of these fragile artefacts. This would also extend the period before interventive conservation treatments become necessary. However the critical factors for silk deterioration have not been determined and so the methods of increasing the lifetime not yet identified.

Amongst the natural fibres found in historic houses, silk is reported to be the most vulnerable to damage, especially from light.[2,3] Historic houses tend to utilise natural lighting from windows, however it can be difficult to balance sufficient light to view collections whilst controlling the dose. Research on historic tapestries reported the poor condition of samples taken from the reverse side, despite their bright colours, indicating light may not be the only important deterioration factor for silk.[4] However there are few published studies on the effect of humidity on silk

deterioration, therefore the extent of the risk to the collection remains to be elucidated.

Silk can be processed in a large number of different ways and these have changed over time and with new equipment and limits on the use of chemicals. European silk from the 19th and 20th centuries is especially likely to have been treated with a range of experimental methods as the reported explosion of weighting patents for silk testifies.[5] A large number of the textiles in the English Heritage collection date from this period. Some of these materials, such as tin-weighted silk, are thought to have an inherent deterioration mechanism due to the presence of the metal salt in the silk.[6] However these textiles are difficult to identify and the amount, and their location within the English Heritage collection was unknown. The research aimed to identify the variety of silks within the English Heritage collection and document their overt state.

Current monitoring within a number of English Heritage properties records the temperature and humidity in the display and storage areas. There are also a small number of light monitors, although each display room has a light plan which specifies the appropriate light level for the collections in that room. However there is no specific display conditions for silk collections, the research aimed to determine these and identify possible modifications. The display environments have been used as the basis of accelerated ageing conditions to determine the critical deterioration factors for silk on open display. This helps elucidate the silk ageing process and its associated dynamics which can be used to improve the preventive conservation and collections management for these objects.

To follow the progress of silk deterioration and quantify the condition of the English Heritage collection a means of analysis was required. Previous research had successfully applied High Performance Size Exclusion Chromatography (HPSEC) to the analysis of micro-samples from historic tapestries to determine the condition of the silk.[7,8,9] This technique follows changes to the molecular weight of silk

which decreases as the silk deteriorates. By taking micro-samples from the English Heritage collection it was hoped to determine their condition using HPSEC. This could be compared with results from analysis of accelerated ageing samples. However this technique is destructive even though the required samples are very small. A way to relate the destructive laboratory analysis of both accelerated ageing and historic samples with a non-invasive and non-destructive method for use within historic houses was desirable.

A further aim of the research was to develop a non-invasive and non-destructive technique to determine the condition of silk collections for use in historic houses. This could then be used to characterise the silk collections in a selected property. The data could be further related to the analytical results and documentary evidence of the collections to give a more complete picture of the collection. The possible improvements to the display lifetime of objects by improving the preventive conservation could also be quantified.

The first section of this thesis presents the research to understand the English Heritage collection and how it may have been processed. This includes a review of the literature on silk, its origins and formation in the silkworm and the processing of silk, particularly the methods that may have been used for silk in the English Heritage collection. There are limited references to the environmental effects on silk deterioration, but the available sources are reviewed. The survey of the English Heritage collection and selection of the properties (Apsley House, Audley End House, Brodsworth Hall, Osborne House and the Wernher Collection at Ranger's House) for further study is included. From the 1000 objects which contain silk a subset of 100 were chosen for further study and micro-samples removed. The display environments for the selected properties are presented and the key conditions selected for further study.

A review of previous elemental analysis for textiles is presented along with the results from the historic micro-samples from English Heritage to identify the types

of silk present in the collection. Problems quantifying the data are discussed along with the limitations to identify the processing methods which have introduced the identified elements. As well as elemental analysis there have been many studies on silk analysing the crystal structure, amino acid composition, silk structure and condition. These methods have been reviewed along with the information they provide on silk. The applicability of the techniques to conservation is discussed to determine their suitability for this research.

The HPSEC equipment parameters and experimental protocols were determined and are discussed. Further analysis of the calibration standards was undertaken to demonstrate these are not disassociated by the HPSEC operating conditions. The protocols were tested using samples from the Dudley Armorial tapestry from the Burrell Collection. This allowed the same thread to be sampled from both the front (faded) and reverse (brightly coloured) of the tapestry and determined the similar condition of samples.

To understand deterioration rates for silk the limited references for the activation energy and rate of silk deterioration were reviewed. However the reported activation energies cover a wide range. A kinetics study was undertaken and a number of methods used to experimentally determine the activation energy. The calculated activation energy is discussed along with the expected increase in deterioration for the accelerated ageing experiments. This preliminary study helped develop the ageing protocols for the longer term study on silk.

The second half of the thesis discusses accelerated ageing experiments, the results and application to preventive conservation. Accelerated ageing experiments have been used to identify the critical deterioration factors for silk. The rate of deterioration during ageing experiments and important parameters for silk degradation are identified. The accelerated ageing results are also compared to those from the English Heritage micro-samples and values in the literature.

The experimental results are discussed in terms of the critical deterioration factors for silk and to make preventive conservation recommendations. The results have been used to develop a silk deterioration curve and its potential use in preventive conservation discussed. The possibility of extending this to isoperms for silk deterioration is also explored. To quantify how these techniques could be utilised within historic collections the effect on display lifetimes of objects has been discussed and examples from the English Heritage collection are given.

The destructive laboratory analysis of samples has been compared with the near-infrared (NIR) spectra of samples. As NIR can be used *in situ* and is both non-invasive and non-destructive it has the potential to be suitable for condition monitoring of silk artefacts. The use of multivariate analysis to develop a model relating the data and make predictions of the tensile strength of samples is discussed. Tests of the model at Brodsworth Hall are presented, including the possibility to rank the condition of objects within a collection.

The research has demonstrated high humidity increases silk deterioration and is more important than previously considered. Despite previous indications on the effect of light on silk deterioration, this has been shown to have less effect than humidity.

References

[1] Guan, J., Yang, C. Q. and Chen, G. (2009) 'Formaldehyde-free flame retardant finishing of silk using a hydroxyl-functional organophosphorus oligomer' *Polymer Degradation and Stability* **94** 450-455.

[2] Tímár-Balázsy, A. and Eastop, D. (1998) 'Fibres' *Chemical Principles of Textile Conservation* Oxford: Butterworth-Heinemann 3-66.

[3] Tucker, P., Kerr, N. and Hersh, S. P. (1980) 'Photochemical Damage of Textiles' *Textiles and Museum Lighting* (The Harpers Ferry Regional Textile Group) December 4 & 5 1980, The Anderson House Museum, National Headquarters of

the Society of the Cincinnati, 2118 Massachusetts Ave, NW Washington DC 20008, 23-40.

[4] Quye, A., Hallett, K. and Herrero Carretero, C. (2009) *'Wrought in Gold and Silk' Preserving the Art of Historic Tapestries* Edinburgh: National Museums Scotland Enterprises Ltd – Publishing.

[5] Hacke, M. (2008) 'Weighted silk: history, analysis and conservation' *Reviews in Conservation* **9** 3-15.

[6] Palmer, A. (2006) ''A bomb in the collection': researching and exhibiting early 20th-century fashion' in *The Future of the 20th Century. Postprints of the AHRC Research Centre for Textile Conservation and Textile Studies Second Annual Conference July 2005*, C. Rogerson and P. Garside (ed.) London: Archetype 41-47.

[7] Howell, D. (1992) 'Silk Degradation Studies' in *Silk: Harpers Ferry Regional Textile Group, 11th Symposium*, Washington DC: Harpers Ferry Regional Textile Group 11-12.

[8] Hallett, K. and Howell, D. (2005) 'Size exclusion chromatography as a tool for monitoring silk degradation in historic tapestries', in *AHRC Research Centre for Textile Conservation and Textile Studies First Annual Conference – Scientific Analysis of Ancient and Historic Textiles Postprints,* Janaway, R. and Wyeth, P. (ed.) London: Archetype 143–150.

[9] Hallett, K. and Howell, D. (2005) 'Size exclusion chromatography of silk: inferring the textile strength and assessing the condition of historic tapestries' in *ICOM Committee for Conservation 14th Triennial Meeting Preprints, The Hague, 12-16th September 2005 Preprints* **2** 911-919.

Chapter 1 – Silk

Textiles provide details of commercial, political and social history; however they are ephemeral organic objects and silk is regarded as particularly vulnerable. This chapter will consider the source and production of silk along with the processing techniques common to historic collections. An overview of silk composition and structure along with its chemical and physical properties are presented to help determine how silk deterioration occurs. The impact of environmental display conditions on silk deterioration is also reviewed.

Within historic houses the collections are used to display how the home would have appeared during use. The use of open display places textiles particularly at risk from the display environment. A balance between the risk of open display and making the collection accessible is therefore sought. When silk deteriorates it becomes brittle limiting the success of sewing conservation methods.[1] Alternatively silk can be treated with adhesives[2] or consolidants[3]; however this affects the appearance and stiffness of silk and is often only carried out when the silk would be completely lost otherwise.[4] Advice for the display of textiles often recommends low light levels, with both the fading of dyes and embrittlement of the fibres cited as damage caused by light.[5,6] The environmental effects on the fading of dyes have been studied[7,8] however there is little research on the effects on the textile substrates.

Silk textiles are commonly reported as more vulnerable to damage, particularly from light, than those made from other natural or synthetic fibres.[9,10,11,12,13] This research looks at the environmental effects causing damage to silk and how these may be mitigated on open display within historic houses. The effects of dyes have been excluded to minimise the number of variables and provide information on the deterioration of silk under varying environmental conditions, which has been rarely

studied previously.[14] Improvements made to increase the longevity of silk on display should also be effective for other textiles, if silk is used as an exemplar for the most vulnerable textile fibre. To understand the risks to silk a review of its production, processing, composition, structure, properties and the available information on environmental effects are presented. Where possible abstracts of papers published in languages other than English have been used, however it has not been possible to thoroughly review literature published in languages other than English.

Silk Production

Early references to the silkworm are reported from the second or third millennium B.C. in China and the earliest surviving fragments of cloth from *Bombyx mori* filaments date from 3630 B.C.[15] Riboud has described the weave and figurative designs on silk fragments from the Warring States period (3rd – 5th Century B.C.).[16] The cultivation of silkworms (sericulture) dispersed slowly to Asia (Korea and Japan), the Middle East (Iran and Turkey) and eventually Europe (Italy and France)[17] although China still produces the greatest amount of silk.[18] The majority of silk is still used as a textile but it is becoming increasingly important in biomedical research for tissue[19,20] and bone[21] repairs and artificial tendons as well as within the cosmetics industry.[22]

Although silk is generated by a number of insect larvae and spiders it is the domesticated silkworm, *Bombyx mori*, which produces the majority of fibres used commercially. Wolfgang reports around 15,000 cocoons are required to produce a pound of silk.[23] A number of wild silk moth species also exist whose silk can be spun and woven. These include both the Chinese and Indian tussah moth (*Antheraea pernyi* and *Antheraea mylitta* respectively) and an African communal caterpillar, *Anaphe moloneyi.*[24]

Bombyx mori larvae (silkworms) are fed exclusively on leaves from the mulberry tree. The lifecycle of a silkworm lasts about 45-55 days but can vary depending on the rearing conditions and changes in diet, it has been suggested this also affects the quality of silk.[25,26,27,28] During the silkworm's lifecycle it moults and rests four times, feeding between each. At the end of the fifth feeding period, or instar, the larva rests for about 24 hours, before forming the cocoon over 3-6 days. The silk is spun by the silkworm moving its head in a figure of eight motion whilst extruding the silk from the spinneret, producing circa 60 cm of thread per minute.[29] The resulting thread (bave) is actually formed of two filaments (brins) made from fibroin – the main silk protein. The brins are held together by another protein gum, sericin (see Figure 1.1). On average the *Bombyx mori* thread is 10-25 μm in diameter with individual brins measuring 5-10 μm, wild silks tend to be coarser, 65 μm in diameter.

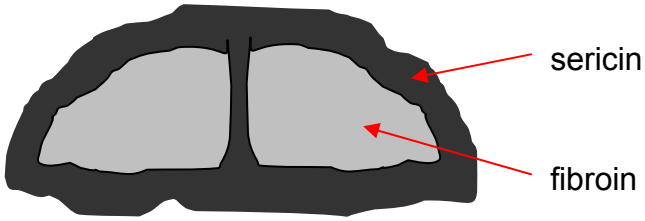

Figure 1.1 – image of silk fibre cross-section

On either side of the *Bombyx mori* silkworm there are glands which produce the silk solution.[30] These have been separated into three regions, or divisions, based on the function taking place.[31,32] The main protein fibroin is generated in the posterior division and stored in the larger middle region, where sericin is also synthesised. The proteins remain separate and move into the anterior division, where the two glands combine and move into the spinneret. Analysis of gland silk has identified it is mostly in a random-coil conformation, known as silk I which during spinning is transformed by shear stress into the β-crystalline or silk II form. Magoshi *et al.* have identified that the extension rate of the silk affects the conformation, with rates higher than 500 mm/min giving β-form silk.[33] The

transformation between the dimorphs of silk fibroin can also occur due to the sample preparation, including solvent treatment.[34,35,36]

The silk thread is spun from an aqueous solution forming an insoluble fibre, this change occurs as a result of an irreversible phase change on spinning.[37] Analysis has shown there are also changes in pH (from 5.6 to 4.8),[38,39] viscosity,[40,41] and ion exchange.[42,43,44,45] During spinning sericin is not reported to undergo a similar conformational change. This is thought to be related to the higher proportion of large side chain amino acids preventing close packing and a higher water content. The sericin layer forms an amorphous, adhesive coating around the fibroin. Willcox describes the silkworm spinning process as analogous to liquid-crystal spinning.

A study of the pupae determined the presence of an enzyme, protease, which was secreted with a liquid, thought to act as a buffer for the enzyme, to soften the sericin and allow the moth to separate the fibres and escape.[46] To prevent damage to the silk filaments from the emerging moth, the chrysalis is stifled with either steam or a low heat.[47] It is then possible to reel a continuous thread from the cocoon. The cocoons are placed in warm water which softens the gum and allows the filaments to be unravelled. In most cocoons the central 500-800 metres are reeled from the approximately 1500 metres of thread. The unravelled threads are reeled into a skein of silk; however it is so fine that it cannot easily be used. To produce a suitable thread several filaments are twisted together forming thrown silk. The outer and inner layers of the cocoon are known as silk waste and are used to produce spun silk. Cocoons from wild silk species are usually collected after the moth has escaped and so tend to be spun. The sericin gum prevents mechanical damage to the fibroin filaments and so usually remains during processing.[48]

Silk Processing

Degumming is the removal of sericin from raw silk, giving the lustrous, soft silk fibre. A variety of methods including boiling water, alkaline or acid solutions and enzymes have all been used to remove sericin. The different composition of sericin to fibroin allows it to be preferentially removed by hydrolysis to smaller water-soluble units.[49] Studies on degumming have shown that either an alkaline (pH 9.5-10.5) or an acidic (pH 1.5-2) solution gives the most effective degumming.[50] However all degumming methods are thought to cause some damage to the fibroin fibres. Studies by Jiang *et al.* looked at the effects of various degumming methods on the tensile behaviour and morphology of silk fibres and found borate buffer degumming was best in terms of mechanical properties and sericin removal.[51]

The level of sericin removal during degumming is controlled depending on the later required processing techniques. Summaries of literature by Brooks *et al.* report raw silk contains 20-30% sericin, ecru silk 24-26%, souple silk 17-18% and in cuite silk around 5% sericin remains. Raw silk is more hygroscopic than silk which has been degummed due to the higher amount of sericin, which may make it more at risk from environmental damage.[14,52]

Silk is naturally coloured, although *Bombyx mori* silk is often white or light yellow wild silks tend to range from yellow to dark brown. This led silk to be bleached in order to have white or lighter coloured dyed silks. Carboni describes how skeins were soaped and placed in a chamber where sulfur was burned. This may account for the high sulfur content found in historic silks analysed by Ballard.[53,54]
Bleaching can occur by oxidation or reduction, although oxidation is favoured as it alters the colouring compounds whereas reduced silk can be reoxidised and yellow again. Common oxidative bleaches include hydrogen peroxide, sodium perborate or persulfate, with sodium hydrosulfite or sodium sulfoxylates used for reductive bleaching. The whiteness of silk can also be increased with optical brighteners.

If fully degummed, silk loses approximately 25% of its weight. As silk was sold by weight, weighting is thought to have originated as a means of replacing the lost weight. When the added material replaces the equivalent lost during degumming, silk is said to be at par. If the weighting introduces less, the silk is described as *below par*, whereas if it increases the weight above that before degumming it is *above par*. Waxes, gums and especially sugars are reported as organic weighting agents. These could be used with light coloured dyes but were removed by washing the silk. Weighting with sugar could increase the weight by 10-20% at most.[55]

Another common weighting material was tannins, although initially this was limited to dark coloured dyed silk as they stain fibres brown. Decolourised tannins are reported from the 1890s and allowed them to be used with light-coloured silks.[48,56] Black silk was often weighted with tannins in combination with iron salts giving weight increases of 25%. Recent research found black dyed samples of both wool and silk had less strength compared with other colours. Within historic tapestries the black and dark brown yarns are often reported as missing or extremely weak by conservators.[57] This work undertaken on the European project, Monitoring of Damage to Historic Tapestries (MODHT) demonstrated the dyeing process itself damages silk fibres. The effects of dyes on raw silk and wild silk species have also been studied.[58,59]

Patents for metallic weighting with inorganic salts of aluminium, iron, lead, magnesium, tungsten and zinc are reported from 1855 by Scott.[60] However tin weighting compounds became common with a range of different methods used from the 1870s onwards. A stannic chloride bath could increase the weight by 10% and was often repeated four or five times. In 1893 Neuhaus patented the “dynamite” method which used an aluminium sulfate bath before treatment with sodium silicate on tin and phosphate loaded silk to increase the weight by around 400%.[48,53] It is reported that greater weighting levels are possible if some sericin

remains on the silk. The methods and technology used to weight silk were reviewed by Scott in the 1930s.[60,61,62] Weighted silk is usually heavier and thicker and has better draping qualities than unweighted degummed silk.[63] This led to weighting becoming an accepted treatment, however dramatic changes in the mechanical properties are reported for metallic weighted silk.[64,65]

Tin weighting is not thought to bond to the fibre but instead be absorbed into the amorphous regions of fibroin. However chemical combination is also proposed as a possible mechanism. Within the fibres of *Bombyx mori* silk are microvoids which vary in size and distribution. These accessible regions have been imaged with silver sulfide particles formed after treatment with hydrogen sulfide gas and then silver nitrate solution.[66] The particles are aligned parallel to the fibre length and are rod-like in shape. Analysis of tin-weighted silk with small-angle X-ray diffraction (SAXD) located stannic acid gel in elongated microvoids which also ran parallel to the fibre axis.[67] Weighting of silk using polymer grafting with methacrylic acid (MAA) has been reported as replacing tin weighting more recently.[68,69]

Silk yarns have been finished using dilute organic acids. Silk finishing with tartaric and citric acids produces a rustling effect known as “scroop”. Citric acid[70,71] and epoxides[72,73,74] have been used to finish silk giving improved launder-ability due to the formation of crosslinks. Flame resistant finishing has also been investigated.[75]

Silk Composition and Structure

Three amino acids, glycine, alanine and serine, make up about 86% of fibroin.[76] The full amino acid composition of both *Bombyx mori* and Tussah silk fibroin and sericin can be seen in Table 1.1, the differences between the silks have been discussed by Schroeder and Kay[77] and Lucas *et al*.[78] The high numbers of small amino acids in fibroin enable the protein chains to form ordered, crystalline regions. *Bombyx mori* silk is reported as having 62-65% crystallinity, whereas wild silks

have 50-63%. The larger amino acids are generally found in the amorphous areas and are reduced in number in deteriorated silk.[79]

	Bombyx mori silk		Tussah silk (*A. mylitta)*	
Amino acid	Fibroin / mol %	Sericin / mol %	Fibroin / mol %	Sericin / mol %
Glycine	44.5	14.7	26.6	14.5
Alanine	29.3	4.3	41.4	5.8
Valine	2.2	3.6	0.9	5.2
Leucine	0.5	1.4	0.3	2.5
Isoleucine	0.7	0.7	0.3	1.3
Serine*	12.1	37.3	11.1	12.3
Threonine*	0.9	8.7	0.4	11.1
Aspartic acid*	1.3	14.8	6.3	10.2
Glutamic acid*	1.0	3.4	0.9	6.9
Lysine*	0.3	2.4	0.2	16.5
Arginine*	0.5	3.6	3.9	1.7
Histidine*	0.2	1.2	1.0	2.1
Tyrosine*	5.2	2.6	4.7	6.8
Phenylalanine	0.6	0.3	0.3	2.0
Proline	0.3	0.7	0.4	0.8
Tryptophan	0.2	-	1.2	0.3
Methionine	0.1	-	-	-
Cysteine*	0.2	0.5	-	-

Table 1.1 – amino acid composition of polypeptides in fibroin and sericin for *Bombyx mori* and Tussah silks[80] (* = polar amino acid)

Cysteine and methionine were initially thought to be absent from fibroin due to their small amount. Cysteine was known to be in sericin, which meant it was regarded as contamination of the results due to insufficient degumming.[81] The presence of cysteine within fibroin was reported by Schroeder and Kay[77] and confirmed by Zuber *et al.*[82] Four cysteine residues per molecule were identified by Lucas[83] and their location and the sequence was determined to be within the amorphous region by Earland and Robins,[84] but the exact nature of the cysteine residues and formation of cystine links was unclear.[85]

The composition of sericin is noticeably different to fibroin with less glycine and alanine. There are also a greater number of polar groups (marked by * in Table

1.1) giving sericin its greater water solubility and absorption. Analysis of sericin has identified a number of different molecular weight proteins,[86,87] and their carbohydrate content.[88]

Chymotrypsin has been used to digest aqueous solutions of fibroin leading to two fractions.[89] One was an insoluble precipitate, Cp, with a molecular weight of approximately 4000. This was highly crystalline and accounted for approximately 60% of the fibroin. The remaining fraction, Cs, was soluble and formed the amorphous parts of the fibroin, with the large side chain amino acids. The chemically resistant fraction has also been prepared by a variety of treatments by Shaw and Smith.[90]

Lucas described how twelve crystalline sections alternate with twelve amorphous regions. Within the Cp fraction a hexapeptide sequence Ser-Gly-Ala-Gly-Ala-Gly (see Figure 1.2) was identified and suggested to form the majority of the crystalline regions within *Bombyx mori* silk fibroin. The hexapeptide has been synthesised[91] and characterised further.[92] A 59-residue sequence was also determined:

---Tyr.Gly.Ala.Gly.Ala.Gly.[Ser.Gly.$(Ala.Gly)_n]_8$.Ser.Gly.Ala.Ala.Gly.Tyr.---

where n is usually 2 and always has a mean value of 2. Genetic studies on *Bombyx mori* silk fibroin have elucidated the complete amino acid sequence and studies have begun to look at the structure based on the composition.[93,94,95,96] This includes indentifying alternating crystalline and amorphous units[97] and the turns related to the location of proline amino acids.[98]

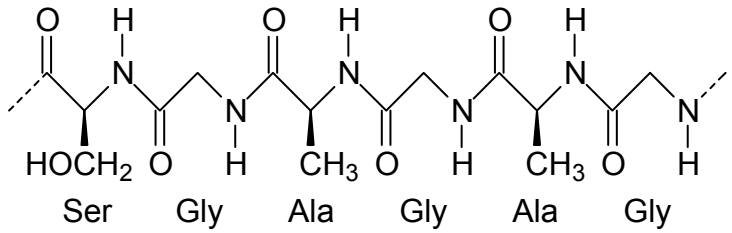

Figure 1.2 – hexapeptide repeating unit in silk (polar arrangement)

Shaw described the highly crystalline fraction Cp as phase I. Phase II was identified as the sequences of glycine, alanine, valine and tyrosine residues that occur with phase I in fractions Tp and Tnd (fibroin dissolved in water or lithium thiocyanate respectively, digested with trypsin). Phase II fractions were not as ordered as those in phase I but not completely disordered. The truly amorphous sequences that remained were labelled phase III and included the polar and large side chain amino acids.[99] The most sensitive regions to alkaline hydrolysis were reported by Shaw as the alternating glycyl residues in phases I and II.[100]

Molecular weights ranging from 33,000 to 400,000 Daltons have been reported due to degradation of fibroin when preparing pure, degummed samples.[24,101,102] Analysis of gland silk solubilised in urea or guanidine-HCl solutions has led to a narrower range of 350,000 to 370,000 Daltons.[,103,104,105] The links between chains has also been debated. Initially it was suggested that the chains may be joined by an intramolecular disulfide bridge from cystine residues, or possibly ester bonds.[106] A number of authors found one large and one to three small components linked by disulfide bonds.[86,105,107,108]

It is now accepted that *Bombyx mori* fibroin is formed of a heavy component (H-chain) of 350,000 Daltons and light component (L-chain) of 25,000 Daltons linked by a disulfide bond. The sequence of these chains, including the cystine bond between them has been elucidated from the gene codes.[109,110,111] Studies on the H-L subunit have identified that the H-chain contains mainly glycine, alanine and serine, whereas the L-chain is reported to contain high amounts of leucine, isoleucine and valine.[112] Six of the H-L subunits are reported to link to a further protein, known as P25, via hydrophobic interactions,[113,114] in a 6:6:1 molar ratio (see Figure 1.3).[115] It has been suggested that this 2.3 MDa complex is only stable in the gland and not after extrusion.[116] For wild silks the H-chain is modified and the L-chain and P25 unit are not found.[117]

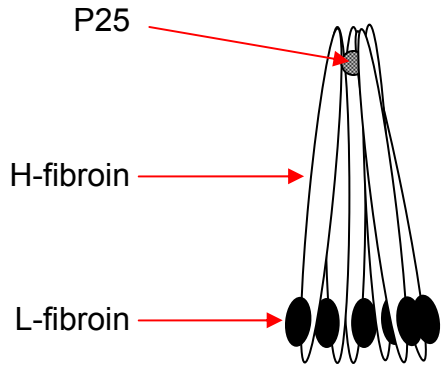

Figure 1.3 – combination of H-L subunits and P25 (redrawn from Inoue *et al.*)

The intramolecular bonding between the chains of the protein influences the conformation or secondary structure of a protein.[118] The polypeptide chains forming the backbone of silk were interpreted as running parallel to the fibre axis in early X-ray investigations.[119,120,121] Within silk a pleated sheet structure is formed that then stacks to form a three-dimensional crystalline structure. The β-sheet and turn structure within the chains can be seen in Figure 1.4.

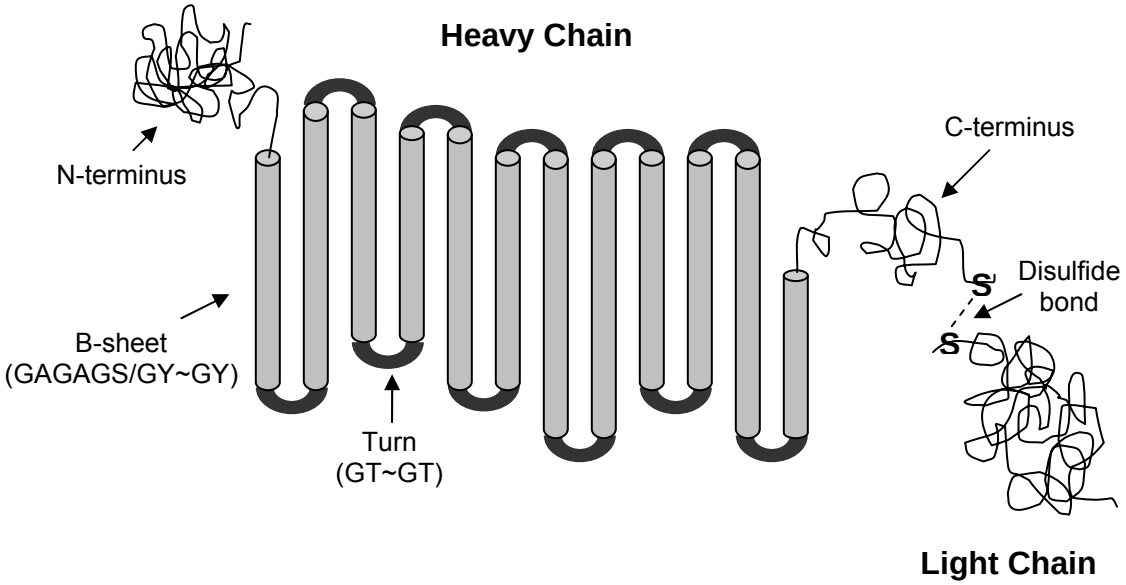

Figure 1.4 – 2D structure of H-L chain subunit (redrawn from Ha *et al.*)

Studies by Marsh *et al.*,[122,123] and Warwicker[124] elucidated the unit cell dimensions for *Bombyx mori* as: *a* (interchain) = 0.94 nm; *b* (fibre axis) = 0.697 nm; *c* (intersheet) = 0.92 nm. They suggest four polypeptide chains or eight amino acid residues fold back to run in opposite directions in an antiparallel arrangement, with the glycine side chains of one sheet opposite those of the next sheet. This was questioned by Crick and Kendrew[125] and more recent X-ray studies[126,127] revealed an antiparallel (antipolar-) arrangement (see Figure 1.5) rather than the antiparallel (polar-) formation described by Marsh *et al*. This has also been observed by NMR[128,129] and Raman spectroscopy.[130] This indicates the methyl groups on the alanine residues alternate from side to side of the sheet instead of running along one face in the (polar-) model (see Figure 1.2).

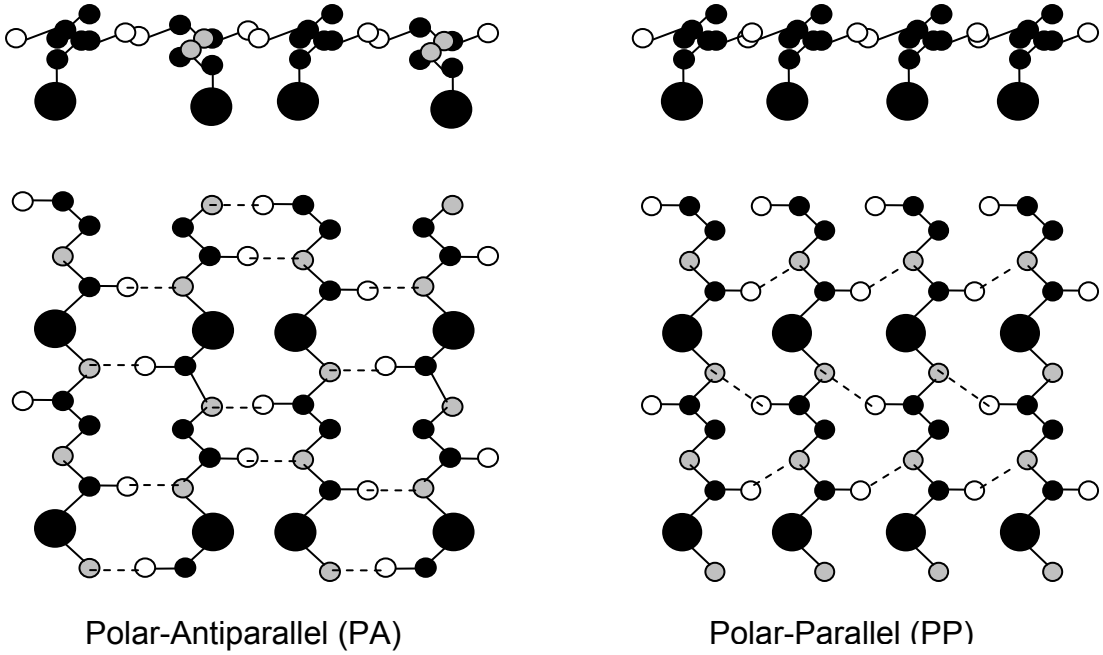

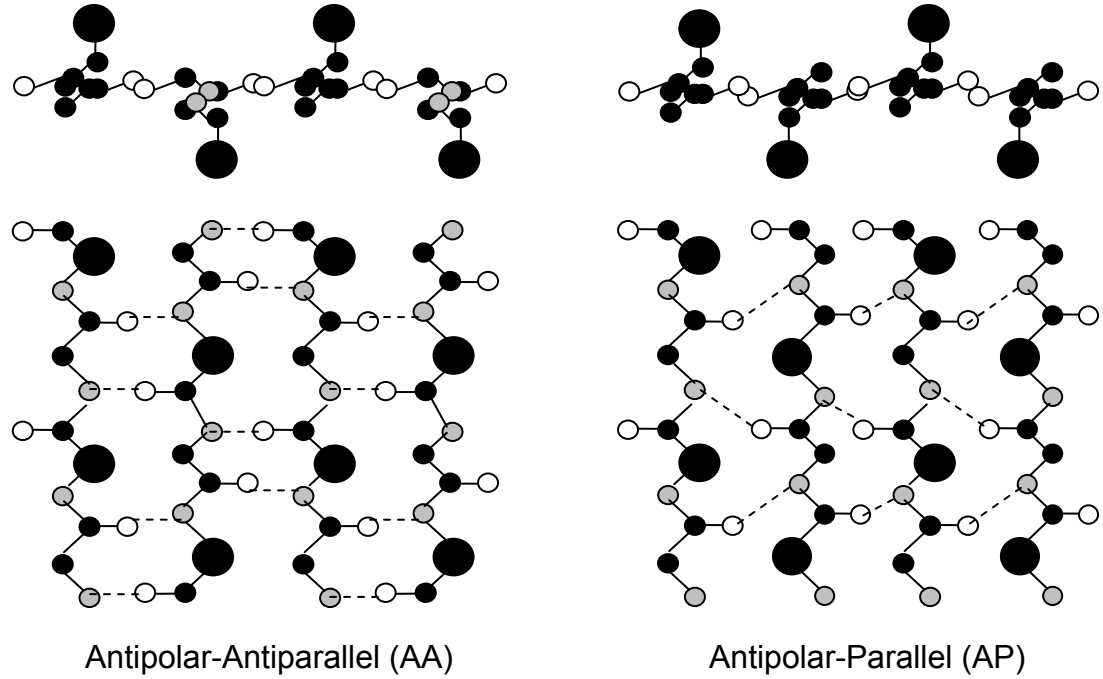

Figure 1.5 – models for sheet structure

Warwicker undertook a number of X-ray studies[131,132] on a number of different types of silk proteins and found that although the fibre axis and interchain spacings (*b* and *a* coordinates) were the same, the intersheet spacings (*c* coordinates)

varied depending on the size of the projecting side-chains. Therefore it is probable that the conformation and the amino acid composition are different in each species. The structure of wild silks have also been studied by Marsh *et al.* [133] and characterized by Sen and Babu.[134]

Twelve of the chains are thought to associate to form β-sheets, five of which associate to form microfibrils (approximately 10nm in diameter). Fibrils are formed from bundles of the microfibrils (about 1 μm), which combine to associate into fibroin filaments (7 – 12 μm). A skin-core structure has been suggested with denser material around the outside.[135] A similar structure has also been observed during studies on the microvoids observed between the fibrils. The nanofibrillar structures (around 70-150 nm in diameter) have been imaged using atomic force microscopy (AFM)[57,136] and scanning electron microscopy (SEM)[137] in unaged, undyed silk. AFM analysis after light ageing observed the fibrils break down into smaller segments, suggesting degradation occurs.[138,139] Nanofibrils have been reported to show helical features, which may relate to the twist reported by Lotz *et al.* in the crystal structure.

AFM has been used to image solutions of gland silk, identifying small rods (60 nm x 15 nm) which aggregated at higher concentrations to form threadlike structures.[140] A similar structure had previously been suggested by Kratky based on X-ray studies.[141] Aggregate formation within gland silk has also been suggested by Li *et al.*[142]

Physical Properties

Cross sections of brins are roughly triangular (*Bombyx mori*), wedge to rectangular (Tussah) or crescent (*Anaphe*) in shape when imaged using a scanning electron microscope (SEM).[143] Degummed silk fibres have few external markings along the length. Whereas raw silk is described as having a striated appearance due to the

filaments being held together by sericin. The coarser wild Tussah silks are ribbon-like and twisting.

The glass transition temperature (T_g) marks changes in a number of physical properties including the specific volume, modulus and heat capacity. Changes in the T_g can be caused by the presence of crosslinks or changes to the chain length.[144] For new *Bombyx mori* silk the T_g is 175 °C[145] and 162 °C for Tussah silk.[146] A number of wild silks (kususan, erisan and tensan) have also been analysed and show higher T_g values (198, 191, and 201 °C respectively).[147] Thermogravimetry, differential thermal analysis (TG-DTA) of cocoons observe a yellowing around the reported T_g values.[148]

Unlike most natural fibres silk is strong with a high breaking extension, being more similar to synthetic fibres with a high work to rupture. Silk has a low yield strain which gives it a low yield point compared with nylon. The mechanical properties, particularly tenacity, breaking extension and modulus, have been shown to relate to fibre fineness.[149] Sen and Babu reported as the silk fibre becomes thinner, the more ordered and the greater the degree of crystallinity it is.[150] The elastic modulus increases with decreasing thickness of the silk thread, which is observed in a number of silkworm species. The changing thickness of the silk fibre has been shown to relate to the position within the cocoon and to enable the cocoon to effectively protect the pupae.[151] Cheung *et al.* demonstrated that *Bombyx mori* fibres can take a higher loading but less extension than Tussah fibres.[152] Similar results are reported by Das who correlates this to the poor orientation and crystalline order in Tussah silk fibres,[153] this is suggested to relate to the higher percent of bulky groups present.[154]

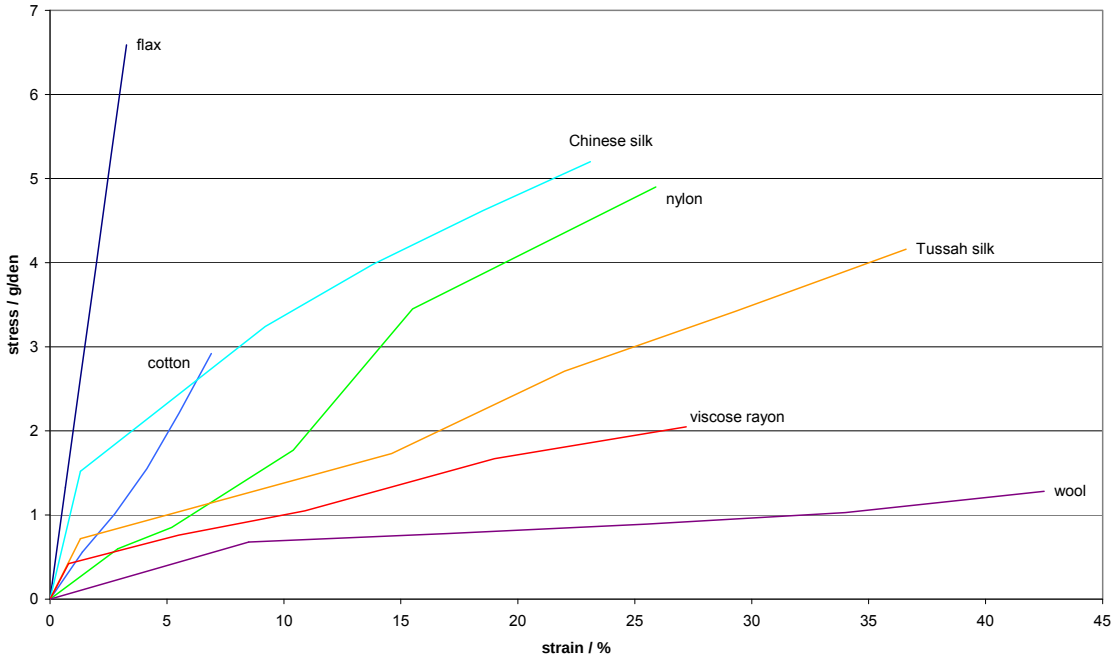

Figure 1.6 – stress-strain plot of common materials (plotted from data in Appendix II of Meredith)

The initial deformation, under tension is reported within the amorphous regions.[155] The relationship between the structure and physical properties have been analysed by Sirichaisit *et al*.[156] More recently the extension of silk has been shown to include elastic deformation of the β-sheet crystals.[157] The ability of the silk fibre to recover in the elastic region is related to the moisture content. At low strains the recovery of silk decreases with increasing humidity, however moving from 60% to 90% RH the recovery increases with increasing strain.[158] At high temperatures, or after chemical treatment, supercontraction of *Bombyx* silk has been reported. Above the elastic region (seen as a sharp change for both Chinese and Tussah silk in Figure 1.6) interchain bonds break and the chains extend past each other, if tension continues to be applied. This can lead to permanent deformation if the bonds reform in the new extended positions.[159]

Chemical Properties

The amorphous regions, due to their less ordered nature, are more accessible to deterioration agents such as oxygen, humidity and salts, and Crighton has suggested that silk deterioration starts here.[160] Warwicker studied the sorption of water by silk and reported no changes between the X-ray diagrams of wet and dry fibroin indicating water does not penetrate the crystalline region.[161]

Silk degradation caused by boiling water or steam, is thought to lead to hydrolysis. Hydrolysis of the peptide links leads to scission of the main polypeptide chain in silk, with a corresponding decrease in molecular weight.[162] The rate of hydrolysis can be altered by changing pH and temperature. The main chain is thought to be hydrolysed by strong acids, with end groups attacked by alkalis. The less acidic and alkaline region between pH 4 and 8 is reported to cause less degradation.

The side chains of amino acids and the terminal residues of the main chain can be oxidised, as can the peptide bonds of the main chain. Two amino acids that are particularly vulnerable to oxidation are tyrosine and threonine.[163] Oxidation caused by hydrogen peroxide or peracetic acid has been followed by changes in viscosity, Methylene Blue absorption, and the reduced tyrosine content of silk. Reactions of silk fibroin with a number of oxidizing agents have been studied by Earland and Stell[164] and crosslinks are suggested to form.[165,166]

Water is reported to bond with the fibroin within the amorphous region forming crosslinks, opening up the structure and reducing the force required to rupture the fibre, giving an increase in extensibility.[167] Crosslinks are also reported to form as a result of ageing in silk, along with loss of amorphous regions leading to a gradual increase in crystallinity.[168] Increasing lengths of dry heat treatment leads to a decreasing level of solubility which is reported to relate to the increased formation of crosslinks.[169] Formaldehyde is known to lead to crosslinks in proteins, with a reaction between the terminal amino group and the carboxyl double bond in

formaldehyde. Methylene crosslinks are then formed between the chains in the amorphous regions.[170] Bifunctional dyes have been reported to form crosslinks in silk and similarly affect mechanical and solubility properties.[171]

Research on silk to improve crease-resistance[172] and washability have introduced crosslinks and studied their effects. The treatment of silk with synthetic resins reacted with tyrosine residues to reduce swelling caused by moisture.[173] The use of electrical discharge to form crosslinks and improve the mechanical properties has also been tested.[174] Work using sodium citrate found improvements to the abrasion resistance and tear strength of the treated silk. This is attributed to reaction of the carboxyl groups in sodium citrate with the side chains in silk to form crosslinks. Reaction mechanisms for sodium citrate with the terminal amino group of arginine and lysine side chains are included and suggest a dehydration reaction occurs.

Work using epoxides to improve the wet resiliency of silk, and therefore its crease-resistance has identified serine, tyrosine, lysine and histidine as the active groups forming covalent bonds with the epoxides. The epoxy groups are reported to react with the hydroxyl groups of serine, the phenol hydroxyl group of tyrosine, amino group of lysine and imino group of histidine.[175] Cai *et al.* report changes in resiliency, moisture regain, whiteness and tensile strength following epoxide treatment and attribute this to a crosslinking reaction between the epoxide and silk in the accessible amorphous regions.

Environmental Effects on Silk

Of all the natural fibres silk is generally regarded as the most vulnerable to damage.[9,11,32,176,177,178] Becker and Tuross report that many environmental factors affect the deterioration of silk but that “light is considered the worst offender” and Hirabayashi *et al.* describe both UV radiation and sunlight as accelerating silk deterioration.[179] It is thought that UV radiation is most damaging[13,22] causing rapid

decreases in strength during artificial ageing tests on silk fibroin.[180] The changes to mechanical strength on light ageing, with and without UV radiation, have been analysed by Korenberg,[181] with greater changes observed when UV radiation was included. Structural transformations have been observed upon light irradiation.[182] The amorphous content increases upon sunlight ageing, reportedly due to UV light breaking bonds between polypeptide chains[183] and ageing outside demonstrated the rapid deterioration of silk in comparison to other textiles.,[176] Treatment of silk with stabilizers to prevent light and heat deterioration have been researched, however stabilizers which protected against light were detrimental to heat stability.[184] Previous research on silk deterioration indicated it may be caused by manufacturing processes and aggravated by light and oxidation.[185] Miller's work subjected new silk to a range of chemical treatments, common to silk processing methods, as well as heat and light, however humidity treatments are not reported.

The decomposition of tryptophan,[186] accelerated by the presence of tyrosine[187] leads to the yellowing of silk on light exposure. Amino acid analysis of a naturally aged silk dress collection found reduced levels of serine and tyrosine. Artificially aged silks demonstrated an increase in solubility with increased light ageing and increasing energy of the radiation used.[188] The formation of double bonds between amino acids with aromatic rings and the peptide backbone leading to photoyellowing has been proposed.[189] The extent of yellowing has been studied under both different light and moisture levels and different mechanisms are proposed.[190]

Experiments have shown oxygen is essential in degradation,[191] although silk photo-deterioration has been recorded in the absence of oxygen at slower rates.[192] The deterioration of silk under urban atmospheres has also been reported and hydrogen peroxide is suggested to form from anthroquinone vat dyes, known as photosensitisers, accelerating silk deterioration,[7,193] moisture can also increase this process. High moisture content in the fibre is also reported to accelerate

photodeterioration. Other factors suggested to affect silk degradation during light exposure include pH,[194] with a maximum stability at about pH 10.[195]

The sensitivity of silk to light has been reported to be increased by the presence of metallic weighting, although damage is still reported during ageing in the dark.[196] Experiments by Roberts and Mack[197] demonstrated that metallic weighting caused a large loss of strength which was increased by greater amounts of weighting in the silk. It is thought the metal salts in weighted silk have a catalytic effect on the deterioration. Samples known to be weighted are also reported to be more soluble in 7M urea than non-weighted samples.

Ballard *et al.*[198] analysed fourteen specimens from historic silk flags using scanning electron microscopy. The silk is described as being shredded, split and in unexhibitable condition by the authors. Ballard notes that such degradation has been ascribed to tin weighting, however the analysis demonstrated only one specimen had been weighted. The major element in all scans was sulfur and Ballard lists various reasons for its prominence including its presence in the fibroin, residues from bleaching, dyeing, mordanting, weighting or pollution. Further work by Ballard noted that fibroin or colorants could not account for the high sulfur content.[199] That shattering of silk may not be due to weighting but a result of other factors such as previous treatment, processing and finishing has also been reported by Yamazaki.[200]

High RH levels are generally avoided during display to prevent biological attack of textiles. However, silk is reported to be resistant to biological deterioration,[11,201] with tests demonstrating silk fibroin is resistant to fungi although can be degraded by bacteria.[202] Enzymes have been used to digest silk fibroin in solution in order to study the crystalline regions of silk fibroin, but the effect of enzymes on silk fibre deterioration have only recently been studied due to the increased use of silk as a biomaterial.[203]

Lower RH levels are recommended by a number of references but without citing any research or literature.[10,204] Within the literature there are very few studies that have determined the effects of humidity on silk degradation. A review by Hansen and Sobel cites a number of studies on the effects of humidity on silk. However a large proportion of the references relate to raw silk which is known to be more hygroscopic and therefore may not be applicable to degummed silk. A number of figures are reproduced from work by Hirabayashi who reported raw silk was strongest at 20% RH and decreased in strength with increasing RH.[205] Increased duration of exposure to high humidity also leads to increased degradation.[206] Hansen and Ginell recorded loss of tensile properties and increased colour change for degummed silk above 50% RH. The review suggests silk should be stored below 50% RH, however the research on degummed silk only analysed the effect of 0%, 50% and higher values of RH with no intermediate values.

Research on the mechanical effects of humidity demonstrated little measureable damage to silk even with extreme fluctuations in the range of 30 to 60% RH.[207] The greatest changes were recorded in samples maintained at 85% RH for six months whereas the strongest sample was that held at 33% RH. Humidification treatments have been found to cause changes in breaking load and elongation of silk particularly for old fabrics.[208] These references all indicate the effect of humidity may be more important than previously considered. Pascoe has suggested that there is scope for detailed investigations to establish the various effects of light, dark, humidity and pH.[209]

Further it has been suggested that for silk deterioration, light may not be the only important parameter. Samples taken from the reverse of historic tapestries were described as “bright and unfaded” in colour due to the lack of light exposure. However, compared with the aged modern model materials the average molecular weight of the silk was still much lower. This indicates a mechanism separate to that causing fading of the dyes and implies humidity may be involved. Fractography of naturally aged historic silk fibres reports that a more complex

mechanism occurs than in laboratory heat or light exposure of modern silk.[210] This indicates that there are likely to be synergistic effects between different environmental ageing parameters.

When silk deteriorates it becomes extremely embrittled and friable (to the point of powdering) as well as discoloured. This makes silk deterioration particularly difficult to repair. Traditional stitching conservation methods are generally unsuccessful as the silk breaks on contact with the needle.[211] Alternatives include adhesives however often the whole object or silk region requires backing. Adhesive treatments often dramatically alter the drape and appearance of the silk as a result the author describes it as "not a long-term solution".[212] The difficulties in finding suitable interventive conservation treatments for silk deterioration mean a preventive conservation approach may offer greater longevity for silk objects. However in order to successfully slow the rate of silk deterioration a better understanding of the causes of deterioration is required.

France states that "the end of the useful life of a textile is usually related to the loss of mechanical properties associated with its function".[213] Comparison of the amino acid content of aged silk suggests that the ratio of neutral to acidic amino acids relates to the point at which degummed silk has suffered extensive light damage and is at risk from handling, with 3.38 or greater being the critical value.[214] These may provide measures of a textiles display lifetime and a method of comparing deterioration mechanisms. Although light has been shown to cause fading of dyes, its role in the embrittlement and deterioration of the substrate textile has not been determined. This research will focus on understanding the effect environmental factors common to open display, particularly humidity, have on the deterioration of degummed, undyed silk.

References

[1] Keyserlingk, M. (1990) 'The Use of Adhesives in Textile Conservation' *ICOM Committee for Conservation 9th Triennial Meeting Dresden, Germany, 26-31 August 1990 Preprints* Paris: ICOM Committee for Conservation **1** 307-312.

[2] Tímár-Balázsy, A. and Eastop, D. (1998) 'Adhesives and consolidants' *Chemical Principles of Textile Conservation* Oxford: Butterworth-Heinemann 304-331.

[3] Hansen, E. F. and Ginell, W. S. (1989) 'The Conservation of Silk with Parylene-C' *Historic Textile and Paper Materials II – Conservation and Characterization* Zeronian, S. H. and Needles, H. L. (ed.) ACS 410 Washington DC, USA: American Chemical Society 108-133.

[4] Hersh, S. P., Hutchins, J. K., Kerr, N. and Tucker, P.A. (1980) 'Prevailing Opinion in the U.S.A. on the Desirable Qualities of Fabric Consolidants' *Proceedings of International Conference on the Conservation and Restoration of Textiles, Milan, Italy* 96-103.

[5] Fikioris, M. (1981) 'Textile Conservation for Period Room Settings in Museums and Historic Houses' in *Preservation of Paper and Textiles of Historic and Artistic Value II* Williams, J. C. (ed.) Washington DC: American Chemical Society **193** 253-274.

[6] Bullock, L. (2005) 'Light as an Agent of Deterioration' *National Trust Manual of Housekeeping* Oxford: Butterworth-Heinemann 94.

[7] Egerton, G. S. (1948) 'Some Aspects of the Photochemical Degradation of Nylon, Silk, and Viscose Rayon' *Textile Research Journal* **18** 659-669.

[8] Giles, C. H. and McKay, R. B. (1963) 'The lightfastness of dyes: a review' *Textile Research Journal* **33** 527-577.

[9] Tímár-Balázsy, A. and Eastop, D. (1998) 'Fibres' *Chemical Principles of Textile Conservation* Oxford: Butterworth-Heinemann 3-66.

[10] Tucker, P., Kerr, N. and Hersh, S. P. (1980) 'Photochemical Damage of Textiles' *Textiles and Museum Lighting* (The Harpers Ferry Regional Textile Group) December 4 & 5 1980, The Anderson House Museum, National Headquarters of

the Society of the Cincinnati, 2118 Massachusetts Ave, NW Washington DC 20008, 23-40.

[11] Vigo, T. L. (1977) 'Preservation of Natural Textile Fibers – Historical Perspectives' in *Preservation of Paper and Textiles of Historic and Artistic Value* Williams, J. C. (ed.) Washington DC: American Chemical Society **164** 189-207.

[12] Becker, M. and Tuross, N. (1992) 'Novel Approaches for Assessing the Preservation of Historic Silks: A Case Study of the First Ladies' Gowns' *Materials Research Society Bulletin* **17** 39-44.

[13] Trotman, S. R. (1936) 'The Determination of Damage in Silk' *Journal of the Society of Chemical Industry (Transactions)* **55** 325T-327T.

[14] Hansen, E. F. and Sobel, H., (1994), 'Effect of the Environment on the Degradation of Silk: A Review', in *The Textile Specialty Group Postprints of Papers Delivered at the Textile Subgroup Session, American Institute for Conservation 20th Annual Meeting, Buffalo, New York, 1992*, Washington DC: American Institute for Conservation, 114-130.

[15] Schoeser, M. (2007) *Silk* New Haven, C.T.: Yale University Press 17

[16] Riboud, K. (1977) 'A Closer View of Early Chinese Silks' in *Studies in Textile History*, Veronika Gervers ed., Toronto: Royal Ontario Museum 252-280.

[17] Merritt, J. L. (1992) 'Silk: History, Cultivation and Processing' in *Silk: Harpers Ferry Regional Textile Group, 11th Symposium*, Washington DC: Harpers Ferry Regional Textile Group 1-3.

[18] Tazima, Y. (1984) 'Silkworm moths' *Evolution of Domesticated Animals* London: Longman 416-424.

[19] Khan, M. M. R., Gotoh, Y., Miura, M., Morikawa, H. and Nagura, M. (2006) 'Influence of an Iodine Treatment on the Structure and Physical Properties of *Bombyx mori* Silk Fibroin Fiber' *Journal of Polymer Science: Part B: Polymer Physics* **44** 3418-3426.

[20] Minoura, N., Tsukada, M. and Nagura, M. (1990) 'Physico-chemical properties of silk fibroin membrane as a biomaterial' *Biomaterials* **11 (6)** 430-434.

[21] Preghenella, M., Pezzotti, G. and Migliaresi, C. (2007) 'Comparative Raman spectroscopic analysis of orientation in fibers and regenerated films of *Bombyx mori* silk fibroin' *Journal of Raman Spectroscopy* **38 (5)** 522-536.

[22] Matsumoto, A., Kim, H. J., Tsai, I. Y., Wang, X., Cebe, P. and Kaplan, D. L. (2007) 'Silk' *Handbook of Fiber Chemistry 3rd Edition* Lewin, M. (ed.) London: Taylor and Francis 383-405.

[23] Wolfgang, W. G. (1970) 'Silk' *Encyclopedia of Polymer Science and Technology* Mark, H. and Gaylord, N. (ed.) **12** New York: John Wiley & Sons, Inc, 578-585.

[24] Robson, R. M. (1998) 'SILK Composition, Structure, and Properties', in, *Handbook of Fiber Chemistry*, International Fiber Science and Technology Series /15 Second Edition Lewin, M. and Pearce, E. M. (ed.) New York: Marcel Dekker 415 – 463.

[25] Bergmann, W. (1940) 'Relations Between the Food and Silk of Silkworms' *Textile Research* **10** 462-475.

[26] Jirousek, C. A. (1998) 'The End of the Silk Road: Implications of the Decline of Turkish Sericulture' *Textile History* **29 (2)** 201-225.

[27] Manisankar, G., Ujjal, M. and Aniruddha, M. (2008) 'Effect Of Environmental Factors (Temperature and Humidity) on Spinning Worms of Silkworm (*Bombyx mori* L.)' *Research Journal of Chemistry and Environment* **12 (4)** 12-18.

[28] Balasundaram, D., Selvisabhanayakam, and Mathivanan, V. (2009) 'Studies on Comparative Feed Efficacy of MR2 Variety Mulberry Leaves and MR2 Treated with Vitamin B-6 on *Bombyx mori* (L.) in Relation to Cocoon Weight and Silk Traits' *Journal of Experimental Zoology India* **12 (1)** 187-190.

[29] Zahn, H. and Krasowski, A. (2005) 'Silk' In *Ullmann's Encyclopedia of Industrial Chemistry* Weinheim: Wiley-VCH GmbH & Co. 1-14.

[30] Bergmann, W. (1939) 'Facts and Theories Concerning the Formation of Natural Silk' *Textile Research* **9** 329-342.

[31] Mercer, E. H. (1954) 'Studies on the Soluble Proteins of the Silk Gland of the Silkworm, *Bombyx mori*' *Textile Research Journal* **24** 135-145.

[32] Lucas, F., Shaw, J. T. B. and Smith, S. G. (1958) 'The Silk Fibroins' *Advances in Protein Chemistry* **13** 107-242.
[33] Magoshi, J., Magoshi, Y. and Nakamura, S. (1985) 'Physical properties and structure of silk: 10. The mechanism of fibre formation from liquid silk of silkworm *Bombyx mori*' *Polymer Communications* **26** 309-311.
[34] Magoshi, J., Mizuide, M., Magoshi, Y., Takahashi, K., Kubo, M. and Nakamura, S. (1979) 'Physical Properties and Structure of Silk. VI. Conformational Changes in Silk Fibroin Induced by Immersion in Water at 2 to 130°C' *Journal of Polymer Science: Polymer Physics Edition* **17** 515-520.
[35] Magoshi, J., Magoshi, Y. and Nakamura, S. (1981) 'Physical Properties and Structure of Silk. VII. Crystallization of Amorphous Silk Fibroin Induced by Immersion in Methanol' *Journal of Polymer Science: Polymer Physics Edition* **19** 185-186.
[36] Fraser, R. D. B., MacRae, T. P. (1973) *Conformation in Fibrous Proteins* New York and London: Academic Press.
[37] Willcox, P. J., Gido, S. P., Muller, W. and Kaplan, D. L. (1996) 'Evidence of a Cholesteric Liquid Crystalline Phase in Natural Silk Spinning Processes' *Macromolecules* **29** 5106-5110.
[38] Lotz, B., Gonthier-Vassal, A., Brack, A. and Magoshi, J. (1982) 'Twisted Single Crystals of *Bombyx mori* Silk Fibroin and Related Model Polypeptides with β-Structure – A Correlation with the Twist of the Beta-Sheets in Globular Proteins' *Journal of Molecular Biology* **156** 345-357.
[39] Wong Po Foo, C., Bini, E., Hensman, J., Knight, D. P., Lewis, R. V. and Kaplan, D. L. (2006) 'Role of pH and charge on silk protein assembly in insects and spiders' *Applied Physics A Materials Science & Processing* **82** 223-233.
[40] Magoshi, J., Magoshi, Y. and Nakamura, S. (1985) 'Crystallization, Liquid Crystal, and Fiber Formation of Silk Fibroin' *Journal of Applied Polymer Science: Applied Polymer Symposium* **41** 187-204.

[41] Iizuka, E. (1985) 'Silk Thread – Mechanism of Spinning and its Mechanical Properties' *Journal of Applied Polymer Science: Applied Polymer Symposium.* **41** 173-185.

[42] Hossain, K. S., Ochi, A., Ooyama, E., Magoshi, J. and Nemoto, N. (2003) 'Dynamic Light Scattering of Native Silk Fibroin Solution Extracted from Different Parts of the Middle Division of the Silk Gland of the *Bombyx mori* Silkworm' *Biomacromolecules* **4** 350-359.

[43] Zong, X.-H., Zhou, P., Shao, Z.-Z., Chen, S.-M., Chen, X., Hu, B.-W., Deng, F. and Yao, W.-H. (2004) 'Effect of pH and Copper (II) on the Conformation Transitions of Silk Fibroin Based on EPR, NMR, and Raman Spectroscopy' *Biochemistry* **43** 11932-11941.

[44] Zhou, P., Xie, X., Knight, D. P., Zong, X.-H., Deng, F. and Yao, W.-H. (2004) 'Effects of pH and Calcium Ions on the Conformational Transitions in Silk Fibroin Using 2D Raman Correlation Spectroscopy and 13C Solid-State NMR' *Biochemistry* **43** 11302-11311.

[45] Zhou, L., Chen, X., Shao, Z., Huang, Y. and Knight, D. P. (2005) 'Effect of Metallic Ions on Silk Formation in the Mulberry Silkworm, *Bombyx mori*' *Journal of Physical Chemistry B.* **109** 16937-16945.

[46] Kafatos, F. C. and Williams, C. M. (1964) 'Enzymatic Mechanism for the Escape of Certain Moths from Their Cocoons' *Science* **146 (3643)** 538-540.

[47] Carboni, P. (1952) *Silk, Biology, Chemistry and Technology* Walter, K. (transl.) London: Chapman and Hall.

[48] Brooks, M. M., O'Connor, S. and McDonnell, J. G. (1996) 'The Application of Low-energy X-radiography in the Examination and Investigation of Degraded Historic Silk Textiles: Preliminary Report', *ICOM Committee for Conservation 11th Triennial Meeting Edinburgh, Scotland, 1-6 September 1996 Preprints* London: James and James (Science Publishers) **2** 670-679.

[49] Gulrajani, M. L., Sethi, S., Gupta, S. (1992), 'Some studies in degumming of silk with organic acids' *Journal of the Society of Dyers and Colourists* **108 (2)** 79-86.

[50] Mosher, H. H. (1932) 'Usual Degumming Methods Prove Harmful to Silk-Wool Unions' *Textile World* (Nov.) 86-87.

[51] Jiang, P., Liu, H., Wang, C., Wu, L., Huang, J. and Guo, C. (2006) 'Tensile behaviour and morphology of differently degummed silkworm (*Bombyx mori*) cocoon silk fibres' *Materials Letters* **60** 919-925.

[52] Yanagi, Y., Hu, W. and Hirabayashi, K. (1986) 'Warp breaking of old silk fabrics made in the Edo period' *Kobunkazai no kagaku* **31** 51-54.

[53] Ballard, M., Koestler, R. J. and Indicator, N. (1986) 'Weighted Silks Observed Using Energy Dispersive X-ray Spectrometry' *Scanning Electron Microscopy* **2** 499-506.

[54] Ballard, M. W., Koestler, R. J. and Indicator, N. (1990) ' Recent results concerning the degradation of historic silk flags' *ICOM Committee for Conservation 9th Triennial Meeting Dresden, Germany, 26-31 August 1990 Preprints* Paris: ICOM Committee for Conservation 277-282.

[55] Sykes, P. (1984) *Textile Conservation Group Newsletter*, 10 May 1984, **6 (5).**

[56] Hacke, M. (2008) 'Weighted silk: history, analysis and conservation' *Reviews in Conservation* **9** 3-15.

[57] Carr, C. M. (2006) 'Monitoring of Damage to Historic Tapestries (MODHT) EVK4-2001-00048 Final Report'.

[58] Sen, K., Babu K, M. (2004) 'Studies on Indian Silk. III. Effect of Structure on Dyeing Behavior' *Journal of Applied Polymer Science* **92(2)** 1116-1123.

[59] Durasevic, V., Machnowski, W. and Kotlinska, A. (2008) 'Dyeing Behaviour of Differently Degummed Silk Fibers' *4th International Textile Clothing and Design Conference Book of Proceedings 5-8th October 2008 Dubrovnik, Croatia* Dragcevic, Z. (ed.) 341-346.

[60] Scott, W. M. (1931) 'The Weighting of Silk I-IV' *American Dyestuff Reporter* **20** 517-518, 539-540, 543, 557-562, 591-594, 621-622.

[61] Scott, W. M. (1934) 'Recent Developments in the Chemistry of Silk and of Silk Processing I-V' *American Dyestuff Reporter* **23** 217-221, 253-254, 283-284, 330-332, 339-340, 363-364.

[62] Scott, W. M. (1935) 'Developments During 1934 in the Chemistry of Silk and Silk Processing' *American Dyestuff Reporter* **24** 443-450.

[63] Miller, J. E. and Reagan, B. M. (1989) 'Degradation in Weighted and Unweighted Historic Silks', *Journal of the American Institute of Conservation* **28** 97-115.

[64] Ross, J. E., Johnson, R. L. and Edgar, R. (1936) 'Degradation of Weighted Silk Fibroin by Acid and Alkali' *Textile Research Journal* **6** 207-216.

[65] Garside, P. and Wyeth, P. (2002) 'Characterization of silk deterioration' *Strengthening the Bond: Science and Textiles. Preprints of the North American Textile Conservation Conference April 2002* Whelan, V.J. (ed.) Philadelphia, PA: North American Textile Conservation Conference 55-60.

[66] Robson, R. M. (1999) 'Microvoids in *Bombyx mori* silk. An electron microscope study' *International Journal of Biological Macromolecules* **24** 145-150.

[67] Kawahara, Y. (1993) 'Analysis of the void structure of silk fibers by tin weighting' *Sen'i Gakkaishi* **49 (12)** 621-627.

[68] Lower, E. S. (1988) 'Silk: its Properties and Main End-Uses' *Textile Month* August 1988 9-14.

[69] Liu, J., Shao, J. and Zheng, J. (2004) 'Radiation Grafting/Crosslinking of Silk Using Electron-Beam Irradiation' *Journal of Applied Polymer Science* **91** 2028-2034.

[70] Yang, Y. and Li, S. (1993) 'Silk Fabric Non-formaldehyde Crease-resistant Finishing Using Citric Acid' *Journal of the Textile Institute* **84 (4)** 638-644.

[71] Leksophee, T., Supansomboon, S. and Sombatsompop, N. (2004) 'Effects of Crosslinking Agents, Dyeing Temperature, and pH on Mechanical Performance and Whiteness of Silk Fabric' *Journal of Applied Polymer Science* **91** 1000-1007.

[72] Cai, Z., Jiang, G. and Yang, S. (2001) 'Chemical finishing of silk fabric' *Coloration Technology* **117** 161-165.

[73] Cai, Z. and Qiu, Y. (2003) 'Using an Aqueous Epoxide in Bombyx mori Silk Fabric Finishing' *Textile Research Journal* **73(1)** 42-46.

[74] Cai, Z., Jiang, G. and Qiu, Y. (2004) 'Chemical Modification of Bombyx Mori Silk with Epoxide EPSIB' *Journal of Applied Polymer Science* **91** 3579-3586.

[75] Guan, J. P. and Chen, G. Q. (2008) 'Flame resistant modification of silk fabric with vinyl phosphate' *Fibers and Polymers* **9 (4)** 438-443.

[76] Garside, P. and Wyeth, P., (2006) 'Textiles' in *Conservation Science Heritage Materials*, Cambridge: The Royal Society for Chemistry, 56-91.

[77] Schroeder, W. A. and Kay, L. M. (1955) 'The Amino Acid Composition of *Bombyx mori* Silk Fibroin and of Tussah Silk Fibroin' *Journal of the American Chemical Society* **77** 3908-3913.

[78] Lucas, F., Shaw, J. T. B. and Smith, S. G. (1960) 'Comparative Studies of Fibroins I The Amino Acid Composition of Various Fibroins and its Significance in Relation to their Crystal Structure and Taxonomy' *Journal of Molecular Biology* **2** 339-349.

[79] Yanagi, Y., Kondo, Y. and Hirabayashi, K. (2000) 'Deterioration of Silk Fabrics and Their Crystallinity' *Textile Research Journal* **70 (10)** 871-875.

[80] Lucas, F. and Rudall, K. M. (1968) 'Extracellular Fibrous Proteins: The Silks' in *Comprehensive Biochemistry* Florkin, M. and Stotz, H. (ed.) **26B** Amsterdam: Elsevier Publishing 475-558.

[81] Otterburn, M. S. (1977) 'The Chemistry and Reactivity of Silk' in *The Chemistry of Natural Fibres* Asquith, R.S. (ed.), New York: John Wiley and Sons, Inc., 53-80.

[82] Zuber, H., Ziegler, K. and Zahn, H. (1957) *Zeitschrift für Naturforschung* **126** 734.

[83] Lucas, F. (1966) 'Cystine Content of Silk Fibroin (*Bombyx mori*)' *Nature* **210 (5039)** 952-953.

[84] Earland, C. and Robins, S. P. (1973) 'A Study of the Cystine Residues in Bombyx mori and Other Silks' *International Journal of Peptide and Protein Research* **5** 327-335.

[85] Robson, A., Woodhouse, J. M. and Zaidi, Z. H. (1970) 'Cystine in Silk Fibroin, Bombyx mori' *International Journal of Protein Research* **2** 181-189.

[86] Gamo, T., Inokuchi, T. and Laufer, H. (1977) 'Polypeptides of Fibroin and Sericin Secreted from the Different Sections of the Silk Gland in *Bombyx mori*' *Insect Biochemistry* **7** 285-295.

[87] Teramoto, H. and Miyazawa, M. (2005) 'Molecular Orientation Behaviour of Silk Sericin Film as Revealed by ATR Infrared Spectroscopy' *Biomacromolecules* **6** 2049-2057.
[88] Sinohara, H. and Asano, Y. (1967) 'Carbohydrate Content of Fibroin and Sericin of the Silkworm, *Bombyx mori*' *The Journal of Biochemistry* **62(1)** 129-130.
[89] Lucas, F., Shaw, J. T. B. and Smith, S. G., (1957) 'The Amino Acid Sequence in a Fraction of the Fibroin of *Bombyx mori*' *Biochemical Journal* **66** 468-479.
[90] Shaw, J. T. B. and Smith, S. G. (1961) 'Comparative Studies of Fibroins IV The Composition and Structure of Chemically Resistant Fractions from Some Silk Fibroins' *Biochimica et Biophysica Acta* **52** 305-318.
[91] Stewart, F. H. C. (1966) 'Poly-L-Alanylglycyl-L-Alanylglycyl-L-Serylglycine: A Synthetic Model of *Bombyx mori* Silk Fibroin' *Australian Journal of Chemistry* **19** 489-501.
[92] Taddei, P., Asakura, T., Yao, J. and Monti, P. (2004) 'Raman Study of Poly(Alanine-Glycine)-Based Peptides Containing Tyrosine, Valine, and Serine as Model for the Semicrystalline Domains of *Bombyx mori* Silk Fibroin' *Biopolymers* **75** 314-324.
[93] Gage, L. P. and Manning, R. F. (1980) 'Internal Structure of the Silk Fibroin Gene of *Bombyx mori*' *The Journal of Biological Chemistry* **255 (19)** 9444-9450.
[94] Couble, P., Chevillard, M., Moine, A., Ravel-Chapuis, P. and Prudhomme, J.-C. (1985) 'Structural Organization of the P_{25} gene of *Bombyx mori* and Comparative analysis of it 5' flanking DNA with that of the Fibroin Gene' *Nucleic Acids Research* **13 (5)** 1801-1814.
[95] Chevillard, M., Couble, P. and Prudhomme, J.-C. (1986) 'Complete Nucleotide Sequence of the Gene Encoding the *Bombyx mori* Silk protein P25 and Predicted Amino Acid Sequence of the Protein' *Nucleic Acids Research* **14 (15)** 6341-6342.
[96] The International Silkworm Genome Consortium (2008) 'The genome of a lepidopteran model insect, the silkworm *Bombyx mori*' *Insect Biochemistry and Molecular Biology* **38** 1036-1045.

[97] Zhou, C. Z., Confalonieri, F., Medina, N., Zivanovic, Y., Esnault, C., Yang, T., Jacquet, M., Janin, J., Duguet, M., Perasso, R., Li, Z.-G. (2000) 'Fine organization of *Bombyx mori* fibroin heavy chain' *Nucleic Acids Research* **28** 2413-2419.

[98] Ha, S.-W., Gracz, H. S., Tonelli, A. E. and Hudson, S. M. (2005) 'Structural Study of Irregular Amino Acid Sequences in the Heavy Chain of *Bombyx mori* Silk Fibroin' *Biomacromolecules* **6** 2563-2569.

[99] Shaw, J. T. B. (1964) 'Fractionation of the Fibroin of *Bombyx mori* with Trypsin' *Biochemical Journal* **93** 45–54.

[100] Shaw, J. T. B. (1964) 'Fractionation of the Fibroin of *Bombyx mori* with Alkali' *Biochemical Journal* **93** 54-61.

[101] Holmes, F. H. and Smith, S. I. (1952) 'Sedimentation and Diffusion of Soluble Fibroin' *Nature* **169 (4292)** 193.

[102] Howitt, F. O. (1955) 'Silk Fibroin as a Fibrous Protein' *Textile Research Journal* **25** 242-246.

[103] Sprague, K. (1975) 'The *Bombyx mori* Silk Proteins: Characterization of Large Polypeptides' *Biochemistry* **14 (5)** 925-931.

[104] Iida, H. (1972) *Sen-i Kako*, **24** 165, 267.

[105] Tashiro, Y., Otsuki, E. and Shimadzu, T. (1972) 'Sedimentation Analyses of Native Silk Fibroin in Urea and Guanidine·HCl' *Biochimica et Biophysica Acta* **257** 198-209.

[106] Zuber, H., (1961), *Kolloid-Zeitschrift* **179** 100.

[107] Sasaki, T. and Noda, H. (1973) 'Studies on Silk Fibroin of *Bombyx mori* Directly Extracted from the Silk Gland I. Molecular Weight Determination in Guanidine Hydrochloride or Urea Solutions' *Biochimica et Biophysica Acta* **310** 76-90.

[108] Sasaki, T. and Noda, H. (1973) 'Studies on Silk Fibroin of *Bombyx mori* Directly Extracted from the Silk Gland II. Effect of Reduction of Disulfide Bonds and Subunit Structure' *Biochimica et Biophysica Acta* **310** 91-103.

[109] Yamaguchi, K., Kikuchi, Y., Takagi, T., Kikuchi, A., Oyama, F., Shimura, K. and Mizuno, S. (1989) 'Primary Structure of the Silk Fibroin Light Chain Determined by

cDNA Sequencing and Peptide Analysis' *Journal of Molecular Biology* **210** 127-139.

[110] Tanaka, K., Mori, K. and Mizuno, S. (1993) 'Immunological Identification of the Major Disulfide-Linked Light Component of Silk Fibroin' *Journal of Biochemistry* **114** 1-4.

[111] Zhou, C.-Z., Confalonieri, F., Jacquet, M., Perasso, R., Li, Z.-G., Janin, J. (2001) 'Silk Fibroin: Structural Implications of a Remarkable Amino Acid Sequence' *Proteins: Structure, Function, and Genetics* **44** 119-122.

[112] Takei, F., Kikuchi, Y., Kikuchi, A., Mizuno, S. and Shimura, K. (1987) 'Further Evidence for Importance of the Subunit Combination of Silk Fibroin in Its Efficient Secretion from the Posterior Silk Gland Cells' *The Journal of Cell Biology* **105** 175-180.

[113] Tanaka, K., Kajiyama, N., Ishikura, K., Waga, S., Kikuchi, A., Ohtomo, K., Takagi, T. and Mizuno, S. (1999) 'Determination of the site of disulfide linkage between heavy and light chains of silk fibroin produced by *Bombyx mori*' *Biochimica et Biophysica Acta* **1432** 92-103.

[114] Tanaka, K., Inoue, S. and Mizuno, S. (1999) 'Hydrophobic interactions of P25, containing Asn-linked oligosaccharide chains, with the H-L complex of silk fibroin produced by *Bombyx mori*' *Insect Biochemistry and Molecular Biology* **29** 269-276.

[115] Inoue, S., Tanaka, K., Arisaka, F., Kimura, S., Ohtomo, K. and Mizuno, S. (2000) 'Silk Fibroin of *Bombyx mori* Is Secreted, Assembling a High Molecular Mass Elementary Unit Consisting of H-chain, L-chain, and P25, with a 6:6:1 Molar Ratio' *Journal of Biological Chemistry* **275 (51)** 40517-40528.

[116] Drummy, L. F., Farmer, B. L. and Naik, R. R. (2007) 'Correlation of the β-sheet crystal size in silk fibers with the protein amino acid sequence' *Soft Matter* **3** 877-882.

[117] Yonemura, N. and Sehnal, F. (2006) 'The Design of Silk Fiber Composition in Moths Has Been Conserved for More Than 150 Million Years' *Journal of Molecular Evolution* **63** 42-53.

[118] Grieff, S., Kutzke, H., Riekel, C., Wyeth, P. and Lahlil, S., (2005) 'Surveying silk fibre degradation by crystallinity determination: a study on the Tang dynasty silk treasure from Famen Temple, China', in *AHRC Research Centre for Textile Conservation and Textile Studies First Annual Conference –Scientific Analysis of Ancient and Historic Textiles Postprints* Janaway, R. and Wyeth, P. (ed.) London: Archetype 38–43.

[119] Meyer, K. H. and Mark, H. (1928) *Chemische Berichte* **61** 1932.

[120] Schnabel, E. and Zahn, H. (1958) *Annalen der Chemie* **614** 141.

[121] Schnabel, E. (1958) *Annalen der Chemie* **615** 173.

[122] Marsh, R. E., Corey, R. B. and Pauling, L. (1955) 'An Investigation of the Structure of Silk Fibroin' *Biochimicia et Biophysica Acta* **16** 1-34.

[123] Marsh, R. E., Corey, R. B. and Pauling, L. (1955) 'The Crystal Structure of Silk Fibroin' *Acta Crystallographica* **8** 62.

[124] Warwicker, J. O. (1954) 'The Crystal Structure of Silk Fibroin' *Acta Crystallographica* **7** 565-573.

[125] Crick, F. H. C. and Kendrew, J. C. (1957) 'X-ray Analysis and Protein Structure' *Advances in Protein Chemistry* **12** 133-214.

[126] Takahashi, Y., Gehoh, M. and Yuzuriha, K. (1991) 'Crystal Structure of Silk (*Bombyx mori*)' *Journal of Polymer Science: Part B: Polymer Physics* **29** 889-891.

[127] Takahashi, Y., Gehoh, M. and Yuzuriha, K. (1999) 'Structure Refinement and Diffuse Streak Scattering of Silk (*Bombyx mori*)' *International Journal of Biological Macromolecules* **24** 127-138.

[128] Asakura, T., Nakazawa, Y., Ohnishi, E. and Moro, F. (2005) 'Evidence from ^{13}C solid-state NMR spectroscopy for a lamella structure in an alanine-glycine copolypeptide: A model for the crystalline domain of *Bombyx mori* silk fiber' *Protein Science* **14** 2654-2657.

[129] Asakura, T., Okonogi, M., Nakazawa, Y. and Yamauchi, K. (2006) 'Structural Analysis of Alanine Tripeptide with Antiparallel and Parallel β-Sheet Structures in Relation to the Analysis of Mixed β-Sheet Structures in *Samia cynthia ricini* Silk

Protein Fiber Using Solid State NMR Spectroscopy' *Journal of the American Chemical Society* **128** 6231-6238.

[130] Lefèvre, T., Rousseau, M.-E. and Pézolet, M. (2007) 'Protein Secondary Structure and Orientation in Silk as Revealed by Raman Spectromicroscopy' *Biophysical Journal* **92** 2885-2895.

[131] Warwicker, J. O. (1956) 'The Crystal Structure of Silk Fibroins' *Transactions of the Faraday Society* **52** 554-557.

[132] Warwicker J. O. (1960) 'Comparative Studies of Fibroins II. The Crystal Structures of Various Fibroins' *Journal of Molecular Biology* **2** 350-362.

[133] Marsh, R. E., Corey, R. B. and Pauling, L. (1955) 'The Structure of Tussah Silk Fibroin' *Acta Crystallographica* **8** 710-715.

[134] Sen, K., Babu K, M. (2004) 'Studies on Indian Silk. I. Macrocharacterization and Analysis of Amino Acid Composition' *Journal of Applied Polymer Science* **92(2)** 1080-1097.

[135] Hakimi, O., Knight, D. P., Knight, M. M., Grahn, M. F. and Vadgama, P. (2006) 'Ultrastructure of Insect and Spider Cocoon Silks' *Bimacromolecules* **7** 2901-2908.

[136] Miller, L. D., Putthanarat, S., Eby, R. K. and Adams, W. W. (1999) 'Investigation of the nanofibrillar morphology in silk fibers by small angle X-ray scattering and atomic force microscopy' *International Journal of Biological Macromolecules* **24** 159-165.

[137] Putthanarat, S., Stribeck, N., Fossey, S. A., Eby, R. K. and Adams, W. W. (2000) 'Investigation of the nanofibrils of silk fibers' *Polymer* **41** 7735-7747.

[138] Odlyha, M., Wang, Q., Foster, G. M., de Groot, J., Horton, M. and Bozec, L., (2005) 'Monitoring of damage to historic tapestries: the application of dynamic mechanical thermal analysis to model and historic tapestries', in *AHRC Research Centre for Textile Conservation and Textile Studies First Annual Conference – Scientific Analysis of Ancient and Historic Textiles Postprints* Janaway, R. and Wyeth, P. (ed.) London: Archetype 126–134.

[139] Odlyha, M., Wang, Q., Foster, G. M., de Groot, J., Horton, M. and Bozec, L. (2005) 'Thermal analysis of Model and Historic Tapestries' *Journal of Thermal Analysis and Calorimetry* **82** 627-636.

[140] Inoue, S.-I., Magoshi, J., Tanaka, T., Magoshi, Y. and Becker, M. (2000) 'Atomic Force Microscopy: *Bombyx mori* Silk Fibroin Molecules and Their Higher Order Structure' *Journal of Polymer Science Part B: Polymer Physics* **38 (11)** 1436-1439.

[141] Kratky, O. (1956) 'An X-ray Investigation of Silk Fibroin' *Transactions of the Faraday Society* **52** 558-570.

[142] Li, G., Zhou, P., Shao, Z., Xie, X., Chen, X., Wang, H., Chunyu, L. and Yu, T. (2001) 'The Natural Silk Spinning Process – A Nucleation-Dependent Aggregation Mechanism?' *European Journal of Biochemistry* **268** 6600-6606.

[143] Anon. (1985) *Identification of Textile Materials* 7th Edition Manchester: The Textile Institute 12-13.

[144] Cowie, J. M. G. (1997) 'The Amorphous State' *Polymers: Chemistry and Physics of Modern Materials 2nd Edition* London: Chapman and Hall 247-273.

[145] Magoshi, J. and Nakamura, S. (1975) 'Studies on Physical Properties and Structure of Silk. Glass Transition and Crystallization of Silk Fibroin' *Journal of Applied Polymer Science* **19** 1013-1015.

[146] Magoshi, J., Magoshi, Y. and Nakamura, S. (1977) 'Physical Properties and Structure of Silk. III. The Glass Transition and Conformational Changes of Tussah Silk Fibroin' *Journal of Applied Polymer Science* **21** 2405-2407.

[147] Nakamura, S., Saegusa, Y., Yamaguchi, Y., Magoshi, J. and Kamiyama, S. (1986) 'Physical Properties and Structures of Silk. XI. Glass Transition Temperature of Wild Silk Fibroins' *Journal of Applied Polymer Science* **31** 955-956.

[148] Zhang, H., Magoshi, J., Becker, M., Chen, J. Y. and Matsunaga, R. (2002) 'Thermal Properties of *Bombyx mori* Silk Fibers' *Journal Applied Polymer Science* **86 (8)** 1817-1820.

[149] Meredith, R. (1945) 'The Tensile Behaviour of Raw Cotton and Other Textile Fibres' *Journal of the Textile Institute* **36** T107-T123.

[150] Sen, K., Babu K, M. (2004) 'Studies on Indian Silk. II. Structure-Property Correlations' *Journal of Applied Polymer Science* **92(2)** 1098-1115.

[151] Zhao, H.-P., Feng, X.-Q., Yu, S.-W., Cui, W.-Z. and Zou, F.-Z. (2005) 'Mechanical Properties of Silkworm Cocoons' *Polymer* **46** 9192-9201.

[152] Cheung, H.-Y., Lau, K.-T., Zhao, Y.-Q. and Lu, J. (2008) 'Tensile Properties of Different Silkworm Silk Fibers' *Advanced Materials Research* **47-50** 1213-1216.

[153] Das, S. (2008) 'Structure, Property, and Relaxation Behaviour of Mulberry (*Bombyx mori*) and Tasar (*Antheraea Mylita*) Silk' *Journal of Natural Fibers* **5 (3)** 218-226.

[154] Ghosh, A. and Das, S. (2008) 'Tensile and Twist Failure of Mulberry and Tasar Silk' *Journal of the Textile Institute* **99 (2)** 165-168.

[155] Seydel, T., Kölln, K., Krasnov, I., Diddens, I., Hauptmann, N., Helms, G., Ogurreck, M., Kang, S.-G. Koza, M. M. and Müller, M. (2007) 'Silkworm Silk under Tensile Strain Investigated by Synchrotron X-ray Diffraction and Neutron Spectroscopy' *Macromolecules* **40** 1035-1042.

[156] Sirichaisit, J., Brookes, V. L., Young, R. J. and Vollrath, F. (2003) 'Analysis of Structure/Property Relationships in Silkworm (*Bombyx mori*) and Spider Dragline (*Nephila edulis*) Silks Using Raman Spectroscopy' *Biomacromolecules* **4** 387-394.

[157] Krasnov, I., Diddens, I., Hauptmann, N., Helms, G., Ogurreck, M., Seydel, T., Funari, S. S. and Müller, M. (2008) 'Mechanical Properties of Silk: Interplay of Deformation on Macroscopic and Molecular Length Scales' *Physical Review Letters* **100 (4)** 048104-1-048104-4.

[158] Beste, L. F. and Hoffman, R. M. (1950) 'A qualitative study of resilience' *Textile Research Journal*, **20 (7)** 441-453.

[159] Denny, M. W. (1980) 'Silks – their Properties and Functions', in *The Mechanical Properties of Biological Materials* (*Symposia of the Society for Experimental Biology*) **34** Vincent J. F. V. and Currey, D. J. (eds.) New York: Cambridge University Press 247-272.

[160] Crighton, J. S., (1993), 'Silk: a Study of its Degradation and Conservation' in *Conservation Science in the UK* Tennent, N. H. (ed.) 96-98.

[161] Warwicker, J. O. (1960) 'An X-ray Study of the Sorption of Water by the Silk Fibroin of *Bombyx mori*' *Journal of the Textile Institute* **57** T289-T292.

[162] McCaffrey, L. M. (1992) 'Some Theory behind Silk Degradation and Stabilization' in *Silk: Harpers Ferry Regional Textile Group, 11th Symposium*, Washington DC: Harpers Ferry Regional Textile Group 15-21.

[163] Sitch, D. A. and Smith, S. G. (1957) 'The Oxidation of Silk Fibroin by Hydrogen Peroxide and by Peracetic Acid' *Journal of the Textile Institute* **48** T341-T355.

[164] Earland, C. and Stell, J. G. P. (1957) 'The Reaction of Silk Fibroin with Oxidizing Agents' *Biochimica et Biophysica Acta* **23** 97-102.

[165] Earland, C., Stell, J. G. P. and Wiseman, A. (1960) 'The Oxidative Insolublization of Proteins' *Journal of the Textile Institute* **51** T817-T827.

[166] Earland, C. and Stell, J. G. P. (1966) 'Formation of New Crosslinkages in Proteins by Oxidation of the Tyrosine Residues with Potassium Nitrosyldisulphonate' *Polymer* **7** 549- 556

[167] Lucas, F., Shaw, J. T. B. and Smith S. G. (1955) 'The Chemical Constitution of Some Silk Fibroins and its Bearing on their Physical Properties' *Journal of the Textile Institute*, **46** T440-T452.

[168] Kerr, N. (1992) 'Understanding the Behaviour of Silk: Structure-Property Relationships' in *Silk: Harpers Ferry Regional Textile Group, 11th Symposium*, Washington DC: Harpers Ferry Regional Textile Group 5-9.

[169] Asquith, R. S., Otterburn, M. S. and Sinclair, W. J. (1974) 'Isopeptide Crosslinks – Their Occurrence and Importance in Protein Structure' *Angewandte Chemie International Edition* **13(8)** 514-520.

[170] French, D. and Edsall, J. T. (1945) 'The Reactions of Formaldehyde with Amino Acids and Proteins' *Advances in Protein Chemistry* **2** 277-335.

[171] Agarwal, D., Sen, K. and Gulrajani, M. L. (1996) 'Formation of crosslinks in silk by bifunctional reactive dyes: effect on solubility and mechanical properties' *Journal of the Society of Dyers and Colourists* **112** 321-325.

[172] Xiaojun, P. Jitao, W. and Jie, S. (1993) 'Silk finishing with Epoxides' *Journal of the Society of Dyers and Colourists* **109 (4)** 159-163.

[173] Kawahara, Y., Furuta, H., Shioya, M., Kikutani, T. and Takaku, A. (1994) 'Analysis of structure and swelling behavior of silk fibers treated with a mixture of glyoxal and urethane resins' *Sen'i Gakkaishi* **50 (11)** 505-509.

[174] Yumusak, C. and Alekberov, V. (2008) 'The Effects of Electrical Discharge on the Mechanical Properties of *Bombyx mori* Silk Fibroin' *Fibers and Polymers* **9 (1)** 15-20.

[175] Tsukada, M., Nagura, M., Ishikawa, H. and Shiozaki, H. (1991) 'Structural Characteristics of Silk Fibers Treated with Epoxides' *Journal of Applied Polymer Science* **43** 643-649.

[176] Turner, A. J. (1920) 'The Influence of Atmospheric Exposure on the Properties of Textiles' *Journal of the Society of Dyers and Colourists* **36** 165-173.

[177] Brill, T. B. (1980) *Light, Its Interaction with Art and Antiquities* New York: Plenum Press 187.

[178] Seeley, N. J. (1997) 'Textiles on Open Display: The Conservation Issues' In *Textiles in Trust* Marko, K. (ed.) London: Archetype 8-13.

[179] Hirabayashi, K., Takei, M. and Kondo, M. (1984) 'Deterioration mechanism of silk fabrics' *Kokogaku to shizen kagaku* **17** 61-72.

[180] Tsukada, M. and Hirabayashi, K. (1980) 'Change of Silk Fibroin Structure by Ultraviolet Radiation' *Journal of Polymer Science: Polymer Letters Edition* **18** 507-511.

[181] Korenberg, C. (2007) 'The effect of ultraviolet-filtered light on the mechanical strength of fabrics' *The British Museum Technical Research Bulletin* **1** 23-27.

[182] Tsuboi, Y., Ikejiri, T., Shiga, S., Yamada, K. and Itaya, A. (2001) 'Light can transform the secondary structure of silk protein' *Applied Physics A: Materials Science and Processing* **73** 637-640.

[183] Okamoto S. and Kikuchi M. (1958) 'The decomposition of silk fibroin by sunlight. V, On the discrystallization of the crystalline parts of silk by light' *Journal of Sericultural Science of Japan* **27** 367-373.

[184] Becker, M. A., Hersh, S. P. and Tucker, P. A. (1989) 'The Stabilization of Silk to Light and Heat' *Historic Textile and Paper Materials II – Conservation and*

Characterization Zeronian, S. H. and Needles, H. L. (ed.) Advances in Chemistry Series No. 410 Washington DC: American Chemical Society 94-107.
[185] Miller, J. E. (1986) 'A Comparative Analysis of Degradation in Naturally Aged and Experimentally Degraded Silk' PhD Dissertation (Kansas State University)
[186] Okamoto, S. and Kimura, T. (1953) *Journal of the Society of Textile and Cellulose Industry Japan.* **9** 284.
[187] Yoshida, Z. and Kato, M. (1955) *Journal of the Chemical Society of Japan.* **58** 274, 667.
[188] Becker, M. A., Willman, P. and Tuross, N. C. (1995) 'The U.S. First Ladies Gowns: A Biochemical Study of Silk Preservation' *Journal of the American Institute of Conservation* **34** 141-152.
[189] Nishi, H. (1979) 'The relations between yellowing of silk and aromatic amino acids' *Nippon snashi-gaku zasshi* **48** 164-170.
[190] Setoyama, K. (1982) 'Effect of water on the heat yellowing of silk fabrics and the changes in amino acid composition in silk fibroin by heated sealed tubes' *Journal of Sericultural Science of Japan* **51** 365-369.
[191] Egerton, G. S. (1948) 'The Action of Light on Viscose Rayon, Silk and Nylon, Undyed and Dyed with Some Vat Dyes' *Journal of the Textile Institute* **39** T293-T304.
[192] Honda, H. (1979) 'Storage of silk fabrics in the environment without oxygen' *Sen-i Seihin Shohi kagaku* **20 (4)** 135-140.
[193] Bamford, C. H. and Dewar, M. J. S. (1949) 'Photosensitisation and Tendering by Vat Dyes' *Journal of the Society of Dyers and Colourists* **65** 674-681.
[194] Harris, M. (1934) 'The Photochemical Decomposition of Silk' *American Dyestuff Reporter Proceedings of the American Association of Textile Chemists and Colorists* **403-405** 215-217.
[195] Harris, M. and Jessup, D. A. (1934) 'The Effect of pH on the Photochemical Decomposition of Silk' *Bureau of Standards Journal of Research* **7** 1179-1184.

[196] D'Olier, A. A. and Mack, P. B. (1936) 'The Effect of Darkroom Storage on Unweighted and Tin Weighted Silk – Paper III' *Rayon and Melliand Textile Monthly* **17** 102.

[197] Roberts, N. M. and Mack, P. B. (1936) 'A Study of the Effects of Light and Air on Unweighted and Tin Weighted Silk – Paper II' *Rayon and Melliand Textile Monthly* 49-51.

[198] Ballard, M., Koestler, R. J., Blair, C. and Indicator, N. (1989) 'Historical Silk Flags Studied by Scanning Electron Microscopy – Energy Dispersive X-ray Spectrometry', in *Archaeological Chemistry IV*, Advances in Chemistry Series No 220 Washington DC: American Chemical Society 419-428.

[199] Ballard, M., Koestler, R. J., Blair, C. Santamaria, C. and Indicator N (1989) 'Historic Silk Flags from Harrisburg' in *Historic Textile and Paper Materials II, Conservation and Characterisation*, Developed from a Symposium by the Cellulose Paper and Textile Division at the 196th National Meeting of the American Chemical Society Washington DC: American Chemical Society 134-142.

[200] Yamazaki, M. (2003) 'Shattered Silk' MA Dissertation (Textile Conservation Centre).

[201] Szostak-Kotowa, J. (2004) 'Biodeterioration of textiles' *International Biodeterioration and Biodegradation* **53** 165-170.

[202] Ciferri, O., Becker, M. E. and de Rossi, E. (2003) 'Characterization of Bacteria Isolated from Naturally Aged Silk Fibroin' *Art, Biology, and Conservation: Biodeterioration of Works of Art The Metropolitan Museum of Art, New York* Koestler, R. J., Koestler, V. H., Charola, A. E. and Nieto-Fernandez, F. E. (ed.) New Haven: Yale University Press 191-207.

[203] Horan, R. L., Antle, K., Collette, A. L., Wang, Y., Huang, J., Moreau, J. E., Volloch, V., Kaplan, D. L. and Altman, G. H. (2005) 'In vitro degradation of silk fibroin' *Biomaterials* **26** 3385-3393.

[204] Rice, J. W. (1968) 'Principles of Textile Conservation Science No. IX How Humidity may affect Rug, Tapestry, and Other Textile Collections' *Textile Museum Journal* **2 (3)** 53-56.

[205] Hirabayashi, K. (1981) 'The deterioration and preservation of silk fabrics' *Kobunkazai no kagaku* **26** 24-34.

[206] Hu, W., Yanagi, Y., Arai, M., Hirabayashi, K. and Yoshitake, N. (1987) 'Effect of humidity on the degradation of silk' *Journal of Sericultural Science of Japan* **52 (2**) 127-130.

[207] Howell, D. (1996) 'Some Mechanical Effects of Inappropriate Humidity on Textiles' *ICOM Committee for Conservation 11th Triennial Meeting Edinburgh, Scotland, 1-6 September 1996 Preprints* London: James and James **2** 692-698.

[208] Stephens, M. (1997) 'The humidification of textiles : a literature review of the effects of moisture on textile fibres and an investigation of the effects of three humidification techniques on the tensile properties of naturally aged and new silk, wool and linen' Student report (PG Diploma in Textile Conservation) University of London, Textile Conservation Centre in affiliation with the Courtauld Institute of Art

[209] Pascoe, M. W. (1980) 'Science and Ethics in Textile Conservation' in *Proceedings of the International Conference on the Conservation and Restoration of Textiles, Milan, Italy* 104-106.

[210] Breese, R. R. and Goodyear, G. E. (1986) 'Fractography of Historic Silk Fibers' in *Historic Textile and Paper Materials Conservation and Characterization* Needles, H. L. and Zeronian, S. H. (ed.) American Chemical Series 212 Washington: American Chemical Society 95-109.

[211] Halvorson, B. G. and Kerr, N. (1994) 'Effect of Light on the Properties of Silk Fabrics Coated with Parylene-C' *Studies in Conservation* **39** 45-56.

[212] Palmer, A. (2006) ''A bomb in the collection': researching and exhibiting early 20th-century fashion' in *The Future of the 20th Century. Postprints of the AHRC Research Centre for Textile Conservation and Textile Studies Second Annual Conference July 2005* Rogerson, C. and Garside, P. (ed.) London: Archetype, 41-47.

[213] France F. G., (2005) 'Scientific Analysis in the identification of textile materials', in *AHRC Research Centre for Textile Conservation and Textile Studies First*

Annual Conference – Scientific Analysis of Ancient and Historic Textiles Postprints, Janaway, R. and Wyeth, P. (ed.) London: Archetype*,* 3–11.

[214] Becker, M. A., Magoshi, Y., Sakai, T. and Tuross, N. C., (1997), 'Chemical and Physical Properties of Old Silk Fabrics', *Studies in Conservation*, **42**, 27-37.

Chapter 2 –The English Heritage Silk Collection

For the research to be relevant to the collection of silk within English Heritage properties a number of questions had to be answered. Which properties contained silk artefacts and how many objects were there? What type of objects were they and what types of silk were used to make them? What was the condition of objects on display? What are the environmental display conditions currently and are improvements possible? In order to answer these questions object and environmental monitoring records were consulted as well as undertaking house surveys. This has identified the properties and environmental conditions which will be studied during the research.

English Heritage provides advice to the Government on the historic environment.[1] The work of English Heritage includes conserving and enhancing the historic environment, broadening public access to heritage and increasing people's understanding of the past.[2] As part of this remit English Heritage opens around 400 properties to the public. These vary from ruins to stately homes and include abbeys, castles, as well as underground tunnels. Of these properties over 130 contain collections. These include historic houses, archaeological museums and a large number of site displays.

The conservation of the collection is undertaken by the Collections Conservation team. The work of the Collections Conservation team includes training for site staff, defining realistic standards and management systems, supporting property presentation projects and research into preventive conservation.[3] Although there are similarities with museums, the open display of collections at English Heritage properties creates different challenges. As houses are presented 'as found' or 'as believed to have been', objects are not grouped by material or material specific environmental parameters. It is also rare within historic houses to use display

cases, unless the collection was historically displayed in this way, increasing the risk to the objects. For this reason a large proportion of the Collections Conservation team's research is characterising the risks and developing appropriate methods to reduce them. This often involves researching the collection *in situ* and looking at specific materials in more detail.

One of the methods used to characterise the risks in English Heritage properties has been the decennial National Collections Condition Audit.[4,5,6] The National Audit has identified areas within the English Heritage collection that require further research, one of these areas recently highlighted is textiles. One of the aims of this research is to provide greater understanding of the deterioration of silk and identify methods of mitigating the risks to silk within historic houses using improved preventive conservation measures. As mentioned in the previous chapter silk has been chosen as it is regarded as the most vulnerable material within textile collections.

To get an initial overview of the magnitude, complexity and locations of the English Heritage silk collection a search of the Historic Object Management System (HOMS) was undertaken. HOMS is the database containing information and object records for the collection within English Heritage. An initial search of the database using silk in the material field identified around 1000 records. This gave a starting point for looking at the English Heritage collection to determine the condition and variety of silk materials held. However this search is limited as it relies on silk being included in the material field for an object. For objects composed of a number of materials it is not uncommon for only the major material to be included, for example a chair made of wood, which has a silk upholstered pad, may only contain wood in the material field. This method also relies on all the objects being recorded on the database. When the search was undertaken records for a number of properties were still being entered into the system; therefore this was not necessarily the case. To overcome these limitations a number of site visits were undertaken.

From the records identified on HOMS as objects containing silk, it could be seen that the majority of the collection was in a small number of properties; Audley End House, Brodsworth Hall and Osborne House. Apsley House and Eltham Palace also contained a large number of silk objects. At Eltham Palace the silks are all reproductions dating from circa 1999 when the house was redisplayed. As the main focus of the research is historic silks, Eltham Palace was not selected for further study. The Wernher Collection at Ranger's House contained a small number of objects with silk but all provided important comparisons with the other houses, for example a number of tapestries on are on display at Ranger's House. In all, five properties were chosen for site visits, to study the collection further and identify objects containing silk. The aim was to include materials and objects that were representative of the collection, covering the range and depth whilst still being a manageable size. The selected properties were Apsley House, Audley End House, Brodsworth Hall, Osborne House and Ranger's House.

English Heritage Properties

Apsley House is situated at Hyde Park Corner in central London. The house was the home of the first Duke of Wellington and was given to the nation in 1947 by the seventh Duke of Wellington. Apsley House displays a number of paintings, some of which were originally in the Spanish Royal Collection. There is also a large silver collection including the Portuguese Service, a gift to the first Duke after his defeat of Napoleon. In addition, the collection has a series of silk Napoleonic standards which are embroidered with the Department in silver metal threads (see Figure 2.1).

Figure 2.1 – silk Napoleonic standard of the Garde Nationale [WM.1654V-1948] from Apsley House

Figure 2.2 – decorative back of address pouch from Osborne House (The Royal Collection copyright 2009 Her Majesty Queen Elizabeth II)

Audley End House in Essex has had numerous owners, including the Suffolk family. However, most of the current interiors date from the third Baron Braybrooke (1783-1858). The collection at Audley End House includes paintings, decorative arts, furniture and natural history. A number of tapestries have recently been redisplayed after 30 years in storage. These were conserved at the Textile Conservation Centre, along with a number of other objects from Audley End House. This has given access to detailed information on the condition and conservation of these objects. Other objects containing silk include curtains and upholstery as well as painted banners, fire screens and state beds.

Brodsworth Hall near Doncaster was built in 1860 for Charles Thellusson and occupied for 150 years by members of his family. When the last resident, Sylvia Grant-Dalton died in 1988 the house was taken over by English Heritage who preserved it as found. This included the peeling wallpaper in one of the bedrooms, the cluttered storage rooms and silverfish damage in the Morning Room. As well as silk upholstery and soft furnishings there are a number of rooms which are silk lined. These silks have suffered extensive light damage and are now extremely fragile. The silk collection at Brodsworth House also includes a number of items of

costume. Some of the collection from Brodsworth Hall is stored off site at Fulford, an English Heritage store.

Osborne House on the Isle of Wight was Queen Victoria's country residence. Rebuilt in the Italianate style, the house is opulently decorated. The collection includes sculpture, paintings as well as decorative arts and furniture, mostly belonging to the Royal Collection. There are numerous objects containing silk including many silk address pouches (see Figure 2.2) from the Durbar Room, costume, upholstery and reproduction silk wall linings. The Swiss Cottage has a number of boxes from the Indian and Colonial Exhibition of 1886 containing silk and cocoons. There are also a number of raw and dyed silk skeins on display in the Swiss Cottage Museum. These may provide a naturally aged, but less processed silk sample.

Ranger's House was built in 1723 and became the official residence of the Ranger of Greenwich Park in 1815. It currently houses the Wernher Collection. Diamond magnate, Sir Julius Wernher (1850-1912) collected a large number of medieval and Renaissance works of art which were displayed first at his London home, Bath House and later in his country home, Luton Hoo. Nearly 700 works of art are on display, including large numbers of ivories, bronzes, ceramics, enamels and paintings. There are four large tapestries and some smaller tapestries displayed in the gallery along with some fragments upstairs. There are also a number of silk velvet objects, including upholstery and a 14th century reliquary bag.

Environmental Conditions

Environmental data from each of the five properties has been collated and interpreted to further understand the display conditions. For each property the environmental conditions in the rooms containing the majority of the textile collections are presented in Appendix 1. This has helped assess the key factors that are likely to affect silk ageing and deterioration. The information can then be

used to determine which environmental conditions should be studied in more detail, through accelerated ageing experiments on silk, in order to identify the critical factors in silk deterioration.

Temperature and Humidity

All of the five properties selected have radio telemetry environmental monitoring systems. The majority of sensors record temperature and relative humidity (RH) conditions, although most properties also have some light sensors with a few combined light and UV sensors. When necessary this data can be supplemented by using stand alone data loggers. In all properties comparison is made with an external sensor. For historic houses this is particularly useful as the external conditions have a significant effect on the internal environment when control systems such as air conditioning are not used, commonly seen when monitoring as a reduced and delayed fluctuation inside after an external change. For example in Figure 2.3 the same trends can be seen during January 2008 between the external and internal conditions, although the temperature is higher and therefore the RH lower inside. The internal conditions are also flattened and respond more slowly to the external changes due to the buffering of the building and its contents. Of the properties studied only the Gallery at Apsley House has any form of air conditioning.

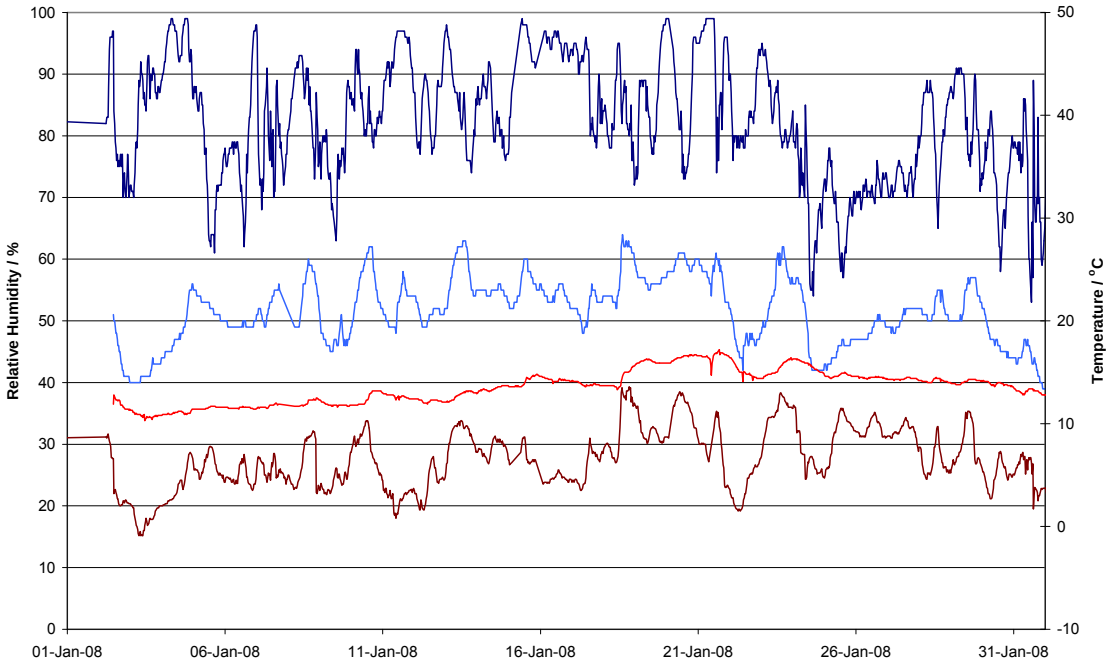

Figure 2.3 – comparison of external and internal conditions at Brodsworth Hall (external RH: dark blue; temp: dark red, internal RH: light blue; temp: red)

The different environmental conditions may affect the method by which the silk deteriorates as well as the rate. Therefore a good understanding of the display environment in each property along with how this might affect silk deterioration is required. This information will allow for improved preventive conservation measures by targeting the environmental conditions which may be detrimental but possible to improve.

Environmental data from each property from January 2005 to December 2008 was analysed using Climate Notebook® software, to determine broad trends. Climate Notebook® can import data from a wide number of environmental monitoring packages. This allows data collected using different software to be easily compared as well as providing a number of additional metrics for deterioration based on the environmental conditions. For each room limits can be set for the environmental parameters as well as selecting the materials in the room. The software allows a number of overviews of the data as well as comparisons

between rooms or groups of rooms. The effect of the environment on the materials specified can also be considered.

The software has been used to condense the data collected over four years from the large number of rooms in each property. This has then helped determine the average value, marked with a yellow spot in both Figures 2.4 and 2.5. As well as the regions within which the environment usually fluctuates (the large blocks contain 95% of the data) and the extreme values (the lines mark the minimum and maximum values). Figure 2.4 shows the temperature data and Figure 2.5 the RH data for each property.

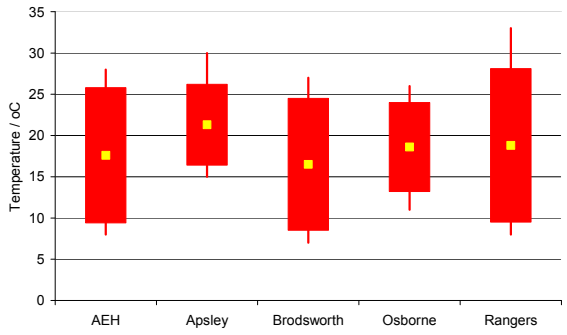

Figure 2.4 – temperature data for each property

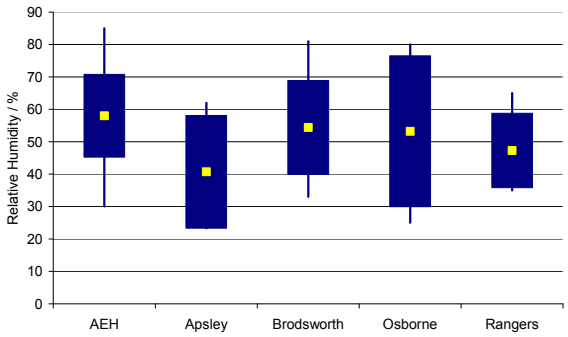

Figure 2.5 – relative humidity data for each property

The Climate Notebook® software uses in-built calculations to give metrics for the risk of chemical (Time Weighted Preservation Index abbreviated to TWPI), biological (Mould risk factor abbreviated to MRF) and physical (% maximum dimensional change abbreviated to % DC max) damage. These can be used to compare rooms and prioritise improvements or select the most suitable rooms to display certain collections in. Table 2.1 gives the averaged results for each metric for the selected properties. For example Osborne House is cold and damp in comparison with Apsley House, the lower temperatures give a higher TWPI than Apsley House, but the large RH variation gives a high %DC max. In Apsley House the higher temperatures mean a lower TWPI value but also give a higher MRF.

When used in combination with the materials section the metrics can help determine possible improvements for example, if there are no organic materials in a room a higher MRF is less of a concern. However, if objects at risk from dimensional change are present e.g. veneers, then the %DC should be lower.

property	**TWPI** (higher better)	**MRF** (lower better)	**%DC max** (lower better)
Apsley House	45.4	2.0	1.1
Audley End House	45.5	0.0	1.1
Brodsworth Hall	50.7	0.3	1.1
Osborne House	49.8	1.2	2.0
Ranger's House	50.3	0.2	0.9

Table 2.1 – summary of damage factors in the selected English Heritage properties

The conditions in Apsley House tend to be warmer and therefore drier throughout the year. This means overall a higher average temperature than the other properties and a lower average RH. The winter months are generally drier in most properties due to heating air with lower moisture content, a result of external conditions. However in Apsley House the winter average can be around 30%. The Gallery in Apsley House has silk lined walls as well as silk upholstered furniture, this room is also air conditioned. This raises the average RH in this room to over 40% during the dry winter months however it also introduces greater variation in the RH (18% compared with 14 - 15% variation in the other rooms on the first floor). This demonstrates the compromises required to control the environment; the average RH can be increased but so is the variation.

Temperatures are generally lower in the other properties, with larger variation. The average RH levels are correspondingly higher, although the RH variation is similar. Audley End House on average is slightly warmer and damper in comparison to Brodsworth Hall, although the reason for this is unclear. In most properties temperature is used to control the RH level – humidistat control. From the data for each property an average room temperature value of 20 °C has been selected for use in the later kinetics studies (see chapter six).

At Ranger's House the majority of the objects are exhibited within display cases. These offer very stable RH levels maintained by silica gel, while the temperature is allowed to vary. In comparison the rooms have a large seasonal variation in temperature, with very low temperatures in winter and very high temperatures in summer. Inside the rooms there are also large RH variations as the humidity is uncontrolled. This provides a sharp contrast with the controlled RH in the cases (see Figure 2.6) although as most objects are within the cases or relatively insensitive to environmental changes this is not problematic.

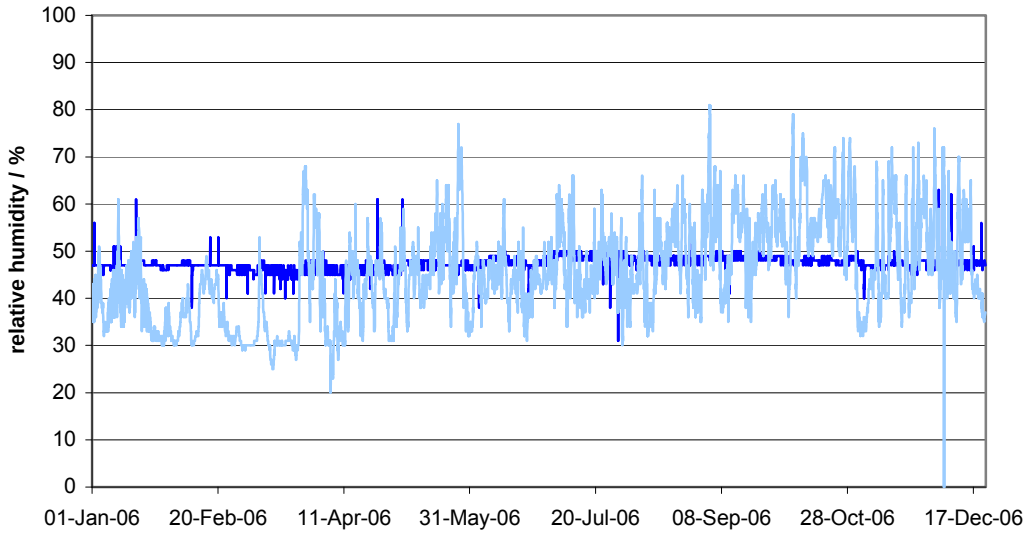

Figure 2.6 – comparison of the RH between the display cases (blue) and room at Ranger's House (light blue) (temperature has been excluded for clarity)

A sensor was placed behind a tapestry, on an outside wall, at Audley End House to study whether there was a difference compared to the room environment. Although there have been signal problems the initial studies demonstrate that the humidity is between 5 and 10% RH higher behind the tapestry (see Figure 2.7). However the temperature is similar in both locations, with slightly smaller fluctuations behind the tapestry. A comparison of the absolute humidity shows it is slightly higher (<0.5 gm^{-3}) behind the tapestry but does not decrease as much as

the room (between 1 and 2 gm^{-3} damper than the room). This may arise from the tapestry acting as a buffer and releasing moisture during drier spells, maintaining a damper microclimate behind the tapestry.

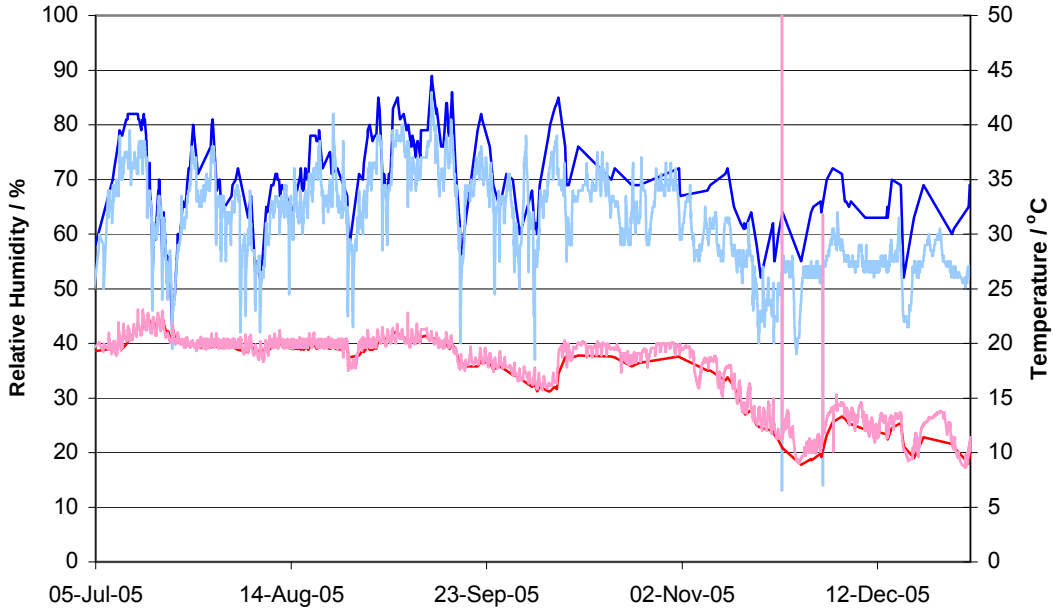

Figure 2.7 – monitoring in the tapestry room at Audley End House
(room: temperature pink; RH light blue; behind tapestry: temperature red; RH blue)

To study this further, additional sensors have been placed behind three tapestries on display at Ranger's House (see Figure 2.8). These tapestries are lined but freely hang against the wall whereas those at Audley End House are fixed to lined walls. Figure 2.9 shows the difference in RH levels which vary behind the three tapestries by up to 10% RH. A difference is particularly evident between the empress tapestry and the other two, which hang on the opposite wall. There is also a corresponding temperature difference with the sensor behind the empress tapestry, around 0.5 °C in the summer increasing to 1 °C in the autumn and around 2 °C in the winter. A comparison of the absolute humidity between the sensors shows a similar trend to the RH, with the empress tapestry 0.5 gm^{-3} higher than the hunting tapestry which is 0.5 gm^{-3} higher than the emperor. There are a number of possible reasons for these differences, including that one or more of the sensors

require calibration. However the sensors were all recalibrated at the same time, so it is also possible that this difference is real.

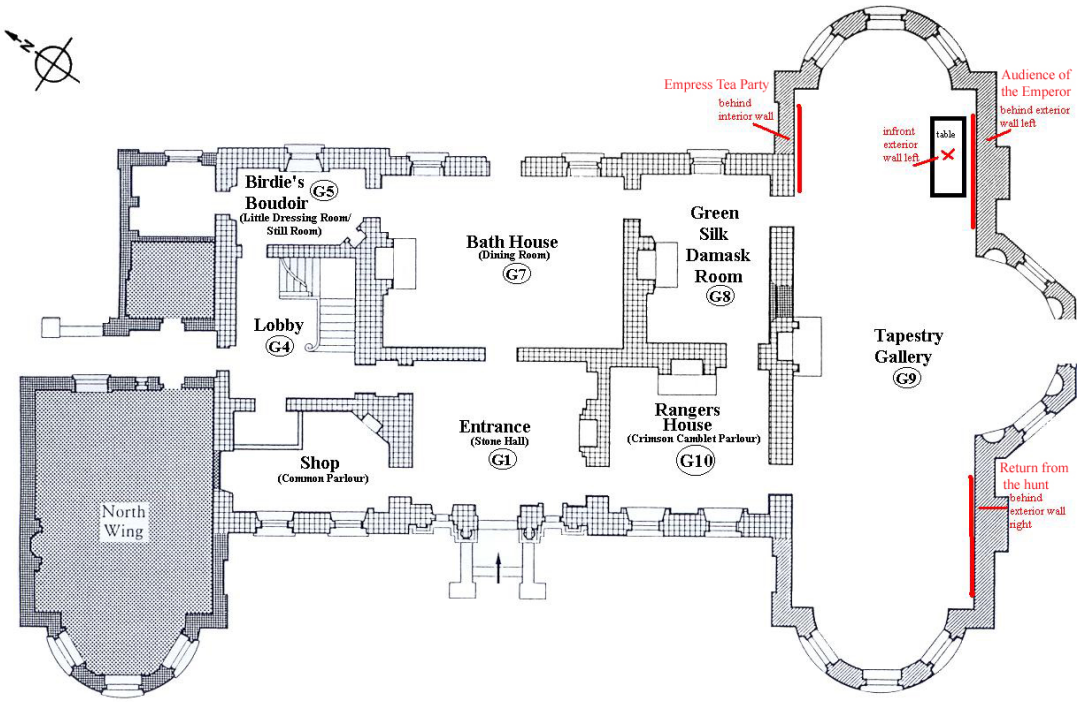

Figure 2.8 – location of tapestries in the gallery at Ranger's House
(copyright English Heritage)

All the tapestries are hung on external walls. However the empress hangs on a north-facing wall which gets little sunlight, compared to the opposite south-facing walls on which the emperor and hunting tapestries hang. It is noticeable that the hunting tapestry hangs on the most south facing wall and also has the highest temperatures. Whether the difference arises from warming due to additional direct sunlight would require further external surface monitoring to verify this is the cause. It is possible that moisture from the wall may lead to the observed differences, especially behind the empress tapestry, however additional investigation would be required to understand this further.

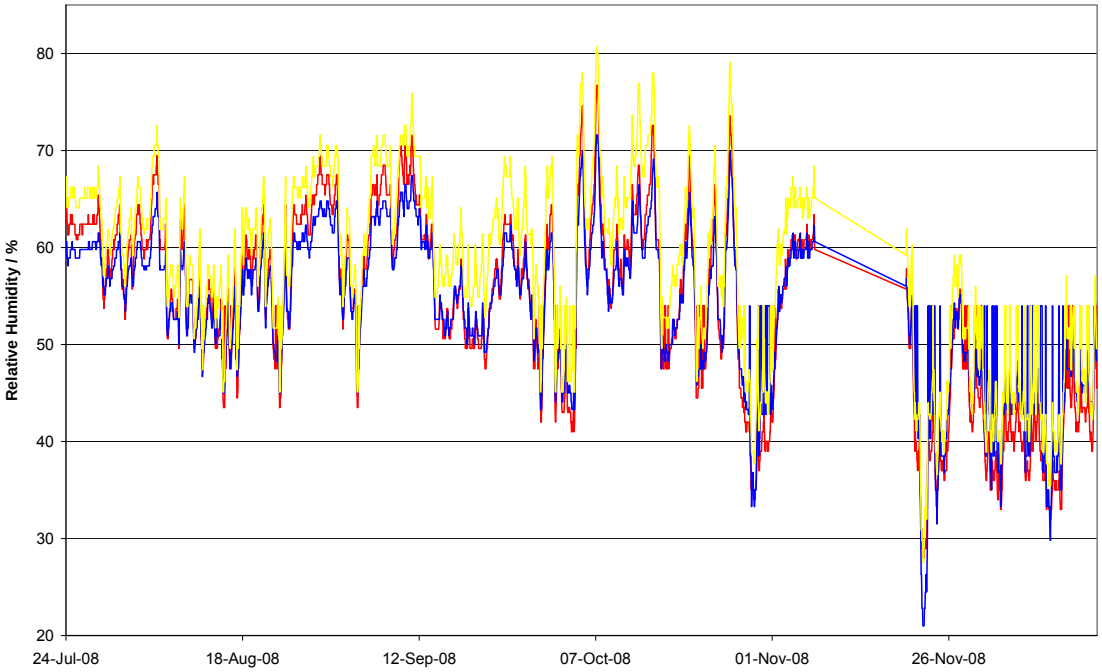

Figure 2.9 – comparison of RH levels behind three tapestries at Ranger's House (hunting tapestry: red, emperor tapestry: blue, empress tapestry: yellow)

Figure 2.10 shows the difference between the sensor behind the emperor tapestry and a sensor placed on the table in front. The sensor behind the tapestry is 1 °C colder than that on the table. There is also an average difference of around 3% RH between the sensor on the table and behind the tapestry. The most noticeable difference however are the increased fluctuations recorded behind the tapestry. The sensor on the table fluctuates less and also shows smaller changes in RH. For example on 23rd November 2008 a significant drop in RH can be observed. In the room the RH decreases from 40 to 30%, which can be damaging for some materials such as veneers. However behind the tapestry the RH drops from 40 to 20%. It may be that the small difference in RH has little effect, but that the more dramatic changes and more frequent fluctuations are the reason unfaded silk, sampled from the reverse of tapestries during MODHT, was in poor condition. The absolute humidity is approximately the same for these two sensors, although the smaller fluctuations are again observed for the table sensor. Further

environmental monitoring would be required to confirm the differences observed as well as accelerated ageing under these fluctuating environments.

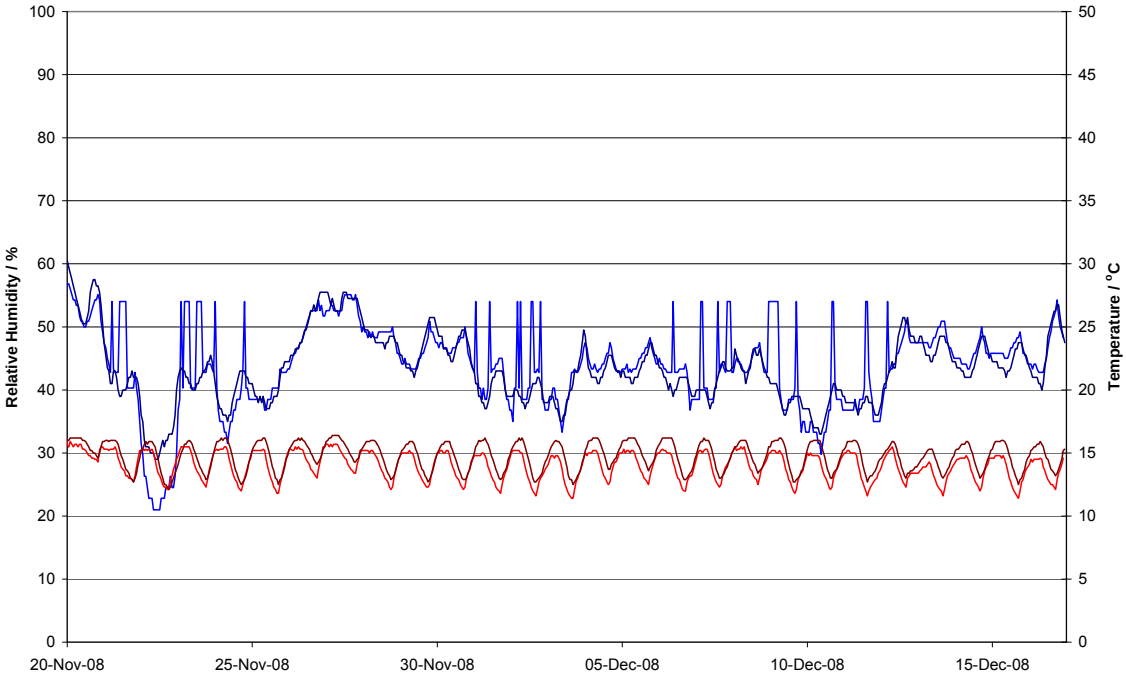

Figure 2.10 – comparison between the front and back of the Emperor tapestry (front: temperature dark red; RH dark blue; behind: temperature red; RH blue)

The conditions that characterise the display environments are: low RH (~30%) mainly seen during the winter dry spells, low average RH (~40%), for example at Apsley House, mid average RH (~50%), high average RH (~60%), for example at Audley End House, and high RH (~75%) recorded during the summer high spells. These environmental conditions should all be considered during accelerated ageing tests. For silk the moisture sorption profile is reported to show little change between 30 and 50% RH,[7] with the regain of silk changing little between 30 and 60% RH.[8] Carlene reported little change in the breaking strength of silk between 33 and 55% RH.[9] These references indicate little change to silk would be expected in this region, but more significant variation outside this region, so studying changes at a wide range of RH levels could help determine if this is true.

It would also be interesting to study the effect of seasonal variation by cycling between a low RH, mid RH, high RH and mid RH again. Cycling of RH is likely to cause physical as well as chemical damage to the silk fibres. As mentioned above it is possible that the more extreme and rapid fluctuations in RH also cause physical damage to the silk and would be interesting to study. However this type of environment is difficult to simulate in accelerated ageing tests and it is unlikely these variations could be prevented or reduced within historic house environments.

Light

Although there are fewer light than temperature and RH sensors, almost all display rooms have been assessed to make light plans. Light levels in historic properties can be controlled in a number of ways but the most common is the use of double blinds. This uses a black out blind with a cream blind in front. By adjusting the blind positions light levels can be reduced and direct sunlight prevented. Blind plans are formulated by making spot readings of the light levels in different positions and at different times of day and adjusting the blinds to reduce the incoming light. Light plans usually specify a maximum light level, measured in lux for a specific object so the light level can be checked and the blinds altered accordingly, often the blind position is also recommended. Maximum light levels are often adjusted to take into account the opening hours of the property, as light doses can be calculated based on annual budgets.

A current English Heritage research project looking at light data from continuous monitoring, has identified that annual light levels are often below the annual light budget. Of the sensors monitoring light 80% record annual exposure levels of 75% or less of the budget. It may be possible light levels could be increased for visitors up to the annual light budget, although this is an ongoing project. As the light budgets set out the maximum annual light dose, it is useful to use these as the basis for further study. Therefore light levels of 50 lux and 200 lux, the maximum

levels used in the annual light budgets will be included in any further ageing studies.

UV

Another method of controlling light levels is to reduce the light entering the room by applying light absorbing films to the windows. These can reduce the transmitted light by varying degrees, depending on the density of the film, although almost all will also reduce the UV content of the light. In most properties a transparent film is used to reduce the UV content of the light only. The current limit used for UV is 75 μW/lumen;[10] this is based on the typical UV content of tungsten bulbs. When new the UV film, reduces the level to 10 μW/lumen, and due to improvements in artificial lighting it is proposed the limit should now be 35 μW/lumen.[11] Therefore it would be useful to look at the effect these low levels of UV have to see if this hastens the silk deterioration, especially as UV is reported to cause rapid damage.[12] It would also be interesting to look at a higher level of UV light exposure to understand the benefits of having the UV absorbing film on the windows for the objects on display.

Combined Effects

As no object on open display is ever subject to humidity or light exposure in isolation it is useful to study a combination of the effect of light and humidity. The initial studies on one factor only will allow the most detrimental to be determined but combining the light and humidity environments should allow any synergistic effects on the deterioration of silk to be studied.

Other Factors

Other factors that may have an impact are pollution and dust. Pollution monitoring usually focuses on a small number of gaseous pollutants: nitrogen dioxide, sulfur

dioxide and ozone. Hydrogen sulfide is usually only monitored at Apsley House due to the large silver collection displayed there as it is known to cause silver tarnish. Chlorides are occasionally monitored, normally at coastal sites. The pollution monitoring has occurred quite recently and gives averaged values for the monitoring period (usually monthly exposures). Pollution effects may be important as we know historically Brodsworth would have been more polluted due to nearby industry. Dust levels are also averaged over the monitoring period and provide information on areas that are particularly at risk. Research has shown that dust levels fall with increased distance from the visitor route and that height and the type of dust found can also be important factors for both the aesthetic impact and damage caused by the dust.[13]

Most of the factors discussed so far will cause microstructural and direct chemical damage. However there is also a risk of macrostructural physical and biological damage during open display. As noted in the previous chapter the risk of biological damage is generally reported as being low, however this is further reduced as far as possible by modifying the environment and checking the objects for signs of damage. Physical damage can be caused by numerous sources, some of which can be reduced, some of which are inherent. The tension a fabric is placed under when used in upholstery or hung for display e.g. tapestries and banners, can cause damage over time. An example of this can be seen at Apsley House in the orders display case, where the weight of the order on the ribbon, has led to tears in the silk (see Figure 2.11). In some cases this can be prevented or reduced by altering the display to improve mounts or provide greater support. Abrasion and other physical damage can also be caused by touching the objects or brushing past them (see Figure 2.12). This can be mitigated by changing visitor routes and ensuring visitors are aware of the damage caused by touching. An example of this is at Eltham Palace where replica samples of materials in the house have been mounted for visitors to touch. A covered sample is also provided demonstrating the damage that is caused over a short time period to the objects by touching and helps discourage visitors from doing so.

Figure 2.11 – damage to ribbon on Jewel of the Order of the Elephant, Denmark [WM.1392-1948] at Apsley House

Figure 2.12 – abrasion to silk fronted cabinet at Osborne House (The Royal Collection copyright 2009 Her Majesty Queen Elizabeth II)

In order to study the causes of silk deterioration a series of accelerated ageing experiments on surrogate materials will be used to study the following environmental effects found in the selected English Heritage properties:

RH:	none (0%), very low (~30%), low (~40%), mid (~50%), high (~60%), very high (~75%) and saturated (100%)
light:	dark (0 lux), low light levels (50 lux) and high light levels (200 lux)
UV*:	none (0 μW/lumen), low (35 μW/lumen), mid (75 μW/lumen) and high (150 μW/lumen)
combined effects:	combination of each RH level with each light level, i.e. 0, 30, 40, 50, 60, 75 and 100% in the dark, at 50 lux and at 200 lux.

*In reality UV and light exposure occur together therefore UV conditions will be combined with a light level of 200 lux for accelerated ageing. This level of illumination has been selected as UV is measured as a proportion of the light and in historic houses at 50 lux the level of UV is not usually measurable.

Sampling English Heritage Silks

Although the object records include condition information this is based on visual observation of the objects. Work on High Performance Size Exclusion Chromatography (HPSEC) had demonstrated the greater sensitivity of this technique to small changes in condition compared with more common methods such as tensile testing, which require large samples.[14] Taking small samples, although destructive, will provide details about the type of silk and its current condition. This information will help improve the care and condition of the collection as a whole.

The object records for each of the five sites were used as the basis for the visits, with each object located and assessed. At most sites a tour of the site by the curator or conservator highlighted any other objects that might contain silk as well as those that might not be included in the records. Assessment of the objects was based on the current condition and display environment, the type of silk (e.g. raw silk, weighted silks, silk velvets), age, uniqueness of the object and possible comparisons with other objects in the collections (e.g. tapestries). After each visit a record was made with details of the object and whether it may be suitable for sampling. (Suitability for sampling was determined by the information that may be gained by sampling and the ease with which the object could be sampled i.e. if there were protruding fibres.) These initial summaries were then discussed with the relevant curators and a final list of objects to sample was created. Where necessary permission from lenders was then obtained before sampling occurred. One store (Fulford) was also visited and samples taken to include the items from Brodsworth Hall which are stored off site.

A database of samples was created and this has been updated regularly to include all the samples taken as well as any further information (see Appendix 2). The database includes where the samples have come from (property, room, object

including accession number and description), size, colour and analysis undertaken (including summary of the results). Each sample has been given a unique identifying code; these consist of my initials (nl), a three letter code for the property (aps, aeh, bro, ful, osb, ran) and a sequential number (starting from 1 for each property). In total 112 samples were taken across the six locations. This represents approximately 10% of the silk collection within English Heritage.

The samples taken from the objects on display in the English Heritage properties will be analysed to determine the types of silk materials within collection. HPSEC results from the analysis of the historic micro-samples will be compared to those from accelerated ageing studies. This will help identify the current condition of the English Heritage silk collection. It may also be possible to use results from the micro-samples to determine the cause of deterioration in some objects and this will be investigated.

References

[1] Funding Agreement Between the Department for Culture, Media and Sport (DCMS), Department for Communities and Local Government (DCLG), Department for Environment, Food and Rural Affairs (DEFRA) and English Heritage 2005/6-2007/8. http://www.culture.gov.uk/NR/rdonlyres/67B548CA-A01C-4FFD-9243-D95208A129CC/0/EHFundingAgreement06_08.pdf accessed 30/07/2007.

[2] http://www.english-heritage.org.uk/server/show/conWebDoc.166 accessed 30/07/2007.

[3] Collections Conservation Research Plan, Internal English Heritage report (2006)

[4] Taylor, J. (2005) 'An Integrated Approach to Risk Assessments and Condition Surveys' *Journal of the American Institute for Conservation* **44** 127-141.

[5] Fry, C., Xavier-Rowe, A., Halahan, J. and Dinsmore, J. (2007) 'What's Causing the Damage! The Use of a Combined Solution-Based Risk Assessment and

Condition Audit' *Preprints of Museum Microclimates Conference The National Museum Denmark 19-23 November 2007* 107-114.

[6] Xavier-Rowe, A., Fry, C. and Stanley, B. (2008) ' Power to Prioritize: Applying Risk and Condition Information to the Management of Dispersed Collections' *Conservation and Access Contributions to the London Congress 15-19 September 2008* Saunders, D., Townsend, J. H. and Woodcock, S. (ed.) London: The International Institute for Conservation of Historic and Artistic Works 186-191.

[7] Zhang, X. and Wyeth, P. (2007) 'Moisture Sorption as a Potential Condition Marker for Historic Silks: Noninvasive Determination by Near-Infrared Spectroscopy' *Applied Spectroscopy* **61(2)** 218-222.

[8] Hutton, E. A. and Gartside, J. (1949) 'The Moisture Regain of Silk. Adsorption and Desorption of Water by Silk at 25 °C' *Journal of the Textile Institute* **40** T161-T169.

[9] Carlene, P. W. (1944) 'The Moisture Relations of Textiles. A Survey of the Literature' *Journal of the Society of Dyers and Colourists* **60** 232-237.

[10] Thomson, G. (1986) *The Museum Environment* Oxford: Butterworth-Heinemann 20.

[11] http://www.tate.org.uk/collections/borrowing/care-and-treatment.shtm accessed 27/07/2009.

[12] Tsukada, M. and Hirabayashi, K. (1980) 'Change of Silk Fibroin Structure by Ultraviolet Radiation' *Journal of Polymer Science: Polymer Letters Edition* **18** 507-511.

[13] Lloyd, H., Lithgow, K., Brimblecombe, P., Yoon, Y. H., Frame, K. and Knight, B. (2002) 'The effects of visitor activity on dust in historic collections' *The Conservator* **26** 72-84.

[14] Howell, D. (1992) 'Silk Degradation Studies', in *Silk: Harpers Ferry Regional Textile Group, 11th Symposium*, Washington DC: Harpers Ferry Regional Textile Group 11-12.

Chapter 3 – Elemental Analysis of Silks

To study the deterioration of the silk in the English Heritage collection, it is important to determine which silk materials should be selected to use in the artificial ageing experiments. As silk can be weighted with metallic salts it was valuable to determine if these materials were present within the collection. A review of elemental analysis in textile conservation is presented along with the experimental analysis undertaken to identify these materials. Difficulties in identifying weighting agents rather than mordants are also discussed in this chapter.

Surveys of the selected properties identified the presence of silk velvets and metal thread decoration. It was also thought the costume collection, although small, may contain weighted silk as this is relatively common in costume collections.[1,2] However there are no simple visual checks to determine the presence of weighting materials. Therefore it is difficult to determine if the majority of the collection is plain silk or if this also contained weighted material.

To identify any weighted materials in the English Heritage collection elemental analysis was undertaken. Elemental analysis of textiles can support conservation, for example identifying the processing techniques used during manufacture, such as tin compounds from weighting agents or chromium as a mordant. Understanding how objects have been produced can highlight possible inherent deterioration problems enabling more informed decisions in relation to treatments or preventive conservation of the collection. Elemental analysis can aid interpretation of collections, for example to identify the composition of metal threads found within textiles. This information can be useful as it may relate to the date of production, with pure or high gold content threads commonly reported from the 12th century or before.[3]

Elemental Analysis in Textile Conservation

Metallic mordants and weighting agents in silk, such as aluminium, chromium, copper, iron and tin, have been identified using scanning electron microscopy with energy dispersive X-ray spectrometry (SEM-EDS).[4,5,6,7] Elements can be identified as X-rays are emitted at characteristic energies depending on the energy of the electron removed. Comparison of the elements in silks from marine environments and historic and modern silk materials has been undertaken with SEM-EDS.[8] Using the technique high levels of sulfur have also been found in silk flags described as shattered. Ballard *et al*. suggest that high sulfur rather than weighting materials may cause the deterioration leading to shattering of the silk.[9] EDS has the advantage of being non-destructive[a] and results can often be obtained from very small samples. Newer systems can detect smaller amounts of materials as well as lighter elements, overcoming earlier reported restrictions. Details on SEM-EDS and its use in conservation are discussed by Stuart.[10] Some constraints still apply, such as contamination from soiling and the inability to differentiate between metals used as mordants and those used as weighting agents.

SEM images can provide additional compositional information, for example greater levels of weighting in one direction (weft) in weighted silks. This is visible as brighter threads running in one direction in the image. The increased brightness arises from the heavier element present in the weighted threads, which more effectively backscatters the primary electrons of the beam. This is not observed for mordants as they tend to be present at much lower concentrations and are usually lower atomic weight elements. In metal threads the manufacturing technique can be visible in SEM images and when coupled with EDS the composition of both the metal and any tarnish layers can be determined.

[a] Non-destructive analytical techniques do not destroy the material during analysis but often require a sample, whereas a non-invasive technique does not require a sample. Within conservation science it is generally preferable for objects to be analysed using techniques that are both non-invasive and non-destructive.

Mordants have been identified using wet-chemistry microanalysis,[11] X-ray fluorescence (XRF),[12] inductively coupled plasma-atomic emission spectroscopy (ICP-AES)[13] and atomic absorption spectroscopy (AAS).[14] Particle induced X-ray emission (PIXE) has been used by William and Indicator to detect the presence of aluminium, but they report their system found detection of magnesium difficult and sodium was not detectable, due to absorption of soft X-rays by the detector window.[15] Another method is neutron activation analysis (NAA) however lead, a known weighting agent, cannot be detected as lead isotopes are stable and are not radioactive unless irradiated for a long time.[16]

Dussubieux and Ballard[17,18] have investigated using inductively coupled plasma – mass spectrometry (ICP-MS) to identify inorganic elements present from dyes or mordants. Their work identifies the expected materials although they also report contamination of samples. Their work concludes that ICP-MS could be used for comparison with results from other analytical techniques when these have not been conclusive. However, this method is destructive and the authors report using larger sample sizes (~10-30 mg) although small quantities are required for modern instruments (usually ~1 mg).

The possible locations of weighting agents in silk have been studied with Transmission Electron Microscopy (TEM). Robson studied the microvoids within silk fibres, by imaging deposited silver sulfide to locate the positions and sizes of voids.[19] Microvoids in a number of non-mulberry varieties of Indian silk have been observed in cross section using SEM.[20] Although not providing elemental information it may be possible to use these methods to establish the presence of any weighting agents within the silk structure.

XRF has been used on textiles previously to identify mordants, weighting agents,[21] painted details,[22] mineral dyes[23] and heavy metal pesticide residues.[24] It has also been used to provide elemental information for comparison with X-radiography images.[25] One of the main advantages of XRF is that direct analysis of an artefact is possible, without sampling. Over short time spans at low energy the material is not altered by the analysis.[26] This

makes XRF both non-invasive and non-destructive. The XRF spectrum (see Figure 3.1) can be used to identify elements present, as each element has characteristic X-ray energies (for details on the use of XRF in conservation see Stuart[27]).

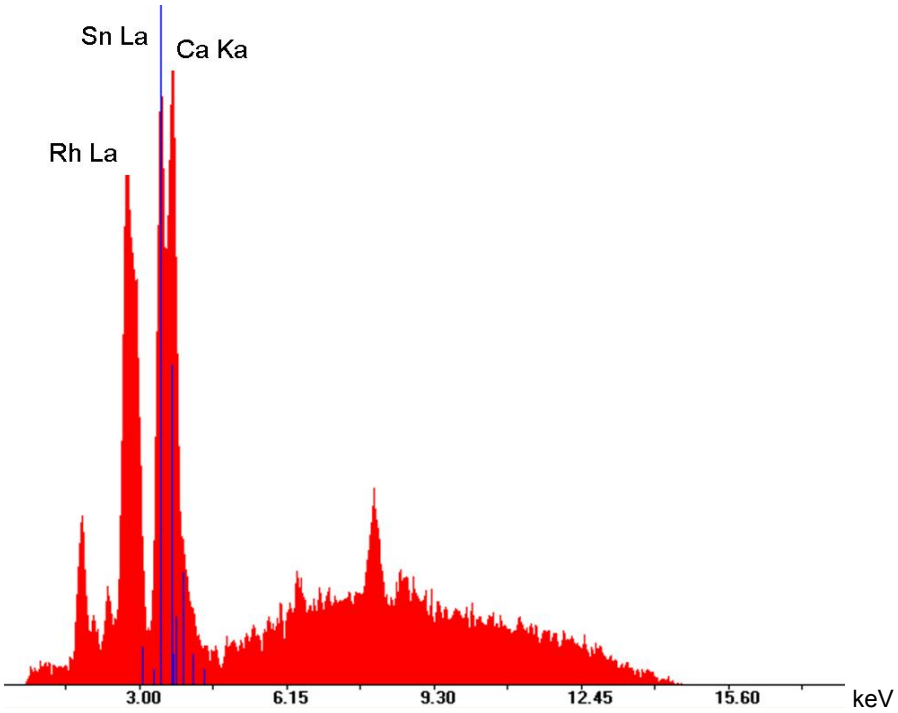

Figure 3.1 – an example XRF spectrum from sample nlbro9, showing characteristic tin lines with tin and calcium peaks, along with the rhodium source peak (the software autoscales the maximum peak to 90% intensity)

Experimental Set Up

Elemental analyses were undertaken to identify whether silks in the English Heritage collection were weighted and if so, how many and what with. Qualitative analysis can determine the presence of elements within the collection from which inferences can be drawn. Such as the presence of tin indicating weighting agents, or iron in black silk as a mordant from the tannin dyeing process. However both iron and tin have been used as mordants and weighting agents and qualitative analysis can not determine the process which has led to the elements presence. This would require quantitative analysis to

determine how much of an element is present and comparison with materials known to be weighted.

The techniques used were chosen based on their availability within conservation departments, for example SEM-EDS and XRF, as well as to answer some of the questions that arose, for example AAS and ICP-OES. It was hoped to obtain quantitative results, which would give a greater understanding of the collection and the materials present. However most of the analyses have yielded qualitative results. These indicate the elements that are present but do not allow for identification of the manufacturing processes used.

SEM-EDS

Scanning Electron Microscopy (SEM) analysis has been performed using a Carl Zeiss S440 scanning electron microscope with an Everhart-Thornley secondary electron detector using an accelerating voltage of 25kV and a probe current of 1.0 nA. SEM images were taken for a number of the samples and used to determine whether there were any differences in the warp and weft fibres. Qualitative Energy Dispersive X-ray Spectroscopy (EDS) analysis was performed on the same instrument with an Oxford Instruments germanium X-ray detector, at a working distance of 25 mm with a standard livetime count of 100 s. The element with the lowest atomic number which can be detected with this equipment was sodium. A single fibre was imaged and magnified to around 5000 times, a square the width of the fibre was selected and the area inside analysed. An initial comparison of three areas on the first sample showed similar results, so for remaining samples only one area was analysed. The silk samples are primarily composed of organic elements (e.g. C, H, N, O) which could not be quantified by the instrument used. The results are expressed as elemental weight %, which were not normalised.

Samples taken from the English Heritage collection were mounted on carbon pads stuck to aluminium stubs and then carbon coated for SEM-EDS analysis. It is very difficult to recover and clean the samples, limiting analysis to the larger specimens from which pieces could be removed. The small size of many

specimens means some are only sufficient to allow High Performance Size Exclusion Chromatography (HPSEC) analysis.

XRF

XRF analysis was performed with a KeyMaster-Bruker TRACeR III-V handheld XRF. The instrument is battery powered with an associated PDA for data analysis, although a laptop and power cables can also be used. When used with the KeyMaster-Bruker vacuum pump attachment elements down to magnesium can be identified. The sample area is an ellipse approximately 5 by 6 mm, with a count time of 40 seconds. The small, portable unit allowed for *in situ* analysis but could also be used to analyse the samples taken from the English Heritage collection. For convenience the XRF was placed upright into a supportive frame and the micro-samples placed on top of the analysing area, which was covered to prevent X-rays escaping. It was possible to analyse samples as small as one fibre, although most consist of a few millimetres of thread.

Due to an overlap between the K_{α} line of calcium (3.67 keV) and L_{β} line of tin the spectra have been checked to determine the presence of calcium as well as tin (see Figure 3.1 for the presence of calcium above the second characteristic tin line).

XRF – In Situ Analysis

There are a number of instances where sampling objects is not possible due to access, or ethically unacceptable such as important items in a very fragile condition. However to accurately represent the English Heritage collection of silk materials it is important to know whether the highly degraded materials are weighted or heavily processed. In this case a technique that is both non-invasive and non-destructive and can be used *in situ* is desirable. To test the applicability in real situations the portable XRF was used on site at Audley End House.

XRF - Calibration

The portable XRF has a number of standard calibrations supplied, however most relate to identification of different standard metal alloys as this was the original use for the equipment. This means the internal quantifications do not apply to textiles and a separate calibration is required for quantitative analysis. As it was not immediately possible to calibrate the XRF for textile samples an alternative method was sought to give qualitative results.

Dussubieux and Ballard used comparison of the signal intensities from inductively coupled plasma – mass spectroscopy (ICP-MS) to determine the presence of mordants where no control material was available. A similar method has been applied to determine the detection limits of the elements by XRF analysis. Although there are difficulties in determining the background level for some materials it has been possible to qualitatively determine those samples with significant content from the current results.

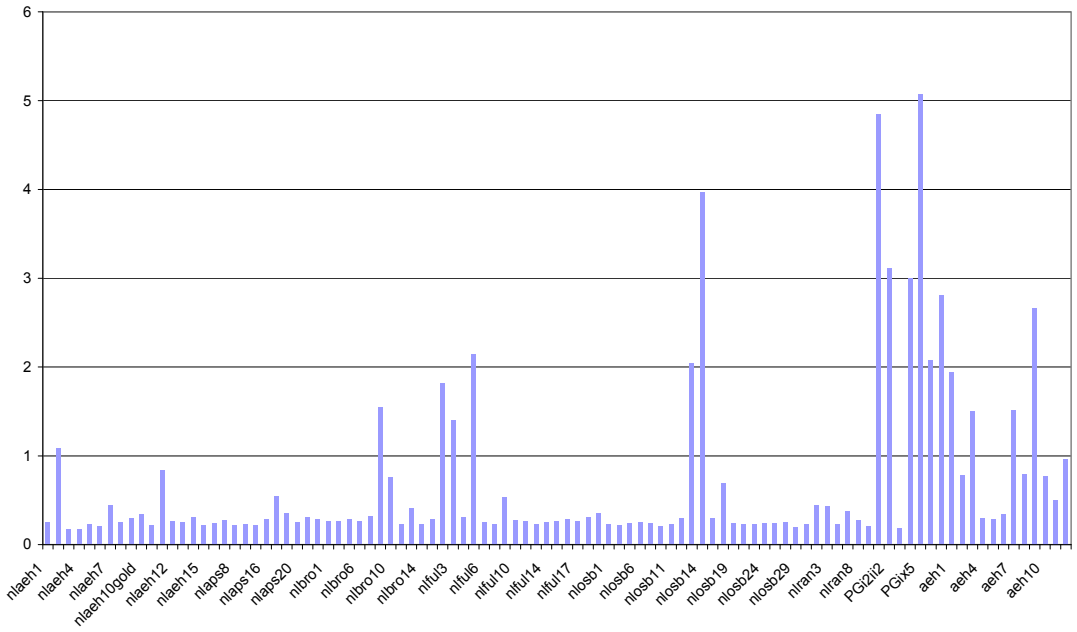

Figure 3.2 – calcium to rhodium peak area ratio results

The XRF spectra are autoscaled by the software, to make the maximum peak height 90%. The autoscale can be adjusted but not turned off; therefore an

alternative method was required to compare the spectra against each other. To provide a correction the ratio of the element peak area against that of the source element, rhodium L_α line has been calculated. For elements with energy lines below 4 keV this worked well, see Figure 3.2, providing a clear difference for samples above the baseline, here at 0.6. However for elements with energy line between 4 and 14 keV the rising background envelope, as seen in Figure 3.3, made this correction less effective, see Figure 3.4. In this case it was harder to determine where the peak ratio is, it could be set at 0.25 which would indicate all the Apsley House samples (nlaps) contain chromium. However as seen in Figure 3.3 the chromium peak is barely visible above the baseline (highlighted in grey). The baseline could be higher at 0.5 but then samples known to contain chromium, such as nlosb29 would be excluded. To avoid erroneous identification, elements with energy lines above 4 keV were corrected by calculating the ratio of the sample to titanium peak areas.

When determining the peak area the software uses a start and end energy for each element (the grey lines in Figure 3.3 for chromium) and the area between the lines are reported. However with the rising background envelope there is a large contribution from the background making peaks between 4 and 14 keV seem greater than the peaks below 4 keV. Titanium has been selected to ratio peaks in this region against as the element is not present in the samples but the peak is on the edge of the rising background envelope and so negates some of these problems. The software does not allow the background envelope to be subtracted and the peak area alone used.

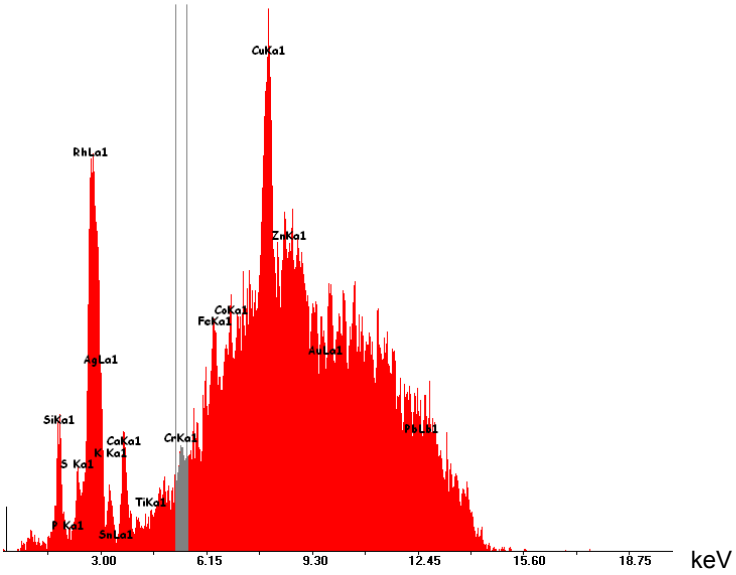

Figure 3.3 – sample nlaps4 showing rising background envelope between 4 and 14 keV

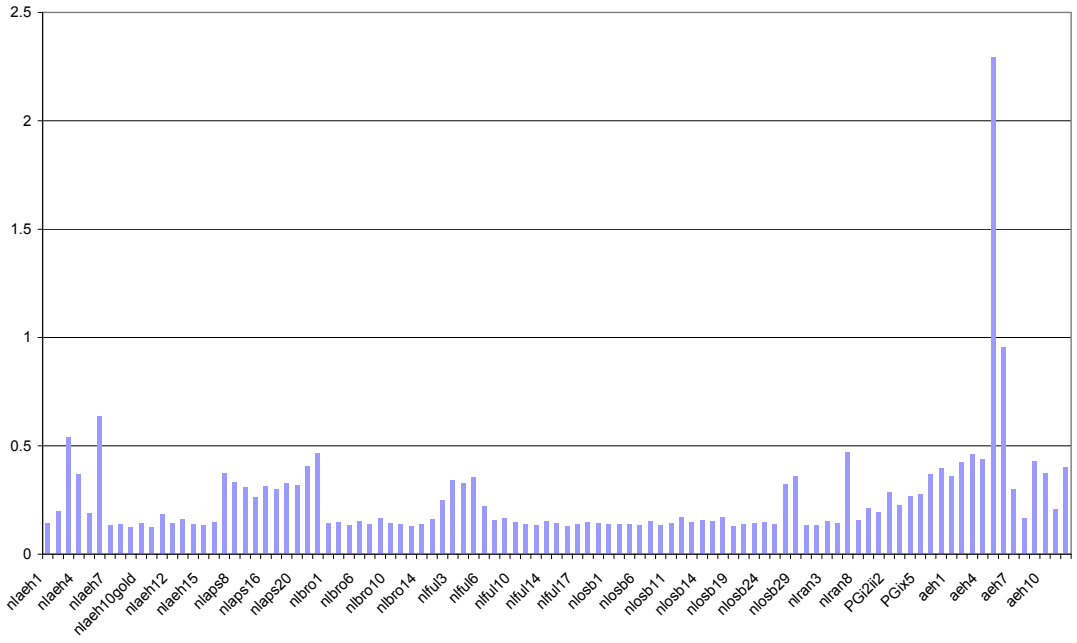

Figure 3.4 – chromium to rhodium peak area ratio results

The further correction using the ratio to the titanium peak area can be seen in Figure 3.5. This has removed difficulties arising from the rising baseline and makes it easier to determine whether chromium is present above the baseline at 3. The ratio results for all elements are included in Appendix 3.

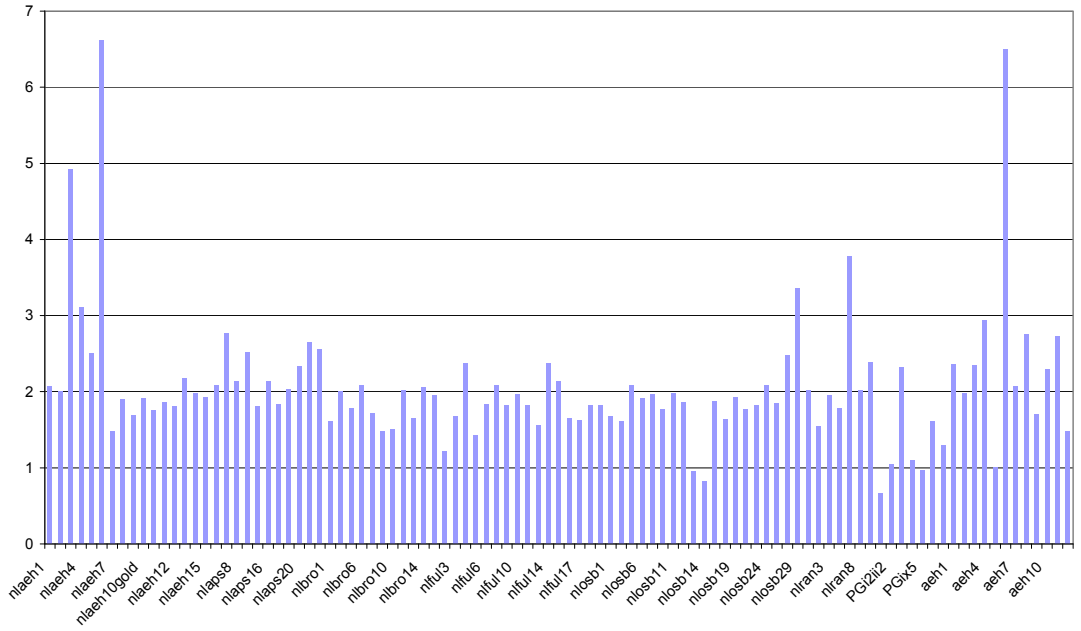

Figure 3.5 – chromium to titanium peak area ratio results

For all elements the amounts present can only be quantitatively determined by calibrating the XRF. In terms of understanding the collection of silk materials within English Heritage there are implications for how much material can be identified as weighted silk. It became apparent that further work was required to determine how the detected element can be quantified.

Atomic Absorption Spectroscopy

Atomic absorption Spectroscopy (AAS) was used to determine the amount of an element present within the silk and provide a basic calibration for the XRF results. Details on AAS and its use in conservation have been discussed by Stuart.[28] Tin, iron and zinc were selected for quantification based on the qualitative XRF results from the English Heritage collection samples. To provide a calibration set model silk materials were produced using atomic absorption standard solutions of iron, tin and zinc, from Sigma Aldrich. These were diluted from a 1000 ppm solution (referred to as 100 %) to produce solutions at 10 % intervals. Silk strips (2 x 5 cm) were immersed in the solution overnight and then left to air dry.

For each condition it was only possible to produce one sample, these were analysed with the portable XRF before being dissolved in concentrated nitric acid (1 ml) and made up to 10 ml of 10% nitric acid with deionised water. This made the model samples comparable with the AAS standard solutions which are in 10% nitric acid. The silk solutions were then analysed using a PU 9100 Atomic Absorption Spectrophotometer with an air/acetylene flame and a detection wavelength of 248 nm (iron), 235 nm (tin) or 214 nm (zinc), to determine the amount of each element present. The average absorbance of three readings was taken and compared to the calibration graph for samples. The calibration standards for iron were from 0-5 ppm (1 ppm interval), tin was 0-200 ppm (50 ppm interval) and zinc 0-1 ppm (0.2 ppm interval).

ICP-OES

Analysis of tin at low concentrations (< 2 mg/L[b]) is usually carried out using graphite furnace atomic absorption spectrometry (GFAAS) rather than flame ionisation. However this was unavailable which increases the detection limit for tin from 5 µg/L for GFAAS to 0.8 mg/L for flame AAS.[29] The calibration standards used for tin also ranged from 0-200 ppm, as most samples fell between 5 and 50 ppm it was difficult to clearly assign concentrations.

To overcome the AAS limitations inductively coupled plasma – optical emission spectroscopy (ICP-OES) was undertaken. This technique is also referred to as inductively coupled plasma – atomic emission spectroscopy (ICP-AES).[30] Analysis was performed using a PerkinElmer Optima 4300DV inductively coupled plasma –optical emission spectrometer with concentric glass nebuliser (Glass Expansion *Conikal*) and a baffled cyclonic spray chamber (Glass Expansion *Twister*). Argon gas was used with the following flow rates: carrier gas 0.8 $Lmin^{-1}$, auxillary gas 1.4 $Lmin^{-1}$ and plasma 18 $Lmin^{-1}$.

For tin there are four emission wavelengths (189.927, 235.484, 283.998 and 242.169 nm) and two different plasma viewing modes possible, of these the

[b] The optimum concentration for analysis with flame AAS is reported to be 10-300 mg/L

axial (rather than radial) measurements gave better repeatability of results. One wavelength (235.484 nm) appeared to have interference due to the presence of iron in one of the known weighted standard samples, therefore this wavelength was omitted. Depending on the selected wavelength the limits of detection were between 3.5 and 7.5 ppb. This is significantly lower than the reported levels of tin in the solutions. All the solutions were filtered through 0.45 µm, 25 mm diameter hydrophilic PTFE syringe filters prior to analysis. Each of the model samples was analysed (the average of 5 repeat measurements for each detection wavelength being quoted) as were the known weighted standard samples. The average readings for the three selected axial wavelengths were used to determine the concentration of tin in each solution. By comparison with prepared standards at 0, 10, 25 and 50 ppm as the AAS had indicated this was concentration range of the prepared model and known weighted samples.

Results

SEM-EDS

For all the samples analysed, fibres in both directions appeared identical suggesting there is no preferential weighting of warp or weft fibres. Silks can be weighted either in the fibre or in the cloth, so these results may suggest any weighting has occurred in the cloth. The images showed greater details of the sampled fibres, for example the velvet pile (Figure 3.6 sample nlful10 from armchair [90003210]), and crepe fabric (Figure 3.7 sample nlful3 from evening dress [90005694]). In Figure 3.7 there is a difference in the contrast between the fibres, which is likely to arise from charging of the sample due to an uneven carbon coating on the crepe weave

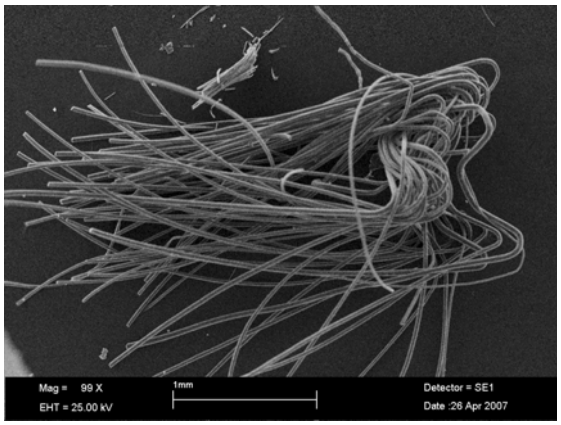

Figure 3.6 – nlful10 velvet pile

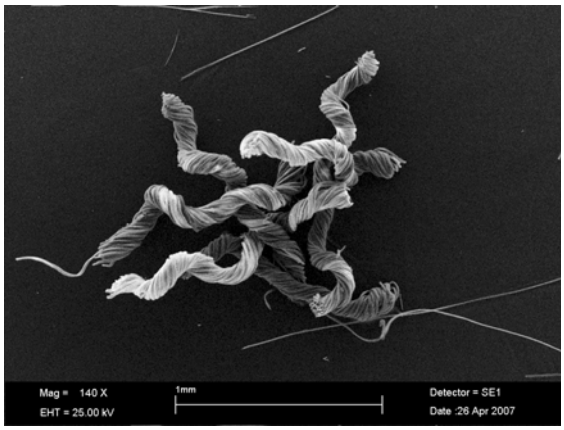

Figure 3.7 – nlful3 crepe fabric

SEM images also made it possible to look at the fractured fibres in more detail. Figure 3.8 shows an example of a fractured fibre from sample nlbro9 taken from a cream silk and lace parasol displayed in bedroom eight. The weave structure could also be seen in more detail, for example sample nlful9 taken from fragments of the silk fronted cabinet [90006945] during conservation (Figure 3.9). There are a number of brighter areas seen in the image arising from charging of the sample, due to an uneven carbon coating as a result of the sample texture.

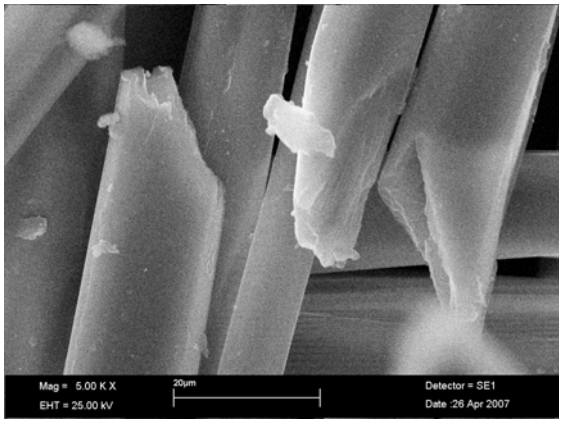

Figure 3.8 – fracture detail from nlbro9

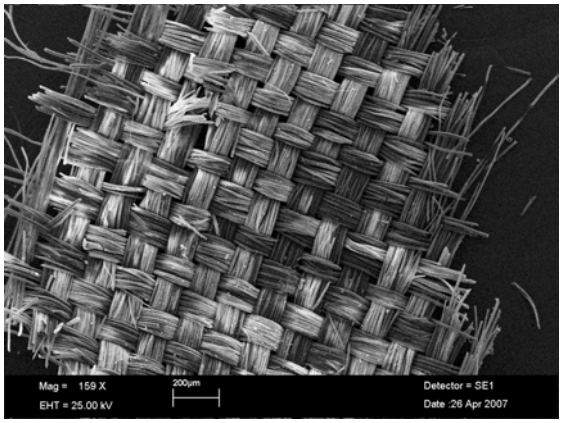

Figure 3.9 – SEM image of nlful9, areas of damage to the weave structure can be seen, along with particulates on the surface

As it was not possible to determine the matrix effects for silk samples, previously determined limits of detection for glass were used to indicate whether

an element was present or not. Of the thirty samples analysed, thirteen contained elements at twice the detection limit (see Table 3.1). The majority of analysed samples contained elements (usually sulfur) at the detection limit but as this has not been determined precisely for silk, trace elements have not been included unless a further element was definitely detected. In some of these cases the elements found suggest weighting materials may be present, for example tin. This has been found in conjunction with silicon and phosphorus on one sample, a cream parasol (nlbro9) (see Figure 3.10), suggesting the "dynamite" weighting method developed by Neuhaus may have been used.

sample id	Si	P	S	Cl	K	Ca	Fe	Sn	Comment
nlful3	-	-	-	-	-	t	-	X	
nlful10	-	-	X	-	-	-	-	-	
nlful15	-	-	-	-	-	-	X	-	
nlbro9	X	X	-	-	-	X	-	X	
nlbro12	-	-	t	-	-	t	t	X	
nlosb13	-	-	-	-	-	-	-	X	
nlosb14	X	-	t	-	-	-	-	X	Cu also present
nlosb20	X	-	t	X	t	X	t	-	analysed glue layer
nlosb23	-	-	-	-	-	X	-	-	
nlaeh11	-	-	X	-	-	X	-	-	possibly soiling deposits
nlaeh10	t	-	X	X	-	X	-	X	Pb also present
nlaeh7	-	-	X	-	-	X	-	X	
nlaeh8	-	-	X	t	X	t	-	-	possibly soiling deposits
limit of detection	0.2	0.2	0.2	0.2	0.1	0.1	0.1	0.1	values are also element %

key: X = present, (>2x detection limit) t = trace, (above detection limit) - = not observed (< detection limit)

Table 3.1 – summary of EDS results

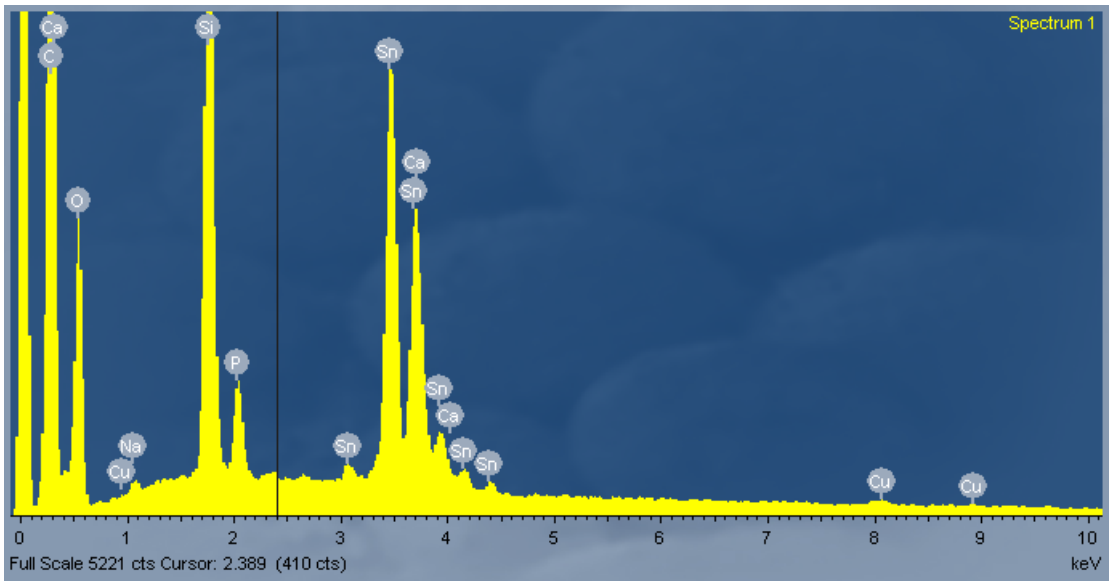

Figure 3.10 – Energy Dispersive X-ray spectrum for sample nlbro9

For EDS analysis of organic materials information can be obtained from a depth of around 5 μm. Heavier elements will absorb the energy reducing the depth to around 1 μm. For nlaeh10, lead, and some of the other elements, may be present as contamination from the paint layer as this is a painted banner, although the unpainted silk on the reverse was analysed. All samples from Audley End House (AEH) showed high levels of sulfur; however one of these samples (nlaeh11) had formed the reverse of a fire screen, so in this example the sulfur may be soot contamination. Sulfur could be present from dust or gaseous pollution as well as processing methods. Although sulfur is found in fibroin, the small amount is below the detection limit of the equipment used.

XRF

To give a better indication of the possible weighting materials present within the English Heritage collection qualitative X-ray Fluorescence Spectroscopy (XRF) analysis was undertaken. The non-destructive nature of XRF enabled a greater number of the English Heritage samples to be analysed. In total seventy nine of the English Heritage samples as well as eight other silks, which were known to be weighted, were analysed. Of the seventy nine samples analysed thirty two contained elements at trace levels or above. Those samples containing an

element at more than twice the baseline value were defined as present and are presented in Table 3.2.

sample id	Si	P	S	K	Ca	Cr	Fe	Sn
nlaeh2	-	-	X	-	t	-	-	-
nlaeh6	-	-	-	-	-	X	-	-
nlaeh10g	-	t	X	-	-	-	-	-
nlbro3	-	-	X	-	-	-	-	-
nlbro8	-	-	X	-	-	-	-	-
nlbro9	t	t	-	t	X	-	-	X
nlful1	X	X	-	t	X	-	-	X
nlful3	t	t	-	t	X	-	-	X
nlful5	X	X	-	X	X	-	-	X
nlful9	-	-	X	-	-	-	-	-
nlful10	-	-	X	-	-	-	-	-
nlosb13	-	-	-	X	X	-	-	X
nlosb14	t	t	t	X	X	-	-	X
nlran2	-	-	X	-	-	-	-	-
baseline (correction element)	0.2 Rh	0.1 Rh	0.25 Rh	0.3 Rh	0.6 Rh	3 Ti	10 Ti	0.4 Rh

key: X = present, (>2x baseline value) t = trace, (above baseline) - = not observed (< baseline)

Table 3.2 – summary of XRF results from English Heritage samples

There are some visible patterns in the XRF results, for example all the samples that contain chromium, including traces amounts, are from modern replicas, either wall silk (nlran7, nlosb29) or materials used in curtains (AEH samples). This is likely to be from the dyeing processes used in the modern fabrics. For a number of samples the results indicate particulate deposits are present, for example nlaeh2, sulfur and trace amounts of calcium suggests inorganic particulates of calcium sulfate. This was also confirmed in some samples imaged and analysed using SEM-EDS.

Trace amounts of gold and lead were found on the gold motif of a painted banner, (sample nlaeh10gold) and probably result from the painted layer. For some samples tin is found in conjunction with silicon and phosphorus (e.g. nlbro9) which implies the Dynamite weighting process has been used to weight the silk. Based on the high levels of tin seen in the XRF results it is probable the following samples from the English Heritage collection are weighted: nlbro9,

nlful1, nlful3, nlful5, nlosb13, nlosb14. It is also possible that nlaps18 and nlbro10 are tin weighted and nlful16 iron weighted as they contain trace levels of these elements.

Some elements are more difficult to assign, such as sulfur. Of the thirty two samples containing elements above trace levels almost all contained sulfur. High levels of sulfur have been reported on shattered silk flags and it is thought that high sulfur rather than weighting materials may cause the deterioration leading to shattering of the silk, but sulfur can also be present due to pollutant contamination. This highlights the uncertainty in the assignment of the source of the elements found by XRF and other elemental analytical techniques.

The *in situ* XRF analysis gave a more comprehensive analysis of objects where only one area could be sampled previously. For example, the festoon curtain in the Little Drawing Room at Audley End House from which a small, cream thread was sampled from a removed section in store. However *in situ* the cream ground and red detail in the decorative bands as well as red flowers (see Figure 3.11) could be analysed giving a greater understanding of the materials present.

Figure 3.11 – detail from the festoon curtain in the Little Drawing Room at Audley End House, numbers indicate representative areas of the different coloured threads analysed

The *in situ* analysis identified a number of different elements in comparison with the sampled threads, for example titanium, cobalt and lead (results are presented in Table 3.3). In some cases these elements may be present due to sampling other materials beneath the textile layer, for example titanium and lead are common in paint and were recorded on spectra from modern replica curtains that are not weighted.

spectrum id	P	S	K	Ca	Ti	Cr	Fe	Co	Cu	Ag	Sn	Au	Pb
aeh1		t		X									
aeh2		t		t			t						
aeh3		t		X			t				t		
aeh4		t						t					
aeh5		t			X								t
aeh6		t				X							t
aeh7		X	t	X									
aeh8	t	X		t					X	X		t	
aeh9	t	t	t	X			t				t		
aeh10		t		t									
aeh11		X							X	X		t	
aeh12		t		t									
baseline (corr. element)	0.1 Rh	0.25 Rh	0.3 Rh	0.6 Rh	0.5 Rh	3 Ti	10 Ti	8 Ti	20 Ti	1 Rh	0.4 Rh	15 Ti	7 Ti

key: X = present, (>2x baseline value) t = trace, (above baseline) - = not observed (< baseline)

Table 3.3 – summary of *in situ* XRF results

Two objects (the green area on the Library ottoman [spectrum aeh8] and counterpane on the Howard Bedroom state bed [spectrum aeh11]) contained metal threads with copper, silver and trace amounts of gold identified. The position of these metal threads within the artefacts means sampling to determine the composition would not have been possible. *In situ* analysis enabled different coloured threads within designs to be identified for example on the Ottoman in the library, which had not been sampled; metal threads, the cream ground and red rose details could all be analysed and differentiated. This is a clear advantage of *in situ* analysis with the portable XRF providing a greater understanding of the object being studied. A single sample, taken from a removed section of fabric or damaged area, cannot be assumed to be representative of the whole. Therefore some of the differences seen between

the *in situ* and sample results may be due to the sample being non-representative.

Atomic Absorption Spectroscopy

Atomic absorption spectroscopy (AAS) results for the zinc solutions made from model samples gave values between 0 and 2.5 ppm. However the XRF peak area ratios (Zn/Ti) range from 4.8 to 6 with no discrimination on increasing zinc concentration. This indicates that the portable XRF cannot detect the presence of zinc below a level equivalent to 2.5 ppm in the solutions prepared from the model samples. A detection limit of 2.5 ppm in the solution relates to a concentration of 2.5×10^{-5} mg mm^{-2} in the silk samples. For sample nlosb12, which had a high intensity peak for zinc (peak area ratio [Zn/Ti] = 15), this means it contains in excess of 2.5×10^{-5} mg mm^{-2}.

For iron AAS the solutions from the prepared model samples measured concentrations in the 1 – 3 ppm range. For comparison the solution from the untreated silk sample gave a concentration of 0.2 ppm. There is a linear increase in the iron concentration above 1.5 ppm (see Figure 3.12). This correlates to an XRF (Fe/Ti) peak area ratio above 5 for the model samples. For the silk samples this is approximately equivalent to an iron concentration of 1.5×10^{-5} mg mm^{-2}.

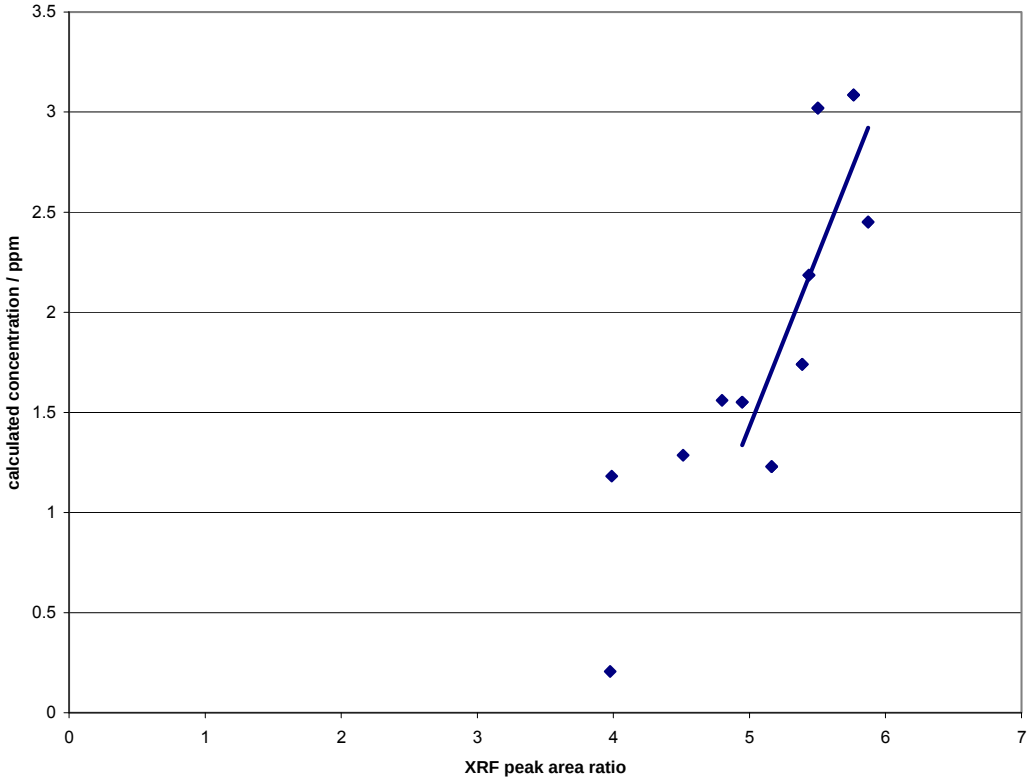

Figure 3.12 – AAS calibration of iron model samples with XRF results
(line shows linear least squares best fit to the data points above 1.5 ppm)

The samples which were known to be weighted with iron, PGiii3 and PGiii1iv1i1, were diluted numerous times to be within the range of the prepared AAS standards (1 to 5 ppm). When this is taken into account the solutions from these samples contain 112 and 45 ppm respectively. The known weighted samples have much greater XRF peak ratios compared with the prepared model samples (see Figure 3.13) and English Heritage historic samples. Although this helped identify the spectra which contain iron it is not possible to determine whether iron is present as a mordant, weighting agent or from contamination.

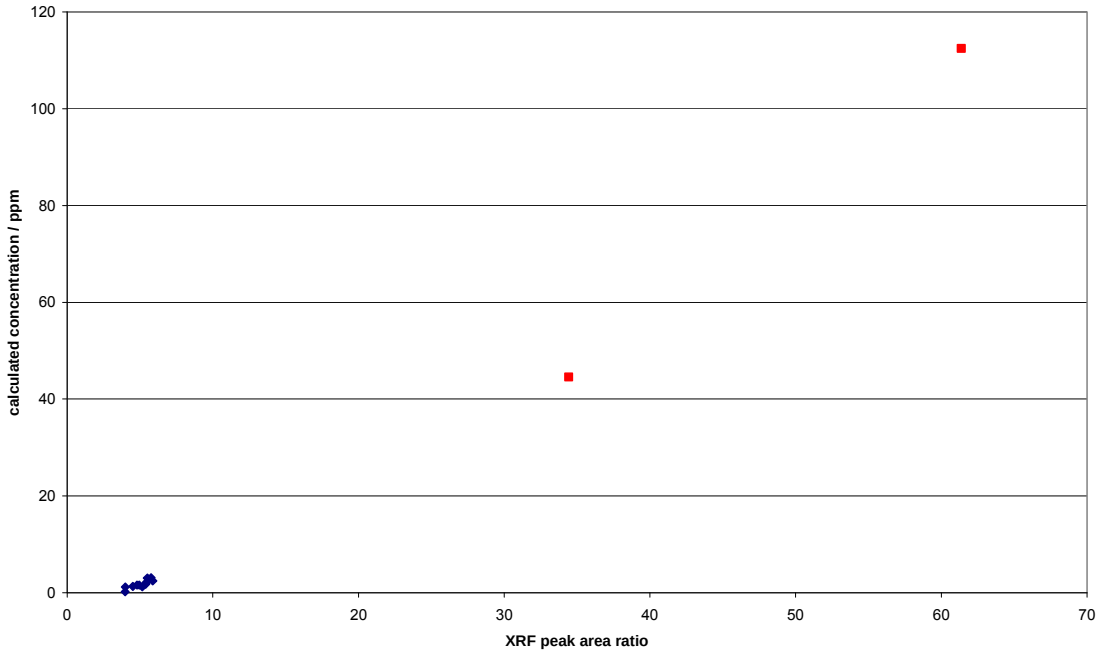

Figure 3.13 – AAS iron calibration from XRF results

(model samples: blue; PG samples: red)

ICP-OES

The solutions from the model samples contained an increasing amount of tin from 0 to 14 ppm (see Figure 3.14). The solutions from the weighted samples varied between 1 to 35 ppm.

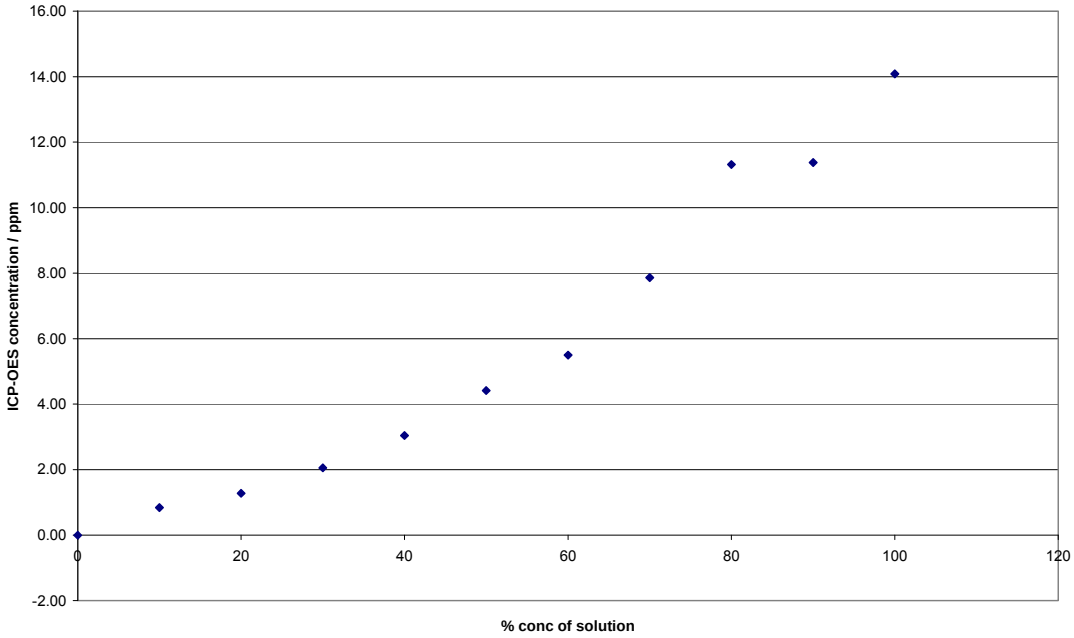

Figure 3.14 – tin ICP-OES results from model samples

Plotting the ICP-OES concentrations against the XRF peak area ratio (Sn/Rh) gives an approximate linear increase for the model samples, with the exception of the untreated sample (see Figure 3.15).

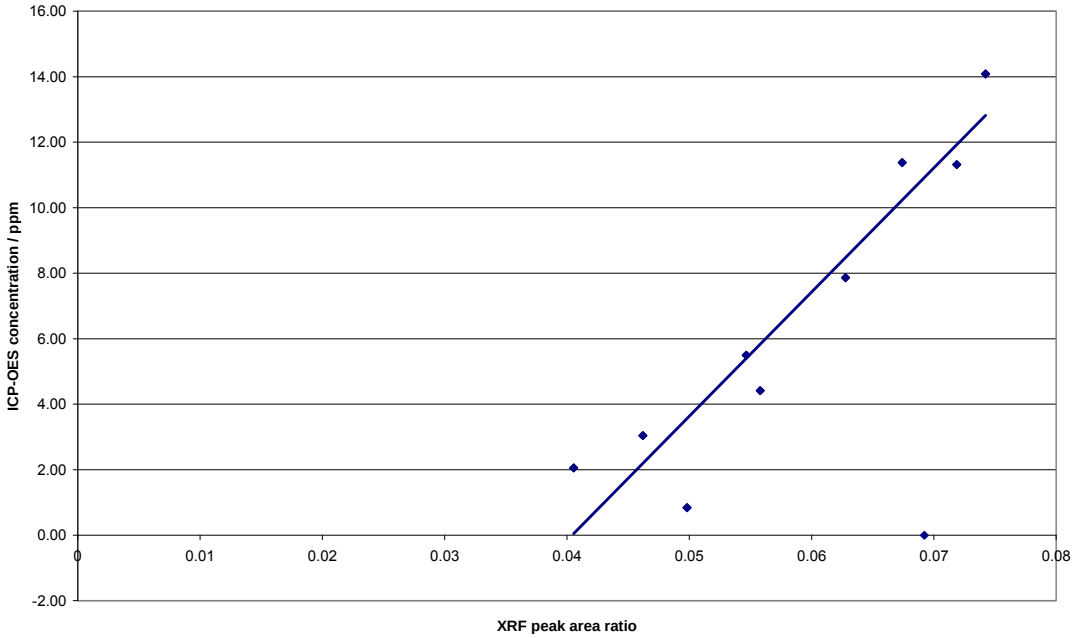

Figure 3.15 – tin XRF calibration with ICP-OES results for the model samples

However when the known weighted samples are included (Figure 3.16) the much higher XRF ratios do not correlate with the low tin concentrations measured by ICP-OES. It is possible the elements have precipitated out of solution or did not pass through the filters during preparation of the samples. However it would be unlikely this would occur for some and not all of the samples. The higher ICP-OES tin concentrations occur when the dynamite tin weighting process has been used. When comparing the results of the standard weighted silk samples the AAS results give higher tin concentrations when iron is not present. This may arise from the same iron interference effect seen at 235 nm (the AAS tin detection wavelength) in the ICP-OES analysis. There are no obvious trends in the XRF data. However this and the scatter in the XRF calibration line using the ICP-OES results, suggests caution should be used when trying to assign concentrations of elements to analysed textile samples.

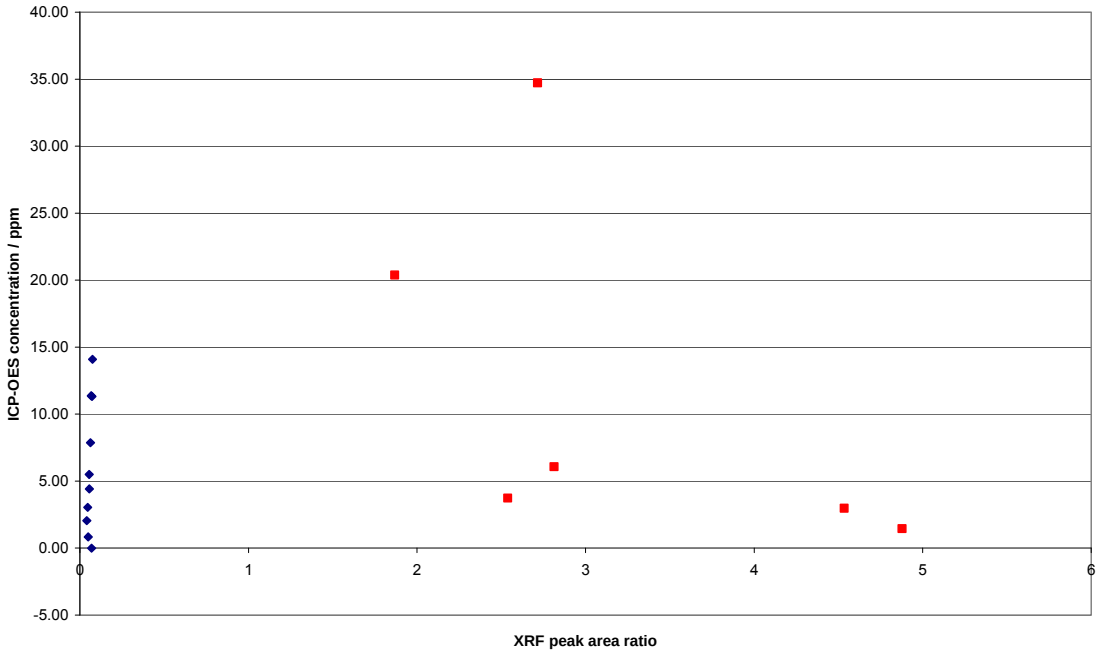

Figure 3.16 – tin XRF calibration with ICP-OES results

(model samples: blue; PG samples: red)

The difficulties in providing a suitable and reliable calibration for samples that are known to be weighted (prefixed PG) means it has not been possible to determine quantitative results. In relation to the English Heritage samples

qualitative results from XRF analysis comparing elemental peak areas to those of rhodium or titanium provide the most useful information. These indicate eight of the historic samples and the six known weighted samples contain tin indicating a small amount of the collection is weighted silk.

Comparison of Techniques

Due to the rapidity and ease of the XRF analyses, this technique enabled a much greater number of samples to be analysed than with SEM-EDS. Only a limited number of samples were analysed using both techniques. There are some similarities, for example nlbro9 where tin, calcium, silicon and phosphorus were identified. For nlosb13 and nlosb14, tin is identified by both techniques, however for nlosb14 copper was observed with SEM-EDS and not by XRF. In the case of nlaeh10 the SEM-EDS found tin and lead in the painted layer. In the XRF analysis these elements were not identified above the baseline although the paint layer had slightly greater amounts of both tin and lead than the unpainted side. It is unclear why there are differences between the results of the two techniques but variations in the detection limits or sampling depths are both possible.

Although only a very limited number of objects could be both sampled and analysed *in situ* some comparisons are possible. The majority of the reproduction material analysed contained chromium, however *in situ* lead and titanium were also identified, as discussed above. For sample nlaeh1, and the corresponding *in situ* analysis aeh1, there was a slight difference with calcium found *in situ*. However the sample was removed from a cleaned section kept in storage and therefore less likely to contain dust than the curtain on permanent display.

Due to the limited number of samples analysed using EDS it is hard to compare the results with those from the XRF analysis, but three samples were shown to contain tin using both methods these are: nlbro9, nlosb13 and nlosb14.

Conclusions

In order to better understand the causes of silk deterioration and therefore to improve the preventive conservation measures it will be necessary to use materials that are found in the English Heritage collection during accelerated ageing experiments. The results have indicated that plain silk dominates, however around 10% of the samples from the collection contained tin, which implies there is a limited amount of weighted materials.

It has been possible to identify elements present within silk textiles both from micro-samples and whilst on display. On-site investigation has not only given a more complete picture of the collection, but also enabled a comprehensive study of the objects. This included selective analysis of differently coloured threads and areas of decoration, such as metal threads. The sampling otherwise needed to obtain this detailed information would generally be ethically unacceptable. This has demonstrated analysis is possible without sampling but interpretation of the elements present can be affected by the presence of other materials such as dust.

Although inorganic elements constituting weighting agents may be readily detected, quantification is not so straightforward. This can have a bearing on the assignment of a detected element to a particular source e.g. mordant, weighting agent or pollutant. Further work would be necessary to definitively determine the process used to incorporate the elements identified using XRF. However XRF analysis may be readily applied to identify objects with possible inherent deterioration mechanisms for example, silks containing tin and enable prioritising of treatments or areas of improvement for preventive conservation.

References

[1] Palmer, A. (2006) ‘’A bomb in the collection’: researching and exhibiting early 20th-century fashion’ in *The Future of the 20th Century. Postprints of the AHRC*

Research Centre for Textile Conservation and Textile Studies Second Annual Conference July 2005, Rogerson, C. and Garside, P. (ed.) London: Archetype 41-47.

[2] Hacke, M. (2008) 'Weighted silk: history, analysis and conservation' *Reviews in Conservation* **9** 3-15.

[3] Hacke, A.-M., Carr, C. M. and Brown, A. (2004) 'Characterisation of metal threads in Renaissance tapestries' *Metal 04* Canberra: National Museum of Australia 415-426.

[4] Indicator, N., Koestler, R. J. and Sheryll, R. (1985) 'The Detection of Mordants by Energy Dispersive X-Ray Spectrometry Part I. Dyed Woolen Textile Fibers' *Journal of the American Institute of Conservation* **24** 104-109.

[5] Koestler, R. J., Indicator, N. and Sheryll, R. (1985) 'The Detection of Metallic Mordants by Energy Dispersive X-Ray Spectrometry Part II. Historical Silk Textiles' *Journal of the American Institute of Conservation* **24** 110-115.

[6] Koestler, R. J., Sheryll, R. and Indicator, N. (1985) 'Identification of Dyeing Mordants and Related Substances on Textile Fibers: A Preliminary Study Using Energy Dispersive X-ray Spectrometry' *Studies in Conservation* **30** 58-62.

[7] Bresee, R. R. and Telthorst, L. A. (1982) 'Energy dispersive X-ray fluorescence and neutron activation analysis of historic silk textiles' CCI Unpublished Technical report.

[8] Srinivasan, R. and Jakes, K. A. (1997) 'Examination of Silk Fibers from a Deep Ocean Site: SEM, EDS, & DSC' *Material Research Society Symposium Proceedings* Washington D.C.: Materials Research Society **462** 375-380.

[9] Ballard, M. W., Koestler, R. J. and Indicator, N. (1990) ' Recent results concerning the degradation of historic silk flags' *ICOM Committee for Conservation 9th Triennial Dresden, German Democratic Republic, 26-31 August 1990 Preprints* Paris: ICOM Committee for Conservation 277-282.

[10] Stuart, B. H. (2007) 'Scanning Electron Microscopy' in *Analytical Techniques in Materials Conservation* Chichester: John Wiley & Sons, Ltd 91-100.

[11] Koch, P.-A. (1963) *Microscopic and Chemical Testing of Textiles*, London: Chapman and Hall **155** 153-158.

[12] Masschelein-Kleiner, L. and Maes, L. R. J. (1978) 'Ancient Dyeing Techniques in Eastern Mediterranean Regions' *ICOM Committee for Conservation 5th Triennial Meeting, Zagreb, 1-8 October 1978 Preprints* Paris: ICOM 78/9/83.

[13] Wakui, M., Yatagai, M., Kohara, N., Sano, C., Ikuno, H., Magoshi, Y. and Saito, M. (2001) 'ICP-AES and X-ray fluorescence determination of mordants on fabric dyed with natural dyes' *Bunkazai Hozon Shufuku Gakkai shi: kobunkazai no kagaku* **45** 12-26.

[14] Tonini, C., (1978) 'Atomic Absorption Spectrophotometry in the Textile Chemistry Laboratory' *Tinctoria* **75** 160-162.

[15] Williams, E. T. and Indicator, N. (1986) 'Detection of Metallic Mordants on Textiles by Particle-Induced X-Ray Emission' *Scanning Electron Microscopy* **3** 847-850.

[16] Miller, J. E. and Reagan, B. M. (1989) 'Degradation in Weighted and Unweighted Historic Silks', *Journal of the American Institute of Conservation* **28** 97-115.

[17] Dussubieux, L. and Ballard, M. W. (2005) 'Using ICP-MS to Detect Inorganic Elements in Organic Materials: A New Tool to Identify Mordants of Dyes on Ancient Textiles' *Materials Issues in Art and Archaeology VII* Materials Research Society Symposium Proceedings **852** Warrendale PA: Materials Research Society 291-296.

[18] Dussubieux, L., Naedel, D., Cunningham, R., Alden, H. and Ballard, M. W. (2005) 'Accuracy, Precision and Investigation: mordant analysis on Antique Textiles by Various Methods' *ICOM Committee for Conservation 14th Triennial Meeting, The Hague, 12-16th September 2005 Preprints* Verger, I. (ed.) London: James & James Ltd **2** 898-903.

[19] Robson, R. M. (1999) 'Microvoids in *Bombyx mori* silk. An electron microscope study' *International Journal of Biological Macromolecules* **24** 145-150.

[20] Sen, K., Babu K, M. (2004) 'Studies on Indian Silk. I. Macrocharacterization and Analysis of Amino Acid Composition' *Journal of Applied Polymer Science* **92 (2)** 1080-1097.

[21] Becker, M. A., Hersh, S. P. and Tucker, P. A. (1987) 'The Influence of Tin Weighting Agents on Silk Degradation Part 1 Inorganic Weighting and Mordanting Agents in Some Historic Silk Fabrics of the 18th and 19th Centuries' *ICOM Committee for Conservation 8th Triennial Meeting, Sydney, Australia, 6-11th September 1987, Preprints* Marina del Ray, C.A.: Getty Conservation Institute **1** 339-344.

[22] Skelton, M. (1995) 'Use of Qualitative Nondestructive X-Ray Fluorescence Analysis in the Characterization of Chinese or Western Provenance for 18th-Century Painted/Printed Silk' *The Conservation of 18th-Century Painted Silk Dress*, Paulozik, C. and Flakerly, S. (ed.) New York: Metropolitan Museum of Art 6-15.

[23] Gardiner, J., Carlson, J., Eaton, L. and Duffy, K. (2000) '"That fabric seems extremely bright": non-destructive characterization of nineteenth century mineral dyes via XRF analysis' *Conservation Combinations: Preprints North American Textile Conservation Conference 2000, Asheville, North Carolina, March 29-31 2000.* Asheville, N.C.: Biltmore House 100-115.

[24] Odegaard, N., Smith, D. R., Boyer, L. V. and Anderson, J. (2006) 'Use of handheld XRF for the study of pesticide residues on museum objects' *Collection Forum* **20** 42-48.

[25] O'Connor, S. personal communication, 06/03/2008.

[26] O'Connor, S. and Maher, J. (2007) 'Assessing the Risks of X-Radiography to Textiles' in *X-Radiography of Textiles, Dress and Related Objects* O'Connor, S and Brooks, M. M. (ed.) Oxford: Butterworth-Heinemann 91-95.

[27] Stuart, B. H. (2007) 'X-Ray Fluorescence Spectroscopy' in *Analytical Techniques in Materials Conservation* Chichester: John Wiley & Sons, Ltd 234-243.

[28] Stuart, B. H. (2007) 'Atomic Absorption Spectroscopy' in *Analytical Techniques in Materials Conservation* Chichester: John Wiley & Sons, Ltd 209-213.

[29] U.S. Environmental Protection Agency (EPA) methods 282.1 Tin (Atomic Absorption, Direct Aspiration) and 282.2 Tin (Atomic Absorption, Furnace

Technique) http://www.caslab.com/EPA-Methods/?term_search=&page=4 accessed 28/07/2009.

[30] Stuart, B. H. (2007) 'Atomic Emission Spectroscopy' in *Analytical Techniques in Materials Conservation* Chichester: John Wiley & Sons, Ltd 213-216.

Chapter 4 – Analysis of silk

A variety of methods have been used to characterise and study silk and its properties. A number of references focus on determining the structure and properties of gland silk or regenerated silk films. However, these methods are often also applicable to the analysis of historic silk. This chapter discusses a number of techniques including the information they provide and their appropriateness to the analysis of historic silk collections.

Silk degradation affects a number of properties including molecular weight, crystallinity and crystal orientation. When considering which property to measure it is necessary to determine what changes will occur on ageing and whether these can be followed easily and with enough accuracy. When working with historic collections whether a technique is non-destructive and the size of sample required are also significant requirements. A large number of analytical techniques and their use within conservation have been discussed by Stuart, for each method below the appropriate pages within this reference are cited.[1]

X-ray Diffraction

Silk has long been studied with X-ray diffraction (XRD)[2] methods because of the interest in determining the structure of the beta-pleated sheet and the role of the high number of simple amino acids found in the crystalline region.[3,4,5,6,7,8] More recently studies have correlated synchrotron[a] XRD with tensile testing and confirmed that deformation occurs in the amorphous region of silk,[9] the viscoelastic properties of silk have also been modelled.[10] Synchrotron radiation microbeam

[a] Synchrotron radiation is an intense light emitted by high energy electrons when their trajectory is changed by a magnetic field. This light source has a spectral range from infrared to X-rays, alongside a small beam size, little diversion and a high flux. As a result it can be used to study very small samples, low concentrations of elements within samples, or to produce maps of elements across samples at much greater speeds.

XRD has been used to analyse excavated ancient silk fibres. These fibres are described as being in a very poor state of preservation however the XRD pattern does not change much with alteration to the silk. This suggests that the crystalline regions are not affected even when deterioration have caused noticeable changes to the mechanical properties of the silk.[11] Using polarized infrared spectroscopy, the crystal orientation parameter can be determined at the same time. This is the ratio of the apparent crystallinities in the fibre measured in the parallel and perpendicular positions and decreases with increasing age of the fibre. For aged silks the orientation parameter has also been correlated with the breaking strength.[12] Only once the deterioration is severe are the crystalline regions attacked. XRD has also been used to determine changes in crystallinity brought about by treatment of silk with iodine. This is thought to enter the amorphous region, disrupting the hydrogen bonding and reducing the crystallite orientation.[13]

Wide Angle X-ray Scattering (WAXS) has been used to determine the effect of temperature on silk structure.[14] With increased scattering from the voids in silk observed as it deteriorates at high temperatures. Synchrotron radiation based Small Angle X-ray Scattering (SAXS) and WAXS have been used to follow the structural changes occurring in regenerated silk fibroin under shear[15] as well as to characterise the decay of ancient Chinese silks.[16] An initial increase in the crystallinity occurs on the loss of the amorphous regions. However as silk continues to decay the crystals are free to move and become increasingly disordered. This led to a widening of the distribution of crystalline orientation and eventually a shift in the peak position with greater decay.

Kennedy *et al*. used SAXS and WAXS to determine changes in the crystallinity of silk after laser cleaning.[17] This work demonstrated that crystallinity decreased upon laser exposure with a corresponding increase in the crystal size. The data was obtained without synchrotron radiation, but the disadvantages of this method include the dramatically increased time of analysis and that the samples must be under vacuum. SAXS has been used to study the effect of weighting treatments

on silk fibres[18] along with demonstrating the presence of nanofibrils.[19] A limitation of these techniques is their availability, especially for synchrotron radiation XRD, for which obtaining beamtime may be a severe constraint. This is important as to study the changes in condition of historic silk information on the crystallite orientation is required and this can be most easily obtained using synchrotron radiation XRD. The advantage is the small sample size required as synchrotron radiation XRD is capable of investigating individual fibres, it is also non destructive as it can be performed in air.

Amino Acid Analysis

Alongside XRD studies on silk there were a number of studies using amino acid analysis[20] to determine the composition of both *Bombyx mori* and Tussah silk fibroin.[21,22,23,24,25,26] As well as studying the composition of silk, amino acid analysis has also been used to follow changes after UV light exposure.[27,28] After light ageing samples were hydrolysed before analysis using ion-exchange high performance liquid chromatography (IE-HPLC).[29] With increased light exposure amounts of hydrolysable serine and tyrosine decreased, there was also a corresponding increase in the amount of hydrolysable ammonia. Other amino acids were reported to show no change with light exposure. The loss of tyrosine on light ageing has also been recorded by other authors.[30,31] Analysis demonstrated accelerated light ageing had a much greater effect on the amount of tyrosine than dyeing or mordanting processes for model silk tapestries. This work also found the historic samples analysed had less tyrosine present than the artificially light aged samples.

Using amino acid analysis, Becker *et al*. recorded greater amounts of tyrosine when a large serine (found in much greater quantities in sericin, than in silk) content was also observed. They suggested that sericin may have a protective effect on silk, against light exposure.[32] However, sericin yellows upon light exposure and due to its solubility in water a sericin coating is at great risk from wet

conservation treatments. Japanese garments analysed showed a greater state of preservation compared with American First Ladies dresses of similar dates. The authors suggest that that the reverence and preventive care practised by the Japanese in caring for kimonos is the reason for the good condition of the silk.[33] One of the advantages of this method described by Becker and Tuross is the small sample size, in the microgram range. Yanagi *et al.* have used amino acid analysis, along with a number of other techniques to study changes to silks including a naturally aged 400 year old sample. This showed the greatest loss to tyrosine and phenylalanine, with much smaller reduction in glycine and alanine.[34] This demonstrates the applicability of this technique to study silk deterioration with potentially microgram samples.

Molecular Weight Analysis

As silk degrades the average molecular weight decreases due to polymer chain scission, allowing the deterioration to be followed. To determine the molecular weight silk has to be dissolved however if the polymer chains are broken the results will not reflect the deterioration of the sample after ageing but the effect of the solvent. Lithium thiocyanate disrupts the hydrogen bonds between the chains, without damaging the main polypeptide chains. The dissolved polymer can then be analysed with high performance size exclusion chromatography (HPSEC)[35] and the molecular weight distribution determined by comparison to standards of known molecular weight. Figure 4.1 shows a typical HPSEC chromatogram of silk dissolved in lithium thiocyanate. As HPSEC is affected by the size of the polymer, urea is used to denature the polymer chains ensuring they are the same shape, and extended rather than globular, which is reported to improve the separation.[36] Similar to amino acid analysis this method requires small samples. Work by Hallett and Howell reduced the quantity of silk required for this method to 0.2 mg.[37]

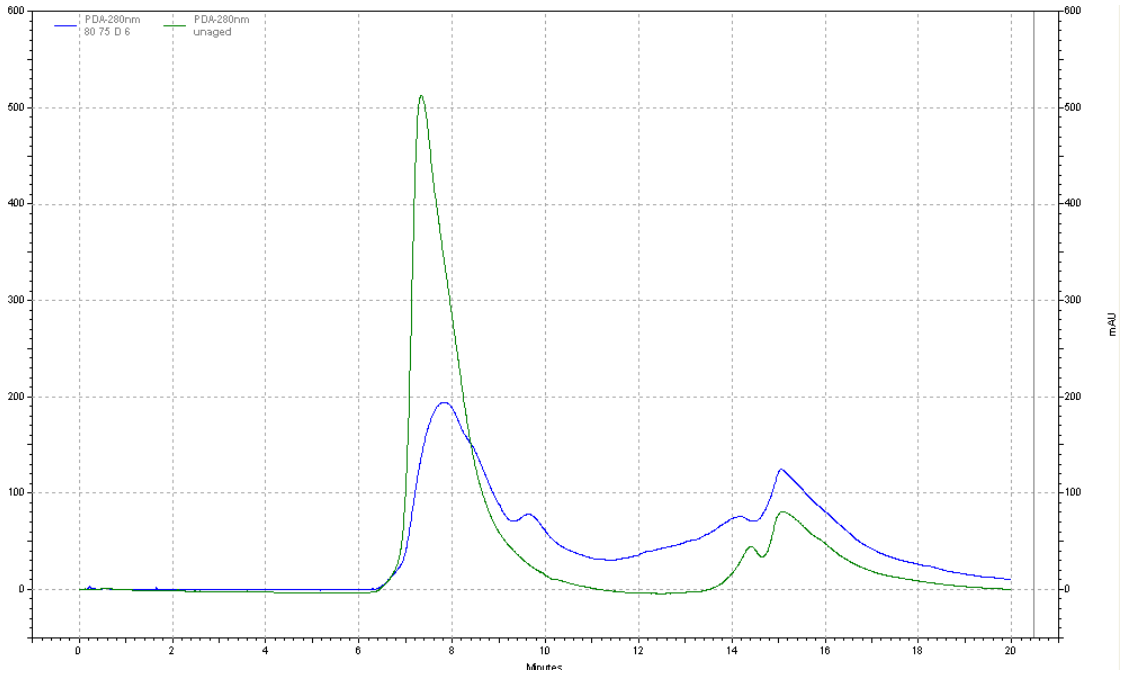

Figure 4.1 – HPSEC chromatogram of silk (the peak at ~15 min is lithium thiocyanate) (unaged silk: green; aged silk: blue)

Hallett and Howell have shown that dyeing and mordanting processes cause a decrease in the molecular weight of silk.[38] Black samples show a significant deterioration after dyeing. Samples from model tapestries showed further decreases in molecular weight after artificial light ageing. However historic samples showed much lower molecular weights than the accelerated aged samples.[37,38] The authors' note this was not expected as the samples were selected from the reverse of historic tapestries and were not faded. This suggests that HPSEC will provide information on the condition of all silks regardless of the mechanism of deterioration. Data from molecular weight analysis has shown good correlation with both percentage extension and breaking strength.[39] A limitation for this technique is that it can only be used on *Bombyx mori* silk as attempts at solubilising wild silks have so far been unsuccessful. It is also reported to be unsuitable for the analysis of weighted silks.[40] Studies with sodium dodecyl sulfate (SDS) polyacrylamide gel electrophoresis,[40,41,42,43,44,45] and agarose-guanidine chromatography[46] have also determined the molecular weight of silk.

Fourier Transform Infrared Spectroscopy

Fourier Transform Infrared (FTIR) spectroscopy[47] has been used to follow changes in the amide I at 1635 cm^{-1} and amide II peak at 1520 cm^{-1} (arising from the α(C=O) and α(N-H) vibrations).[48] As silk degrades the peaks are reported to decrease in intensity before forming a single peak when heavily deteriorated.[49] The structure of silk was studied by Elliot and Malcolm using infrared spectroscopy[50] and structural changes to silk under stress have been studied with dynamic step scan FTIR.[51] FTIR has also been used to monitor conformation transitions between silk I and II, which have been observed by changes in the amide I peaks.[52] However it has been reported that it is difficult to differentiate between random coil and silk I conformations using FTIR. More recently changes in the tyrosine absorption with light ageing have been recorded.[53,54] The effect of pulverization to form silk powders, for the cosmetic industry and biomaterials research, has also been followed using FTIR.[55] These studies demonstrate that the conformation and structure of silk can be observed with FTIR, allowing the changes upon deterioration to be followed. An example FTIR absorbance spectrum for silk can be seen in Figure 4.2.

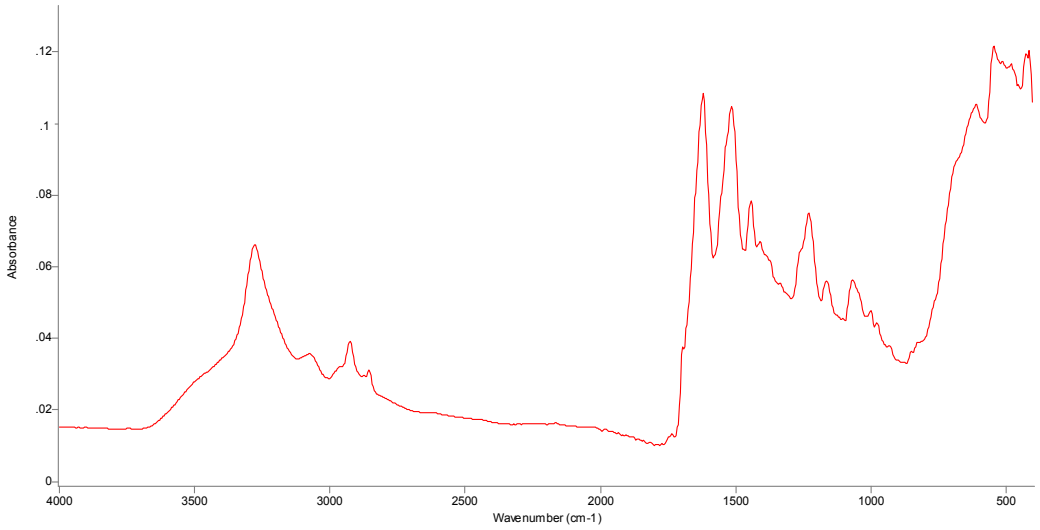

Figure 4.2 – absorbance FTIR spectrum of silk

The polarised infrared spectrum of silk fibroin was recorded by Suzuki who demonstrated treatment with deuterium oxide had no effect on the dichroic components indicating the crystalline region was not affected.[56] Dichroism in silk has also been reported by Ambrose and Elliott.[57] Attenuated total reflectance (ATR)[58] has been used to study sericin and the effects of solvent treatment on orientation.[59] More recently it has been reported that the conventional FTIR spectra show little change for aged silk samples although changes were observed in the polarised spectra. It is suggested that the crystallites are able to move and reorient due to the loss of the amorphous regions. This method has been developed to analyse changes in silk on ageing and is known as polarised attenuated total reflectance FTIR (Pol-ATR). This has the advantage of being non-destructive and in certain circumstances it may also be possible to use non-invasively.

Using pol-ATR Garside *et al*. have defined a crystallinity index, X, based on the intensity ratios of the amide I band at the theoretical maxima for the β-sheet (1615 cm^{-1}) and α-helix / random coil (1655 cm^{-1}) motifs, $X = I_{\beta}/I_{\alpha}$.[60] An orientation parameter has been defined, $\Omega = X_{90^\circ}/X_{0^\circ}$, from the crystallinity indices measured with the fibre perpendicular (X_{90°) and parallel (X_{0°) to the incident electric vector. Higher values of Ω are reported to reflect a greater alignment of the β-crystallites in fibroin to the fibre axis. However the fibres must be completely degummed for the technique to be used and axially aligned in the yarn. This means it is difficult to use on fragile materials. This technique has been further developed to quantify the conformation of silk and determine the orientation of a silk fibroin filament.[61]

Near-Infrared Spectroscopy

FTIR spectroscopy commonly uses mid-infrared (400-4000 cm^{-1}) however near-infrared (4000-13,000 cm^{-1}) instruments are also available. Near-infrared (NIR) spectroscopy has become increasingly utilised due to the rapid collection of

spectra and its non-destructive nature.[62,63] However the technique requires large datasets for comparison when used for identification purposes.[64] NIR spectra are complex combinations of peaks making interpretation complex (see Figure 4.3) and often multivariate analysis (MVA) is required to study differences between spectra.[65] Similar statistical methods have been applied to study silk properties.[66] NIR spectroscopy with multivariate analysis has been used to study the level of degumming achieved during processing.[67]

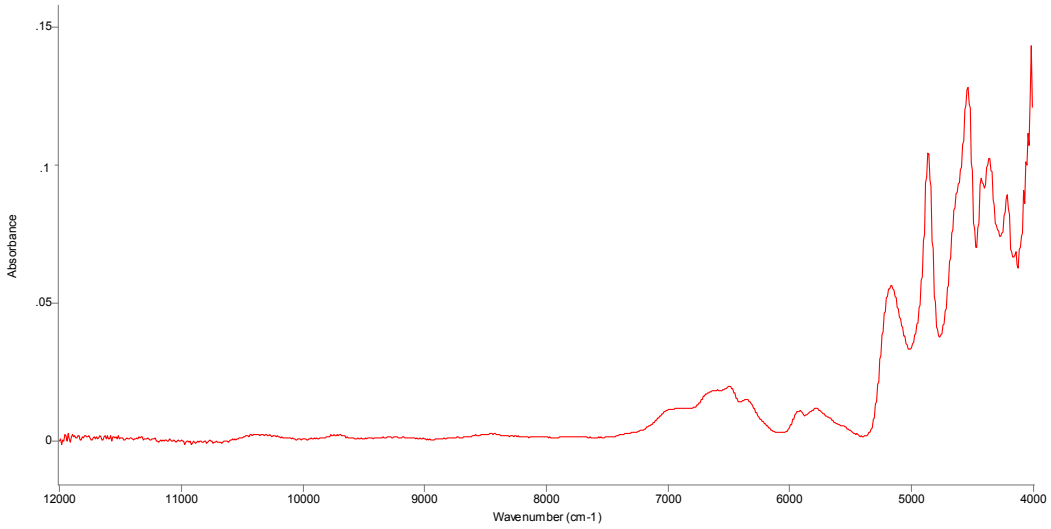

Figure 4.3 – NIR spectrum of silk

Amide bands have been assigned within NIR spectra[68] and used to characterise the secondary structure of silk, most notably in regenerated silk films.[69] Changes to water bands upon exposure to deuterium oxide have been observed using NIR spectroscopy.[70] The authors report the intensity of the band at 5170 cm^{-1} changed based on the ageing method used and propose this as a condition marker for historic silks in collections. Portable NIR spectrometers are available and the use of fibre optic probes enables spectra to be collected non-invasively, this makes it suitable for use within collections.

Raman Spectroscopy

Raman Spectroscopy[71] has been used similarly to FTIR, to determine structural changes in fibroin by shifts in the positions and ratios of amide bands.[72,73,74,75,] Changes in the tyrosine bands for silk after UV / ozone irradiation have also been observed using FT-Raman.[76] Shao *et al*. also reported a reduction in intensity of the C-N bond vibration after irradiation and suggest this may be due to peptide chain scission. Monti *et al*. have commented on the difficulty of separating silk I and random coil conformations using the amide I and III bands in the Raman spectrum.[77] This group have also determined changes in the tyrosine bands depending upon its location within silk and therefore concluded whether it was acting as an electron donor or acceptor. Monti *et al*. have described bands in the Raman spectra that could be used to identify silk I conformations.[78] More recently polarized Raman spectra have been used to assess the molecular orientation of silk fibres in regenerated silk films.[79,80] FT-Raman spectra have been collected at various stages of silk processing,[81] but not yet been reported for historic materials. However most of these studies have been carried out on undyed silk and Raman spectroscopy is commonly used to analyse dyes. Therefore possible fluorescence and spectra from any dyes present in the silk may limit the usefulness of this technique for analysis of the condition of historic silk samples.

Mechanical Testing

Mechanical testing[82] methods are commonly used to study the effects of conservation treatments however these are undertaken on model test materials due to the large sample required.[83,84] An example extension load curve can be seen in Figure 4.4. The effect of processing methods, such as different degumming treatments[85] and dyes and mordants[86] have also been assessed using mechanical properties to determine the level of damage caused. As samples from historic collections are rarely available tensile testing is often not undertaken.[27,87] Where analysis of modern surrogate materials is undertaken it is

often correlated with other techniques, such as FTIR. This is used so micro-samples taken from objects can be analysed non-destructively and provide information on the mechanical properties that could not be obtained from the actual object. Mechanical properties of silk are affected by the moisture content,[88,89] as a result there is a standard test environment.[90] Practical considerations for the mechanical testing of textiles have been discussed by Saville.[91]

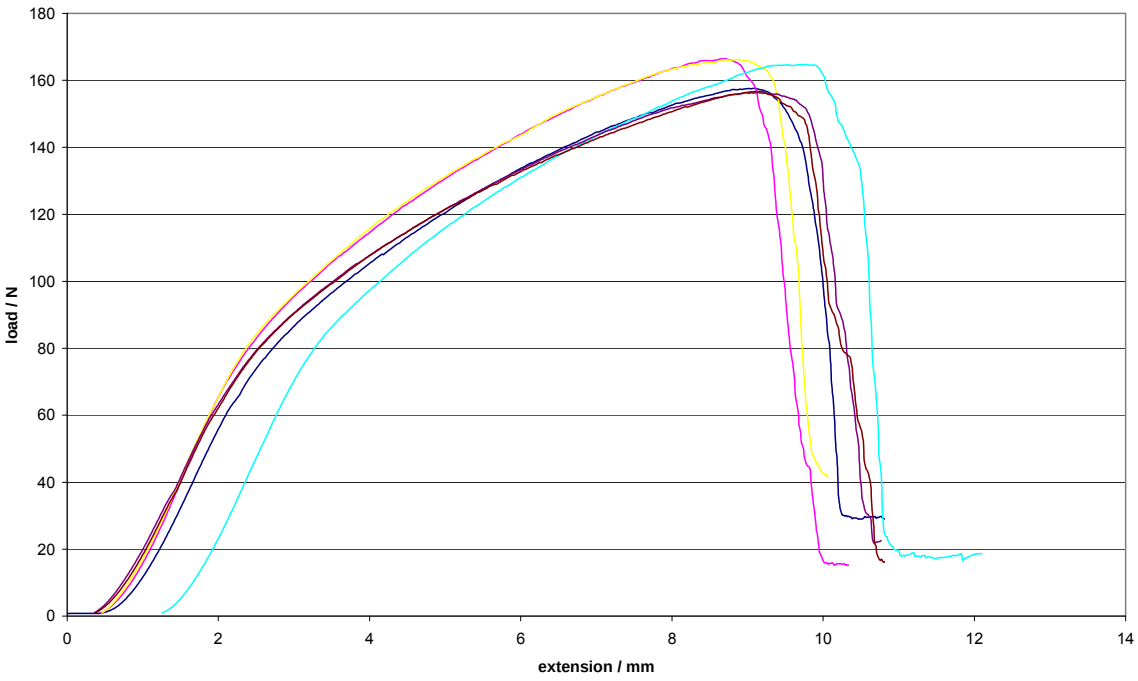

Figure 4.4 – mechanical testing (extension vs. load curve) of unaged silk
(6 replicates analysed at 21.5 ± 0.5 °C and 49.5 ± 1.5% RH)

The tensile behaviour of both natural and synthetic fibres have been determined by Meredith who found silk had high strength and extension, comparable with nylon.[92] Mulberry silk has been shown to have a higher tensile and twist strength compared with Tussah.[93] The authors suggest the performance of Tussah is due to poor orientation arising from a greater number of bulky groups in the fibroin. Tensile strain analysis combined with synchrotron XRD have also been used to study the deformation of silk fibres as discussed above.[9,10] The use of complementary techniques can provide further information on the changes occurring during

mechanical testing.[94] This can increase the understanding of how the fibre changes and what causes the eventual failure of the material.

Thermal Analysis

Thermal methods, such as differential scanning calorimetry (DSC)[95] have been used to determine the glass transition temperature (T_g) of a number of species of silkworm.[96,97,98] The loss of water around 100°C has also been measured using DSC,[99] thermogravimetry (TG)[100] and differential thermal analysis (DTA)[96,101,102] along with the breaking of intramolecular and intermolecular hydrogen bonds between 150 and 180°C.[101,102] FTIR analysis alongside the T_g has been used to quantify the amount of β-sheet crystals in silk[103] and the changes in crystallinity on heating silk have been monitored with XRD and correlated with DSC results.[104] Temperature effects have also been studied by Zhang *et al*. who used thermogravimetry, differential thermal analysis, Fourier transform infrared absorption spectrometry (TG-DTA-FTIR) and report yellowing of silk fibres and cocoons close to the T_g followed by blackening as the fibre degrades.[105]

On ageing the T_g of silk changes which can be recorded with DSC, with artificial light ageing reported to move the T_g to higher temperatures.[106] The peak area for the exothermic peak (210-420°C) is also affected, decreasing after both artificial and natural ageing. The changes in thermal properties are reported to reflect the changes to the chemical composition caused by ageing. Changes to the T_g have also been reported for marine, historic and modern silks.[107] Thermal techniques, although requiring small samples, give limited information on the condition of the silk and therefore may be difficult to interpret.

pH

Conservators often determine the pH of textiles as high acidity can be an indication of deterioration. Work by Kim *et al*. has attempted to use pH as a

measure of silk condition.[108] The authors report surface pH values do not reflect the bulk silk acidity well and instead use a saline extract from a small sample of silk. This is reported to show good correlation with the tensile strength of the silk artificially aged using light and high humidity and the earlier time points of thermal ageing. However changes in pH can also be caused by the presence of contamination, such as dust, which can be common in historic materials on open display and may be difficult to separate from the silk deterioration.

Silk is reported to be most stable to light at pH 10, which was important due to the materials used in commercial finishing of silk.[109] More recent studies on changing pH in gland silk have demonstrated the effect of pH on the conformation of silk for both silkworms and spiders.[110,111,112,113] This has been developed to characterise the structural changes in silk fibroin with varying pH, monitored using both Raman and NMR two-dimensional (2D) correlation spectroscopy .[114] Simple pH tests provide limited information on the condition of fibres and the effect of contamination cannot be easily separated reducing the usefulness of this method.

Fibre Fractography

Scanning electron microscopy (SEM)[115] has been used to study the fibre fractures and provide information on the cause of the type of damage.[116] For unaged modern silk a study found the majority of samples had fracture Type 7 (see Figure 4.5), which is reported as developing from surface flaws.[117] The authors indicate that light might increase or enhance the surface flaws within the fibres. For artificially heat aged samples Type 5 fractures (loss of cohesion between fibrils) became the most common. All the modern samples had a similar amount (10%) of fractures with large internal voids which was assigned Type 11. Eighteen categories of break have been identified and illustrated by Hearle *et al*.[118]

Type 5 Type 7 Type 11

Figure 4.5 – fracture types for silk (redrawn from Breese and Goodyear)

The naturally aged historic samples had more variation in the fracture types, including a number of combination fracture types. The difference in the historic samples could be due to the quality of the original silk or arise from the complexity and greater variety of natural ageing mechanisms compared with laboratory ageing conditions. Similar amounts of fractures due to embrittlement of the silk were recorded for both the modern aged and historic samples. However the samples were pre-treated to erase the effects of physical ageing, which is known to cause embrittlement. In order to determine the cause of different fractures on ageing a detailed atlas of SEM images and an experienced analyst are required, limiting the information available to most people.

Other Methods

Silk molecules have been imaged using Atomic Force Microscopy (AFM)[119] which determined the shape and size as well as changes with increased concentration.[120] AFM has also been used to demonstrate the presence of nanofibrils in silk fibres,[121] and in conjunction with SAXS. The formation of a three dimensional structure of nanofibrils has been imaged with AFM and SEM.[122] Recent work on tapestries used AFM to look at the nanofibrils in unaged and artificially light aged samples. These images indicated the fibril structure is lost with ageing. However it is difficult to quantify the amount of damage or change observed without a large number of samples which restricts the use of AFM within conservation, similarly access to equipment is limited.

Structural changes in silk have been studied using nuclear magnetic resonance (NMR) spectroscopy[123]. Asakura has used NMR to analyse the structure of silk and model silk polypeptides including investigating the structural role of tyrosine.[124] This work has mainly focussed on gland silk including changes between silk I and II conformations and determining their structures.[125,126] Asakura reports solid-state NMR can be applied to noncrystalline samples and is also non-destructive.[127] He has recently also helped develop a microcoil NMR probe which reduces the sample volume required and can be used to analyse the orientation in a small number of fibres.[128] The amount of physisorbed water in cocoons of different silk species has been studied with solid state NMR as a means of identification.[129] This technique could also be used to look at changing conformation and possibly crystallite orientation of silk with age, but has not been reported for use with historic silks. Although not providing information on deterioration of silk, methods for radiocarbon dating silk have been reported.[130]

Conclusions

A number of techniques have been discussed in relation to monitoring the condition of silk, these are summarised in Table 4.1. In analysing the current level of deterioration of historic samples the most suitable technique should provide detailed information on the condition and be sensitive to small changes. It should also be possible to compare this data with that available in the literature. The technique should be non-destructive or require a micro-sample. Importantly the technique should also be available. This is particularly relevant to the synchrotron radiation techniques discussed as it is very difficult to obtain beamtime, which limits the availability of these methods.

Analytical Technique	quantity of silk required	preparation of silk required	technique availability*	is technique destructive / invasive?**	condition assessment sensitivity
μ-XRD	~0.1 mg	none (SR)	very limited access (SR)	non-destructive	good
amino acid analysis	1.0 mg	hydrolysis	available (req column)	destructive	currently limited
HPSEC	0.2 mg	solubilised	available	destructive	good
pol-ATR	~0.2 mg	none	available	non-destructive (~non-invasive)	limited
NIR	analysis of object possible	none	available	non-invasive & non-destructive	good
Raman	~0.1 mg	none	possible access	non-destructive (~non-invasive)	unknown
Mechanical testing	>5 cm of thread	fibres need mounting	available	destructive	good
DSC	0.4 mg	none	possible access	destructive	limited
pH	10 mg	saline extract	available	destructive	limited
fractography	~1.5 mg	C/Au coating	available	~non-destructive	limited
AFM	~0.2 mg	mounting	limited access	~non-destructive	limited
NMR	1 mg (with microcoil)	none (solid-state)	limited access	non-destructive (solid-state)	unknown

Table 4.1 – summary of techniques that may be used to monitor the condition of silk

*available in the Textile Conservation Centre laboratory (SR = synchrotron radiation sources are required)

**destructive means sample is required which cannot be recovered or reused after analysis, non-destructive means sample is required but remains intact after analysis, non-invasive means sample is not required for analysis and object is not destroyed by analysis

In order to analyse the silk samples obtained, HPSEC will be used. Although this is a destructive technique it provides detailed information on the molecular weight and is sensitive to small changes. HPSEC can also be performed on very small samples, which minimises the need for sampling. This technique can be compared to work that has already been published and it will be possible to compare with later samples from accelerated ageing. Critically this technique is also available.

Accelerated ageing experiments will use model materials which can be analysed with both mechanical testing and HPSEC. In order to undertake a much wider condition survey of a historic property and the collection of silks it will be necessary to use a technique that is both non-destructive and non-invasive. NIR spectroscopy may provide a suitable means of analysing the collection *in situ* and this will be further developed.

References

[1] Stuart, B. H. (2007) *Analytical Techniques in Materials Conservation* Chichester: John Wiley & Sons, Ltd.

[2] Stuart, B. H. (2007) 'X-ray Diffraction' in *Analytical Techniques in Materials Conservation* Chichester: John Wiley & Sons, Ltd 230-234.

[3] Warwicker, J. O. (1954) 'The Crystal Structure of Silk Fibroin' *Acta Crystallographica* **7** 565-573.

[4] Marsh, R. E., Corey, R. B. and Pauling, L. (1955) 'The Structure of Tussah Silk Fibroin' *Acta Crystallographica* **8** 710-715.

[5] Marsh, R. E., Corey, R. B. and Pauling, L. (1955) 'The Crystal Structure of Silk Fibroin' *Acta Crystallographica* **8** 62.

[6] Howitt, F. O. (1955) 'Silk Fibroin as a Fibrous Protein' *Textile Research Journal* **25** 242-246.

[7] Kratky, O. (1956) 'An X-ray Investigation of Silk Fibroin' *Transactions of the Faraday Society* **52** 558-570.

[8] Lucas, F. J., Shaw, T. B. and Smith, S. G. (1958) 'The silk fibroins', *Advances in Protein Chemistry* **13** 107-242.

[9] Seydel, T., Kölln, K., Krasnov, I., Diddens, I., Hauptmann, N., Helms, G., Ogurreck, M., Kang, S.-G. Koza, M. M. and Müller, M. (2007) 'Silkworm Silk under Tensile Strain Investigated by Synchrotron X-ray Diffraction and Neutron Spectroscopy' *Macromolecules* **40** 1035-1042.

[10] Krasnov, I., Diddens, I., Hauptmann, N., Helms, G., Ogurreck, M., Seydel, T., Funari, S. S. and Müller, M. (2008) 'Mechanical Properties of Silk: Interplay of

Deformation on Macroscopic and Molecular Length Scales' *Physical Review Letters* **100 (4)** 048104-1-048104-4.

[11] Grieff, S., Kutzke, H., Riekel, C., Wyeth, P. and Lahlil, S., (2005) 'Surveying silk fibre degradation by crystallinity determination: a study on the Tang dynasty silk treasure from Famen Temple, China', in *AHRC Research Centre for Textile Conservation and Textile Studies First Annual Conference –Scientific Analysis of Ancient and Historic Textiles Postprints* Janaway, R. and Wyeth, P. (ed.) London: Archetype 38–43.

[12] Wyeth, P., (2005) 'Signatures of ageing: correlations with behaviour', in *AHRC Research Centre for Textile Conservation and Textile Studies First Annual Conference – Scientific Analysis of Ancient and Historic Textiles Postprints* Janaway, R. and Wyeth, P. (ed.) London: Archetype 137–142.

[13] Khan, M. M. R., Gotoh, Y., Miura, M., Morikawa, H. and Nagura, M. (2006) 'Influence of an Iodine Treatment on the Structure and Physical Properties of *Bombyx mori* Silk Fibroin Fiber' *Journal of Polymer Science Part B: Polymer Physics* **44** 3418-3426.

[14] Drummy, L. F., Phillips, D. M., Stone, M. O., Farmer B. L. and Naik, R. R. (2005) 'Thermally Induced α-Helix to β-Sheet Transition in Regenerated Silk Fibers and Films' *Biomacromolecules* **6** 3328-3333.

[15] Rössle, M., Panine, P., Urban, V. S. and Riekel, C. (2004) 'Structural Evolution of Regenerated Silk Fibroin Under Shear: Combined Wide- and Small-Angle X-ray Scattering Experiments Using Synchrotron Radiation' *Biopolymers* **74 (4)** 316-327.

[16] Hermes, A. C., Davies, R. J., Grieff, S., Kutzke, H., Wyeth, P. and Riekel, C. (2006) 'Characterization of Decay of Ancient Chinese Silk Fabrics by Microbeam Synchrotron Radiation Diffraction' *Biomacromolecules* **7** 777-783.

[17] Kennedy, C. J., Von Lerber, K. and Wess, T. J. (2005) 'Measuring Crystallinity of Laser Cleaned Silk by X-ray Diffraction' *e-Preservation Science* **2** 31-37.

[18] Kawahara, Y., Shioya, M., Kikutani, T. and Takaku, A. (1994) 'Analysis of swelling behavior of silk fibers by small angle x-ray scattering' *Sen'i Gakkaishi* **50 (5)** 199-207.

[19] Miller, L. D., Putthanarat, S., Eby, R. K. and Adams, W. W. (1999) 'Investigation of the nanofibrillar morphology in silk fibers by small angle X-ray scattering and atomic force microscopy' *International Journal of Biological Macromolecules* **24** 159-165.

[20] Stuart, B. H. (2007) 'High Performance Liquid Chromatography' in *Analytical Techniques in Materials Conservation* Chichester: John Wiley & Sons, Ltd 318-319.

[21] Schroeder, W. A. and Kay, L. M. (1955) 'The Amino Acid Composition of *Bombyx mori* Silk Fibroin and of Tussah Silk Fibroin' *Journal of the American Chemical Society* **77** 3908-3913.

[22] Lucas, F., Shaw, J. T. B. and Smith, S. G. (1955) 'The Chemical Constitution of Some Silk Fibroins and its Bearing on their Physical Properties' *Journal of the Textile Institute* **46** T440-T452.

[23] Lucas, F., Shaw, J. T. B. and Smith, S. G. (1957) 'The Amino Acid Sequence in a Fraction of the Fibroin of *Bombyx mori*' *Biochemical Journal* **66** 468-479.

[24] Lucas, F., Shaw, J. T. B. and Smith, S. G. (1960) 'Comparative Studies of Fibroins I The Amino Acid Composition of Various Fibroins and its Significance in Relation to their Crystal Structure and Taxonomy' *Journal of Molecular Biology* **2** 339-349.

[25] Lucas, F., Shaw, J. T. B. and Smith, S. G. (1962) 'Some Amino Acid Sequences in the Amorphous Fraction of the Fibroin of *Bombyx mori*' *Biochemical Journal* **83** 164-171.

[26] Shaw, J. T. B. and Smith, S. G. (1961) 'Comparative Studies of Fibroins IV The Composition and Structure of Chemically Resistant Fractions from Some Silk Fibroins' *Biochimica et Biophysica Acta* **52** 305-318.

[27] Becker, M. and Tuross, N. (1992) 'Novel Approaches for Assessing the Preservation of Historic Silks: A Case Study of the First Ladies' Gowns' *Material Research Society Bulletin* **17** 39-44.

[28] Hirabayashi, K., Takei, M. and Kondo, M. (1984) 'Deterioration mechanism of silk fabrics' *Archaeology and Natural Science* **17** 61-72.

[29] Stuart, B. H. (2007) 'Ion Chromatography' in *Analytical Techniques in Materials Conservation* Chichester: John Wiley & Sons, Ltd. 323-325.

[30] Carr, C. M. (2006) 'Monitoring of Damage to Historic Tapestries (MODHT) EVK4-2001-00048 Final Report'.

[31] Rutherford, H. A. and Harris, M. (1941) 'Photochemical Reactions in Silk' *American Dyestuff Reporter* **14** 345-346 and 363-364.

[32] Becker, M. A., Willman, P. and Tuross, N. C. (1995) 'The U.S. First Ladies Gowns: A Biochemical Study of Silk Preservation' *Journal of the American Institute of Conservation* **34** 141-52.

[33] Becker, M. A., Magoshi, Y., Sakai, T. and Tuross, N. C. (1997) 'Chemical and Physical Properties of Old Silk Fabrics' *Studies in Conservation* **42** 27-37.

[34] Yanagi, Y., Kondo, Y. and Hirabayashi, K. (2000) 'Deterioration of Silk Fabrics and Their Crystallinity' *Textile Research Journal* **70 (10)** 871-875.

[35] Stuart, B. H. (2007) 'Size Exclusion Chromatography' in *Analytical Techniques in Materials Conservation* Chichester: John Wiley & Sons, Ltd 320-323.

[36] Howell, D. (1992) 'Silk Degradation Studies' in *Silk: Harpers Ferry Regional Textile Group, 11th Symposium*, Washington DC: Harpers Ferry Regional Textile Group 11-12.

[37] Hallett, K. and Howell, D. (2005) 'Size exclusion chromatography as a tool for monitoring silk degradation in historic tapestries', in *AHRC Research Centre for Textile Conservation and Textile Studies First Annual Conference – Scientific Analysis of Ancient and Historic Textiles Postprints,* Janaway, R. and Wyeth, P. (ed.) 143–150.

[38] Hallett, K. and Howell, D. (2005) 'Size exclusion chromatography of silk: inferring the textile strength and assessing the condition of historic tapestries' in *ICOM Committee for Conservation 14th Triennial Meeting Preprints, The Hague, 12-16th September 2005 Preprints* **2** 911-919.

[39] Garside, P. and Wyeth, P. (2002) 'Characterization of silk deterioration' *Strengthening the Bond: Science and Textiles. Preprints of the North American*

Textile Conservation Conference April 2002 Whelan, V.J. (ed.) Philadelphia, PA: North American Textile Conservation Conference 55-60.

[40] Tse, S. and Dupont, A.-L. (2001) 'Measuring Silk Deterioration by High-Performance Size-Exclusion Chromatography, Viscometry, and Electrophoresis' *Historic Textiles, Papers, and Polymers in Museums* Cardamone, J. M. and Baker, M. T. (ed.) ACS Symposium Series **779** Washington DC: American Chemical Society 98-114.

[41] Gamo, T., Inokuchi, T. and Laufer, H. (1977) 'Polypeptides of Fibroin and Sericin Secreted from the Different Sections of the Silk Gland in *Bombyx mori*' *Insect Biochemistry* **7** 285-295.

[42] Horan, R. L., Antle, K., Collette, A. L., Wang, Y., Huang, J., Moreau, J. E., Volloch, V., Kaplan, D. L. and Altman, G. H. (2005) 'In vitro degradation of silk fibroin' *Biomaterials* **26** 3385-3393.

[43] Sasaki, T. and Noda, H. (1973) 'Studies on Silk Fibroin of *Bombyx mori* Directly Extracted from the Silk Gland I. Molecular Weight Determination in Guanidine Hydrochloride or Urea Solutions' *Biochimica et Biophysica Acta* **310** 76-90.

[44] Sasaki, T. and Noda, H. (1973) 'Studies on Silk Fibroin of *Bombyx mori* Directly Extracted from the Silk Gland II Effect of Reduction of Disulfide Bonds and Subunit Structure' *Biochimica et Biophysica Acta* **310** 91-103.

[45] Sung, N. Y., Byun, E. B., Kwon, S. K., Kim, J. H., Song, B. S., Choi, J. I., Kim, J. K., Yoon, Y., Byun, M. W., Kim, M. R., Yook, H. S. and Lee, J.W. (2009) 'Effect of Gamma Irradiation on the Structural and Physiological Properties of Silk Fibroin' *Food Science and Biotechnology* **18(1)** 228-233.

[46] Sprague, K. U. (1975) 'The *Bombyx mori* Silk Proteins: Characterization of Large Polypeptides' *Biochemistry* **14 (5)** 925-931.

[47] Stuart, B. H. (2007) 'Infrared Spectroscopy' in *Analytical Techniques in Materials Conservation* Chichester: John Wiley & Sons, Ltd 110-112.

[48] Garside, P. and Brooks, M. M. (2006) 'Probing the Microstructure of Protein and Polyamide Fibres' in *The Future of the 20th Century. Postprints of the AHRC Research Centre for Textile Conservation and Textile Studies Second Annual*

Conference July 2005, Rogerson, C. and Garside, P. (ed.) London: Archetype 67-71.

[49] Sato, M. and Sasaki, Y., (2005) 'Studies on ancient Japanese silk fibres using FTIR microscopy', in *AHRC Research Centre for Textile Conservation and Textile Studies First Annual Conference – Scientific Analysis of Ancient and Historic Textiles Postprints,* Janaway, R. and Wyeth, P. (ed.) London: Archetype 44–47.

[50] Elliott, A. and Malcolm, B. R. (1956) 'Infrared Studies of Polypeptides Related to Silk' *Transactions of the Faraday Society* **52** 528-536.

[51] Sonoyama, M. and Nakano, T. (2000) 'Infrared Rheo-Optics of *Bombyx mori* Fibroin Film by Dynamic Step-Scan FT-IR Spectroscopy Combined with Digital Signal Processing' *Applied Spectroscopy* **54 (7)** 968-973.

[52] Chen, X., Shao, Z., Marinkovic, N. S., Miller, L. M., Zhou, P. and Chance, M. R. (2001) 'Conformation transition kinetics of regenerated *Bombyx mori* silk fibroin membrane monitored by time-resolved FTIR microscopy' *Biophysical Chemistry* **89** 25-34.

[53] Odlyha, M., Theodorakopoulos, C. and Campana, R., (n.d.), 'Damage Assessment of Tapestries by Infrared Spectroscopy (ATR-FTIR)' MODHT poster.

[54] Shao, J. Z., Zheng, J. H., Liu, J. Q. and Carr, C. M. (2004) 'FT-Raman and FT-IR spectroscopic studies of silk fibroin' *Quality Textiles for Quality Life 83rd Textile Institute World Conference 23-27th May 2004, Shanghai, PR China* 427-431.

[55] Li, Y., Yuen, C. W. M., Hu, J. Y. and Cheng, Y. F. (2006) 'Analysis of the Structural Characteristics of Nanoscale Silk Particles' *Journal of Applied Polymer Science* **100** 268-274.

[56] Suzuki, E. (1967) 'A quantitative study of the amide vibrations in the infra-red spectrum of silk fibroin' *Spectrochimica Acta* **23A** 2303-2308.

[57] Ambrose, E. J. and Elliott, A. (1951) 'Infra-red Spectra and Structure of Fibrous Proteins' *Proceedings of the Royal Society of London. Series A Mathematical and Physical Sciences* **206 (1085)** 206-219.

[58] Stuart, B. H. (2007) 'Infrared Spectroscopy' in *Analytical Techniques in Materials Conservation* Chichester: John Wiley & Sons, Ltd 113-114.

[59] Teramoto, H. and Miyazawa, M. (2005) 'Molecular Orientation Behaviour of Silk Sericin Film as Revealed by ATR Infrared Spectroscopy' *Biomacromolecules* **6** 2049-2057.

[60] Garside, P., Lahlil, S. and Wyeth, P. (2005) 'Characterization of Historic Silk by Polarized Attenuated Total Reflectance Fourier Transform Infrared Spectroscopy for Informed Conservation' *Applied Spectroscopy* **59 (10)** 90-95.

[61] Boulet-Audet, M., Lefèvre, T., Buffeteau, T. and Pézolet, M. (2008) 'Attenuated Total Reflection Infrared Spectroscopy: An Efficient Technique to Quantitatively Determine the Orientation and Conformation of Proteins in Single Silk Fibers' *Applied Spectroscopy* **62 (9)** 956-962.

[62] Bokobza, L. (2002) 'Origin of Near-Infrared Absorption Bands' in *Near-Infrared Spectroscopy Principles, Instruments, Applications* Siesler, H. W., Ozaki, Y., Kawata, S. and Heise, H. M. (ed.) Weinheim: Wiley-VCH 11-41.

[63] Zhou, Y., Xu, H. R. and Ying, Y. B. (2008) 'NIR Analysis of Textile Raw Material' *Spectroscopy and Spectral Analysis* **28 (12)** 2804-2807.

[64] Kawano, S. (2002) 'Sampling and Sample Presentation' in *Near-Infrared Spectroscopy Principles, Instruments, Applications* Siesler, H. W., Ozaki, Y., Kawata, S. and Heise, H. M. (ed.) Weinheim: Wiley-VCH 115-124.

[65] Heise, H. M. and Winzen, R. (2002) 'Chemometrics in Near-Infrared Spectroscopy' in *Near-Infrared Spectroscopy Principles, Instruments, Applications* Siesler, H. W., Ozaki, Y., Kawata, S. and Heise, H. M. (ed.) Weinheim: Wiley-VCH 125-162.

[66] Zbilut, J. P., Scheibel, T., Huemmerich, D., Webber, C. L., Colafranceschi, M. and Giuliani, A. (2006) 'Statistical approaches for investigating silk properties' *Applied Physics A: Materials Science & Processing* **82** 243-251.

[67] Mossotti, R., Innocenti, R., Zoccola, M., Anghileri, A. and Freddi, G. (2006) 'The degumming of silk fabrics: a preliminary near infrared spectroscopy study' *Journal of Near Infrared Spectroscopy* **14 (3)** 201-208.

[68] Miyazawa, M. and Sonoyama, M. (1998) 'Second derivative near infrared studies on the structural characterisation of proteins' *Journal of Near Infrared Spectroscopy* **6** A253-A257.

[69] Mo, C., Wu, P., Chen, X. and Shao, Z.-Z. (2006) 'Near-Infrared Characterization on the Secondary Structure of Regenerated *Bombyx mori* Silk Fibroin' *Applied Spectroscopy* **60(12)** 1438-1441.

[70] Zhang, X. and Wyeth, P. (2007) 'Moisture Sorption as a Potential Condition Marker for Historic Silks: Noninvasive Determination by Near-Infrared Spectroscopy' *Applied Spectroscopy* **61(2)** 218-222.

[71] Stuart, B. H. (2007) 'Raman Spectroscopy' in *Analytical Techniques in Materials Conservation* Chichester: John Wiley & Sons, Ltd 136-157.

[72] Magoshi, J., Magoshi, Y. and Nakamura, S. (1985) 'Crystallization, Liquid Crystal, and Fiber Formation of Silk Fibroin' *Journal of Applied Polymer Science: Applied Polymer Symposium* **41** 187-204.

[73] Zheng, S., Li, G., Yao, W. and Yu, T. (1989) 'Raman Spectroscopic Investigation of the Denaturation Process of Silk Fibroin' *Applied Spectroscopy* **43 (7)** 1269-1272.

[74] Lefèvre, T., Rousseau, M.-E. and Pézolet, M. (2007) 'Protein Structure and Orientation in Silk as Revealed by Raman Spectromicroscopy' *Biophysical Journal* **92** 2885-2895.

[75] Taddei, P., Asakura, T., Yao, J. and Monti, P. (2004) 'Raman Study of Poly(Alanine-Glycine)-Based Peptides Containing Tyrosine, Valine, and Serine as Model for the Semicrystalline Domains of *Bombyx mori* Silk Fibroin' *Biopolymers* **75** 314-324.

[76] Shao, J., Zheng, J., Liu, J., Carr, C. M. (2005) 'Fourier Transform Raman and Fourier Transform Infrared Spectroscopy Studies of Silk Fibroin' *Journal of Applied Polymer Science* **96** 1999-2004.

[77] Monti, P., Freddi, G., Bertoluzza, A., Kasai, N. and Tsukada, M. (1998) 'Raman Spectroscopic Studies of Silk Fibroin from *Bombyx mori*' *Journal of Raman Spectroscopy'* **29** 297-304.

[78] Monti, P., Taddei, P. Freddi, G., Asakura, T. and Tsukada, M. (2001) 'Raman spectroscopic characterization of *Bombyx mori* silk fibroin: Raman spectrum of Silk I' *Journal of Raman Spectroscopy* **32** 103-107.

[79] Lefèvre, T., Rousseau, M.-E. and Pézolet, M. (2006) 'Orientation-Insensitive Spectra for Raman Microspectroscopy' *Applied Spectroscopy* **60 (8)** 841-846.

[80] Preghenella, M., Pezzotti, G. and Migliaresi, C. (2007) 'Comparative Raman spectroscopic analysis of orientation in fibers and regenerated films of *Bombyx mori* silk fibroin' *Journal of Raman Spectroscopy* **38 (5)** 522-536.

[81] Edwards, H. G. M and Farwell, D. W. (2005) 'Raman Spectroscopic Studies of Silk' *Journal of Raman Spectroscopy* **26** 901-909.

[82] Stuart, B. H. (2007) 'Tensile Testing' in *Analytical Techniques in Materials Conservation* Chichester: John Wiley & Sons, Ltd 358-363.

[83] Daniels, V. and Leese, M. (1995) 'The Degradation of Silk by Verdigris' *Restaurator* **16** 45-63.

[84] Hansen, E. F. and Ginell, W. S. (1989) 'The Conservation of Silk with Parylene-C' *Historic Textile and Paper Materials II – Conservation and Characterization* Zeronian, S. H. and Needles, H. L. (ed.) ACS 410 Washington DC, USA: American Chemical Society 108-133.

[85] Jiang, P., Liu, H., Wang, C., Wu, L., Huang, J. and Guo, C. (2006) 'Tensile behaviour and morphology of differently degummed silkworm (*Bombyx mori*) cocoon silk fibres' *Materials Letters* **60** 919-925.

[86] Needles, H. L., Cassman, V. and Collins, M. J. (1986) 'Mordanted, Natural-Dyed Wool and Silk Fabrics' *Historic Textile and Paper Materials Conservation and Characterization* Needles, H. L. and Zeronian, S. H. (ed.) **212** Washington DC: American Chemical Society 199-210.

[87] Tímár-Balázsy, A. and Eastop, D. (1998) 'Fibres' *Chemical Principles of Textile Conservation* Oxford: Butterworth-Heinemann 3-66.

[88] Beste, L. F. and Hoffman, R. M. (1950) 'A qualitative study of resilience' *Textile Research Journal* **20 (7)** 441-453.

[89] Saville, B. P. (2003) 'Textiles and Moisture' *Physical Testing of Textiles* Cambridge: Woodhead Publishing 26-43.

[90] BS EN 20139:1992 ISO 139:1973 Textiles – Standard Atmospheres for Conditioning and Testing.

[91] Saville, B. P. (2003) 'Strength and Elongation Tests' *Physical Testing of Textiles* Cambridge: Woodhead Publishing 115-167.

[92] Meredith, R. (1945) 'The Tensile Behaviour of Raw Cotton and Other Textile Fibres' *Journal of the Textile Institute* **36** T107-T123.

[93] Ghosh, A. and Das, S. (2008) 'Tensile and Twist Failure of Mulberry and Tasar Silk' *Journal of the Textile Institute* **99 (2)** 165-168.

[94] Sirichaisit, J., Brookes, V. L., Young, R. J. and Vollrath, F. (2003) 'Analysis of Structure/Property Relationships in Silkworm (*Bombyx mori*) and Spider Dragline (*Nephila edulis*) Silks Using Raman Spectroscopy' *Biomacromolecules* **4** 387-394.

[95] Stuart, B. H. (2007) 'Differential Scanning Calorimetry / Differential Thermal Analysis' in *Analytical Techniques in Materials Conservation* Chichester: John Wiley & Sons, Ltd 347-358.

[96] Magoshi, J. and Nakamura, S. (1975) 'Studies on Physical Properties and Structure of Silk. Glass Transition and Crystallization of Silk Fibroin' *Journal of Applied Polymer Science* **19** 1013-1015.

[97] Magoshi, J., Magoshi, Y. and Nakamura, S. (1977) 'Physical Properties and Structure of Silk. III. The Glass Transition and Conformational Changes of Tussah Silk Fibroin' *Journal of Applied Polymer Science* **21** 2405-2407.

[98] Nakamura, S., Saegusa, Y., Yamaguchi, Y., Magoshi, J. and Kamiyama, S. (1986) 'Physical Properties and Structures of Silk. XI. Glass Transition Temperature of Wild Silk Fibroins' *Journal of Applied Polymer Science* **31** 955-956.

[99] Bora, M. N., Baruah, G. C. and Talukdar, C. L. (1993) 'Investigation on the Thermodynamical Properties of Some Natural Silk Fibres with Various Physical Methods' *Thermochimica Acta* **218** 425-434.

[100] Stuart, B. H. (2007) 'Thermogravimetric Analysis' in *Analytical Techniques in Materials Conservation* Chichester: John Wiley & Sons, Ltd 341-347.

[101] Magoshi, J. and Magoshi, Y. (1975) 'Physical Properties and Structure of Silk. II. Dynamic Mechanical and Dielectric Properties of Silk Fibroin' *Journal of Polymer Science: Polymer Physics Edition* **13** 1347-1351.

[102] Magoshi, J., Magoshi, Y., Nakamura, S., Kasai, N. and Kakudo, M. (1977) 'Physical properties and structure of silk. V. Thermal Behavior of Silk Fibroin in the Random-Coil Conformation' *Journal of Polymer Science: Polymer Physics Edition* **15** 1675-1683.

[103] Hu, X., Kaplan, D. and Cebe, P. (2006) 'Determining Beta-Sheet Crystallinity in Fibrous Proteins by Thermal Analysis and Infrared Spectroscopy' *Macromolecules* **39** 6161-6170.

[104] Glišović, A. and Salditt, T. (2007) 'Temperature dependent structure of spider silk by X-ray diffraction' *Applied Physics A: Materials Science and Processing* **87** 63-69.

[105] Zhang, H., Magoshi, J., Becker, M., Chen, J. Y. and Matsunaga, R. (2002) 'Thermal Properties of *Bombyx mori* Silk Fibers' *Journal of Applied Polymer Science* **86 (8)** 1817-1820.

[106] Odlyha, M., Wang, Q., Foster, G. M., de Groot, J., Horton, M. and Bozec, L. (2005) 'Thermal analysis of Model and Historic Tapestries' *Journal of Thermal Analysis and Calorimetry* **82** 627-636.

[107] Srinivasan, R. and Jakes, K. A. (1997) 'Examination of Silk Fibers from a Deep Ocean Site: SEM, EDS, & DSC' *Material Research Society Symposium Proceedings* **462** Washington D.C.: Materials Research Society 375-380.

[108] Kim, J.-J., Zhang, X. and Wyeth, P. (2008) 'The Inherent Acidic Characteristics of Aged Silk' *e-Preservation Science* **5** 41-46.

[109] Harris, M. and Jessup, D. A. (1934) 'The effect of pH on the Photochemical Decomposition of Silk' *Journal of Research of the National Bureau of Standards* **7(6)** 1179-1184.

[110] Dicko, C., Vollrath, F. and Kenney, J. M. (2004) 'Spider Silk Protein Refolding Is Controlled by Changing pH' *Biomacromolecules* **5** 704-710.

[111] Zhou, P., Xie, X., Knight, D. P., Zong, X.-H., Deng, F. and Yao, W.-H. (2004) 'Effects of pH and Calcium Ions on the Conformational Transitions in Silk Fibroin Using 2D Raman Correlation Spectroscopy and 13C Solid-State NMR' *Biochemistry* **43** 11302-11311.

[112] Zong, X.-H., Zhou, P., Shao, Z.-Z., Chen, S.-M., Chen, X., Hu, B.-W., Deng, F. and Yao, W.-H. (2004) 'Effect of pH and Copper (II) on the Conformation Transitions of Silk Fibroin Based on EPR, NMR, and Raman Spectroscopy' *Biochemistry* **43** 11932-11941.

[113] Wong Po Foo, C., Bini, E., Hensman, J., Knight, D. P., Lewis, R. V. and Kaplan, D. L. (2006) 'Role of pH and charge on silk protein assembly in insects and spiders' *Applied Physics A: Materials Science & Processing* **82** 223-233.

[114] Hu, B.-W., Zhou, P., Noda, I. and Ruan, Q.-X. (2006) 'Generalized Two-Dimensional Correlation Analysis of NMR and Raman Spectra for Structural Evolution Characterizations of Silk Fibroin' *Journal of Physical Chemistry B* **110** 18046-18051.

[115] Stuart, B. H. (2007) 'Scanning Electron Microscopy' in *Analytical Techniques in Materials Conservation* Chichester: John Wiley & Sons, Ltd 91-100.

[116] Zeronian, S. H., Alger, K. W., Ellison, M. S. and Al-Khayatt, S. M. (1986) 'Studying the Cause and Type of Fiber Damage in Textile Materials by Scanning Electron Microscopy' in *Historic Textile and Paper Materials Conservation and Characterization* Needles, H. L. and Zeronian, S. H. (ed.) American Chemical Series 212 Washington DC: American Chemical Society 77-94.

[117] Breese, R. R. and Goodyear, G. E. (1986) 'Fractography of Historic Silk Fibers' in *Historic Textile and Paper Materials Conservation and Characterization* Needles, H. L. and Zeronian, S. H. (ed.) American Chemical Series 212 Washington DC: American Chemical Society 95-109.

[118] Hearle, J. W. S., Lomas, B. and Cooke, W. D. (1998) 'Single Fibre Failure' in *Atlas of Fibre Fracture and Damage to Textiles* 2nd Edition Cambridge: Woodhead Publishing Ltd 13-24.

[119] Stuart, B. H. (2007) 'Scanning Probe Microscopy' in *Analytical Techniques in Materials Conservation* Chichester: John Wiley & Sons, Ltd 100-103.

[120] Inoue, S.-I., Magoshi, J., Tanaka, T., Magoshi, Y. and Becker, M. (2000) 'Atomic Force Microscopy: *Bombyx mori* Silk Fibroin Molecules and Their Higher Order Structure' *Journal of Polymer Science: Part B Polymer Physics* **38 (11)** 1436-1439.

[121] Hakimi, O., Knight, D. P., Knight, M. M., Grahn, M. F. and Vadgama, P. (2006) 'Ultrastructure of Insect and Spider Cocoon Silks' *Bimacromolecules* **7** 2901-2908.

[122] Putthanarat, S., Stribeck, N., Fossey, S. A., Eby, R. K. and Adams, W. W. (2000) 'Investigation of the nanofibrils of silk fibers' *Polymer* **41** 7735-7747.

[123] Stuart, B. H. (2007) 'Nuclear Magnetic Resonance Spectroscopy' in *Analytical Techniques in Materials Conservation* Chichester: John Wiley & Sons, Ltd 168-177.

[124] Asakura, T., Suita, K., Kameda, T., Afonin, S. and Ulrich, A. S. (2004) 'Structural role of tyrosine in *Bombyx mori* silk fibroin studied by solid-state NMR and molecular mechanics on a model peptide prepared as silk I and II' *Magnetic Resonance in Chemistry* **42** 258-266.

[125] Asakura, T., Nakazawa, Y., Ohnishi, E. and Moro, F. (2005) 'Evidence from ^{13}C solid-state NMR spectroscopy for a lamella structure in an alanine-glycine copolypeptide: A model for the crystalline domain of *Bombyx mori* silk fiber' *Protein Science* **14** 2654-2657.

[126] Asakura, T., Okonogi, M., Nakazawa, Y. and Yamauchi, K. (2006) 'Structural Analysis of Alanine Tripeptide with Antiparallel and Parallel β-Sheet Structures in Relation to the Analysis of Mixed β-Sheet Structures in *Samia cynthia ricini* Silk Protein Fiber Using Solid State NMR Spectroscopy' *Journal of the American Chemical Society* **128** 6231-6238.

[127] Asakura, T., Iwadate, M., Demura, M. and Williamson, M. P. (1999) 'Structural analysis of silk with ^{13}C NMR chemical shift contour plots' *International Journal of Biological Macromolecules* **24** 167-171.

[128] Yamauchi, K., Imada, T. and Asakura, T. (2005) 'Use of Microcoil Probehead for Determination of the Structure of Oriented Silk Fibers by Solid-State NMR' *Journal of Physical Chemistry B* **109** 17689-17692.
[129] Borsacchi, S., Cappellozza, S., Catalano, D., Geppi, M. and Ierardi, V. (2006) 'Solid State NMR Investigation of the Molecular Dynamics of Cocoon Silks Produced by Different *Bombyx mori* (Lepidoptera) Strains' *Biomacromolecules* **7** 1266-1273.
[130] Kim, K. J., Southon, J., Imamura, M. and Sparks, R. (2008) 'Development of Sample Pretreatment of Silk for Radiocarbon Dating' *Radiocarbon* **50 (1)** 131-138.

Chapter 5 – High Performance Size Exclusion Chromatography of Silk

As outlined in the previous chapter, the molecular weight of silk can be determined using high performance size exclusion chromatography (HPSEC). This chapter presents the calibration of the HPSEC with questions on the interactions of the protein standards and the eluents used, which was studied using dynamic light scattering (DLS). The development of the HPSEC methodology and parameter protocols are discussed and tested with a tapestry case study.

Initial work to develop the HPSEC method was undertaken by Howell[1] and later Tse and Dupont.[2] The technique was then further developed by Hallett and Howell[3,4] improving the peak separation between silk and the lithium thiocyanate (LiSCN) used to dissolve the silk, as well as reducing the sample size. This formed part of the European project on tapestries, MODHT.[5] As silk deteriorates the polymer breaks into smaller fragments, reducing the molecular weight of the silk and these changes can be followed with HPSEC.

The sample is injected onto the size exclusion column, which contains a packing material. The packing material contains 5 μm particles of silica gel which have pores around 500 Å,[6] allowing materials to be separated based on their molecular weight. Large molecules are too big to interact with the pores and travel straight through the column, eluting first. The smaller molecules enter the pores, with decreasing size leading to an increased time to pass through the column and elute. As the silk deterioration proceeds and smaller fragments are formed, the retention time of the silk increases and the changes can be monitored.

To determine the effective molecular weight, the silk is compared to a calibration curve produced from standard protein samples of known molecular weight. As the protein standards and silk interact with the pores in the packing material the shape of the polymer has an effect, i.e. a long linear molecule will interact less than a long round molecule with the same composition. Therefore HPSEC does not measure the mass but rather the space of the polymer in solution, known as the hydrodynamic volume. By calibrating the column it is possible to determine the molecular weight as it is related to the hydrodynamic volume. This allows the approximate molecular mass to be deduced however it is not an absolute measurement technique.

In previous work the molecular weight distribution has been quantified from the weight-averaged molecular weight, M_w, as the larger molecules contain more of the total mass M_w is biased. These larger molecules (and M_w) also have the most influence on the tensile strength. However there are other methods to calculate the molecular weight and a comparison of these methods would probably be a useful area of further study. For example, the number-averaged molecular weight (M_n) of polystyrene is reported to have a strong effect on the fracture toughness.[7] Whereas Tse and Dupont used the peak molecular weight (M_p) and report this had less solvent effects and was more sensitive to the changes caused by ageing of the silk.

Initial work focussed on developing the methodology and improving the repeatability of the analysis. All work has been carried out on a Thermo Scientific Finnigan SpectraSYSTEM HPLC which includes a solvent degasser, P4000 pump, AS3000 autosampler, and UV6000LP Photodiode Array (PDA) Detector. The HPLC is fitted with a GCF-4000 4 x 3.0 mm filter cartridge, BioSEP-SEC-S4000 30 x 4.6 mm narrow bore guard column and BioSEP-SEC-S4000 300 x 4.6 mm narrow bore column, all from Phenomenex. This column has an exclusion range of 15,000 to 2,000,000 Daltons for proteins in their native state however denaturing solvents will change the exclusion range. The effect of using 8M urea is not

reported by the manufacturer but Pace reported proteins are similarly denatured by 6M GnHCl and 8M urea with GnHCl 1.5 to 2.5 more times more effective.[8] Therefore the exclusion range for 8M urea is likely to be similar to that for 6M GnHCl (5,000 to 700,000 Daltons) rather than 0.5% SDS (15,000 to 500,000 Daltons) which are the denaturing solvents reported.[9] Data processing has used EZChrom Elite with SEC option from Agilent. All chemicals are from Sigma Aldrich and HPLC grade.

Silk Sample Preparation

For method development and analysis of modern silk samples 1.5 mg of silk was used. For historic materials the amount of silk removed was limited and varied between 0.1 and 1.5 mg. The modern silk samples were dissolved overnight in 0.6 ml of 21.5M lithium thiocyanate (0.2 ml for historic samples). The solutions were filtered through Ultrafree-MC centrifugal filter devices with microporous membrane of 0.45 µm pore size from Millipore, in an Eppendorf Minispin centrifuge (5 min at 12,000 rpm).

General Procedure

The samples are placed in the autosampler and 20 µl of the sample is injected onto the column. The sample is carried through the column by the mobile phase, 8M urea, with a flow rate of 0.3 ml min^{-1}. The sample is separated on the column, as described above. The PDA detector scans between 220 to 360 nm as well as recording on a discrete channel at 280nm. The proteins and amino acids producing UV absorption spectra at this wavelength were discussed by Beaven and Holiday[10] and changes in the conformation monitored by Georgakoudi *et al*.[11] The chromatogram from the discrete channel is analysed to determine the relative molecular weight in comparison with the calibration data. Three repeated runs per sample were performed, each of 20 minutes to ensure complete elution.

Methodology Development

The following improvements, determined using samples of unaged and aged silk, have all helped improve reproducibility. Unless specified unaged silk samples are shown in the chromatograms below.

Detector Response Rate

Initial problems included the silk and lithium thiocyanate peaks merging together. Both also had significant tailing (see Figure 5.1). Reducing tailing is important because the software uses the area under the peak to calculate the molecular weight, and for M_w, the distribution is important therefore the results could be skewed by this effect. Peak resolution and reduction of the tailing were both minimised by changing the rise time setting in the SEC software. The rise time is a detector parameter which controls the response time and is inversely proportional to the amount of baseline noise. Initially the rise time was 2 seconds but this gave broad, tailing peaks which almost overlapped. Halving the rise time to 1 s made little change to the resolution or tailing of the peaks. However reducing this further to 0.1 s gave much better resolution and reduced the tailing significantly. This has been chosen as the rise time for the method.

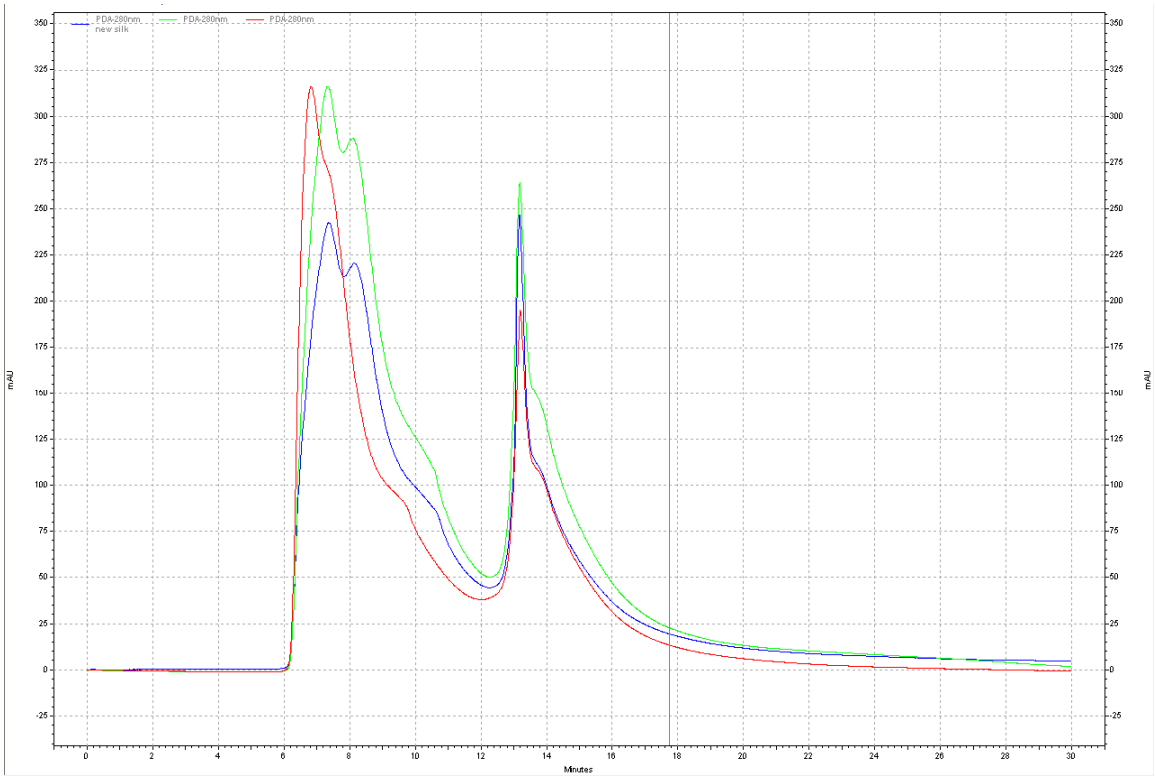

Figure 5.1 – effect of changing rise time settings

(rise time = 2 s: blue; rise time = 1 s: green; rise time = 0.1 s: red)

To determine if rise time was the only parameter controlling the detector response, changes in the data rate were also studied. However no difference was observed between samples run with data rates of 20 Hz, 10 Hz and 5 Hz (see Figure 5.2) and these settings do not seem to be relevant to the PDA UV/Vis detector. Therefore the original setting of 10 Hz has been retained.

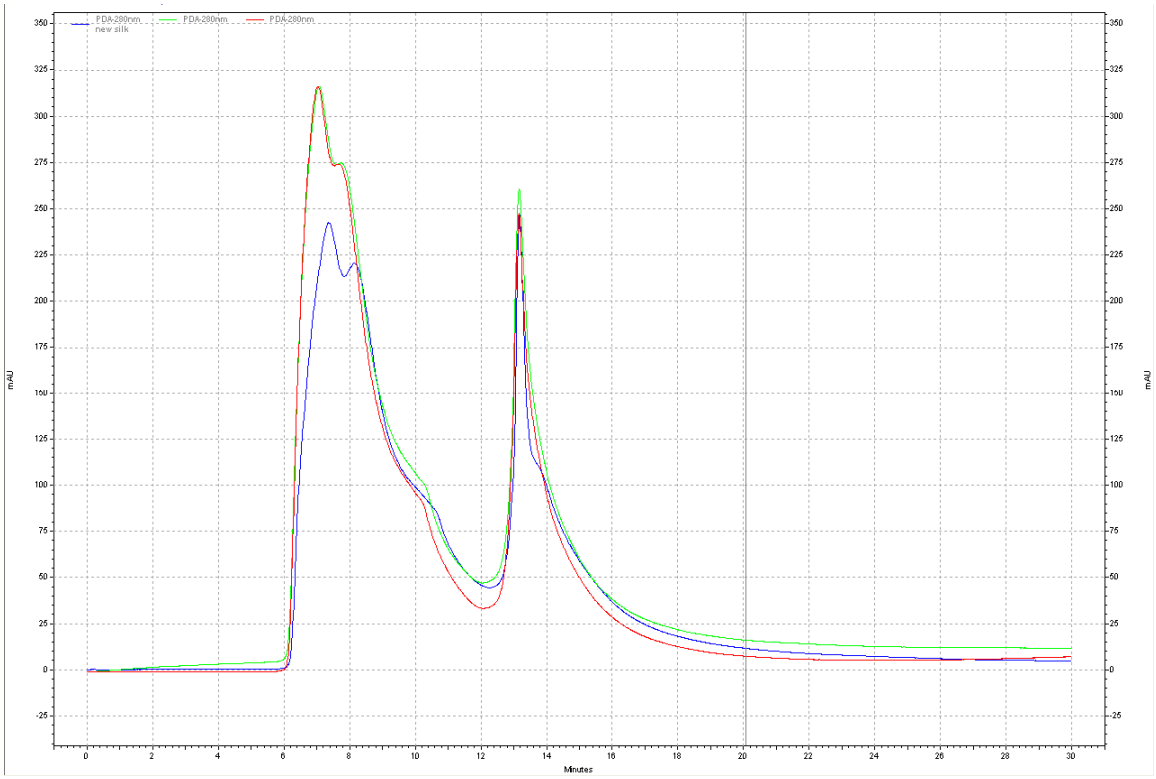

Figure 5.2 – effect of changing data rate settings

(data rate = 10 Hz: blue; data rate = 5 Hz: green; data rate = 20 Hz: red)

Sample Loop

When work started the sample loop on the HPLC was in excess of 100 µl, however the sample injection volume is around 20 µl. It is generally recommended to use a sample loop that is the same volume as the injection volume.[12] A 20 µl sample loop was installed, which also improved the peak resolution and reduced tailing.

Sample Storage

After dissolution silk samples are stored in the fridge to slow any possible deterioration of the samples. The autosampler is directly above the column oven (30 °C), and samples are generally loaded into the autosampler and then run in sequence. This means for the first sample there is a sudden change in temperature compared with the others which sit above the oven while the previous

samples are run. It was unclear whether this difference in temperature might be responsible for differences seen in chromatograms. To study the effect of temperature, two samples were kept in the fridge while two were placed into the autosampler. The two samples in the fridge were placed individually in the autosampler immediately before running. No difference was observed between the chromatogram of the cold samples and those of the room temperature samples (see Figure 5.3). This suggests the temperature change is not problematic.

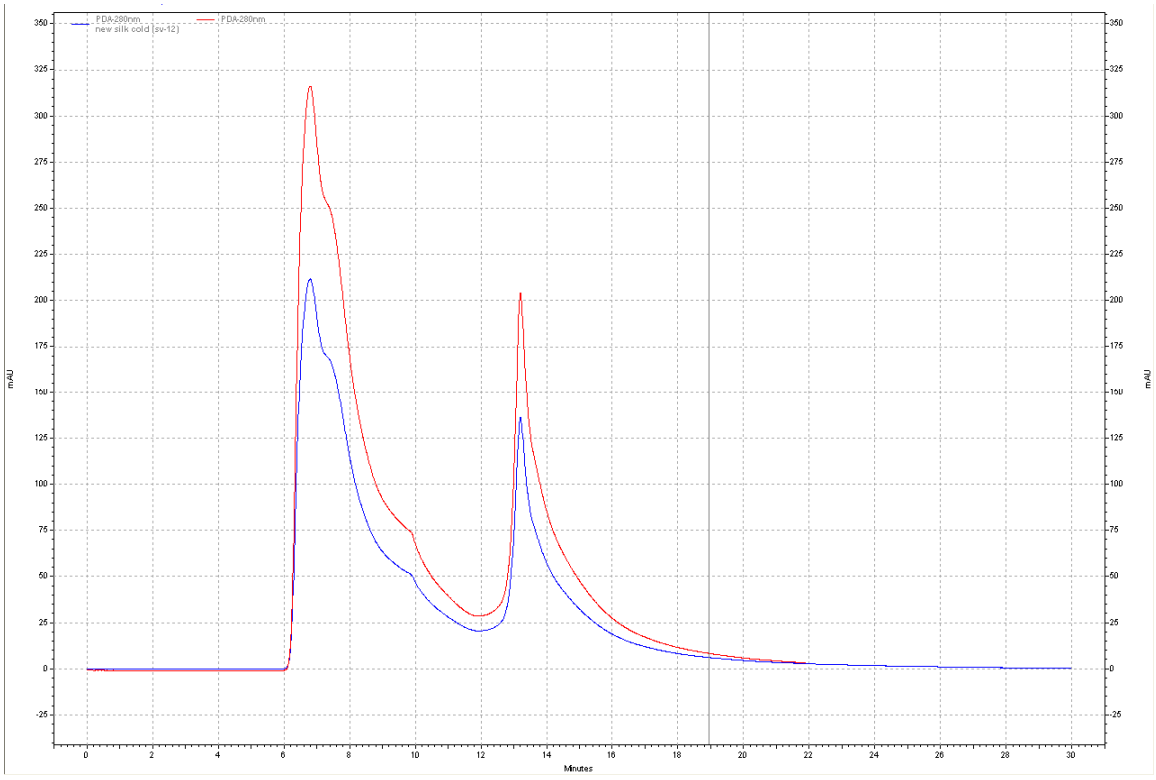

Figure 5.3 – effect of sample temperature

(sample from fridge: blue; sample left in autosampler: red)

When the method to analyse silk was developed the author reported one of the biggest problems was finding a suitable solvent to dissolve the silk without causing degradation. A number of solvents have been used to dissolve gland silk but during tests these were found to only swell silk fibres.[13] Tests on viscosity have dissolved silk in zinc chloride; however it is unclear whether this leads to degradation of the fibre, due to decreases in the viscosity.[14,15] Both lithium

bromide and lithium thiocyanate have been tested, with the latter more easily dissolving silk.[16] However what is not clear is whether lithium thiocyanate causes degradation of the silk in solution with time.

To determine if there were any changes, two samples were stored at reduced temperatures (~5 °C) in the fridge for two weeks, while two samples were stored at room temperature (~25 °C) on the bench for two weeks. Although the intensity of the chromatograms is different the shape and retention times of these samples were identical (see Figure 5.4). This suggests that on this short timescale, commensurate with the HPSEC experiments, damage is not caused. Yamada *et al*. have shown processing reduces the molecular weight of silk more than the dissolution in LiSCN.[17]

Lucas *et al.* report that to dissolve Tussah silk requires hot concentrated aqueous lithium thiocyanate solution although not all the fibroin is soluble.[18] This solution is not reported to be very stable and the solution tends to gel. More recently SDS has been reported for the solubilisation of non-mulberry gland silk,[19] and may be worth further investigation to solubilise Tussah silk for HPSEC analysis.

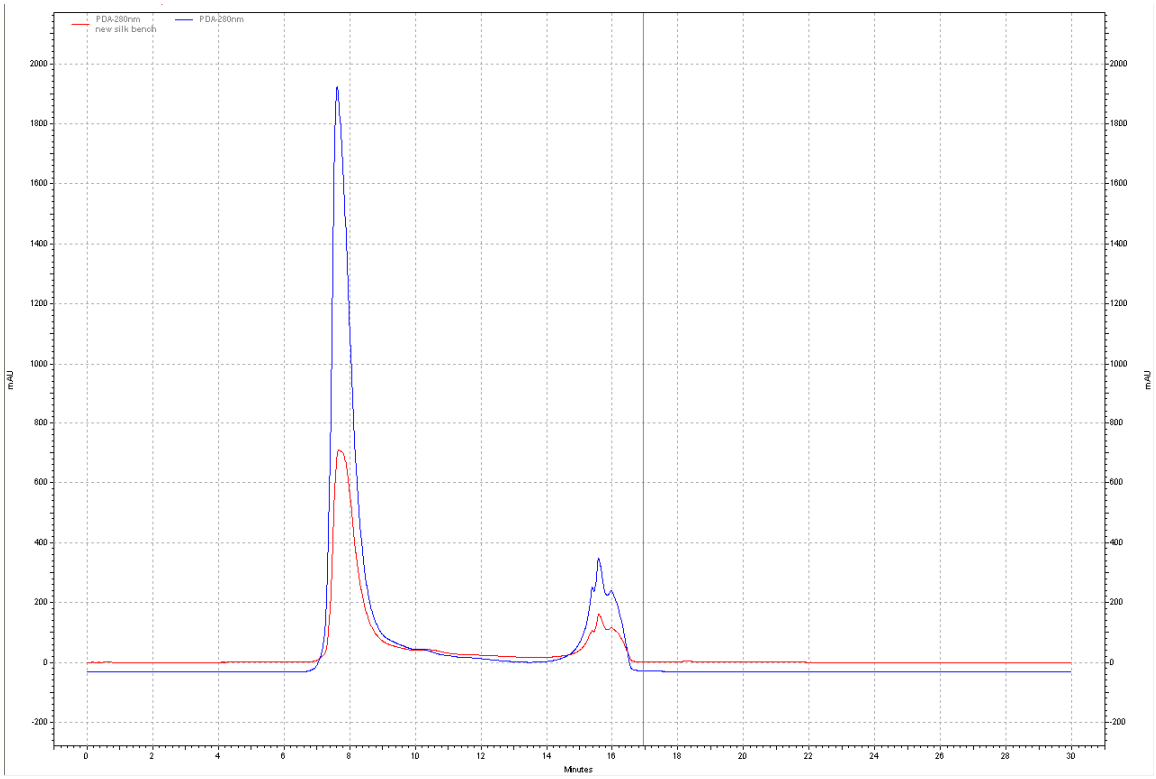

Figure 5.4 – effect of sample storage

(cold storage for 2 weeks: blue; room temperature storage for 2 weeks: red)

Fibre Direction

A further test was run to determine whether any differences existed between the warp and weft samples. Generally samples are from woven fabrics, therefore including both warp and weft fibres. A number of aged samples were separated into warp and weft fibres to distinguish any variations however the chromatograms were identical in all cases (see Figure 5.5). Therefore it seems most practical to analyse samples from woven fabric, rather than separated fibres, as this will give representative results. However, where it is suspected that the warp and weft were not originally processed in the same way then it would be appropriate to look at separated fibres if possible.

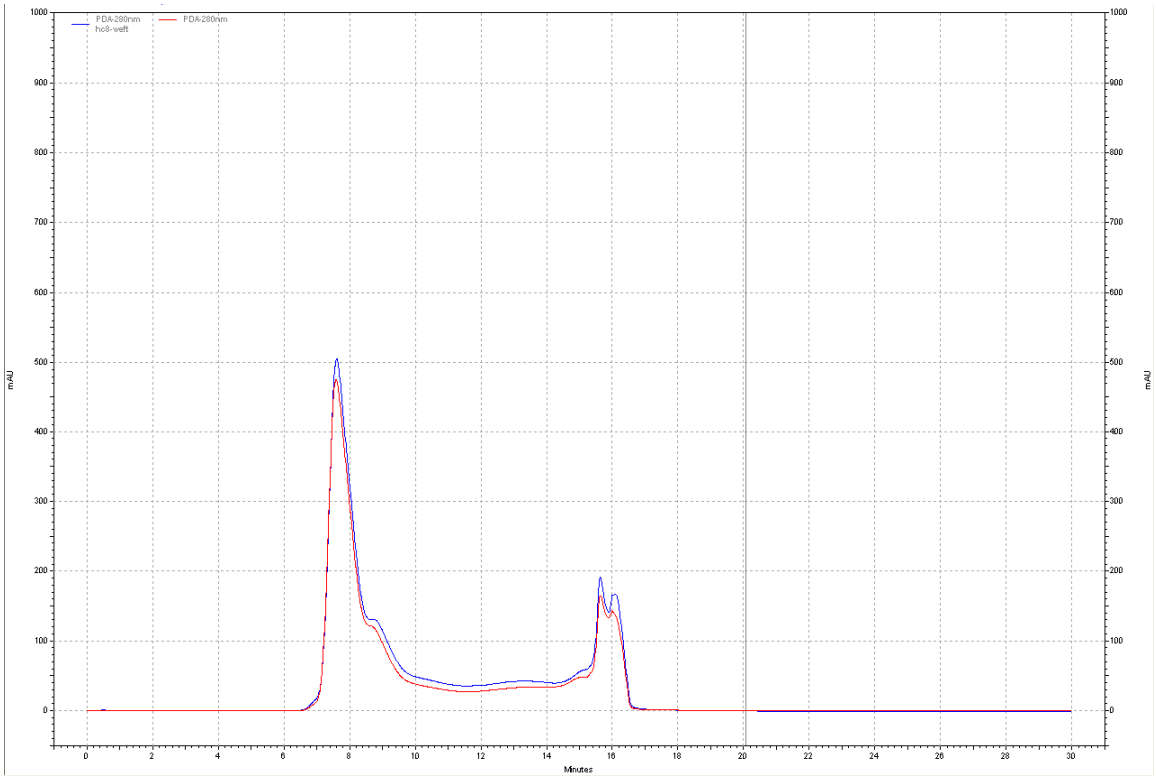

Figure 5.5 – effect of fibre direction (samples are humidity aged silk)
(weft fibres: blue; warp fibres: red)

Effect of Sample Incubation

The rate at which urea denatures the protein affects the change in the hydrodynamic volume and therefore the retention time. However the silk samples and protein standards are all run under the same denaturing conditions therefore this should not affect the analysis results. To test that the silk samples are fully denatured when run, new silk samples were prepared and incubated in 10M urea (1.2 ml) for the following intervals; 0, 1, 2, 4, 8 and 24 hours.

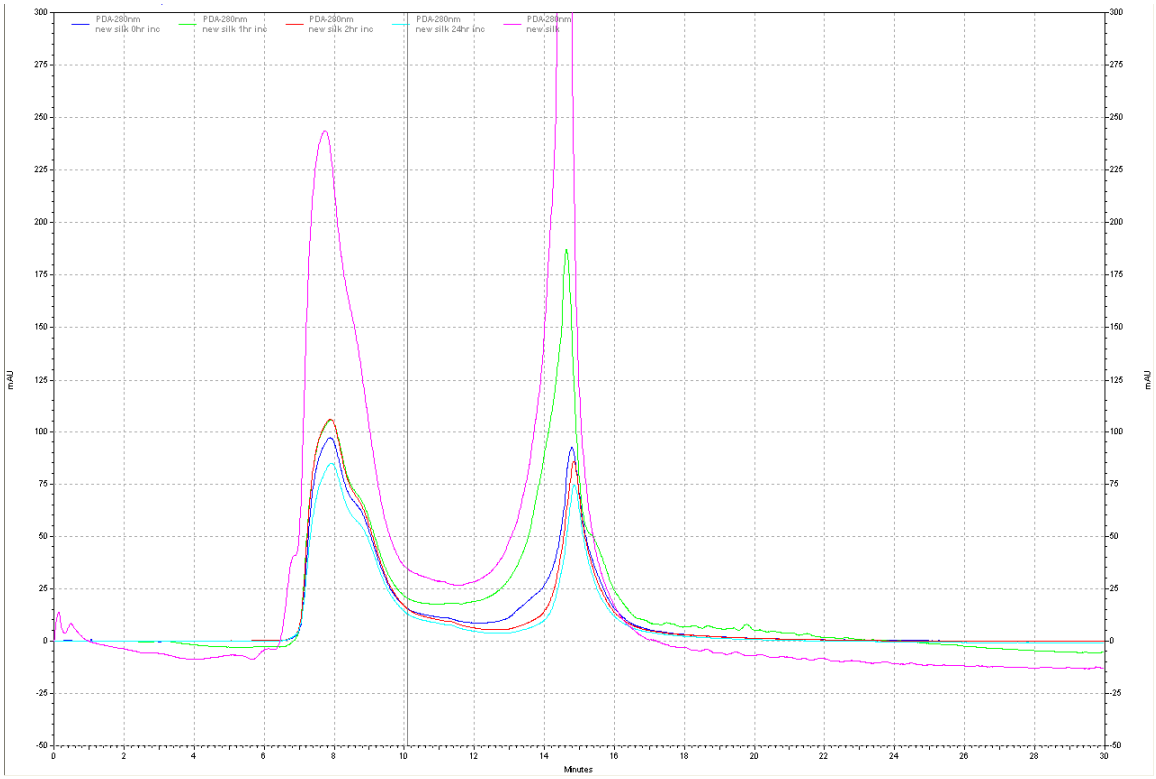

Figure 5.6 – effect of sample incubation

(no urea added: pink; no incubation – 0 hr: blue; 1 hr incubation: green; 2 hr incubation: red; 24 hr incubation: aqua)

Figure 5.6 shows the chromatograms from urea incubated samples (4 and 8 hours have been omitted for clarity), as well as a sample to which no urea was added but the mobile phase was urea. The chromatograms are similar, with the silk and lithium thiocyanate peaks occurring at the same retention times, regardless of the length of urea incubation and whether urea was added or not. This indicates that the normal running conditions do fully denature the silk. It is possible that the protein calibration standards could be denatured at a different rate, although Pace reported proteins were unfolded in 8M urea. The effect of HPSEC running conditions on the protein standards have been studied using dynamic light scattering (DLS) and are discussed below.

Mobile Phase

Another question identified related to the mobile phase. Initial work by Hallett and Howell had used a mixture of 0.05M urea with 0.05M tris-HCl as a buffer, however the silk and lithium thiocyanate peak overlapped and so the mobile phase was changed to 8M urea. 8M urea was chosen as it is reported to denature silk unfolding the globular protein into a long "rod-like" conformation. However lithium thiocyanate is a hydrogen bond competitor, as is 8M urea,[20] therefore it is more likely that 8M urea maintains the unfolded conformation rather than denatures the protein. The polymer now takes up a larger hydrodynamic volume although the chain length remains unaffected. The silk molecules pass through the column more quickly under denaturing conditions as they interact with the pores less. However 8M urea has no effect on lithium thiocyanate, which elutes at the same time, thus separating the peaks.

At the higher concentration of urea the tris-HCl is no longer added to the mobile phase. However it was unclear whether the absence or presence of tris-HCl would have an effect. A test showed the presence of tris-HCl did not affect the retention time in the chromatogram (see Figure 5.7) and so 8M urea only is used as the mobile phase. All mobile phases tested were also checked for pH, which was neutral (7) in all cases.

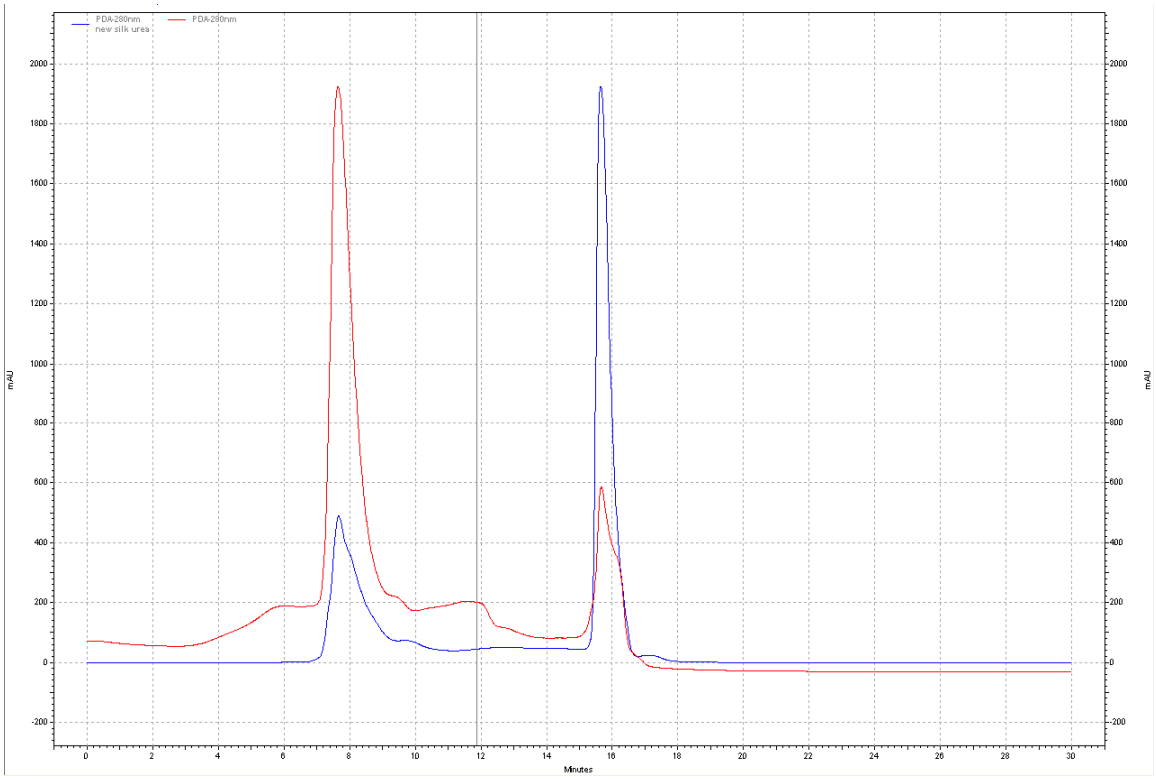

Figure 5.7 – effect of tris-HCl in the mobile phase

(8M urea only: blue; 8M urea and 0.05M tris-HCl: red)

Changes in Mobile Phase Concentration

It has been reported that the choice of 8M urea was made as it is known to denature silk. However a study of the change with increasing molarity has not been reported. In initial work using HPSEC to analyse silk, 0.05M urea was used. It is possible that the peak separation could be achieved with a lower molarity solution of urea. Work by Pace on the effect of urea concentration on the denaturation of ribonuclease showed it was fully denatured by 4M urea. The effect of changing urea molarity on a number of globular proteins has been calculated and the formation of intermediates was noted.[21]

In order to study this effect a number of solutions of increasing molarity from 0.05M to 10M were prepared and used as the mobile phase. For new silk samples no change in the peak position was observed with changing molarity. Changes in the

peak position with differing mobile phase concentration for aged silk samples have been inconclusive and further work would be required to understand this. Trathnigg reports that unlike other types of HPLC, in HPSEC the separation of compounds is due to the stationary phase of the column and the mobile phase should have no effect, as observed in this test.[22] A new publication indicates that 8M urea has separated the peaks although the lithium thiocyanate peak rather than the silk peak is shown to have moved.[23] However running the HPLC with 8M urea allows for comparison with previous published work and gives reproducible results and so has been used as the mobile phase for all further work.

Calibration

To calibrate the column, protein standards of known molecular weight are prepared (see Table 5.1 for details). The calibration standards are Sigma gel filtration molecular weight markers 12,400 to 200,000 kDa. Each standard is made up individually following the instructions provided to make 0.5 ml in 0.05M Tris-HCl buffer (trizma hydrochloride) pH 7. The molecular weight of blue dextran exceeds the exclusion range of the column and therefore is totally excluded, providing the exclusion volume.

protein	molecular weight / kDa	amount required / mg
Blue Dextran	2,000	1
β Amylase	200	2
Alcohol Dehydrogenase	150	2.5
Albumin	66	5
Carbonic Anhydrase	29	1.5
Cytochrome C	12.4	1

Table 5.1 – protein calibration standards

The standards are prepared and left overnight to ensure full dissolution. These are filtered to 0.45 µm using the same method as the silk samples. The standard protein solutions are then run on the HPSEC, under the same denaturing conditions as the silk samples. The maximum peak retention times are noted (see Figure 5.8) and the calibration method file updated with the line of best fit and saved with the most recent date. The line of best fit is rarely linear, with polynomial lines often giving a better match, however due to the limited number of calibration standards; a high order polynomial fit may give an erroneous calibration file. Therefore the highest polynomial fit used has been a quadratic equation. This method file is used to run future samples until the column is recalibrated. An example of the calibration curve produced can be seen in Figure 5.9.

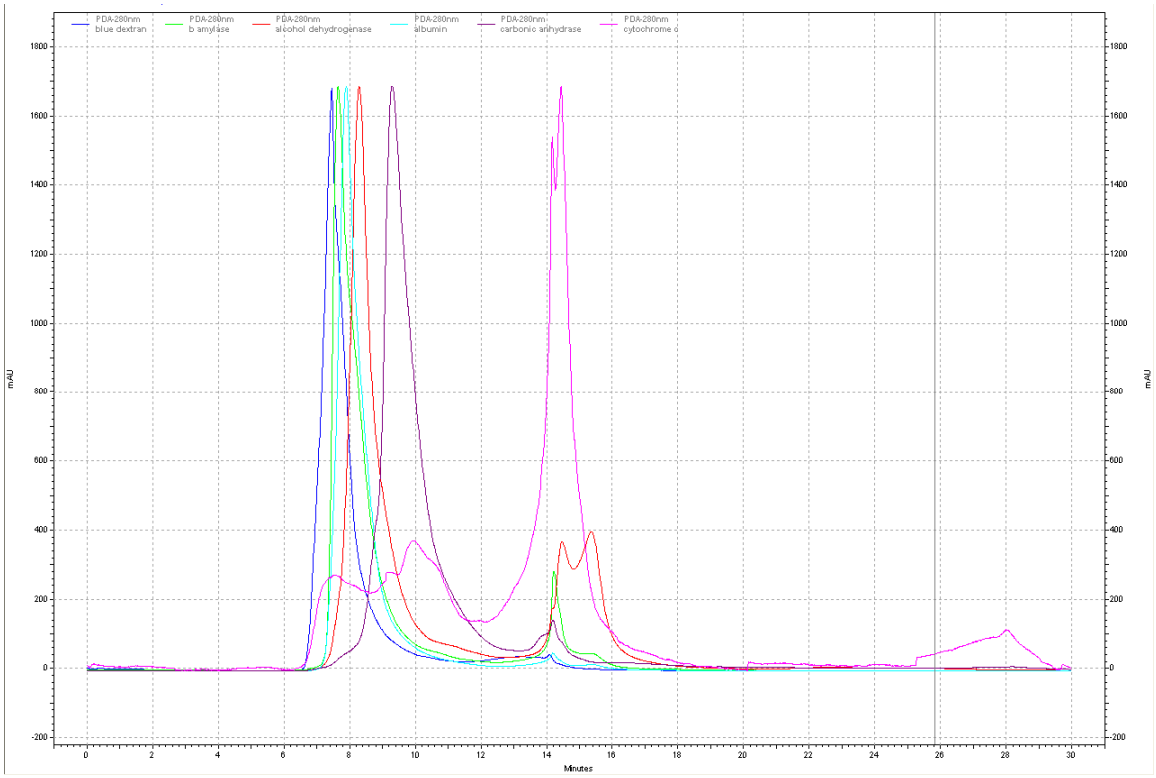

Figure 5.8 – overlaid HPSEC chromatograms of calibration standards
(blue dextran: blue; β amylase: green; alcohol dehydrogenase: red; albumin: aqua; carbonic anhydrase: purple; cytochrome c: pink)

Generally the column should be recalibrated every week. Silk can precipitate out while running samples, seen as an increase in the column back pressure. This change in pressure affects the flow rate of the sample on the column and hence the retention time. As this process is constant it is advisable to check the flow rate each day. This can be done by running one of the calibration standards and comparing the retention time with that in the calibration file. If there is a difference this can be adjusted in the SEC method calibration file by selecting a reference peak and adding a retention time. However as the silk is dissolved in lithium thiocyanate which also has a peak in the chromatogram this can also be used as an internal standard to provide a further check for changes in retention time.

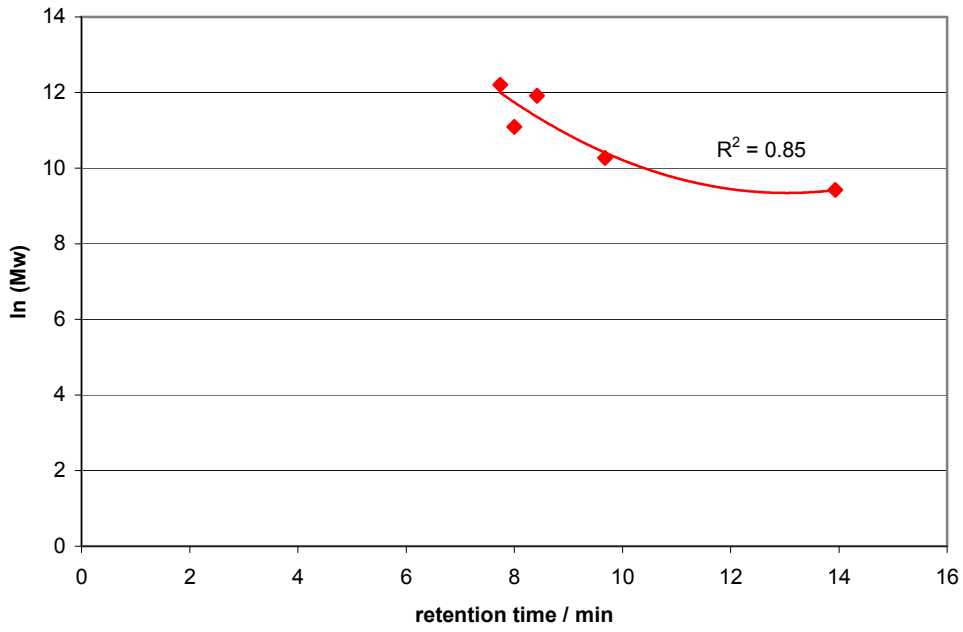

Figure 5.9 – calibration curve (here the line of best fit is a quadratic trendline)

Both β amylase (200 kDa) and alcohol dehydrogenase (150 kDa) exist as tetramers of smaller polypeptides, 56 kDa[24] and 35 kDa[25] respectively, which can separate under denaturing conditions. 8M urea is used as the eluent to denature the proteins, which would be expected to lead to the tetramers separating into their

monomeric units. However when run on the HPLC, the elution times were very close to the blue dextran peak which suggested that the tetramers were observed. A further complication was caused by the albumin peak, which is sold in the monomer form but the elution peak was also close to the blue dextran time. Albumin is reported to form oligomers, with either two, three or four monomers combining. This may explain why the albumin peak often appears between those of β amylase and alcohol dehydrogenase.

In a study on protein interactions using HPSEC, the authors comment that no universal calibration is available.[26] It has also been observed that narrow standards of the same chemical structure are rarely available, affecting the molecular weight calculations.[27] Therefore it is important to fully understand the behaviour of the calibration standards to provide calibration data. Protein molecular weights determined by HPSEC have been compared to results from light scattering by Oliva *et al*.[28] To understanding the behaviour of the calibration standards a series of further tests were run using dynamic light scattering (DLS). DLS measurements have been reported on gland silk[29] however its use to study historic fibres has not been reported.

DLS measurements were made on a Malvern Zetasizer Nano S (Malvern Instruments Ltd) with a detection angle of 173° and a 4mW He-Ne laser at a wavelength of 633 nm. These measurements were all taken at 25 °C with 3 repeat measurements on each sample. DLS has been used to study sub nanometre particles of sucrose,[30] but can also be used to visualise the size and shape of the proteins. By collecting the light scattered by a protein solution, information on its size and shape can be determined.

The effect of the solvent can be included by analysing this individually and correcting both the viscosity effects as well as the refractive index. Samples have been corrected for the presence of both lithium thiocyanate and 8M urea. One feature in the software, *protein utilities*, can be used to determine the expected

diameter (in nanometres) of the protein in globular, linear, starburst or branched conformations from the molecular weight (see Table 5.2). Using the measured diameter, the molecular weight can in turn be calculated for each conformation. The shape of the protein will have an effect on the scattering of the light and therefore the measured diameter as well as the calculated molecular weight.

protein	molecular weight / kDa	expected diameter / nm for each conformation			
		globular	linear	starburst	branched
blue dextran	2000*	30.7	89.4	21.7	43.5
b amylase (tetramer)	200*	11.5	25.1	11.0	15.8
b amylase (monomer)	56**	6.7	12.5	7.5	9.0
alcohol dehydrogenase (tetramer)	150*	10.1	21.4	10.1	13.9
alcohol dehydrogenase (monomer)	35**	5.4	9.6	6.5	7.3
albumin (tetramer)	264***	12.9	29.3	11.9	17.8
albumin (trimer)	198***	11.4	25.0	10.9	15.7
albumin (dimer)	132***	9.6	20.0	9.7	13.1
albumin (monomer)	66*	7.1	13.6	7.9	9.7
carbonic anhydrase	29*	5.0	8.7	6.2	6.7
cytochrome c	12.4*	3.5	5.4	4.8	4.6

Table 5.2 – expected diameters calculated from molecular weight

* Molecular weight taken from product literature

** Molecular weight reported in literature (references 24 and 25)

*** Molecular weight calculated from albumin monomer value

The calculated diameters in Table 5.2 can be compared with the actual measured diameters of the proteins (Table 5.3) to determine the conformation and molecular weight. The same conformation should give the expected diameter value which is closest to the actual diameter and the actual diameters give the closest molecular

weight with that conformation. For example, blue dextran is reported as 2000 kDa by the manufacturer, which would give an expected diameter of 89.4 nm for a linear conformation. The measured diameter is 110 nm which gives a calculated molecular weight of 2904 kDa for a linear conformation. It can be seen in Table 5.3 that the other conformations give excessively high molecular weights for this standard. Table 5.3 contains the calculated molecular weights for each protein based on the measured diameter for each conformation; the highlighted cells indicate the most likely conformation for each protein. Carbonic anhydrase may be either starburst or branched conformation from the DLS results as the measured diameter, and therefore calculated molecular weights both give values close to the manufacturer's value. For alcohol dehydrogenase the DLS results seem to indicate the protein is a trimer rather than a tetramer (~100 kDa instead of ~150 kDa) and so may be partially rather than fully denatured.

protein	average measured diameter / nm	calculated molecular weight / kDa for each conformation			
		globular	linear	starburst	branched
blue dextran	109.83	39603.7	2903.7	462534.3	16427.0
b amylase	11.73	211.2	50.3	252.0	102.1
alcohol dehydrogenase	8.46	98.2	27.8	83.9	48.6
albumin	11.87	217.1	51.8	262	104.9
carbonic anhydrase	6.39	51.1	16.7	32.8	25.7
cytochrome c	5.36	33.8	12.1	18.1	17.2

Table 5.3 – calculated molecular weight from average measured diameters

If the proteins, such as β amylase, were forming both monomeric and oligomeric structures then two or more peaks would be expected in the DLS scans. Most of the spectra showed more than one peak however the second and third peaks

occur at diameters of 100 nm or more. A sample of lithium thiocyanate was run without any silk (see Figure 5.10) which showed only the second and third peaks suggesting these arise from salt-related particles in the samples.

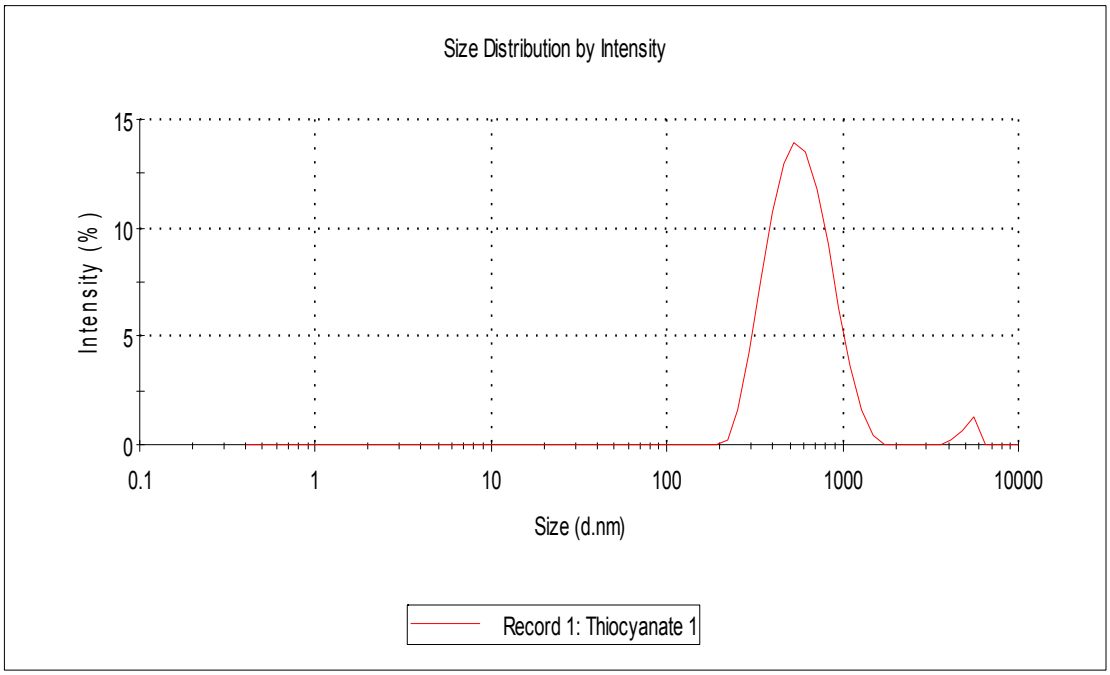

Figure 5.10 – DLS spectrum of lithium thiocyanate

For each sample three replicate runs were performed and the average diameter at the peak maxima has been used to calculate the molecular weight. Figures 5.11 to 5.13 show the DLS spectra for β amylase, alcohol dehydrogenase and albumin. Although the larger diameter peaks move slightly they are too big to be the proteins peaks, which all occur around 10 nm. For each peak there is a size distribution, but there are not separate peaks. This means that although small amounts of material may be present in different conformations or oligomeric numbers, one form dominates.

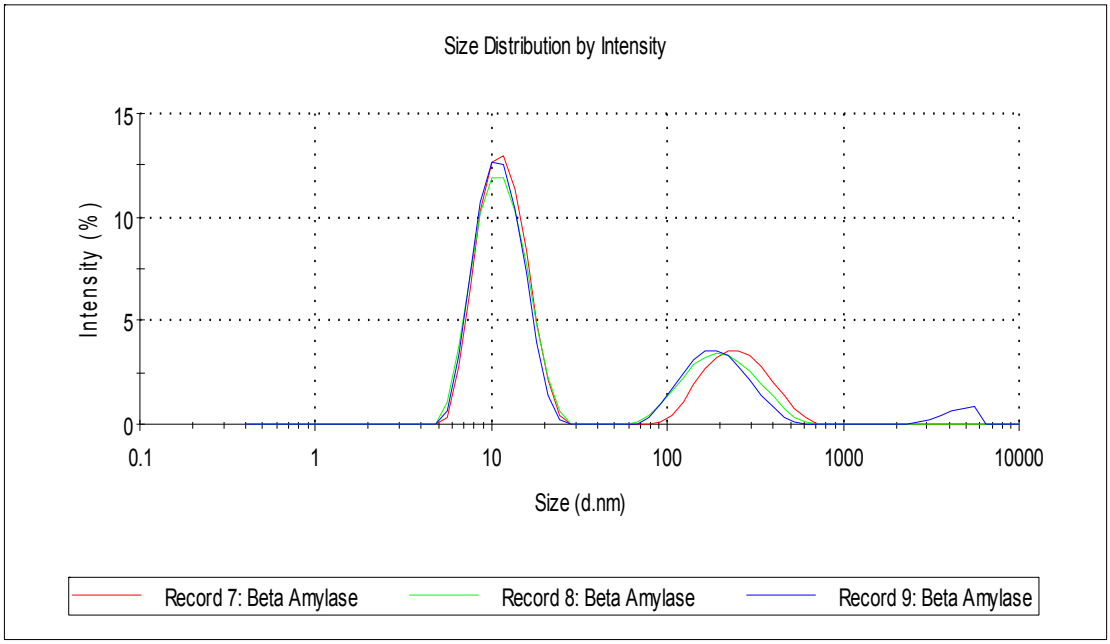

Figure 5.11 – DLS spectra of β amylase

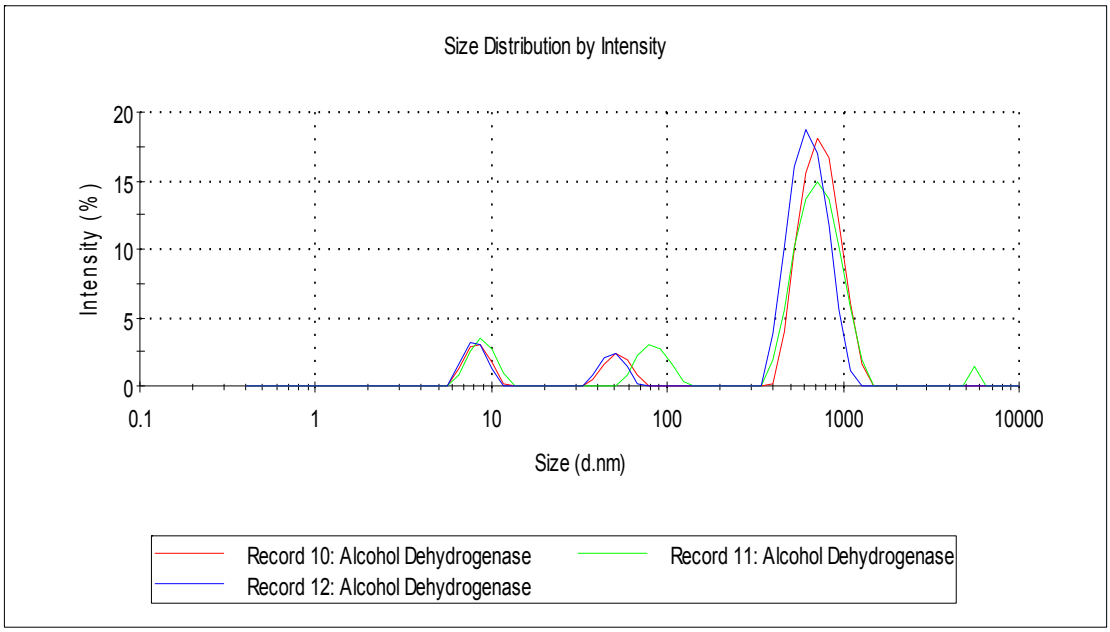

Figure 5.12 – DLS spectra of alcohol dehydrogenase

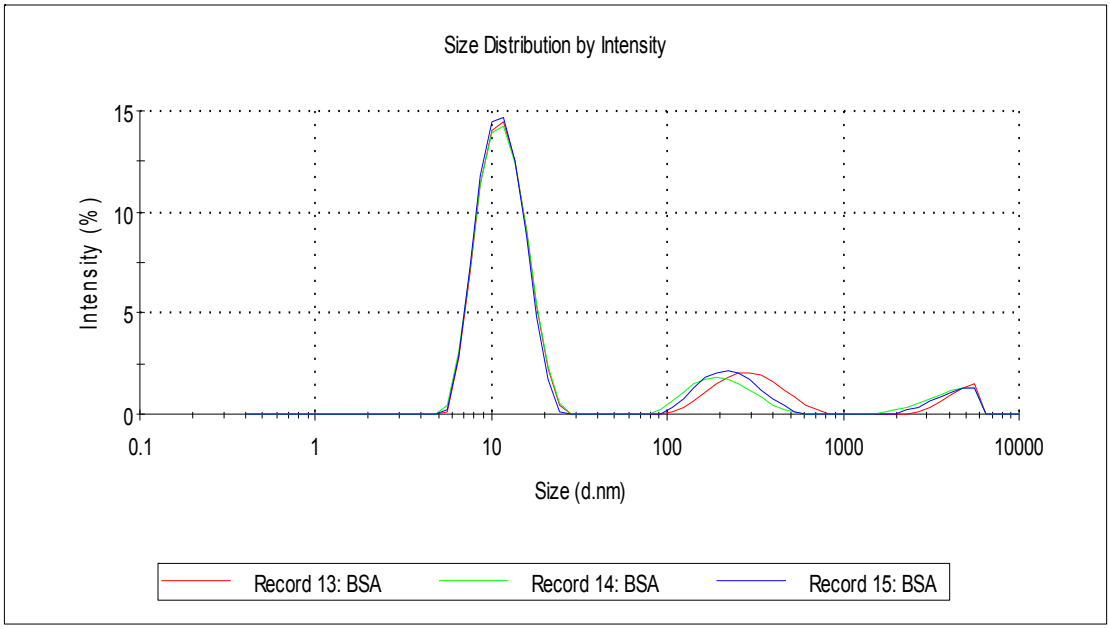

Figure 5.13 – DLS spectra of albumin

The single protein peak seen in DLS spectra, along with the calculated molecular weights have helped determine the exact nature of the calibration standards. For example with β amylase, if the protein was monomeric and linear then a diameter of 12.5 nm would be expected, whereas if the protein is a tetramer and globular then the diameter would be expected to be 11.5 nm. The average measured diameter is 11.73 nm, which is much closer to the tetramer size and gives a similar molecular weight in the globular conformation.

The DLS work has demonstrated that β amylase and alcohol dehydrogenase are not denatured on the column by the 8M urea but are in the tetrameric form and globular proteins. Albumin is generally seen as the trimer rather than the monomer although on some occasions it has been noted that the albumin peak appears before the β amylase which would indicate a tetramer has been formed. In the HPSEC calibration files the molecular weights given in Table 5.4 are used. The blue dextran peak is not included in the calibration file but is run to determine the totally excluded retention time of the column. This may not be seen in all HPSEC systems but is observed with the HPSEC and parameters described above, and highlight the uncertainties within the calibration.

protein standard	molecular weight / kDa	protein standard	molecular weight / kDa
blue dextran	2000	albumin	198
β amylase	200	carbonic anhydrase	29
alcohol dehydrogenase	150	cytochrome c	12.4

Table 5.4 – molecular weights of protein standards as used in the HPSEC calibration file

Implications for English Heritage Silks

The results of the HPSEC analysis will provide information on the current condition of the silks within the English Heritage collection. This information can be compared with data from accelerated ageing tests to allow a greater understanding of the causes of the silk deterioration. The results of the HPSEC analysis can also be compared with published results for historic silk samples analysed as part of MODHT. This research noted greater deterioration for historic samples compared to artificially aged samples. As only light accelerated ageing was utilised this adds weight to the theory that other factors as well as light may be responsible for silk deterioration.

Burrell Tapestry

In MODHT only artificially aged silks were sampled with both the front and back of the same thread. A small number of historic samples were removed from the front of tapestries and these were found to be in a similar condition to those from the reverse. To determine whether the similarity found in MODHT was due to sampling position or dyeing processes rather than age and condition of the silk a number of samples were taken from the same thread on both the front and back of a historic tapestry.

Figure 5.14 – light yellow silk in the leaves of the tapestry border
(reproduced by permission of the Burrell Collection, Glasgow Museums, Culture and Sport Glasgow)

The tapestry is one of a series of three woven for Robert Dudley, Earl of Leicester (d.1588). It depicts the Dudley coat of arms, held by lion supporters and surrounded by English flowering plants and a border of flowers and fruit. Conservation work on the tapestry at the Textile Conservation Centre (TCC) made access to individual threads easier. During conservation it was noticed that there were a large number of fragments of lost silk that were seemingly the same light yellow colour (see Figure 5.14). There were a large number of details within the tapestry border as well as highlights on the central lion in this colour. The same thread was sampled from both the front and the back of the tapestry in seven different locations (see Figure 5.15). Visual assessment suggested that locations 1 to 3 were in a rather poor condition (front and back), whereas the reverse sections of samples 5 to 7 had retained more colour.

Figure 5.15 – Dudley Armorial tapestry overview (reverse) with sampling locations marked (reproduced by permission of the Burrell Collection, Glasgow Museums, Culture and Sport Glasgow)

This light yellow colour was selected due to ease of access to samples arising from previous damage, as well as the relatively even distribution of this colour across the tapestry. It was hoped that by running these samples any effects from the dye

would be minimised due to the similar colour and that a number of locations would be more representative than a single area of damage. Therefore any differences observed between the front and back samples would be due to the actual condition of the silk by limiting the other possible variables.

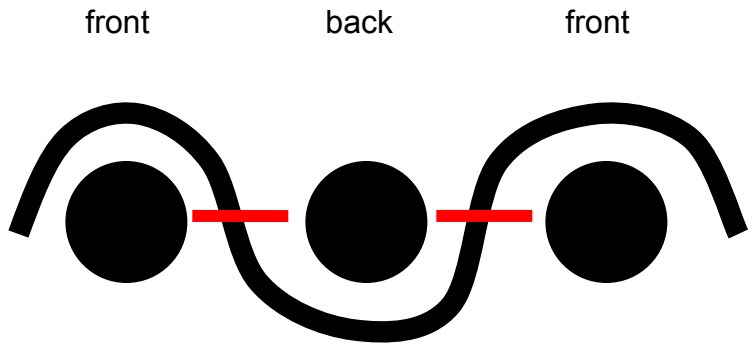

Figure 5.16 – cross section of tapestry weave structure

Figure 5.16 shows a cross section of the weave structure. The sampled threads were removed and separated into a front and back section by cutting along the red lines in the illustration. Samples labelled as from the front are from the displayed side. The resulting samples, such as that in Figure 5.17 were around 3 mm long. The sampling is difficult as the threads are unpicked to provide a sample which has definitely come from the front or back region. Ethically this means not only removing material for a destructive technique but also removing some material that forms the image on the front. To minimise the impact sampling had, material was carefully removed from the edges of areas with previous damage. In each case only one thread was removed and just one front and back section taken. This has implications for how representative the samples may be as the areas had already suffered some damage, as well as the limited number of samples that could be justified.

Figure 5.17 – sample 5 back

As can be seen in Figure 5.18, there is little difference in the traces for the front and back samples. For the seven samples there were some differences mainly in the intensity of the signal for the unfaded backs in samples 5 to 7. However the retention time and over all shape of the molecular weight distributions are similar for all samples when comparing the front and back sections. When the peak area is integrated to determine the weight-averaged molecular weight (M_w) the differences between the front and back sections show little change (see Figure 5.19). These initial results suggest that samples, which at first sight seemed in better condition (5-7) are as deteriorated as the others, according to the molecular weight criterion. Furthermore, within experimental error, the extent of deterioration for the front and back samples seems to be much the same.

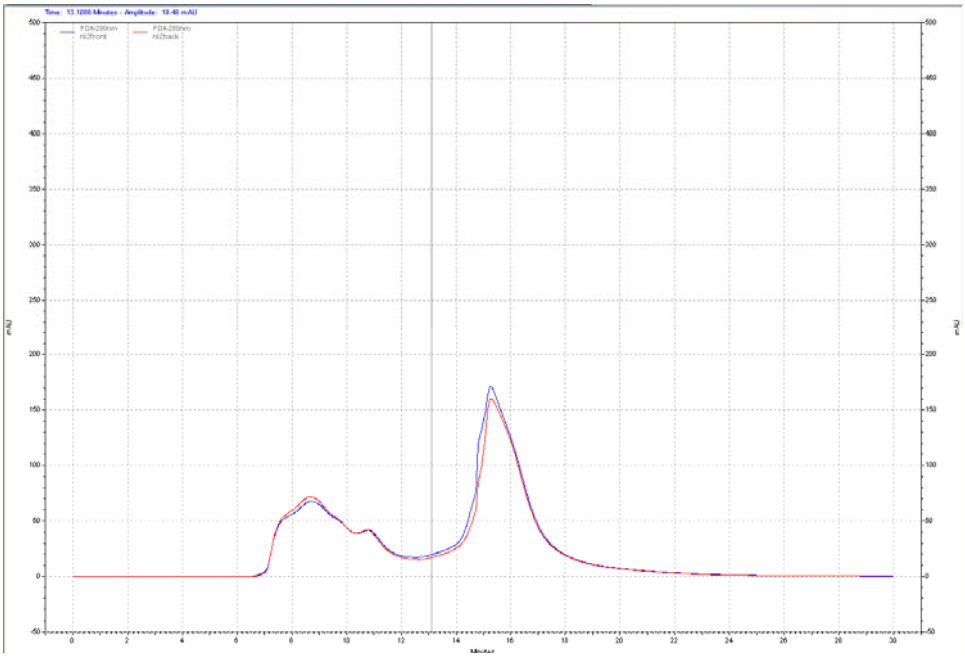

Figure 5.18 – sample 2 HPSEC chromatograms (front: blue; back: red)

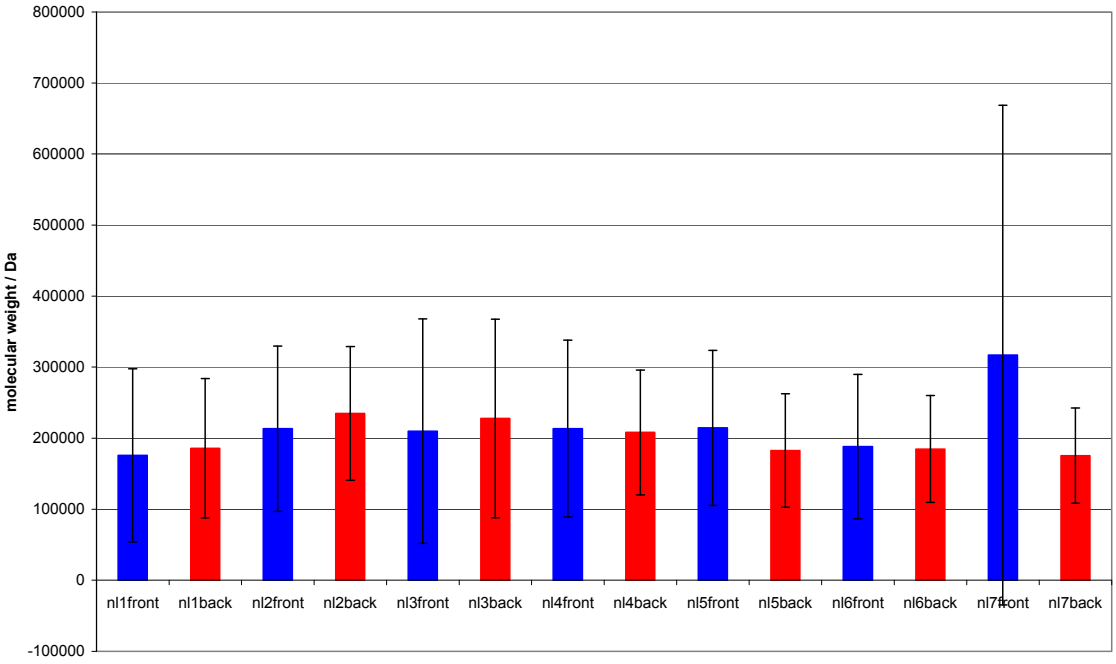

Figure 5.19 – molecular weight results; the average and range for the triplicate analyses are shown in each case (front: blue; back: red)

In relation to the sampling position there does not seem to be any correlation between the condition of the silk and its location on the tapestry. The results indicate that any difference in the fading of the dye cannot be taken as an indication of the level of silk deterioration. It appears that light is not the only important factor in silk deterioration, confirming that the critical factors promoting silk degradation need to be reassessed.

Conclusions

Tests using the HPSEC have demonstrated the repeatability of analysis and its ability to provide information on the molecular weight of samples. The small amount of sample required allows historic samples taken from the English Heritage collection to be analysed and information on the condition to be obtained. Comparison with results from accelerated ageing experiments should also allow correlation between a number of analytical methods providing further information on the condition and potentially remaining lifetime of the historic collections. However a number of difficulties with the calibration methods have been identified and these may be problematic in determining the molecular weight of samples. To determine whether HPSEC could be successfully applied it was used as one of the analytical methods for the kinetics ageing experiments.

References

[1] Howell, D. (1992) 'Silk Degradation Studies' in *Silk: Harpers Ferry Regional Textile Group, 11th Symposium*, Washington DC: Harpers Ferry Regional Textile Group 11-12.

[2] Tse, S. and Dupont, A.-L. (2001) 'Measuring silk deterioration by high-performance size-exclusion chromatography, viscometry and electrophoresis' in *Historic Textiles, Papers, and Polymers in Museums, ACS Symposium Series 779* Cardamone, J. and Baker, M. (ed.) Washington DC: American Chemical Society 98-114.

[3] Hallett, K. and Howell, D. (2005) 'Size exclusion chromatography as a tool for monitoring silk degradation in historic tapestries', in *AHRC Research Centre for Textile Conservation and Textile Studies First Annual Conference – Scientific Analysis of Ancient and Historic Textiles Postprints,* Janaway, R. and Wyeth, P. (ed.) London: Archetype 143–150.

[4] Hallett, K. and Howell, D. (2005) 'Size exclusion chromatography of silk: inferring the textile strength and assessing the condition of historic tapestries' in *ICOM Committee for Conservation 14th Triennial Meeting Preprints, The Hague, 12-16th September 2005 Preprints* **2** 911-919.

[5] Carr, C. M. (2006) 'Monitoring of Damage to Historic Tapestries (MODHT) EVK4-2001-00048 Final Report'.

[6] http://www.phenomenex.com/products/brands/view.aspx?id=9705 accessed 31/07/2009.

[7] Dai, C.-A., Kramer, E. J., Washiyama, J. and Hui, C.-Y. (1996) 'Fracture Toughness of Polymer Interface Reinforced With Diblock Copolymer: Effect of Homopolymer Molecular Weight' *Macromolecules* **29 (23)** 7536-7543.

[8] Pace, C. N. (1986) 'Determination and Analysis of Urea and Guanidine Hydrochloride Denaturation Curves' *Methods in Enzymology* **131** 266-280.

[9] BioSep brochure http://www.phenomenex.com/WorkArea/showcontent.aspx?id=8143 accessed 31/07/2009.

[10] Beaven, G. H. and Holiday, E. R. (1952) 'Ultraviolet Absorption Spectra of Proteins and Amino Acids' *Advances in Protein Chemistry* **7** 319-386.

[11] Georgakoudi, I., Tsai, I., Greiner, C., Wong, C., DeFelice, J. and Kaplan, D. (2007) 'Intrinsic fluorescence changes associated with the conformational state of silk fibroin in biomaterial matrices' *Optics Express* **15 (3)** 1043-1053.

[12] Mitchell, S. personal communication, 23/07/2007.

[13] Hallett, K. personal communication, 05/04/2007.

[14] Trotman, S. R. and Bell, H. S. (1935) 'The Determination of Damage in Silk' *Journal of the Society of Chemical Industry (Transactions)* **54** 141T-142T.

[15] Tweedie, A. S. (1938) 'A Study of the Viscosity Method for the Determination of Damage in Silk' *Canadian Journal of Research* **16B** 134-150.

[16] Goto, Y., Tsukada, M. and Minoura, N. (1990) 'Molecular Cleavage of Silk Fibroin by an Aqueous Solution of Lithium Thiocyanate' *Journal of Sericultural Science of Japan* **59 (6)** 402-409.

[17] Yamada, H., Nakao, H., Takasu, Y. and Tsubouchi, K. (2001) 'Preparation of undegraded native molecular fibroin solution from silkworm cocoons' *Materials Science and Engineering C* **14** 41-46.

[18] Lucas, F., Shaw, J. T. B. and Smith, S. G. (1958) 'The Silk Fibroins' *Advances in Protein Chemistry* **13** 107-242.

[19] Mandal, B. B. and Kundu, S. C. (2008) 'A Novel Method for Dissolution and Stabilization of Non-Mulberry Silk Gland Protein Fibroin Using Anionic Surfactant Sodium Dodecyl Sulfate' *Biotechnology and Bioengineering* **99 (6)** 1482-1489.

[20] Denny, M. W. (1980) 'Silks – their Properties and Functions', in *The Mechanical Properties of Biological Materials* (*Symposia of the Society for Experimental Biology*) **34** Vincent J. F. V. and Currey, D. J. (eds.) New York: Cambridge University Press 247-272.

[21] Tanford, C. (1964) 'Isothermal Unfolding of Globular Proteins in Aqueous Urea Solutions' *Journal of the American Chemical Society* **86** 2050-2059.

[22] Trathnigg, B. (2000) 'Size-exclusion Chromatography of Polymers' in *Encyclopedia of Analytical Chemistry* Meyers, R. A. (ed.) Chichester: Wiley 8008-8034.

[23] Hacke, M., Hallett, K., Odlyha, M., Peggie, D., Quye, A. and Berghe, I. V. (2009) 'Appendix 1 Technical Details and Protocols for Scientific Analysis' in '*Wrought in Gold and Silk' Preserving the Art of Historic Tapestries* Edinburgh: NMS Enterprises Limited – Publishing 111.

[24] Ramjeesingh, M., Huan, L.-J., Garami, E. and Bear, C. E. (1999) 'Novel method for evaluation of the oligomeric structure of membrane proteins' *Biochemical Journal* **342** 119-123.

[25] Bühner, M. and Sund, H. (1969) 'Yeast Alcohol Dehydrogenase: - SH Groups, Disulfide Groups, Quaternary Structure, and Reactivation by Reductive Cleavage of Disulfide Groups' *European Journal of Biochemistry* **11** 73-79.
[26] Bloustine, J., Berejnov, V. and Fraden, S. (2003) 'Measurements of Protein-Protein Interactions by Size Exclusion Chromatography' *Biophysical Journal* **85** 2619-2623.
[27] Goetz, H., Elgass, H. and Huber, L. (1985) 'Determination of Molecular Weight Data in Size-Exclusion Chromatography by Use of Broad-Molecular-Weight-Distributed Standards' *Journal of Chromatography* **349** 357-367.
[28] Oliva, A., Llabrés, M. and Fariña, J. B. (2001) 'Comparative study of protein molecular weights by size-exclusion chromatography and laser-light scattering' *Journal of Pharmaceutical and Biomedical Analysis* **25** 833-841.
[29] Hossain, K. S., Ochi, A., Ooyama, E., Magoshi, J. and Nemoto, N. (2003) 'Dynamic Light Scattering of Native Silk Fibroin Solution Extracted from Different Parts of the Middle Division of the Silk Gland of the *Bombyx mori* Silkworm' *Biomacromolecules* **4** 350-359.
[30] Kaszuba, M., McKnight, D., Connah, M. T., McNeil-Watson, F. K. and Nobbmann, U. (2008) 'Measuring Sub Nanometre Sizes Using Dynamic Light Scattering' *Journal of Nanoparticle Research* **10** 823-829.

Chapter 6 – Silk Deterioration Kinetics Study

To study the rate of deterioration of silk a kinetics study has been undertaken. This chapter reviews the available literature values for the activation energy of silk reactions. The experimental conditions used for the kinetics study and the results are presented. A number of methods to determine the activation energy are included with the experimentally determined value for silk deterioration. Design optimisation of the accelerated ageing experiments on the basis of this result is discussed.

Accelerated ageing experiments will be used to mimic silk deterioration occurring on open display. Ageing under the range of display conditions identified in chapter two, will help determine the critical deterioration factors for silk. However, to put the results into context, the length of ageing needs to be related to an equivalent length of time on display. For example is 100 years light exposure at 200 lux, causing more damage than 100 years exposure to high humidity? To answer this question requires knowledge of the increase in the rate of deterioration caused by the higher temperatures used for accelerated ageing. For some other materials in conservation (most extensively paper and photographic media) this has been done using the activation energy, E_a. However for silk there has been little research on the rates of reaction or determination of E_a.

The kinetics work is a preliminary study, designed to supplement the available published data with the rate of silk deterioration and the associated activation energy of the reaction. The complexity of kinetics studies and limited time means the results will not be an exact prediction, more a guide to what might happen. The study should also put the available data in the literature into perspective and determine whether any of the values of E_a are suitable for relating the ageing to display intervals. Some of the information in this chapter was presented at *Natural Fibres in Australasia*, the paper from which is in Appendix 4.

Published Activation Energies for Silk

There are a limited number of studies which quote a value of E_a for silk including two with values extracted from thermal analyses. However these methods may not be relevant to silk deterioration occurring on open display. Work by Bora *et al.*[1] gives activation energies for three different types of silk analysed using DSC. For each type of silk a value is given for the dehydration reaction, around 100 – 150 °C, with E_a between 10 – 13 kJmol^{-1}. The E_a is also reported for the decomposition reaction, around 300 °C, with activation energies between 30 – 39 kJmol^{-1}. Work by Garside and Wyeth[2] gives calculated activation energies from TGA traces. However, these are suggested to relate to fibroin crystallite melting, and the values (between 45 and 79 kJ g^{-1}) on conversion to standard units (kJmol^{-1}) seem inconsistent with lower E_a decomposition reactions.

Thermal chemiluminescence of fibrous proteins determined a change in the activation energy at the glass transition temperature, T_g. Below the T_g the activation energy is reported as 54 kJ mol^{-1} however this rises to 147 kJ mol^{-1} above the T_g.[3] Studies on conservation processes have also reported the activation energy including silk degradation caused by copper acetate (used as a pigment, verdigris) which calculated the activation energy as 100 kJ mol^{-1}.[4] A study on the use of Parylene-C as a consolidant for silk, determined the activation energy from tensile testing after ageing between 70 °C and 110 °C. Depending on the tensile property used the activation energies for uncoated aged silk were between 59.5 – 66.4 kJ mol^{-1}.[5]

The variation in these values means it is difficult to determine whether any of these activation energies can be used to determine the increase in rate of deterioration. It is also likely that the silk deterioration occurring on open display in historic houses is different to some of the reactions above, so the activation energy is also liable to be different. To relate the ageing and display intervals a kinetics study was undertaken on silk deterioration reactions. The experiments also act as a

preliminary test for the accelerated ageing set up to minimise experimental design problems for the later long-term ageing tests.

Methodology

Experimental Set Up

For this initial study a limited number of the accelerated ageing parameters were selected. Hybridisation tubes were used for ageing as they can be sealed and heated without contaminating the samples inside. These have been prepared as shown in Figure 6.1. RH levels will be created with saturated salt solutions with a piece of glass wool above to prevent salt migration and reduce possible contamination of the silk. The silk samples are suspended above from a filter paper via a loop of polyester thread. The lid is then firmly closed with the rubber seal inside (PTFE coated side onto the filter paper).

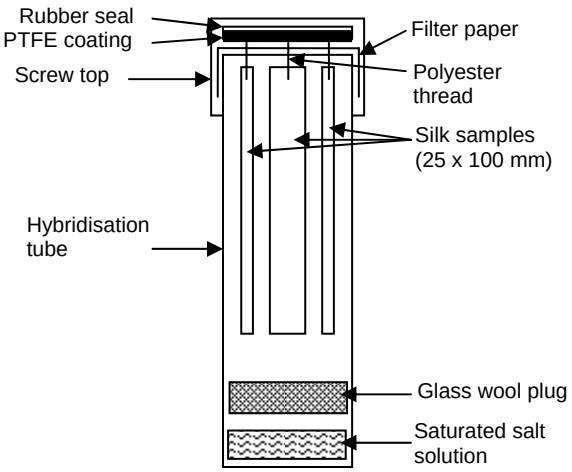

Figure 6.1 – kinetics ageing experimental set up

Elemental analysis of the English Heritage collection (see chapter three) found that the majority of the objects are made of plain silk; this will be replicated using medium weight habotai silk in the kinetics ageing tests. This will also be used in

the accelerated ageing tests. Three pieces of silk, 25 x 100 mm (warp in the longest direction) provide replicates for each ageing condition. The size of the silk is limited due to the size of the hybridisation tubes. Samples were prepared for each set of ageing conditions with one tube removed weekly for 6 weeks.

Environmental Conditions and Creation

As the dehydration of silk crystals is reported around 100 °C[1,6,7] ageing was undertaken at 50, 60, 70, 80 and 90 °C. Saturated salt solutions were used to produce environments of approximately 30% ($MgCl_2.6H_2O$), 50% (NaBr) and 75% (NaCl) RH for ageing. The RH levels vary by up to 6% between 50 and 90 °C[8].

To compare the effect of light on the ageing of silk some samples were placed in a daylight ageing light box (for full details see chapter seven). The direct light level under the UV filter was measured as 7000 lux but the hybridisation tubes and the angle reduce this to 1900 lux. To ensure an equal comparison half the hybridisation tubes were wrapped in aluminium foil and placed in the light box (20 °C dark samples). Ageing samples have been given an identification code relating to the conditions used. This is made up of the temperature (20, 50, 60, 70, 80, 90), RH level (30, 50, 75) and lighting conditions (L / D) with the time interval in weeks (1-6), for example 20 30 L 4 has been aged in the light box at 30% RH for 4 weeks.

Method of Analysis

After ageing each sample was tensile tested to measure the maximum load and the tensile extension at maximum load, as well as determining the molecular weight of the samples with HPSEC. Tensile testing data was acquired at 22 ± 2 °C, 52 ± 5% RH on an Instron 5544 instrument, adapting the standard method for fabric strips BS EN ISO 13934-1:1999,[9] with gauge lengths of 50 mm and a crosshead speed of 10 mm/min. Results for strips which broke close to the jaws were discarded and average values calculated. As the sample size selected differs

to that given in the British Standard[10] a series of tests were carried out to study the effects of varying the sample size. These looked at differences based on the sample direction (warp or weft threads in the longest direction), width and length as well as the extension rate.

For the HPSEC, 1.5 mg of silk was dissolved in 0.6ml of ~21M lithium thiocyanate solution, with the greater concentration and volume allowing three replicate runs to be performed on the HPSEC. In most cases material was taken from replicate number one. The equipment and method used is described in chapter five.

Determination of the Rate of Deterioration

Previous silk accelerated ageing studies, at 0 and 100% RH, have found that tensile properties show an exponential decrease over time[11]. For this work, the apparent first order rate constants of deterioration, k, were determined from the slopes of plots of the log (load or extension) versus time, following linear regression. The degradation of silk has also been described as having first order rate constants after light and heat ageing measured using breaking strength.[12] The same method was also used for the HPSEC data.

Determination of the Activation Energy

The Arrhenius equation (Equation 6.1) was then applied to determine the activation energy for deterioration at each RH level.

$$k = Ae^{-Ea/RT} \qquad \textbf{Equation 6.1}$$

In Equation 6.1 k is the rate constant, A the pre-exponential factor, E_a the activation energy, R the gas constant and T the temperature (in K). E_a values were estimated from the slopes of graphs of ln(k) against the reciprocal temperature (see Figure 6.2).

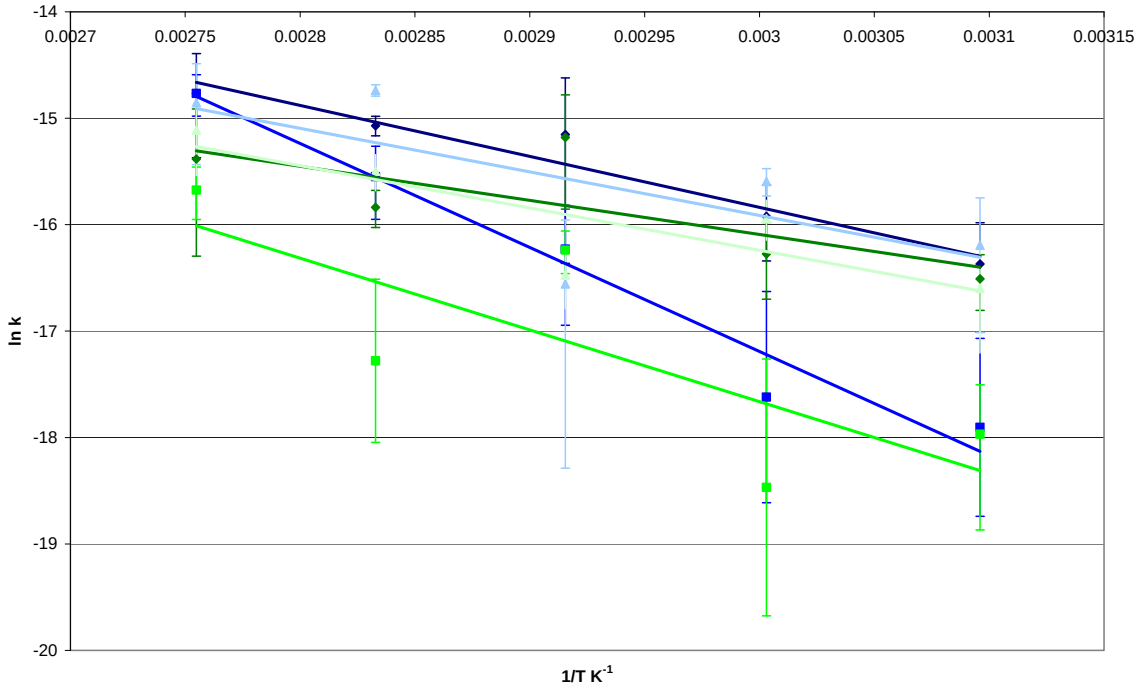

Figure 6.2 – Arrhenius plot for tensile testing results

(extension: 30% dark blue; 50% blue; 75% light blue; load: 30% dark green; 50% green; 75% light green)

Results and Discussion

Tensile Testing - Parameter Variation Trial

Due to the size of the hybridisation tubes the silk samples were limited to 25 x 100 mm. To study the effects this reduced size would have, compared with the size given in the British Standard, a trial was undertaken. Five replicate samples of 100, 150, 200 and 250 mm in length, by 25 and 50 mm in width were compared at extension rates of 10 and 20 mm min^{-1}. The gauge length was increased from 50 mm (for the 100 mm long samples) by 50 mm increments with increasing sample length, to 200 mm for the 250 mm long samples. Samples were prepared with both the warp and weft in the longest direction to determine if this would have any

difference. The trial was conducted on the same plain weave silk habotai used for the kinetics study.

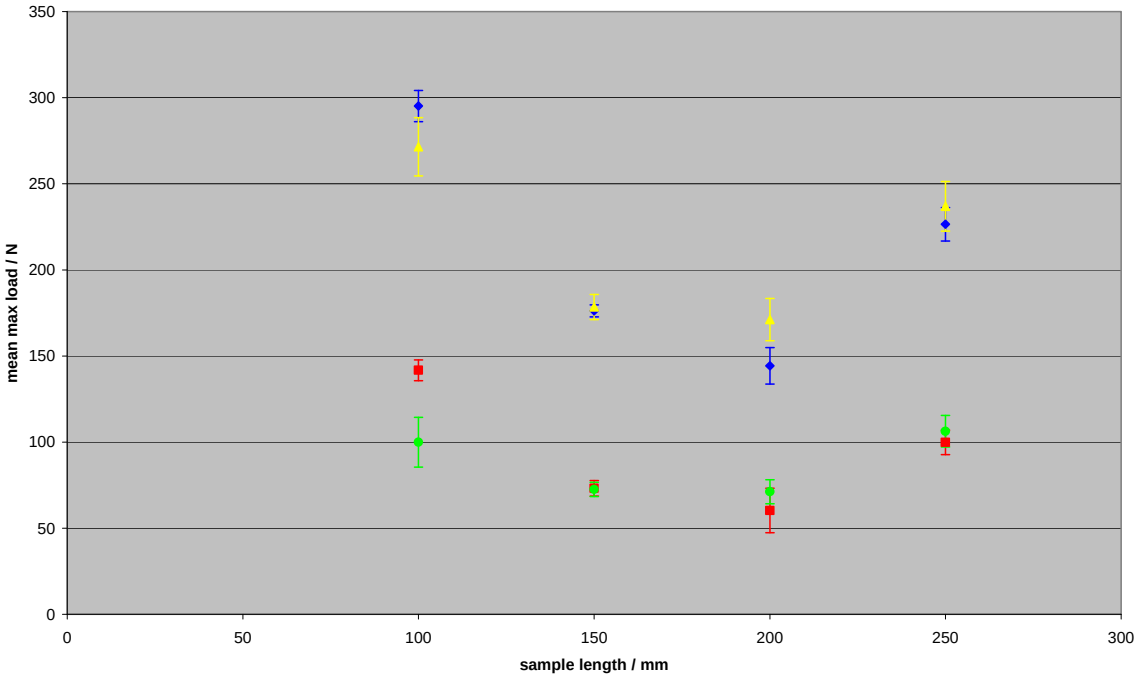

Figure 6.3 – variation in maximum load with increasing length of weft samples

(width 50 mm, speed 20 mm/min: blue; width 25 mm, speed 20 mm/min: red; width 50 mm, speed 10 mm/min: yellow; width 25 mm, speed 10 mm/min: green)

For samples cut with the weft fibres in the longest direction (referred to as weft samples) there was a drop in the maximum load between the 100 and 200 mm long samples (see Figure 6.3). From 200 to 250 mm the maximum load increased. Doubling the width of the samples from 25 to 50 mm increases the maximum load by approximately a factor of two, as might be expected. Doubling the extension rate had almost no effect.

In the extension at maximum load there is very little change between the 100 and 150 mm long samples in the weft direction. This is followed by an increase in the extension at maximum load between 150 to 250 mm (see Figure 6.4). In the weft

direction the length of sample seems to affect the results therefore weft samples will not be analysed in further work.

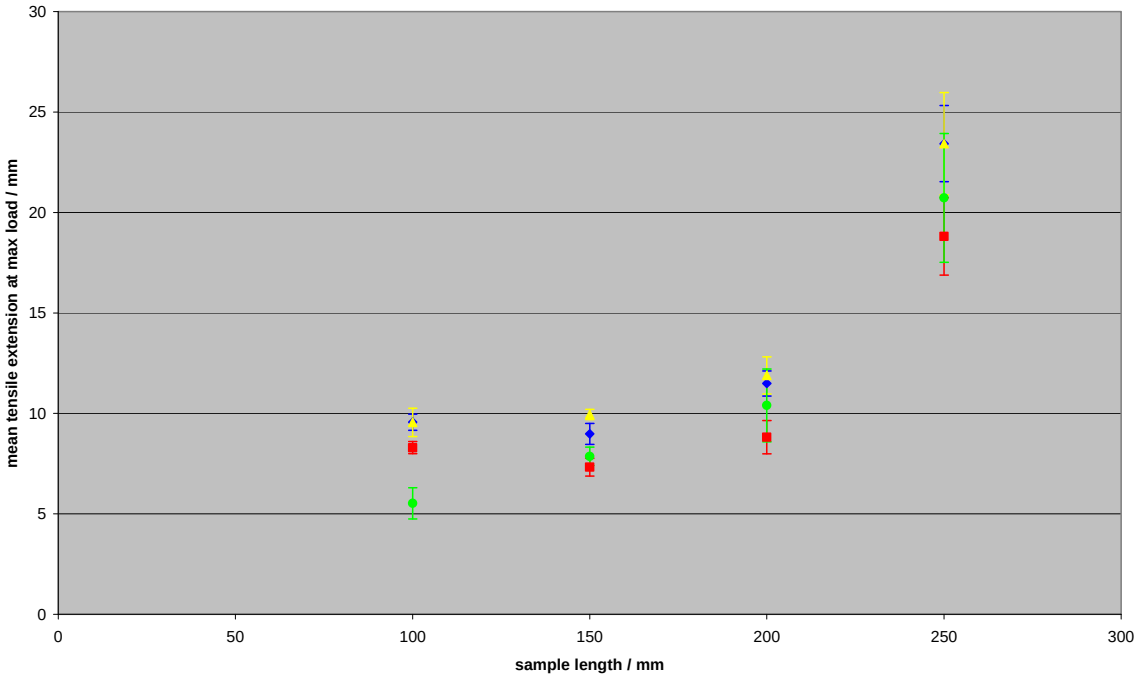

Figure 6.4 – variation in extension at maximum load with increasing length of weft samples

(width 50 mm, speed 20 mm/min: blue; width 25 mm, speed 20 mm/min: red; width 50 mm, speed 10 mm/min: yellow; width 25 mm, speed 10 mm/min: green)

For warp samples increasing the length had little effect on the maximum load measured. This is especially true for 25 mm wide strips (see Figure 6.5). Changes in the extension rate also had a minimal effect, again especially on the 25 mm wide samples, although a ten fold increase in extension rate has been reported to affect the strength of mulberry and Tussah silk filaments.[13] Increasing the width from 25 to 50 mm approximately doubled the maximum load, as with the weft samples. For the wider samples (50 mm) wider jaws were used. To determine if this had any impact on the results the narrower (25 x 100 mm) samples were run with both sets of jaws and at both extension rates. These values are within the experimental

error of each other therefore the effect of changing the jaws can be seen as negligible.

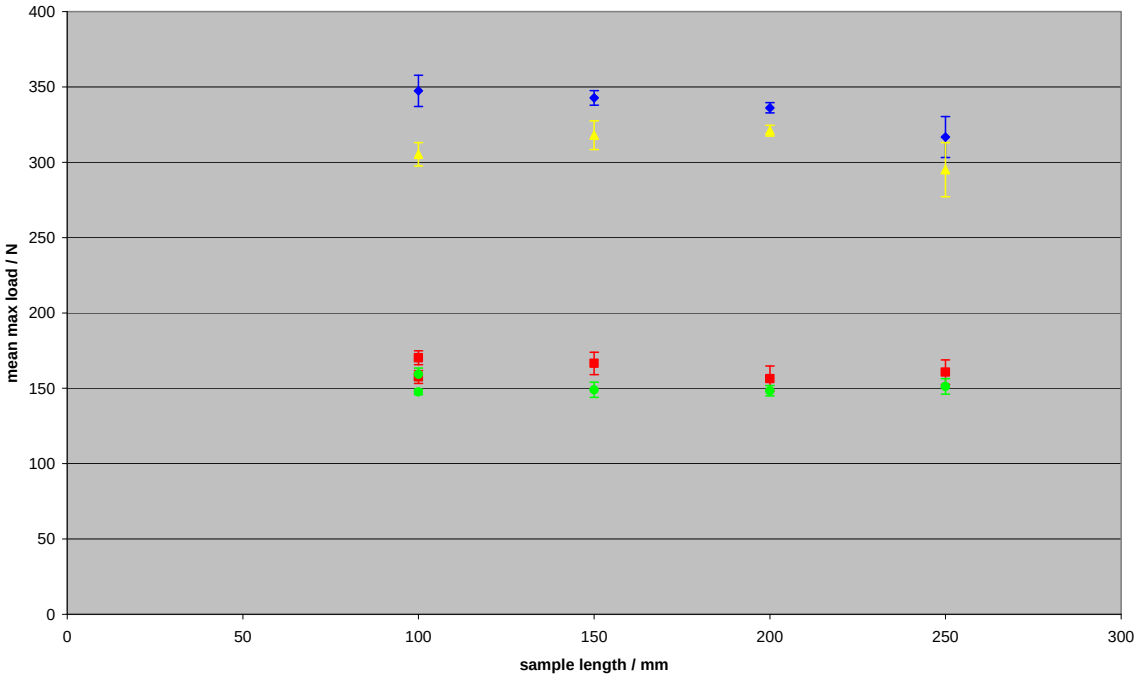

Figure 6.5 – variation in maximum load with increasing length of warp samples

(width 50 mm, speed 20 mm/min: blue; width 25 mm, speed 20 mm/min: red; width 50 mm, speed 10 mm/min: yellow; width 25 mm, speed 10 mm/min: green)

For the extension at maximum load data there is a linear increase with increasing sample, and therefore gauge length. These results seem to be regardless of the sample width, extension rate or jaw width (see Figure 6.6). These results suggest that using 25 x 100 mm silk strips for the kinetics trial will give meaningful data in comparison with the standard method. The final parameters chosen for the tensile testing were: 25 x 100 mm warp direction strips with an extension rate of 10 mm min^{-1} as this gave a smaller standard deviation from the mean. The jaw width used should have no bearing but for consistency the same jaws will be used throughout.

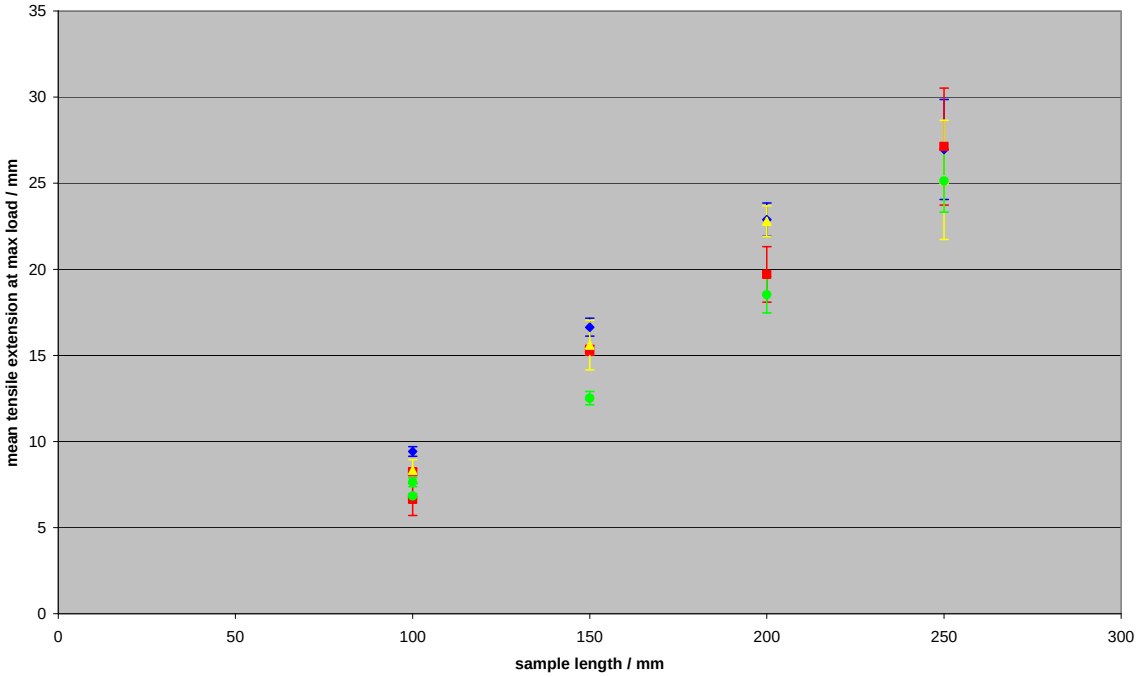

Figure 6.6 – variation in extension at maximum load with increasing length of warp samples

(width 50 mm, speed 20 mm/min: blue; width 25 mm, speed 20 mm/min: red; width 50 mm, speed 10 mm/min: yellow; width 25 mm, speed 10 mm/min: green)

Tensile Testing - Kinetics Samples

The tensile strength (measured as the maximum load at break) and tensile extension at break showed comparable changes. Figure 6.7 shows the maximum load at break results for samples aged at 75% RH and over the range of temperatures; similar trends were observed at 30% and 50% RH. Data in Figure 6.7 have exponential best-fit trendlines, which indicate a first-order deterioration rate for silk. There was a gradual reduction in the performance over the length of each set of heat and humidity ageing conditions, with the most marked effects at higher temperature and high humidity. For example, at 75% RH and 90 °C the maximum load was halved after just one to two weeks. There was also a noticeable increase in the yellowing of the samples at higher temperatures and humidities.

The ageing dependence on relative humidity is illustrated with the extension at maximum load for samples treated at 60 °C (see Figure 6.8). Perhaps surprisingly, at all temperatures the smallest change was observed for the samples kept at 50% RH. Although this is a tentative conclusion requiring confirmation, given the relatively small decrease in values coupled with the data scatter and size of the experimental error, it was confirmed by the maximum load results. Ageing at 75% RH caused the most deterioration.

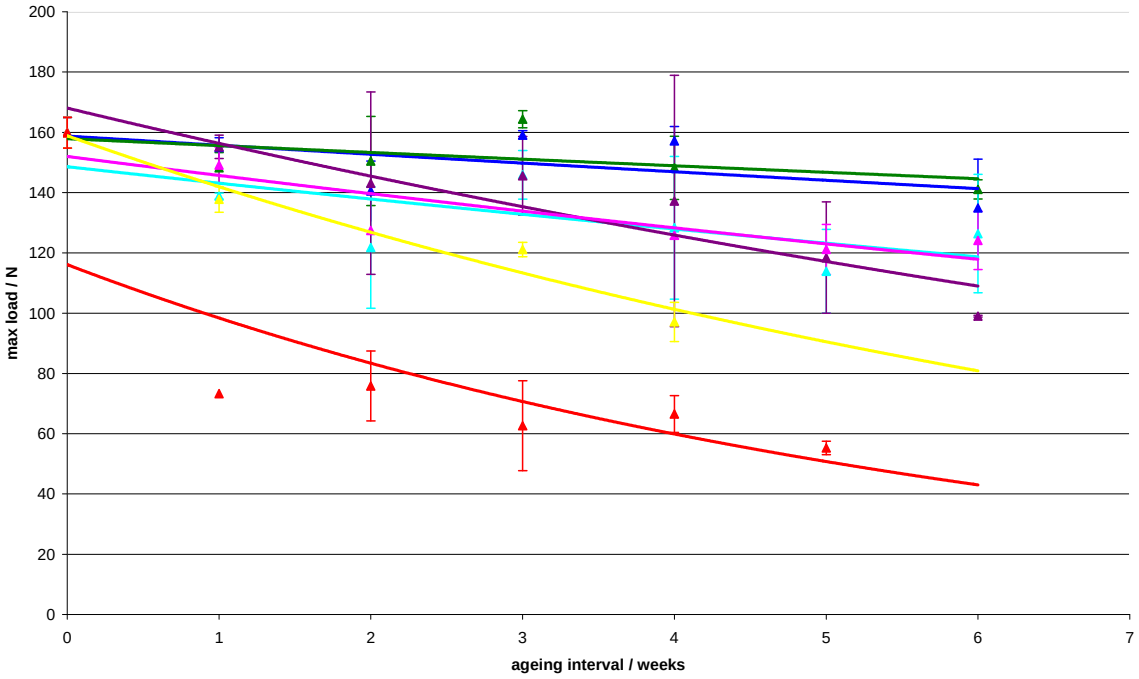

Figure 6.7 – changes in maximum load after ageing at 75% RH (other RH levels removed for clarity)

(20 °C light: blue; 20 °C dark: green; 50 °C: aqua; 60 °C: purple; 70 °C: pink; 80 °C: yellow; 90 °C: red)

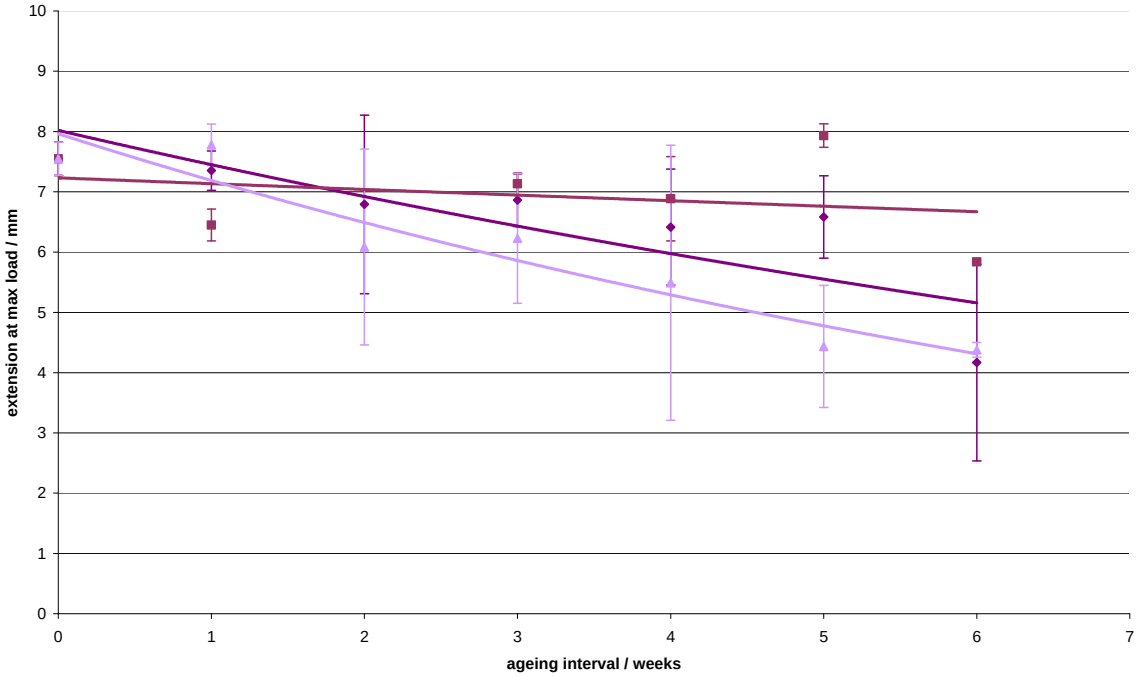

Figure 6.8 – changes in extension at maximum load after ageing at 60 °C
(30% RH: dark purple; 50% RH: purple; 75% RH: light purple)

For samples aged in the light box at room temperature (20 °C light and 20 °C dark) there was a small change after 6 weeks with little significant difference between the two sets of samples (see Figure 6.7). For the light aged samples those aged at 30% and 50% RH show a slight increase in strength with ageing (see Figure 6.9). This may be caused by experimental variations (such as changing RH during tensile testing) as the same effect is not observed in the HPSEC results which show little change on ageing. The small changes, with approximately flat slopes, and the slight increases giving positive slopes for the trend lines have implications for determining the rate of reaction later.

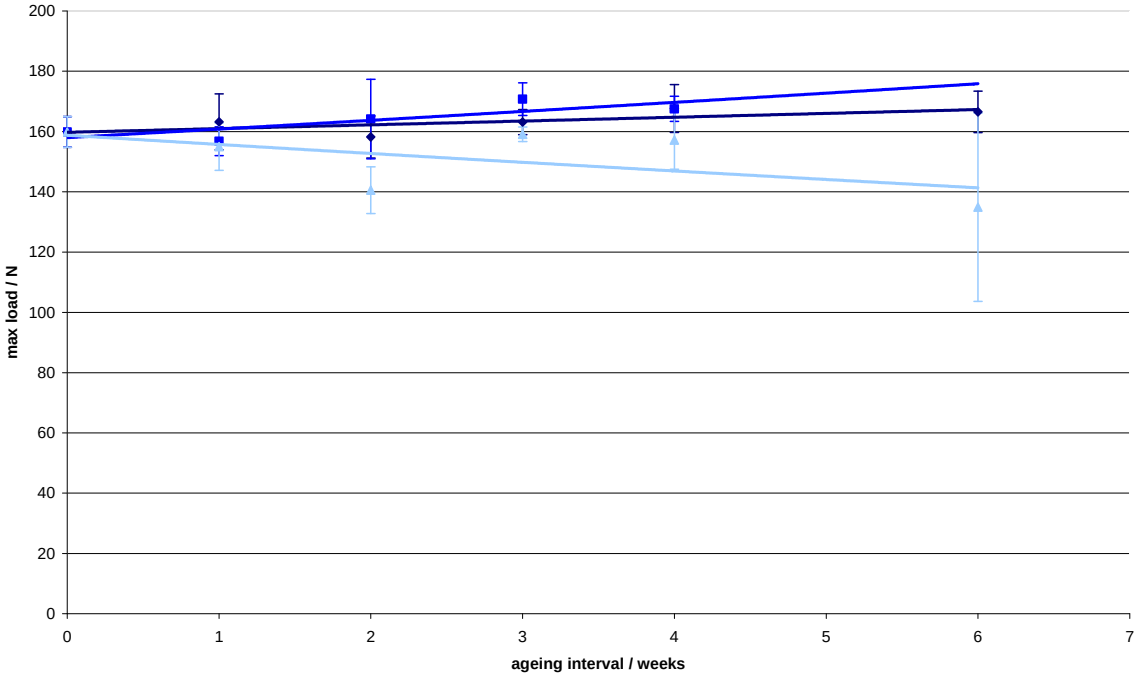

Figure 6.9 – maximum load results for samples light aged at 20 °C
(30% RH: dark blue; 50% RH: blue; 75% RH: light blue)

Tensile Testing - Rate Determinations

As described above the rate has been determined from the slopes of plots of the log (load or extension) versus time, following linear regression for example in Figure 6.10. The rate constant, k can be determined from the slope of each trend line, (which equals –k) these values are given in Table 6.1.

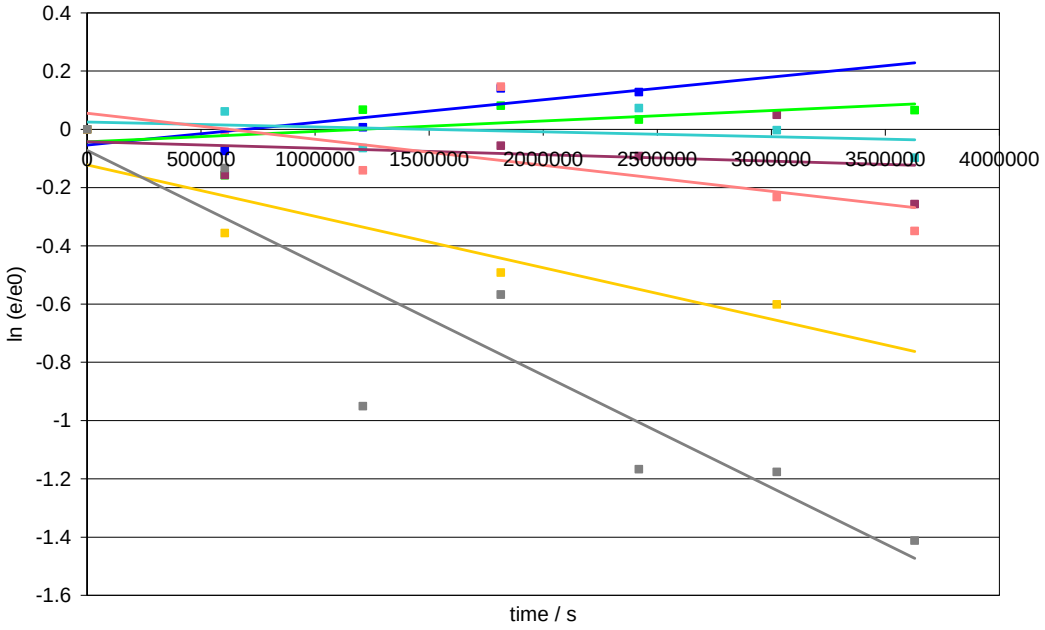

Figure 6.10 – calculating the rate constant from extension data after ageing at 50% RH (20 °C light: blue; 20 °C dark: light green; 50 °C: aqua; 60 °C: purple; 70 °C: pink; 80 °C: light orange; 90 °C: grey)

	30% RH	50% RH	75% RH
extension 20 °C L	-5.53E-09	-7.79E-08	4.10E-08
extension 20 °C D	-1.05E-09	-3.59E-08	4.33E-08
extension 50 °C	7.78E-08	1.67E-08	9.28E-08
extension 60 °C	1.22E-07	2.23E-08	1.69E-07
extension 70 °C	2.62E-07	8.93E-08	6.44E-08
extension 80 °C	2.85E-07	1.77E-07	3.97E-07
extension 90 °C	3.86E-07	3.86E-07	3.54E-07
load 20 °C L	-1.27E-08	-2.95E-08	3.21E-08
load 20 °C D	-4.67E-09	-1.42E-08	2.42E-08
load 50 °C	6.75E-08	1.57E-08	6.19E-08
load 60 °C	8.54E-08	9.53E-09	1.19E-07
load 70 °C	2.56E-07	8.86E-08	7.00E-08
load 80 °C	1.32E-07	3.13E-08	1.86E-07
load 90 °C	2.09E-07	1.56E-07	2.73E-07

Table 6.1 – rate constants (k) in s^{-1} determined from tensile results

Tensile Testing – Activation Energies

The 20 °C samples show little alteration on ageing, with either no change or a small increase in the slope (see Figure 6.10). The activation energy is determined by calculating ln(k), therefore if the slope (i.e. –k) is not negative but positive (or flat) then k becomes a negative number. This is problematic as the log of a negative number cannot be calculated. Table 6.1 includes a number of negative values of k for the samples aged at 20 °C, so only the samples aged at elevated temperatures (50 °C to 90 °C) have been used to determine the activation energies. The slopes of the lines in Figure 6.2 equals $-E_a/R$, where R is the gas constant (8.314 J K^{-1} mol^{-1}), these have been used to determine the activation energies in Table 6.2.

	30% RH	50% RH	75% RH
extension	40 ± 6	81 ± 9	34 ± 21
load	27 ± 13	56 ± 26	33 ± 12

Table 6.2 – activation energies (in kJ mol^{-1}) determined from tensile testing results

Although the calculated errors are relatively large, it is interesting to note that the activation energy is higher at 50% RH compared with the other two ageing conditions.

HPSEC - Kinetics Samples

The HPSEC results from the kinetics samples show a similar trend to the tensile testing results. For the majority of ageing conditions higher levels of relative humidity (RH) give a larger decrease in the weight-averaged molecular weight (M_w) of the silk (see Figure 6.11). Increases in temperature also caused larger decreases in the M_w, so the most deterioration was seen for the samples aged at

90°C and 75% RH. There are small changes observed in the samples aged at 20°C whether they were exposed to light or not, although the highest RH levels do seem to have caused slightly more deterioration. The molecular weight can also be measured by the number-averaged molecular weight (M_n) or the maximum peak position in the chromatogram (M_p). Both show similar trends to the M_w results.

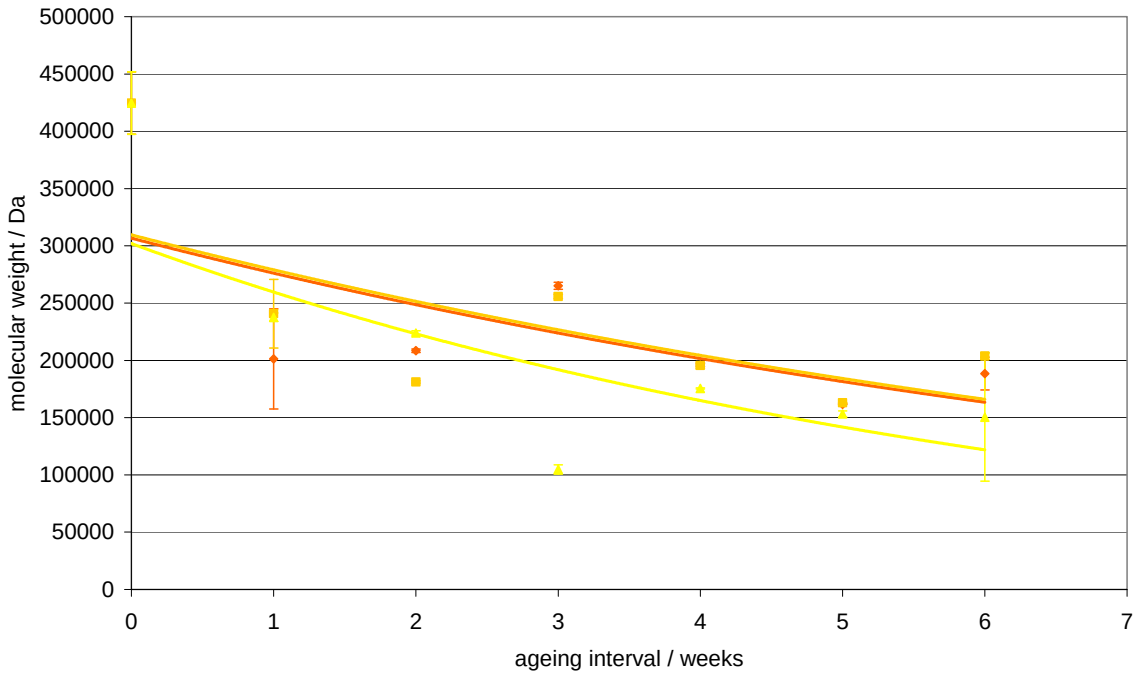

Figure 6.11 – changes in weight-averaged molecular weight after ageing at 80°C (30% RH: dark orange; 50% RH: orange; 75% RH: yellow)

When initially processing the HPSEC data it became apparent that very small changes in retention times for the calibration standards gave wildly different molecular weight values, often for the same sample. These difficulties and the solutions are discussed in more detail in chapter eight. However, due to these problems the values determined for the activation energy, using the method above; included some negative numbers with errors in the same region as the calculated activation energy. Therefore alternative methods of determining E_a were sought.

A review of similar experimental work from within paper conservation suggested two alternative methods to determine E_a. Work has shown that paper, or more accurately cellulose deterioration reactions can be more accurately followed using changes in the degree of polymerisation (DP) before and after ageing. A HPSEC study on cellulose reports DP is equivalent to the number-averaged molecular weight (M_n)[14] which may also apply to silk. The second method is time-temperature superposition (TTSP) which involves shifting the data along a time axis to align data from different temperatures to form a master curve for the deterioration reaction at a reference temperature, usually lower than the ageing temperatures. These are both investigated further using the data obtained.

Degree of Polymerisation

In cellulose deterioration, the degree of polymerisation (DP) has been used to follow the degradation reaction. Using the linear Ekenstam's relationship[15,16] a pseudo-zero order approximation can be calculated from Equation 6.2 or the first order reaction from Equation 6.3.

$$1/DP - 1/DP_0 = kt \qquad \textbf{Equation 6.2}$$

$$\ln (1-1/DP_0) - \ln (1-1/DP) = kt \qquad \textbf{Equation 6.3}$$

Where DP is the number-averaged degree of polymerisation and DP_0 the value at the start, t=0. Silk is a natural polymer, similar to cellulose, and the number-averaged molecular weight (M_n) has been reported to be equal to the degree of polymerisation (DP) in cellulose. Therefore it may be possible to use these equations to determine the rate of silk deterioration. An interesting difference with this method is that each time interval gives a rate of reaction k, which means for each week of ageing the activation energy can be calculated (see Figure 6.12 and Table 6.3).

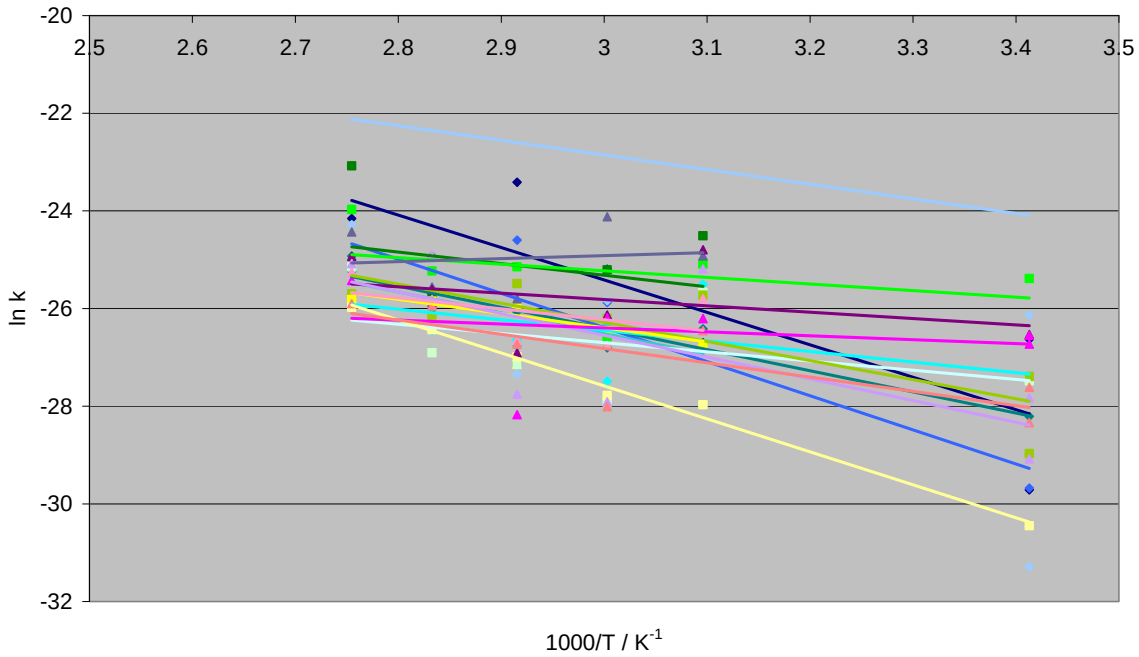

Figure 6.12 – Arrhenius plots using degree of polymerisation calculations (30% RH: week 1 dark blue; week 2 blue; week 3 light blue; week 4 dark aqua; week 5 aqua; week 6 light aqua; 50% RH: week 1 dark green; week 2 green; week 3 light green; week 4 olive green; week 5 yellow; week 6 light yellow; 75% RH: week 1 slate; week 2 dark purple; week 3 light purple; week 4 dark pink; week 5 light pink; week 6 coral)

RH/%	30	50	75
week 1	54 ± 31	20 ± 52	-5 ± 25
week 2	6 ± 35	34 ±27	1± 31
week 3	55 ± 59	18 ±39	29 ± 51
week 4	35 ±14	1 ± 11	17 ± 36
week 5	36 ±14	24 ± 5	19 ± 20
week 6	14 ±32	52 ±5	30 ± 25

Table 6.3 – activation energies (in kJ mol^{-1}) from degree of polymerisation calculations

As previously the values for ageing at 20 °C have been excluded, however as can be seen in Table 6.3 in most cases the errors within these calculations are similar

to the values themselves with relatively high variation between the weeks. It seems to suggest that this method of analysing the data does not improve on the previous, more traditional method or that M_n for silk cannot be used for the degree of polymerisation (DP) as with cellulose.

Time-Temperature Superposition

Another method which has been applied to paper deterioration but originally was used for polymers, such as neoprene, is time-temperature superposition (TTSP)[17]. This is used for thermal ageing predictions by shifting data from a number of higher temperatures by different shift factors along the time axis to produce a master deterioration curve for a lower temperature, at which the experiments would take too long. For paper deterioration the activation energy calculated by this method is similar to that calculated using the normal kinetics analysis for the same type of paper[18]. One of the initial stages for this method is to produce Arrhenius plots from time to equivalent damage (TED) data. This technique has been used to look at the deterioration processes for various materials within the film and photography conservation fields.

To produce the TED data, the analytical results are plotted as a ratio against the initial value, for example in Figure 6.13, the extension of the aged sample is divided by the extension of the unaged sample (e/e_0). Extension values have been used to provide a comparison with the molecular weight values and also to compare the activation energies calculated using this method with those given in Table 6.2 above. Figure 6.13 shows data from the 20 50 dark aged samples along with those aged at varying RH levels at both 60 and 80 °C. With increased ageing this ratio decreases, as the extension of the sample decreases with ageing. To produce an Arrhenius plot a measure of the deterioration is chosen, for example $e/e_0 = 0.9$, and the time taken for each ageing condition to reach this point is calculated, this is the TED value.

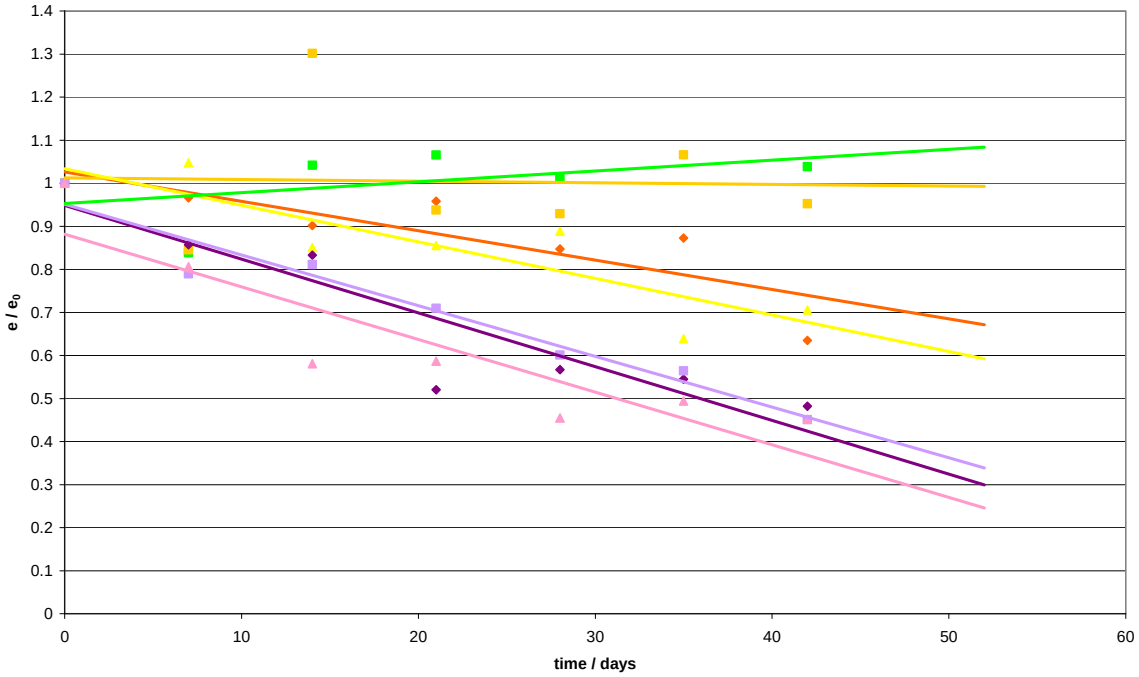

Figure 6.13 – the change in the extension ratio (e/e_0) with ageing time
(20 °C dark: green; 60 °C 30% RH: dark orange; 60 °C 50% RH: orange;
60 °C 75% RH: yellow; 80 °C 30% RH: dark purple; 80 °C 50% RH: light purple;
80 °C 75% RH: pink)

The Arrhenius plot uses the log of this time (ln(TED)) on the y axis against the reciprocal temperature used for ageing (1/T) on the x axis (see Figure 6.14) . The slope of the line equals E_a/R. Here the temperature axis is 1000/T which means the slope multiplied by R gives the activation energy in $kJmol^{-1}$ (as shown in Table 6.4). These graphs have positive slopes as ln(TED) rather than the reciprocal value is plotted, however the values obtained for the slope are identical regardless of this factor.

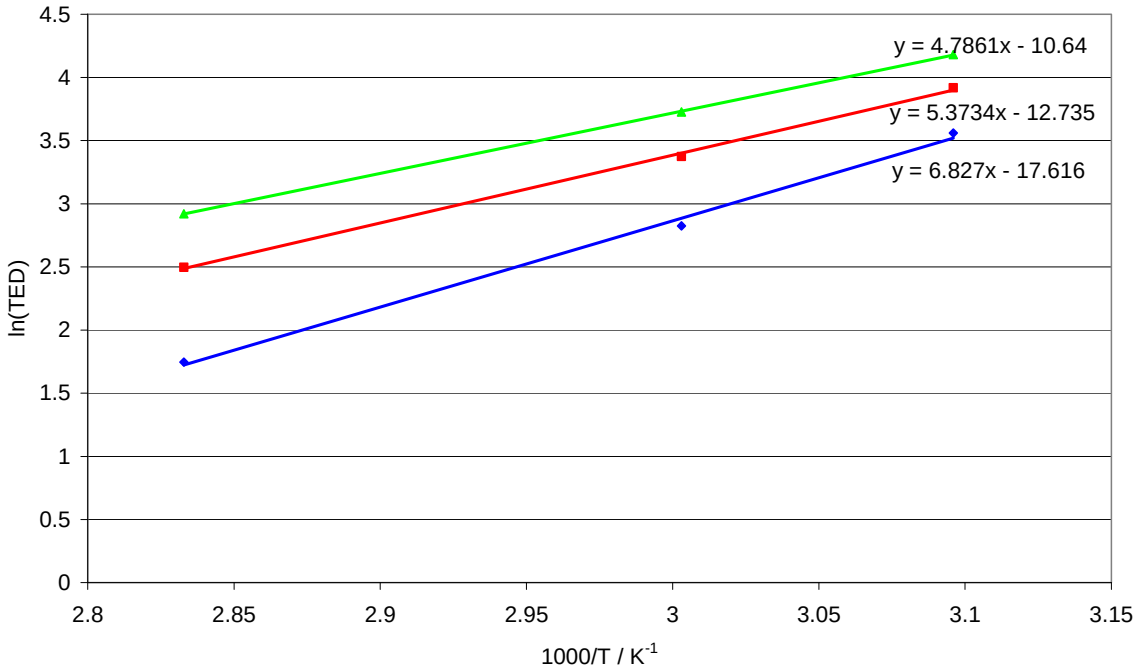

Figure 6.14 – Arrhenius plot for thermal ageing data at 30% RH

(e/e_0 = 0.9: blue; e/e_0 = 0.8: red; e/e_0 = 0.7: green)

For the extension data there are still some problems with this method, for example ageing at 70 °C and 30% RH gives negative values due to contamination of the samples by salt. To provide comparisons the TED data for e/e_0 = 0.9, 0.8 and 0.7 were all plotted, with at least three temperatures for each line. Generally these values are much closer together than those in Table 6.2, particularly within each RH level. However the same trend is seen as before with higher activation energies for 50% RH. The average activation energy for silk deterioration from this method was calculated as 50 kJ mol^{-1}.

RH / %	e/e_0 = 0.9	e/e_0 = 0.8	e/e_0 = 0.7	average
30	57 ± 3	45 ± 1	40 ±0.3	47
50	63 ± 11	66 ± 13	67 ± 21	65
75	39 ± 29	39 ± 10	38 ± 5	39

Table 6.4 – activation energies (in kJ mol^{-1}) calculated from TED extension

The TTSP method was also applied to the molecular weight results determined by HPSEC, using the weight-averaged molecular weight M_w values. The process used was the same as for the extension data above, with M_w/M_{w0} = 0.6, 0.5 and 0.4 being selected as the TED values. The calculated activation energies are given in Table 6.5. Again the values are close together, although much lower and with large errors, however the 50% RH values are higher as before. The low activation energies and high associated errors, along with the difficulties experienced in the molecular weight calculations mean the results of the HPSEC analysis have not been used to determine the activation energy.

RH / %	M_w/M_{w0} = 0.6	M_w/M_{w0} = 0.5	M_w/M_{w0} = 0.4	average
30	18 ± 10	14 ± 3	11 ± 4	14
50	28 ± 26	24 ± 14	22 ± 8	24
75	4 ± 6	14 ± 23	17 ± 28	12

Table 6.5 – activation energies (in kJ mol^{-1}) calculated from TED M_w

Having determined the activation energy for the reaction the master curve can be plotted (see Figure 6.15). Although not used further in this research the curve shows the loss of extension takes around 1200 days (or approximately three years). However this is strongly affected by a change in activation energy, increasing the activation energy from 50 kJ mol^{-1} (used to plot Figure 6.15) to 75 kJ mol^{-1} would shift the curve so e/e_0 = 0 takes around 10000 days. This could be useful to determine the predicted lifetime of materials where the activation energy is more certain, but has not been pursued as part of this research.

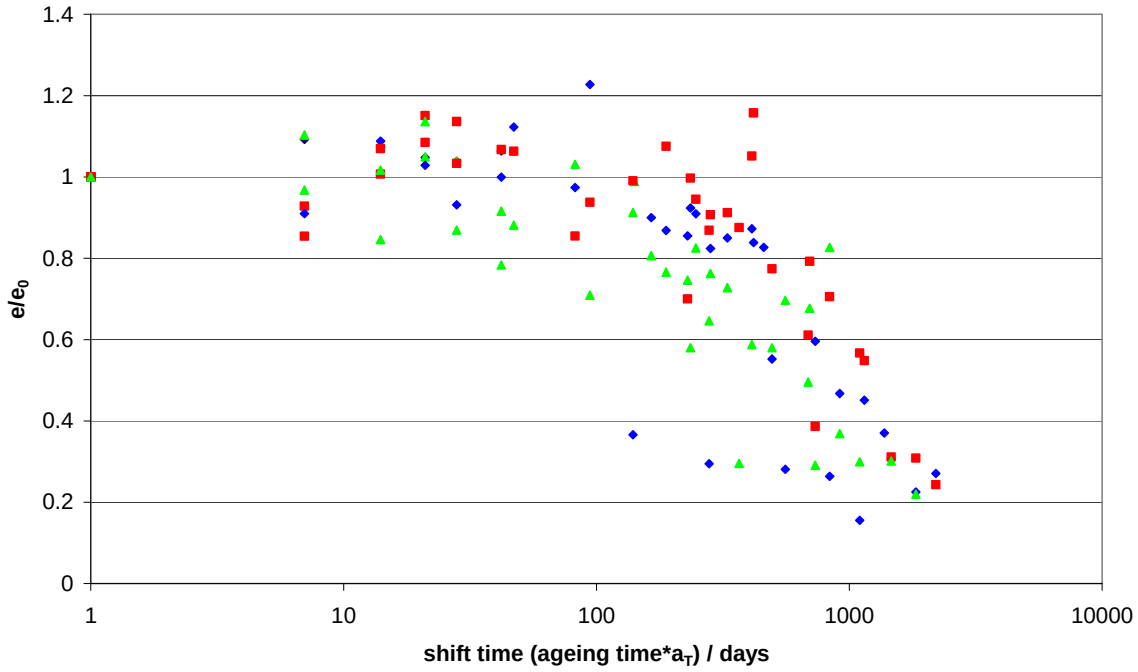

Figure 6.15 – master curve based on TTSP method using average E_a (50 kJ mol^{-1}) (30% RH: blue; 50% RH: red; 75% RH: green)

Research by the Image Permanence Institute (IPI) on film and photographic media has demonstrated that the activation energy (and therefore the predicted lifetimes) varies depending on the measure of deterioration used.[19] However methods that measure chemical deterioration, such as molecular weight, are favoured over those that use physical methods to measure the deterioration as this is a secondary effect caused by the chemical changes.[20] As Zou *et al.* mention in relation to paper deterioration "the loss of mechanical properties is a consequence but not a direct indication of the chemical degradation of cellulose". There is also a large variation in the reported activation energies for paper deterioration.[21]

Conclusions

The kinetics experiments have helped identify a number of changes to the experimental procedure for the accelerated ageing experiments. These include using six replicates for each ageing condition to improve the repeatability of the

tensile testing results. All six replicates can be aged within a single hybridisation tube. The samples will remain the same size (25 x 100 mm) in order to fit in hybridisation tubes, but this has an understandable and linear effect on the tensile testing data.

For the long-term accelerated ageing experiments 80 °C has been chosen as the elevated temperature to increase rate of reaction. This will cause a substantial increase in the rate of reaction allowing silk deterioration to be studied. However it will also enable the samples to be aged for longer time intervals. The accelerated ageing experiments include samples aged for up to one year; in the kinetics experiments samples aged at 90 °C and 75% RH had lost approximately 50% of their initial strength after six weeks. Therefore ageing under these conditions is unlikely to proceed for the desired time interval. The choice of 80 °C should also ensure that the silk does not undergo dehydration reactions that have been observed during thermal analysis.

This study was also undertaken in order to determine the approximate activation energy for silk deterioration reactions. As reported by other investigators the activation energy varies with the analytical technique chosen. There are also a wide range of values from the results of this study. However the majority of values indicate higher activation energies for silk deterioration at 50% RH compared to the other levels of RH studied. The longer term accelerated ageing study incorporates a wider range of RH levels for ageing and the effect on the rate of deterioration will be studied further. But it may indicate, similar to other organic materials, that there is a plateau region (middle RH levels) with little change in the deterioration rate for silk. However the extreme regions may have sudden increases in deterioration, this would be useful to understand for environmental control in order to slow the degradation of silk collections on display. The effect of salt contamination on silk deterioration (particularly at 30% RH) is discussed further in chapters seven and eight. These results indicate the kinetics data at 30% RH has a number of uncertainties.

The results of the kinetics study indicate the average activation energy for silk deterioration is approximately 50 kJ mol^{-1}. This is similar to the values determined by thermal chemiluminescence below the T_g and for untreated samples in the consolidation study. The average activation energy (50 kJ mol^{-1}) has been used to determine the increase in deterioration rate for the longer term accelerated ageing experiments (chapter seven), although it is an approximation it will allow the display time and ageing interval to be compared.

References

[1] Bora, M. N., Baruah, G. C. and Talukdar, C. L. (1993) 'Investigation on the Thermodynamical Properties of Some Natural Silk Fibres with Various Physical Methods' *Thermochimica Acta* **218** 425-434.

[2] Garside, P. and Wyeth, P. (2002) 'Characterization of Silk Deterioration' In *Strengthening the Bond: Science and Textiles Preprints* North American Textile Conservation Conference 2002, 5-6th April 2002, Whelan V. J. (ed.) 55-60.

[3] Millington, K. R., Maurdev, G. and Jones, M. J. (2007) 'Thermal chemiluminescence of fibrous proteins' *Polymer Degradation and Stability* **92** 1504-1512.

[4] Daniels, V. and Leese, M. (1995) 'The Degradation of Silk by Verdigris' *Restaurator* **16** 45-63.

[5] Hansen, E. F. and Ginell, W. S. (1989) 'The Conservation of Silk with Parylene-C' *Historic Textile and Paper Materials II – Conservation and Characterization* Zeronian, S. H. and Needles, H. L. (ed.) ACS 410 Washington DC, USA: American Chemical Society 108-133.

[6] Magoshi, J., Magoshi, Y., Nakamura, S., Kasai, N. and Kakudo, M. (1977) 'Physical properties and structure of silk. V. Thermal Behavior of Silk Fibroin in the Random-Coil Conformation' *Journal of Polymer Science: Polymer Physics Edition* **15** 1675-1683.

[7] Magoshi, J., Magoshi, Y. and Nakamura, S. (1985) 'Crystallization, Liquid Crystal, and Fiber Formation of Silk Fibroin' *Journal of Applied Polymer Science: Applied Polymer Symposium* **41** 187-204.

[8] Greenspan, L., (1977), Humidity Fixed Points of Binary Saturated Aqueous Solutions, *Journal of Research of the National Bureau of Standards – A. Physics and Chemistry*, **81A** (1), 89 – 96.

[9] BS EN ISO 13934-1:1999 Textiles. Textile properties of fabrics. Determination of maximum force and elongation at maximum force using the strip method.

[10] BS EN ISO 13934-1:1999 Textiles. Textile properties of fabrics. Determination of maximum force and elongation at maximum force using the strip method.

[11] Kim, J., Zhang, X., Wyeth, P. (2008) 'The inherent acidic characteristics of aged silk' *e-Preservation Science* **5** 41-46.

[12] Kuruppillai, R. V., Hersh, S. P. and Tucker, P. A. (1985) 'Degradation of Silk by Heat and Light' *AIC Preprints of Papers Presented at the 13th Annual Meeting Washington DC 22-26th May 1985* Washington, DC: American Institute for Conservation of Historical and Artistic Works 157.

[13] Ghosh, A. and Das, S. (2008) 'Tensile and Twist Failure of Mulberry and Tasar Silk' *Journal of the Textile Institute* **99 (2)** 165-168.

[14] Emsley, A. M., Ali, M. and Heywood, R. J. (2000) 'A size exclusion chromatography study of cellulose degradation' *Polymer* **41** 8513-8521.

[15] Emsley, A. M. and Stevens, G. C. (1994) 'Kinetics and mechanisms of the low-temperature degradation of cellulose' *Cellulose* **1(1)** 26-56.

[16] Zou, X., Uesaka, T. and Gurnagul, N. (1996) 'Prediction of paper permanence by accelerated aging I. Kinetic analysis of the aging process' *Cellulose* **3** 243-267.

[17] Gillen, K. T. and Clough, R. L. (1989) 'Time-Temperature-Dose Rate Superposition: A Methodology for Extrapolating Accelerated Radiation Aging Data to Low Dose Rate Conditions' *Polymer Degradation and Stability* **24** 137-168.

[18] Ding, H.-Z. and Wang, Z. D. (2007) 'Time-temperature superposition method for predicting the permanence of paper by extrapolating accelerated ageing data to ambient conditions' *Cellulose* **14** 171-181.

[19] Adelstein, P. Z., Reilly, J. M., Nishimura, D. W. and Erbland, C. J. (1992) 'Stability of Cellulose Ester Base Photographic Film: Part 1 – Laboratory Testing Procedures' *Society of Motion Picture and Television Engineers (SMPTE) Journal* 336-346.

[20] Ram, A. T., Masaryk-Morris, S., Kopperi, D. and Bauer, R. W. (1992) 'Simulated Aging of Processed Cellulose Triacetate Motion Picture Films' *Journal of Imaging Science and Technology* **36(1)** 21-28.

[21] Michalski, S. (2002) 'Double the life for each five-degree drop, more than double the life for each halving of relative humidity' *ICOM Committee for Conservation 13th Triennial Meeting, Rio de Janeiro, 22-27 September 2002 Preprints* Vontobel, R. (ed.) London: James & James **1** 66-72.

Chapter 7 – Accelerated Ageing Experimental Design

This chapter discusses the use of accelerated ageing experiments to study deterioration reactions, including the selection of environmental parameters and design of the experiments used. The calculations to determine the length of ageing are presented and potential problems suggested. Tests of the ageing conditions used are reported with observations made during the ageing experiments, which may affect the results.

To identify the critical factors for silk deterioration in historic houses, in the timescale of the project, accelerated ageing experiments are required. To study ageing processes under real conditions and timescales is difficult, as Erhardt and Mecklenburg have noted, ageing experiments either have to occur over very long time intervals or very small changes must be measured and then extrapolated.[1] To overcome this problem ageing reactions are often artificially accelerated so quantifiable changes occur over shorter time periods.

There are two general approaches: either to mimic natural ageing as accurately as possible, or to increase reactions to understand a specific problem, such as off-gassing. In the first it is vital that the reactions occurring during accelerated ageing are the same as those that would take place normally. Also that the increase in the rate of reaction applies similarly to all the reactions occurring rather than leading to a different degradation mechanism dominating. In the second it is more important that if off-gassing is going to occur during actual use of the material studied, it will be observed under the artificial ageing regime. However off-gassing can be caused by the artificial ageing which might never occur in reality.

The aim of these experiments is to understand silk deterioration which would occur on open display, therefore it is important to simulate the natural ageing environments. This helps relate the deterioration seen during accelerated

ageing back to real display environments and find ways of controlling or mitigating the damage. The first assumption made during these accelerated ageing experiments is that the deterioration caused arises from the same reactions which occur under natural ageing and each has been similarly increased in rate. Due to the complexity of natural polymers, such as silk, it is very likely that multiple reactions are occurring both under natural and accelerated ageing conditions. The ageing experiments can be used to give a holistic view and study how the series of reactions behave as a whole since this governs how the physical properties change.[2]

There is no universal method for accelerated ageing, so two separate approaches have been used to relate the accelerated ageing experiments to display parameters. For light ageing the reciprocal principle[3,4] has been applied to calculate the length of ageing at much higher light levels than those used for display. The reciprocal principal demonstrates, for example, that 10 hours at 50 lux is equivalent to 5 hours at 100 lux, both equal 500 lux hours.

An elevated temperature has been chosen for accelerated ageing at different humidity levels. Two further assumptions are then used, that the deterioration processes occurring are chemical and that the increase in temperature will increase the rate of those chemical reactions. The Arrhenius equation can then be applied. These assumptions have been discussed in relation to paper deterioration by Ding and Wang[5] and Zou *et al.*[6] The determined activation energy is therefore an average of the multiple reactions occurring however this is reported to still be linear.[1,6] For paper it has been shown that increasing the temperature, at constant RH, increases the rate of deterioration without significantly altering it, whereas changes in RH change the ageing processes occurring. From the kinetics study (chapter six) it appears that this is also true for silk and the reactions do alter, as seen in the changing activation energies at different levels of RH.

Although there is no standard method for accelerated ageing experiments, the approach chosen is similar to those used to study deterioration reactions for both paper[1,6,7,8] and photographic media.[9,10,11,12,13,14] The Arrhenius equation

relates to reactions occurring in the gas or solution phase but has been applied by these authors to solid materials for various types of both paper and photographic media. The Arrhenius approach uses an elevated temperature to increase the rate of reaction, here silk deterioration. The activation energy of the reaction can be used to determine the increase in rate at the elevated temperature compared with room temperature. The deterioration can then be extrapolated back to that occurring over longer display times at room temperature, relating a length of accelerated ageing with a period of display under the same level of relative humidity (RH). The results should allow comparison between the deterioration caused at different levels of RH, to determine the optimal display environment. By light ageing at different RH levels any synergistic effects of light and humidity can also be considered.

Using display intervals for the time axis rather than ageing intervals enables more accurate comparisons between the light and humidity ageing regimes. It is not uncommon to see light ageing reported as the cause of greatest deterioration for a material, but for the light level used for ageing over a short period to relate to a much greater display time than the thermal ageing reported. The method used here aims to make the two very different methods of ageing comparable and therefore relate the results more directly to the display of collections. This links to a further aim of the research; to predict a display lifetime for silk. With no knowledge of the reaction kinetics and just an ageing period under a certain set of conditions, it is very difficult to say how long that might equate to on display. By using display intervals the endpoint, or a lifetime, is easier to determine. However an understanding of how silk deteriorates with time and at what point it is no longer able to be displayed is still required.

The display end point is often determined from physical properties, such as mechanical strength, such as changes in the strength of tapestries.[15] However this type of analysis is destructive and requires large samples. Therefore surrogate samples that replicate the materials identified within the English Heritage collection are used instead. Chemical analysis of the surrogates can also be undertaken, with the aim of correlating changes in mechanical and

chemical properties. This data can be used to understand the results of chemical analysis performed on small samples removed from the English Heritage collection. By correlating the accelerated ageing experiments with the results from the historic samples it can be determined whether the ageing has produced deterioration similar to that arising from natural ageing on display.

Environmental Criteria

English Heritage Properties Data

Compositional analysis of silks from the English Heritage collection revealed that the majority of the collection is unweighted, plain silk (chapter three). There is a small percentage (~10%) of tin weighted and high sulfur content silk, with a few items that contain iron or zinc. To limit the number of variables but have results which are applicable to the collection plain, unweighted, medium-weight silk habotai (used in the kinetics tests) was selected for the accelerated ageing experiments.

Analysis of environmental monitoring data from the selected English Heritage properties (chapter two) highlighted the following conditions were of interest for further study.

relative humidity:	none (0%), very low (~30%), low (~40%), mid (~50%), high (~60%), very high (~75%) and saturated (100%)
light:	dark (0 lux), low light levels (50 lux) and high light levels (200 lux)
UV:	none (0 μW/lumen), low (35 μW/lumen), mid (75 μW/lumen) and high (150 μW/lumen) at 200 lux
combined effects:	combination of each RH level with each light level, i.e. 0, 30, 40, 50, 60, 75 and 100% in the dark, at 50 lux and at 200 lux.

For relative humidity (RH) the levels were selected from typical display environments and two outer extremes (0 and 100% RH). Light levels were

chosen to reflect storage (0 lux) and the two maxima used to calculate annual light budgets for display (50 and 200 lux). UV levels were chosen to represent an ideal (0 μW/lumen) as well as the effects of UV absorbing film on windows when new (35 μW/lumen), before replacement (75 μW/lumen) and if not installed (150 μW/lumen) at 200 lux. A combination of all the RH levels with all the lighting conditions was then proposed. A number of changes, outlined below, have been made in order to carry out the experiments within a suitable time frame and with the equipment available. However these still cover the majority of display environments and should provide a basis for making display recommendations.

Experimental Design – Temperature and RH

Experimental Calculations

In designing the thermal and hydrolytic ageing experiments there are two factors to consider; which temperature to use and how to maintain the desired RH levels. The length of ageing required and how long it relates to on display can be calculated based on the chosen elevated temperature.

Selecting an appropriate temperature is important as the reactions causing the deterioration should be those that will occur at room temperature. This is difficult to ensure but there are a number of factors that are likely to cause alterations to the type of reactions which take place. The first is the glass transition temperature, T_g, above this point the properties of the polymer change and for most polymers the reactivity will also change. For silk the T_g is around 160 – 175 °C, depending on the species of silkworm.[16]

There is a further factor, occurring below the T_g, which means it does not need to be considered in these experiments. Silk contains both associated and bound water molecules within the crystallites. The amount of associated water changes with RH and these are the effects being studied. However the bound water can also be removed at high temperatures. This is likely to change the reactivity of the crystallites as there will be a structural change on the loss of

water. Therefore ageing should occur below the point at which the bound water is lost as this is present during natural ageing. Silk crystallites are reported to undergo dehydration around 100 °C,[17] hence the chosen temperature should be lower than this value.

To ensure crystallite dehydration does not occur, but there is still a sufficient increase in the rate of reaction, 80 °C has been selected for accelerated ageing tests. This will allow noticeable levels of silk deterioration to be caused but still allow analysis of the samples after ageing. During the kinetics study (chapter six) the samples aged at 90 °C and 75% RH had lost around 50% of their strength in six weeks and so samples aged for longer than six months would be too fragile to be differentiated. A study on silk degumming in 8M urea reported fibroin degradation occurred at 90 °C and was incomplete at 70 °C and report a preference for 80 °C.[18] Ageing at 80 °C will reduce the likelihood of fibroin degradation arising from heating, with the effect of humidity compared by selecting a single ageing temperature.

There are a number of possible methods to create varying levels of RH for ageing environments. These include saturated salt solutions, humidity ageing chambers and glycerol solutions. Saturated salt solutions control the RH by absorbing moisture from the air if the RH is higher than desired or releasing moisture if it is lower. The RH created depends on the salt chosen and the temperature. The range of possible RH levels that can be created is dependent on the available salts and the temperature which ageing experiments will be carried out at. There are two considerations with this technique, firstly that the solution has to be saturated at the ageing temperature in order to release or absorb moisture and secondly that the salts can migrate out of the solution and contaminate samples.

Humidity ageing chambers can be set to create any RH level. The accuracy to which this is maintained will depend both on the equipment measuring the RH within the chamber and the mechanism by which RH is controlled within the chamber. Ageing with saturated salt or glycerol solutions is usually done in sealed containers to ensure the RH is maintained. In RH chambers the

samples are sealed within the chamber, the limit in these experiments is the size of the chamber. The length of experiment provides a further limitation as only one RH level can be maintained at any one time. With the use of solutions a number of RH levels can be used simultaneously in different containers within the same oven. RH ovens are relatively expensive, which limits their availability and so within conservation their use is often limited.

Glycerol solutions can be prepared to create any RH level. Similar to saturated salt solutions they are used in sealed containers and absorb or release moisture depending upon the concentration of the solution. Glycerol does not migrate in the way that saturated salt solutions do, however it does form a vapour phase.[19] This may contaminate the samples with glycerol and therefore has not been selected for use in these experiments. With both methods there is a possibility of contamination of the samples. However glycerol contamination is unlikely to occur under natural ageing conditions, whereas salt contamination can occur, particularly in coastal areas.

At 80 °C, most of the selected RH levels can be created with saturated salt solutions (see Table 7.1). However in Greenspan's tables there is no quoted saturated salt solution to create 40% RH at this temperature.[20] Therefore the 40% RH conditions have been created using a humidity ageing chamber.

RH / %	saturated salt solution	notes
0	-	dry ageing, nothing will be added to give ~0% RH
30	$MgCl_2.6H_2O$	
40	-	no suitable salt, therefore humidity ageing chamber will be used
50	NaBr	
60	KI	
75	NaCl	
100	-	liquid water will be used to give ~100% RH

Table 7.1 – RH levels and chosen method of creation

To determine the increase in rate of reaction at 80 °C the activation energy for the reaction is used. By rearranging the Arrhenius equation the rate of reaction at room temperature (20 °C selected as this is an annual average in English Heritage properties) can be compared to the rate of reaction at 80 °C. The increase in rate can then be used to determine the length of ageing required. For example if ageing at 80 °C causes a ten fold increase in the rate of reaction then 1 years accelerated ageing is equivalent to 10 years on display. One problem with this method is the reliance on the activation energy to determine the length of ageing.

For longer term ageing the experiments needed to be underway before the activation energy had been determined. Therefore ageing intervals were based upon calendar intervals which may be correlated to equivalent display periods when the activation energy was known. Those chosen were 1, 2, 3, 6, 9 and 12 months to give a spread of deterioration levels. Previous humidity ageing for silk has been performed over relatively short time scales (a maximum of around 30 days). These accelerated ageing experiments should enable a much greater amount of deterioration to be created and studied giving more information about what happens over longer time spans. Using the average activation energy (from chapter six) the increase in rate has been calculated as 33 times. This means accelerated ageing for 1 month is approximately equivalent to 2.7 years on display and 1 year of artificial ageing would equal 33 years on display. For the discussion below the ageing interval used is referred to however this will be expanded upon within the results (chapter eight).

Experimental Set Up

The same experimental set up has been used as during the kinetics experiments (see Figure 7.1), with the number of replicates increased to six. For the 0% RH samples glass wool has been included for consistency, although there is no solution beneath it. For 100% RH liquid water replaces the saturated salt solution as recorded in Table 7.1. Due to space limitations, the 6,9 and 12 months samples were aged for the initial 6 months in a Binder® APT heating and drying oven in the English Heritage paintings conservation studio at

Ranger's House. The remaining time and further shorter ageing periods were undertaken in a Heraeus Kendro® UT6P Air Circulation Oven. Both were set at 80 °C and are reported to fluctuate by ± 3 °C.

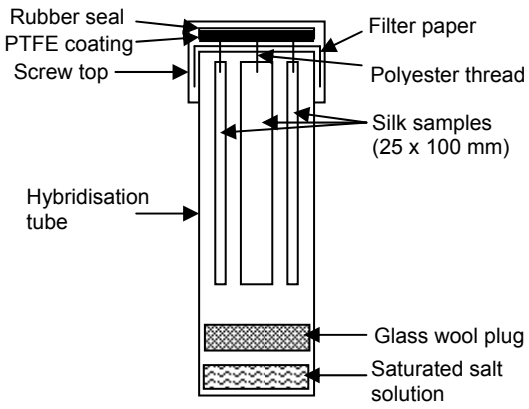

Figure 7.1 – accelerated ageing T/RH experimental set up

The 40% RH samples have been sewn to filter paper in the same way as shown in Figure 7.1. These were suspended from the shelf within the Espec® SH-221 bench top temperature and humidity chamber. This was set to 80 °C (± 0.3 °C) and 40% RH (± 3% RH). All samples were aged in the dark and have been given an identification code with the letter D. This code starts with the ageing RH (0, 30, 40, 50, 60, 75 or 100), the letter D and then the length of ageing, in months (1, 2, 3, 6, 9 or 12). For example 50D9 indicates the samples have been aged at 50% RH in the dark for nine months.

Experimental Design – Light

Experimental Calculations

The length of time required for light ageing can be calculated relatively simply due to the reciprocal principle. For English Heritage properties an annual light budget is set for each display area. These take into account the opening hours of the house and the collections within the room. The annual light budgets are calculated based on two different maxima, 50 lux for light sensitive materials (146100 lux hours) and 200 lux for general collections (584400 lux hours).

Within the houses light levels are then controlled using a double blind at the windows. The black out blind and lighter coloured blind can be positioned to alter the light level and reduce the incoming light and prevent direct sunlight on objects.

Light levels in the light ageing chamber were measured at 7000 lux beneath the UV filter, and a UV level of 2 μW/lumen. For each chosen display time interval, the number of years is multiplied by the annual light budget in lux hours to calculate a total required exposure, for both 50 and 200 lux maxima. The total exposure is then divided by the ageing light level (7000 lux) to give a number of ageing hours. For example, four years on display at 200 lux gives 2337600 lux hours exposure. To obtain this, ageing at 7000 lux, will require 334 hours or approximately 14 days. The reciprocal principle has been used to reduce the number of samples due to limited space in the light box. As 2 years at 200 lux is the same as 8 years at 50 lux, some samples will provide data for different time intervals at both 50 and 200 lux.

Ultraviolet (UV) absorbing film is on all windows within the selected English Heritage properties, reducing the UV light level inside the rooms. However the film breaks down with time and needs replacing so the level of UV entering the room will vary from below 10 μW/lumen to almost 75 μW/lumen (the current recommended maximum). However with improvements in lighting the recommended maximum may be reduced to 35 μW/lumen.[21] As this measure of UV light is a proportion of the visible light, which is reduced by the use of blinds, it is common to find that UV levels are less than 5 μW/lumen in rooms at 200 lux.

It was hoped to look at a variety of UV light levels with the visible light set at 200 lux. However with the light box design it was not possible to control the UV levels in this way, without obtaining further filters. As a result it has only been possible to compare the low UV levels beneath the filter with the much higher levels above. The UV filter reduces the transmitted light so the same calculations as above have been applied to determine the length of ageing above the filter. This means the results are on the same display time scale with

and without UV rather than the same ageing timescale. The light level above the UV filter was measured as 12500 lux and 350 µW/lumen.

Experimental Set Up

Light ageing was carried out in a custom made light box from Complete Lighting Systems in St. Albans (see Figure 7.2). The light box contains twelve F20W/AD artificial daylight, fluorescent bulbs. These bulbs are specifically designed to replicate daylight effects, with a high colour temperature (6500K) and good colour rendering index (Ra = 92).[22] This is desirable as English Heritage properties are lit using natural light supplemented by artificial lighting when required.

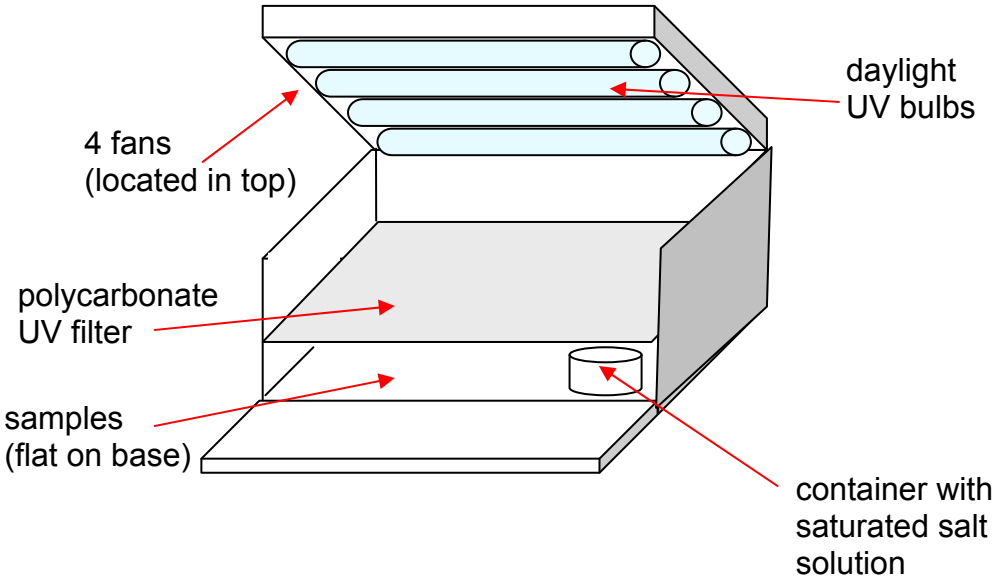

Figure 7.2 – experimental set up in the light ageing chamber

To reduce the length of experiments and number of samples to be analysed a low (33%, $MgCl_2.6H_2O$), middle (50%, NaBr) and high (75%, NaCl) RH value based on display conditions have been selected for comparison. Ageing under dry (0%) and saturated (100%) conditions would be difficult to maintain due to the ventilation from the fans in the lid (four SUNON SF23092A fans). At room temperature a saturated salt solution could be used to maintain 40% RH.

However, this may not be comparable to the samples aged in the dark as a humidity chamber will be used for this ageing condition.

To maintain the RH levels, saturated salt solutions were placed in an open plastic container insider the light box. This was half filled with a perforated covering to reduce possible salt migration. The UV ageing will be carried out solely at the middle RH to reduce the number of samples for analysis, whilst still providing comparison with the other ageing conditions. To ensure that the deterioration caused is due to light ageing the temperature should remain at room temperature. The fans provide ventilation to maintain the light box at room temperature thus ensuring that there is no further deterioration arising from elevated temperatures. RH levels were checked weekly and the salt solutions maintained as and when required to keep the RH at the desired value.

Identifying codes were used for light aged samples based on the ageing conditions, similar to the thermal ageing samples. These begin with the RH level during ageing (30, 50 or 75) and then L or UV to indicate light ageing or light ageing with UV radiation respectively. This is followed by the maximum light level used to calculate the annual light budget (50l or 200l), where l indicates lux. The final number indicates the equivalent number of years on display created during ageing (2, 4, 6, 8, 15 or 16). For example 30L50l6 indicates the samples have been light aged at 30% RH for the equivalent of 6 years on display at a maximum light level of 50 lux.

Possible Experimental Problems

There are a number of differences between the experiments that may affect the results. The most obvious one is the 40% RH experiments as this uses a different method to create the RH level. The likely impact of this was difficult to determine in advance, although it removes the possibility of salt contamination. For the thermal and hydrolytic ageing the effect of the filter paper, polyester thread and PTFE/rubber seals in the hybridisation tubes may also cause contamination. However the majority of samples were all exposed to these factors therefore any effects will at least be consistent.

For the light ageing saturated salts have been used to maintain an environment inside a ventilated light box. As this is not a sealed unit, and relies on the ventilation to maintain room temperature the RH levels are unlikely to be constant. However the solutions were checked regularly and additional salt or water added as required to try and ensure constant levels. Due to space limitations within the light ageing chamber it is possible that samples have not received uniform light exposure. To reduce this effect samples have been removed from across the base to get a spread of any differences.

Saturated Salt Test

As the saturated salt solutions within the hybridisation tubes require occasional additional water or salt it is probable that these are not perfectly sealed. Therefore the stability of the saturated salt solutions within the hybridisation tubes was tested and the actual RH level for each of the chosen RH conditions determined.

To monitor the environment within the sealed tube a hole was drilled through the lid and PTFE coated rubber seal of a hybridisation tube. A Rotronic HygroClip® SC05 temperature and humidity probe was inserted through the lid and seal and the top of the probe sealed to the outside of the hybridisation tube lid using a silicone sealant (see Figure 7.3). To monitor the environment the probe is connected to a Rotronic HygroPalm 2 connected to a laptop running the Rotronic HW3 software. Using this set up the temperature and humidity data were logged every five minutes for a week.

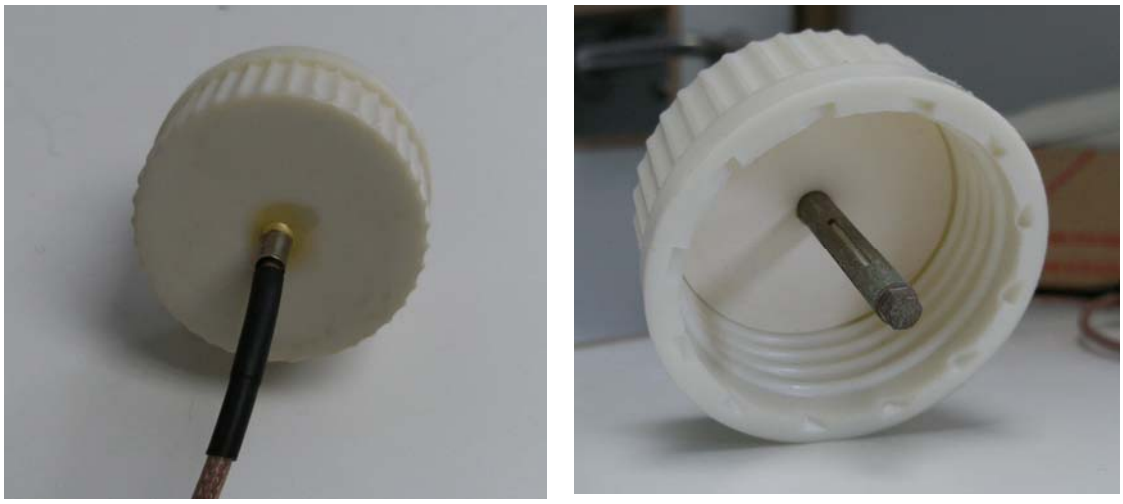

Figure 7.3 – hybridisation tube lid with hygroclip probe from outside (left) and inside (right)

A hybridisation tube was prepared with glass wool in the bottom to replicate the 0% RH tube. This was then attached to the prepared lid and placed in the oven at 80 °C. The lead for the probe passes out of the top of the oven door (the compression seal of the door allows the cable out while maintaining the seal) and into the HygroPalm (see Figure 7.4). Each saturated salt was tested in turn by placing a saturated solution in the hybridisation tube, as done for the accelerated ageing experiments. The environment in the RH oven was also tested by placing the probe (without a hybridisation tube attached) through a port in the side of the chamber and logging the environmental conditions (see Figure 7.5). For each RH level the probe recorded data for one week.

Figure 7.4 – saturated salt experimental set up

Figure 7.5 – testing humidity levels in the RH ageing oven

condition name	method / salt	Greenspan value /%	Measured value / %
0	none	N/A	1.5
30	$MgCl_2.6H_2O$	26.05 ± 0.34	29
40	RH oven	N/A	37
50	NaBr	51.43 ± 1.5	53
60	KI	60.97 ±0.48	62.5
75	NaCl	76.29±0.65	79
100	liquid water	N/A	96

Table 7.2 – results of RH level tests at 80°C

The accuracy of the Hygroclip sensor is reported as 1.5% RH and 0.3 K at 23 °C by the manufacturer. However the sensor was last calibrated by the manufacturers in February 2005. Comparison between the Hygroclip probe and a recently calibrated Novasina MS1 T/ RH sensor initially showed the Hygroclip was reading approximately 4% RH higher and results have been corrected accordingly and are presented in Table 7.2. In most cases calibration of the sensor would be done at three RH levels and corrected, however recalibration was not undertaken and the readings have just been corrected for the observed difference. Although the calibration is unlikely to be linear, a linear correction

was simplest for the purposes of this test. During the 100% RH test the temperature sensor on the Hygroclip probe failed and after the RH readings were noticeable higher. A further check against the Novasina MS1 sensor showed the Hygroclip was now reading 30% RH higher; the RH oven test has been adjusted to take this into consideration.

Monitoring shows 1% RH variation during the week long test implying the conditions are stable over shorter time periods. However, these values are only applicable as long as the water levels are maintained, as the hybridisation tubes still require additional deionised water to maintain saturated salt solutions. As calibration of the Hygroclip would occur at room temperature and there is a slight variation in most calibration lines with changes in temperature this may also have an effect on the accuracy. Generally the values measured are close to the reported values and offer a range of RH levels to study.

Observations during Ageing

Despite the glass wool to act as a barrier above the saturated salt solution, salt migration was still observed. In some cases the silk samples had heavy deposits of salt. This makes the silk brittle and if stuck to the side of the hybridisation tube can cause fragments of the silk to break off. From the earlier kinetics experiments it was observed that the salt affects the tensile testing analysis, altering the shape and breaking point of the sample and leading to samples being excluded from the results. To try and overcome the problem heavy salt deposits were rinsed out of silk samples. This is not ideal as it introduces a further variation in the samples. It has been reported that washing silk gives improved physical properties, which imply this rinsing may affect the results.[23] In hindsight it may have been preferable to rinse all samples in order to prevent a further variable being introduced.

Although the RH oven removes the possibility of salt contamination some 40% RH aged samples had small areas missing after ageing (see Figure 7.6). These seem to be burn marks from contact with the metal wire shelf as the samples have blown around due to the circulation fan. This had not been

anticipated as there was no shelf beneath the samples and they had been suspended from the filter paper through the shelf to hang freely beneath. One likely result of this will be reduced tensile testing values as the missing areas will introduce weaknesses in the affected samples. The number of replicates will also be reduced as some samples will be too short to be tested, for example the second sample in the right hand picture of Figure 7.6.

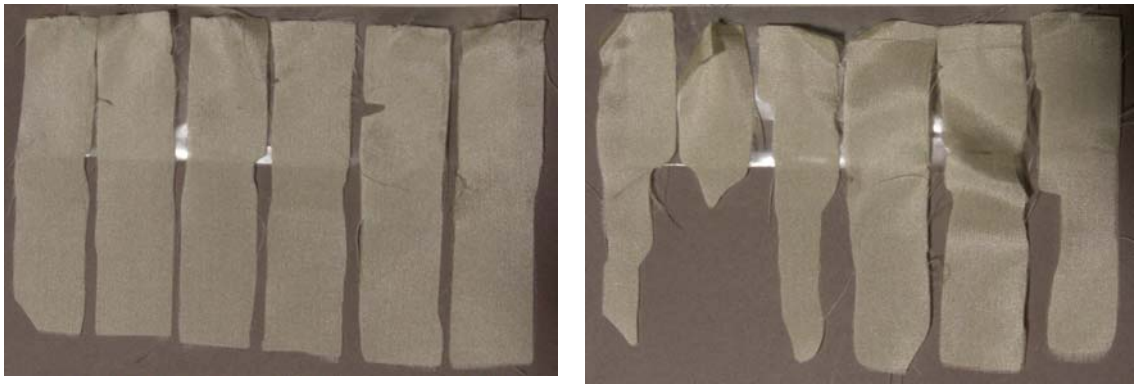

Figure 7.6 – samples aged at 80°C and 40% RH for 6 months (left) and 9 months (right) showing increasing damaged areas and missing sections

There were also some unanticipated changes to some of the samples aged with saturated salt solutions. When moving the samples after the initial six months ageing, the silk inside the hybridisation tube labelled 9 months at 30% RH was brown and gel-like. The saturated salt solution also appeared brown. When the tube was opened the silk remained stuck to the sides and was very difficult to remove. Those sections that were removed and rinsed appeared to have shrunk (see Figure 7.7) and a deposit remained on the inside of the tube (see Figure 7.8). The reason for this is unclear. All the magnesium chloride solutions had been prepared together and the other hybridisation tubes at 30% RH had not been affected. Rather than omit this time interval the 6 month samples were aged for a further 3 months and new samples were prepared and aged for 6 months.

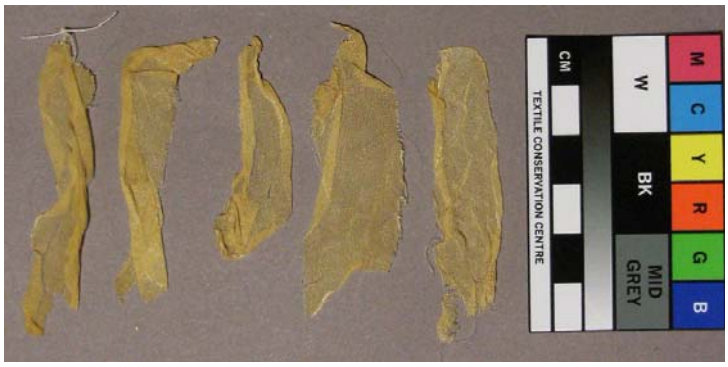

Figure 7.7 – remaining silk samples after ageing for 6 months at 30% RH

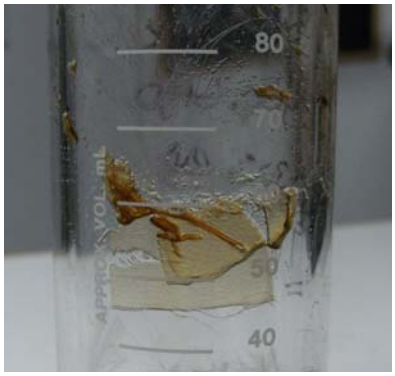

Figure 7.8 – silk remaining in the hybridisation tube

The 60% RH samples have also been affected by the choice of saturated salt solution. From the literature a saturated solution of potassium iodide was selected to maintain 60% RH at 80 °C. However upon moving the samples after the initial six months ageing they were a dark brown colour and although a saturated solution remained in the tubes it was no longer a white salt with clear liquid but yellow salt in a brown solution. Although not tested the smell on the removal of the lids and the appearance was that of iodine solution, which had seemingly dyed the samples suspended above it. The samples aged after, were observed more closely and samples half dyed and half undyed were noted (see Figure 7.9). The effect of this dyeing on the samples aged at 60% RH will be determined during analysis.

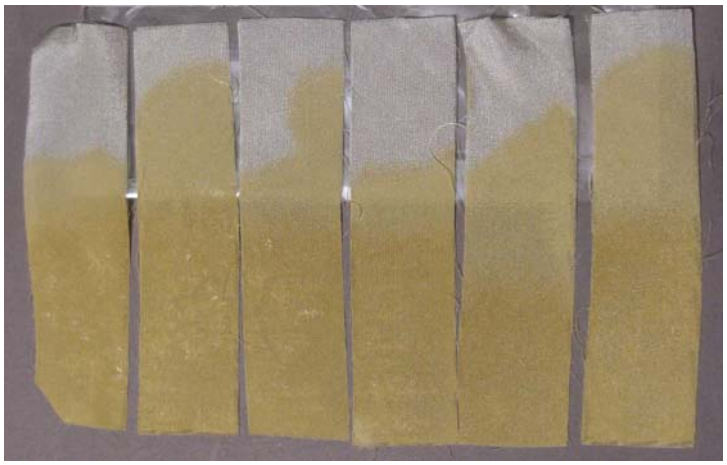

Figure 7.9 – colour change observed on samples aged for 2 months with saturated potassium iodide solution

Yellowing due to accelerated ageing is commonly observed for a range of materials.[24,25,26] During the kinetics ageing it was noted that samples became increasingly yellow as the temperature increased. However all the accelerated ageing was carried out at 80 °C, yet different degrees of yellowing were again observed. This time there was an obvious increase in the amount of yellowing related to humidity. Higher levels of RH produced noticeably yellower samples (see Figure 7.10). Although ageing in the humidity oven seemed to produce less yellowing with samples aged for 12 months less yellow than those aged at 30% RH using a saturated salt solution.

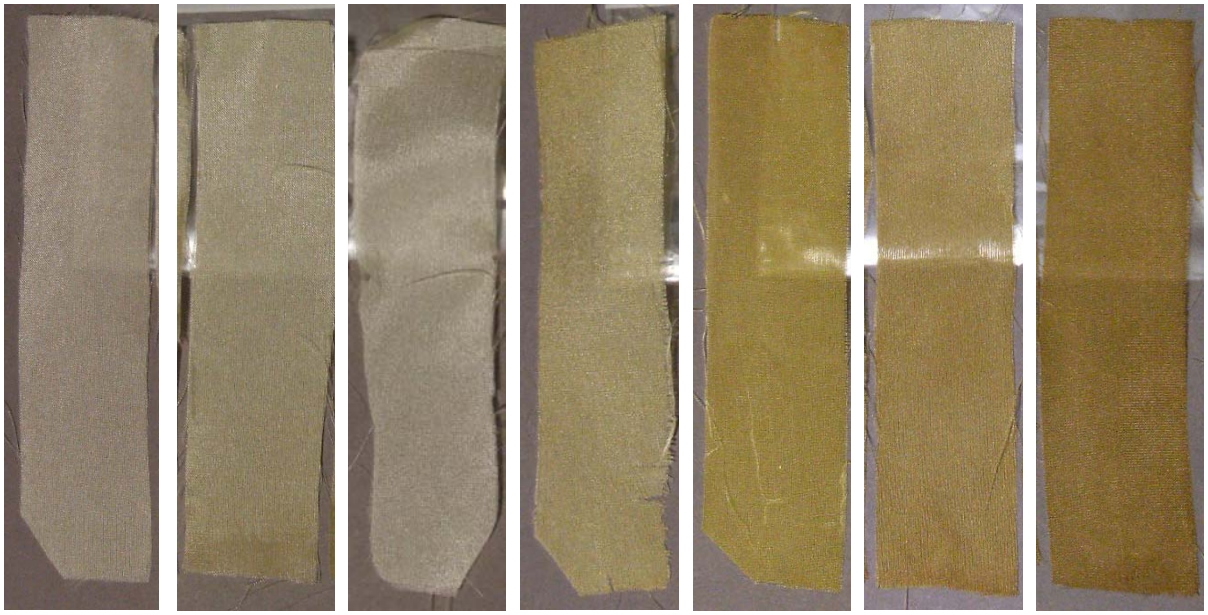

Figure 7.10 – increasing yellowing of samples with increased RH

Conclusions

Ageing has been undertaken under a range of RH levels at 80 °C as well as light and UV exposures. This has led to a range of silk deterioration to be analysed and discussed in subsequent chapters. A number of experimental observations have identified some problems which may affect the analysis of the samples, such as salt contamination or heat damage of the samples (humidity oven ageing). However the RH levels have been verified by separate

environmental monitoring and the approximate length of display time, replicated by the ageing, calculated from the kinetics results. These results will help understand the analytical results presented in the next chapter.

References

[1] Erhardt, D. and Mecklenburg, M. F., (1995), Accelerated VS Natural Aging: Effect of Aging Conditions on the Aging Process of Cellulose, *Materials Issues in Art and Archaeology IV* Vandiver, P. B., Druzik, J. R., Madrid, G., Luis, J., Freestone, I. C. and Wheeler, G. S. (ed.) Warrendale P. A.: Materials Research Society **352**, 247 – 270.

[2] Nishimura, D. personal communication, 28/03/2008.

[3] Thomson, G. (1986) *The Museum Environment* Oxford: Butterworth-Heinemann.

[4] Saunders, D. and Kirby, Jo (1996) 'Light-Induced Damage: Investigating the Reciprocity Principle' *ICOM Committee for Conservation, 11th Triennial Meeting, Edinburgh, Scotland 1-6 September 1996 Preprints* Bridgland, J. (ed.) London: James and James Ltd 87-90.

[5] Ding, H. Z. and Wang, Z. D. (2007) 'Time-temperature superposition method for predicting the permanence of paper by extrapolating accelerated ageing data to ambient conditions' *Cellulose* **14** 171-181.

[6] Zou, X., Uesaka, T. and Gurnagul, N. (1996) 'Prediction of paper permanence by accelerated aging I. Kinetic analysis of the aging process' *Cellulose* **3** 243-267.

[7] Emsley, A. M. and Stevens, G. C. (1994) 'Kinetics and mechanisms of the low-temperature degradation of cellulose' *Cellulose* **1(1)** 26-56.

[8] Roberson, D. D. (1981) 'Permanence / Durability and Preservation Research at the Barrow Laboratory' *Preservation of Paper and Textiles of Historic and Artistic Value II* Advances in Chemistry Series 193 Washington D.C.: American Chemical Society 45-55.

[9] Adelstein, P. Z. (1981) 'Stability of Processed Polyester Base Photographic Films' *Journal of Applied Photographic Engineering* **7 (6)** 160-167.

[10] Adelstein, P. Z., Reilly, J. M., Nishimura, D. W. and Erbland, C. J. (1992) 'Stability of Cellulose Ester Base Photographic Film: Part 1 – Laboratory Testing

Procedures' *Society of Motion Picture and Television Engineers (SMPTE) Journal* 336-346.

[11] Adelstein, P. Z., Reilly, J. M., Nishimura, D. W. and Erbland, C. J. (1992) 'Stability of Cellulose Ester Base Photographic Film: Part 2 – Practical Storage Considerations' *Society of Motion Picture and Television Engineers (SMPTE) Journal* 347-353.

[12] Adelstein, P. Z., Reilly, J. M., Nishimura, D. W. and Erbland, C. J. (1995) 'Stability of Cellulose Ester Base Photographic Film: Part 3 – Measurement of Film Degradation' *Society of Motion Picture and Television Engineers (SMPTE) Journal* **104** 281-291.

[13] Adelstein, P. Z., Reilly, J. M., Nishimura, D. W. and Erbland, C. J. (1995) 'Stability of Cellulose Ester Base Photographic Film: Part 4 – Behavior of Nitrate Base Film' *Society of Motion Picture and Television Engineers (SMPTE) Journal* **104** 359-369.

[14] Adelstein, P. Z., Reilly, J. M., Nishimura, D. W., Erbland, C. J. and Bigourdan, J. L. (1995) 'Stability of Cellulose Ester Base Photographic Film: Part 5 – Recent Findings' *Society of Motion Picture and Television Engineers (SMPTE) Journal* 439-447.

[15] Hallett, K. and Howell, D. (2005) 'Size exclusion chromatography of silk: inferring the textile strength and assessing the condition of historic tapestries' in *ICOM Committee for Conservation 14th Triennial Meeting Preprints, The Hague, 12-16th September 2005 Preprints* **2** 911-919.

[16] Magoshi, J. and Nakamura, S. (1975) 'Studies on Physical Properties and Structure of Silk. Glass Transition and Crystallization of Silk Fibroin' *Journal of Applied Polymer Science* **19** 1013-1015.

[17] Bora, M. N., Baruah, G. C. and Talukdar, C. L. (1993) 'Investigation on the Thermodynamical Properties of Some Natural Silk Fibres with Various Physical Methods' *Thermochimica Acta* **218** 425-434.

[18] Yamada, H., Nakao, H., Takasu, Y. and Tsubouchi, K. (2001) 'Preparation of undegraded native molecular fibroin solution from silkworm cocoons' *Materials Science and Engineering C* **14** 41-46.

[19]http://www.dow.com/PublishedLiterature/dh_0032/0901b803800322bb.pdf?filepath=glycerine/pdfs/noreg/115-00677.pdf&fromPage=GetDoc accessed 03/08/2009.

[20] Greenspan, L. (1977) Humidity Fixed Points of Binary Saturated Aqueous Solutions, *Journal of Research of the National Bureau of Standards – A. Physics and Chemistry* **81A (1)** 89 – 96.

[21] http://www.tate.org.uk/collections/borrowing/care-and-treatment.shtm accessed 27/07/2009.

[22]http://www.geciasia.com/apo/resources/library/lighting/prod_catalogues/downloads/Fluorescent.pdf accessed 03/08/2009.

[23] Breese, R. R. and Goodyear, G. E. (1986) 'Fractography of Historic Silk Fibers' in *Historic Textile and Paper Materials Conservation and Characterization* Needles, H. L. and Zeronian, S. H. (ed.) American Chemical Series 212 Washington: American Chemical Society 95-109.

[24] Richards, H. R. (1984) 'Thermal Degradation of Fabrics and Yarns Part 1: Fabrics' *Journal of the Textile Institute* **1** 28-36.

[25] Korenberg, C. (2007) 'The effect of ultraviolet-filtered light on the mechanical strength of fabrics' *The British Museum Technical Research Bulletin* **1** 23-27.

[26] Hansen, E. F. and Ginell, W. S. (1989) 'The Conservation of Silk with Parylene-C' *Historic Textile and Paper Materials II – Conservation and Characterization* Zeronian, S. H. and Needles, H. L. (ed.) American Chemical Series 410 Washington D.C.: American Chemical Society 108-133.

Chapter 8 – Accelerated Ageing Experimental Results

Changes to the silk samples during accelerated ageing have been determined using tensile testing and High Performance Size Exclusion Chromatography (HPSEC). Difficulties with the HPSEC data processing are discussed alongside the method used to normalise the results. The experimental results are presented and the results from each technique are compared. The chapter reports the rates of deterioration caused by the accelerated ageing experimental conditions.

Two methods were selected to analyse the accelerated aged samples; tensile testing and High Performance Size Exclusion Chromatography (HPSEC). This allowed both the physical and chemical deterioration of the silk samples to be assessed. Chemical measures, such as the degree of polymerisation are reported to be more sensitive to initial changes compared with physical measures of deterioration such as tensile strength.[1] To test whether HPSEC can be used to monitor silk deterioration before physical changes occur, the results from both techniques have been compared.

Tensile Testing

Results

After accelerated ageing each sample was subjected to tensile testing to determine the maximum load at break and the tensile extension at maximum load, using the same equipment as discussed in chapter six. Results for the maximum load at break showed greater reproducibility and so are discussed in greater detail.

To make the accelerated ageing results from different ageing methods comparable (as discussed in chapter six) results were plotted using equivalent display time.

However to gain a better appreciation of the differential degrees of deterioration effected by the various ageing regimes, the raw 'extension vs. load' results for each replicate were plotted first. Figure 8.1 illustrates that light ageing causes a maximum decrease in the tensile strength of 25%, compared to the unaged samples. For some samples the tensile strength actually increases upon ageing, most noticeably for some of the UV aged samples. In comparison there is a bigger decrease in extension, closer to 50%. Extension may therefore be the more sensitive indicator of deterioration in the earlier stages of ageing.

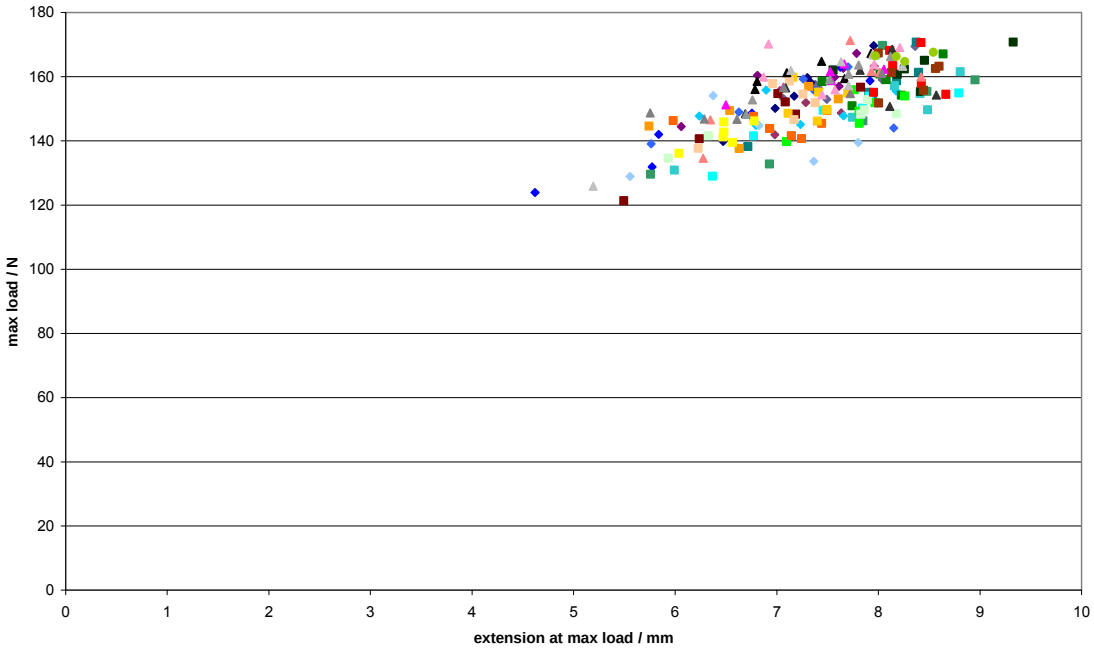

Figure 8.1 – scatter plot of extension vs. load for each light aged replicate

(For an explanation of sample labelling see chapter 7; 30% RH (♦) 30L50l2: slate; 30L50l4: dark purple; 30L50l6: purple; 30L200l2: dark blue; 30L200l4: blue; 30L200l6: mid blue; 30L200l8: light blue; 30L200l15: pale blue; 50% RH (■) 50L50l2: dark aqua; 50L50l4: aqua; 50L50l6: light aqua; 50L200l2: dark green; 50L200l4: green; 50L200l6: mid green; 50L200l8: bright green; 50L200l15: light green; 50UV50l2: dark red; 50UV50l4: red; 50UV50l6: brown; 50UV200l2: dark orange; 50UV200l4: orange; 50UV200l6: pale orange; 50UV200l8: peach; 50UV200l15: yellow; 75% RH (▲) 75L50l2: dark pink; 75L50l4: coral; 75L50l6: light pink; 75L200l2: black; 75L200l4: dark grey; 75L200l6: mid grey; 75L200l8: grey; 75L200l15: light grey; unaged: olive green ●)

In comparison to the accelerated light ageing results in Figure 8.1, where the unaged samples are scattered amongst the light aged results, in Figure 8.2 the unaged samples are clearly visible against the thermally aged samples. This is the first indication that ageing at increased temperature and humidity leads to more deterioration than accelerated light ageing, under the conditions selected. Figure 8.2 shows that with increasing humidity and increased length of ageing, the tensile strength of the silk decreases rapidly. To the extent that the samples aged at 100% RH for 12 months were too deteriorated for tensile testing to take place. The silk strips formed a bundle of fibres when removed from the hybridisation tube, which could not be separated without tearing the sample strips.

Figure 8.2 shows an initial trend similar to the light aged samples up to an extension of 3-4 mm, after this point the trend has a steeper slope, although still linear. An extension of 4 mm is roughly approximate to a decrease in maximum load of 40 N, roughly a quarter, which has been reported to be the elastic limit of silk.[2] As described in chapter seven, the silk from some samples aged at 30% RH had formed a gel-like material inside the hybridisation tubes. Figure 8.2 shows the 30% RH aged samples (green diamonds) are generally more deteriorated than the 40% RH aged samples (aqua plus signs). The samples aged for 6 and 12 months were so deteriorated that samples tore as soon as the load was applied. Hence no results are presented for these samples.

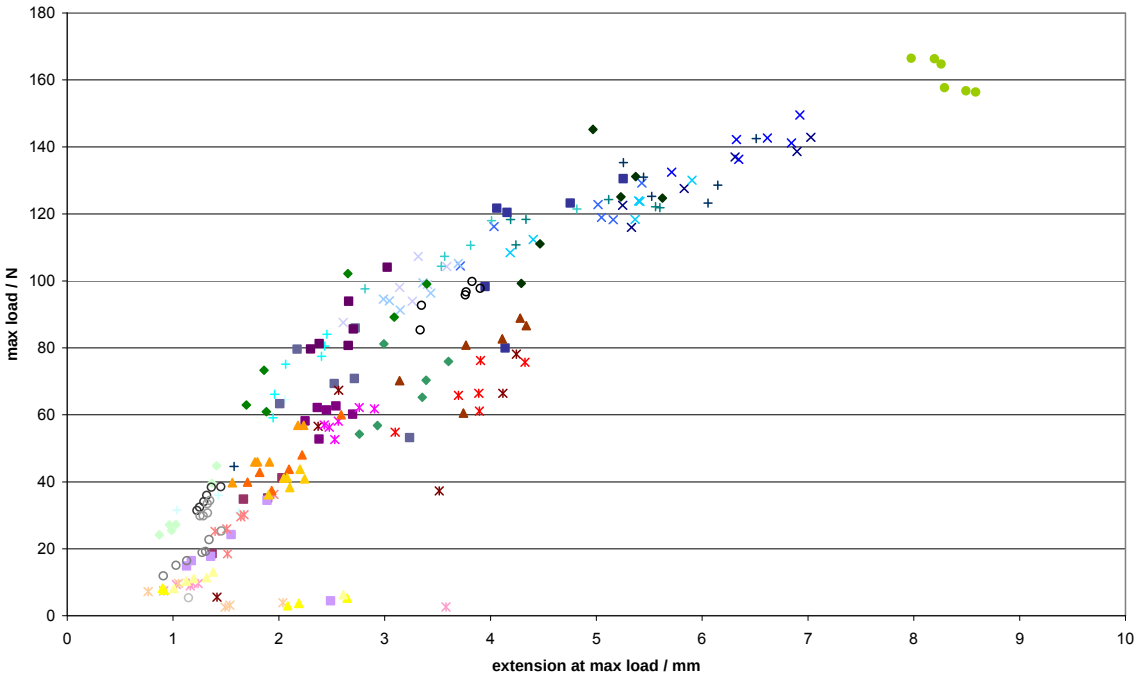

Figure 8.2 – scatter plot of extension vs. load for each thermal aged replicate

(For an explanation of sample labelling see chapter 7; unaged: olive green (●); 0% RH (x) 0D1: dark blue; 0D2: blue; 0D3: mid blue; 0D6: light blue; 0D9: pale blue; 0D12 ice blue; 30% RH (♦) 30D1: dark green; 30D2: green; 30D3: mid green; 30D9: pale green; 40% RH (+) 40D1 dark aqua; 40D2: aqua; 40D3: mid aqua; 40D6: bright aqua; 40D9: pale aqua; 40D12: teal; 50% RH (■) 50D1: indigo; 50D2: slate; 50D3: violet; 50D6: dark purple; 50D9: purple; 50D12: light purple; 60% RH (ж) 60D1: dark red; 60D2: red; 60D3: dark pink; 60D6: coral; 60D9: light pink; 60D12: pale pink; 75% RH (▲) 75D1: brown; 75D2: dark orange; 75D3: orange; 75D6: pale orange; 75D9: yellow; 75D12: peach; 100% RH (○) 100D1: black; 100D2: dark grey; 100D3: grey; 100D6: light grey; 100D9: pale grey)

The load versus extension plot (Figure 8.3) shows the effect of salt contamination on the sample aged at 30% RH for 9 months (pink curve). As well as a dramatic decrease in the tensile strength from the unaged sample (blue curve), there is a noticeable change in the shape of the curve. The salt contamination makes the silk more brittle leading to the sudden failure of the sample. Samples with visible salt contamination after ageing had been rinsed in deionised water, however evidence for salt was still observed in NIR spectra (see chapter eleven) and the

tensile testing curves. In comparison the unaged sample has a gradual increase in the extension of the sample with increasing load before the sample breaks, and there is not a sudden, brittle failure.

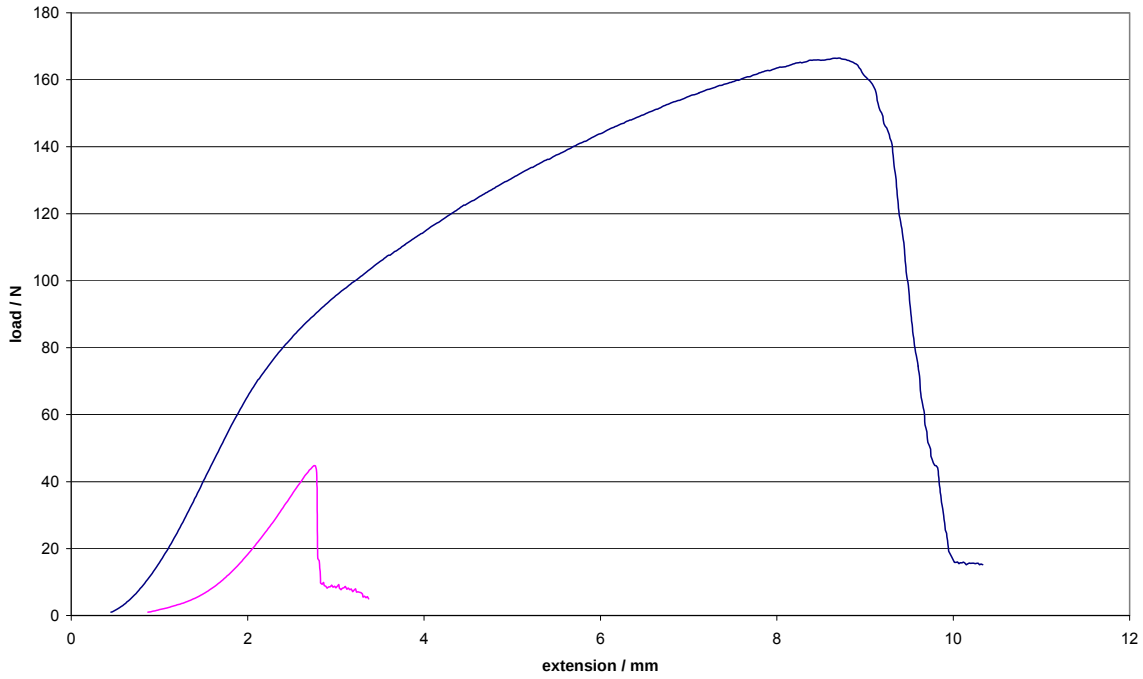

Figure 8.3 – comparison of unaged (blue) and 30% RH sample aged for 9 months (pink)

To plot the results on a time axis equivalent to display time, the length of ageing for the light acceleration had been determined from the annual light budgets. The light aged samples replicated a maximum dose equivalent to 15 years on display at 200 lux (an annual dose of 584400 lux hours) or equivalent to 16 years at 50 lux (an annual dose of 146100 lux hours). For simplicity these are referred to as 50 lux and 200 lux to denote which annual light budget has been used, with a separate equivalent display time (e.g. 4 years) and an ageing RH (e.g. 50%). The average value of the data for the six replicates for each ageing condition was determined and used to plot Figure 8.4. Although there is quite a large standard deviation in the data some trends are still visible. There is very little change in the tensile strength of samples aged at 50% RH and 50 lux or at 75% RH at either light level.

Increasing the light level at 50% RH to 200 lux had a noticeable effect, leading to a greater decrease in the tensile strength.

Both samples aged at 30% RH showed decreased tensile strength compared to samples aged at 50% and 75% RH. This is in contrast to the kinetics aged samples were the samples aged at 75% RH consistently showed greatest deterioration (measured as decreased tensile strength). However the reason for this is likely to reflect the changes in the ageing set up. The kinetics aged samples used sealed hybridisation tubes for both the light and thermal ageing, which maintain the RH level to a greater extent than the trays of saturated salt solution in the ventilated light box.

The use of hybridisation tubes also dramatically decreased the light levels samples were exposed to. The change in angle from lying flat directly under the light tubes, to hanging within the tubes decreased the ageing light level from 7000 to 1900 lux. In order to age a sufficient number of samples over a long enough time interval at the various RH levels, in the available time, a higher light level was required than had been used for the kinetics experiments. This meant compromises had to be made including moving from light ageing in sealed tubes to maintain the RH to using trays of saturated salt solution. Although the solutions in the light ageing chamber were checked regularly it is likely that the RH conditions have not been as successfully maintained. For the 75% RH samples it is probable that water evaporated readily and the RH in the chamber has been somewhat lower.

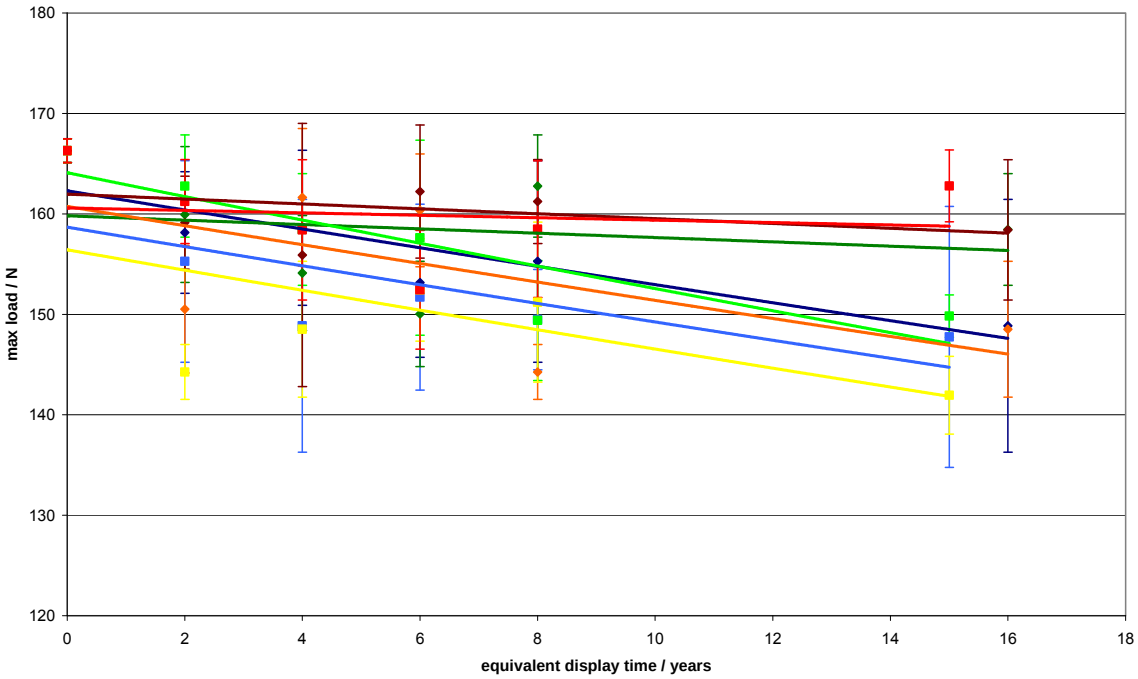

Figure 8.4 – average tensile strength results of light aged samples plot includes exponential regression lines determined by MS Excel

(50 lux (♦) 200 lux (■) 30L50l: dark blue; 30L200l: blue; 50L50l: green; 50L200l: bright green; 50UV50l: orange; 50UV200l: yellow; 75L50l: dark red; 75L200l: red)

The greatest decrease in the tensile strength was observed with the samples exposed to UV radiation. This was further increased when light levels were also higher. Although it was not possible to control the level of UV exposure, it demonstrates the damaging effect UV light has on silk deterioration. Especially when compared with the samples light aged at 50% RH, which were aged simultaneously but beneath the UV filter in the light box. The UV exposed samples show a maximum decrease of 25% in the tensile strength, which is relatively small in comparison to the changes recorded after thermal ageing. This can be seen very clearly in Figure 8.7 with the light and thermal ageing results plotted on the same equivalent display time axis.

The loss of tensile strength for thermally aged samples can be seen in Figure 8.5, again this uses equivalent display time. However for the thermally aged samples

the display time has been calculated using the activation energy to determine the increase in deterioration rate between room temperature (20 °C in the historic properties) and the ageing temperature (80 °C). In general, with increasing RH there is an increase in deterioration. The decrease in tensile strength is particularly rapid at 100% RH, with a drop of 75% after 2 months ageing, equivalent to approximately 5 years on display. Although the rate of deterioration is much slower at 0% RH, the tensile strength still decreases by over a third after a years' ageing, or about 33 years on display.

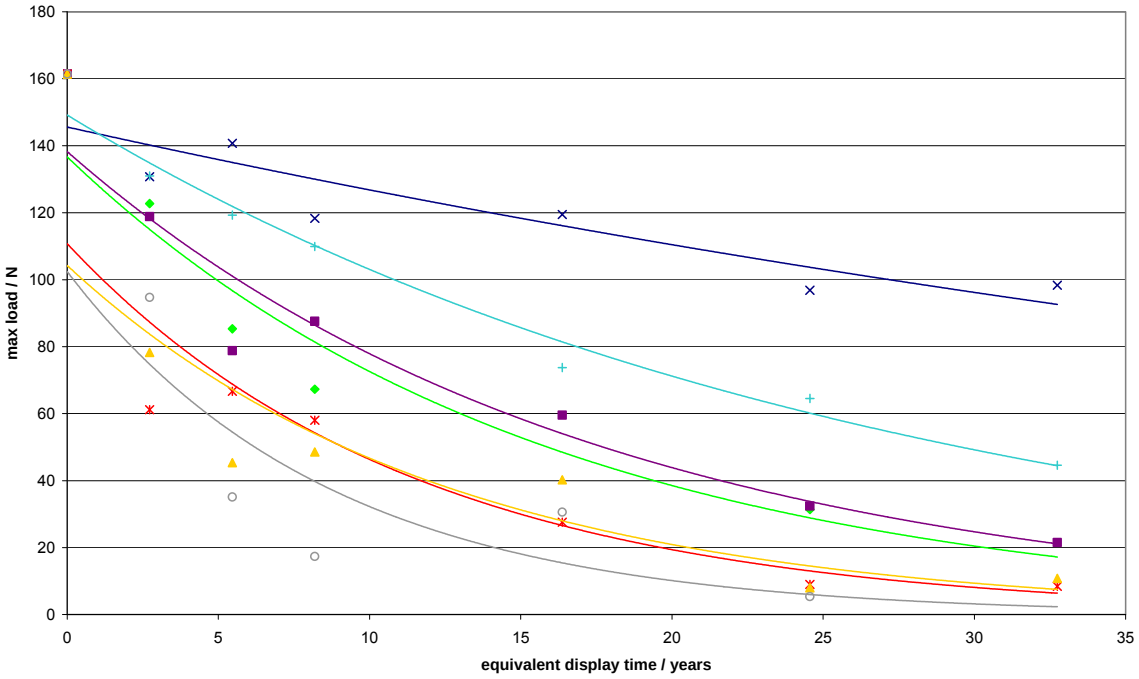

Figure 8.5 – tensile strength results of thermal aged samples plot includes exponential regression lines determined by MS Excel

(0% RH: blue x; 30% RH: dark green ♦; 40% RH: aqua +; 50% RH: dark purple ■; 60% RH: red ж; 75% RH: dark orange▲; 100% RH: grey ○)

Figure 8.5 demonstrates that silk deterioration at 30% RH is more rapid than the samples aged at both 40% and 50% RH. This is likely to result from the salt ($MgCl_2.6H_2O$) contamination observed on these samples and implies that the

presence of salt dramatically increases the rate of silk deterioration. Silk deterioration is thought to proceed from the amorphous areas and moisture is thought to form cross-links between the chains,[3] acting as a plasticiser. It may be that salt contamination on the silk retains moisture and therefore increases the deterioration of the textile.

The samples aged at 60% RH show a similar decrease in the tensile strength as those aged at 75% RH. Checks on the saturated salt solutions (see chapter seven) measured the RH of the 60% RH samples at 62.5% RH and the 75% RH samples at 79% RH, which implies the salt solutions are not forming similar RH environments leading to similar deterioration. However, the 60% RH samples were also found to have a degree of salt (KI) contamination and it is possible the larger decrease in tensile strength arises from the same mechanism as the samples aged at 30% RH.

The effect of salt contamination demonstrates the importance of considering how to display textiles within historic houses. In properties where salt efflorescence is observed, a barrier layer between the wall and textile could be used to prevent salt migration into the silk. The type and construction of this would have to be carefully considered to ensure sufficient moisture permeability to prevent or minimise damage to the masonry behind. Microclimates with higher RH levels have been recorded behind tapestries within English Heritage properties (see chapter two). Therefore the use of barrier layers may be appropriate for a range of large-scale, wall-hung textiles and may require further consideration by conservators and buildings engineers.

To try and determine the amount of deterioration that would occur after one year's ageing the results from the kinetics study (chapter six) at 80 °C had been extrapolated (see Figure 8.6). This predicted there would be no tensile strength after approximately 9 months for the 75% RH samples and after one year for the 30% RH samples. The kinetics study seemed to indicate samples aged at 50%

RH had less deterioration and there might be a central RH region where the silk deterioration was slower. For the 50% RH samples the prediction was after one year of ageing the samples would have approximately 60 N of remaining tensile strength. However the accelerated ageing results show that the increased deterioration of samples at 30% RH arises from salt contamination. Reviews of the data and samples from the kinetics experiments (chapter eleven) seem to confirm this assumption.

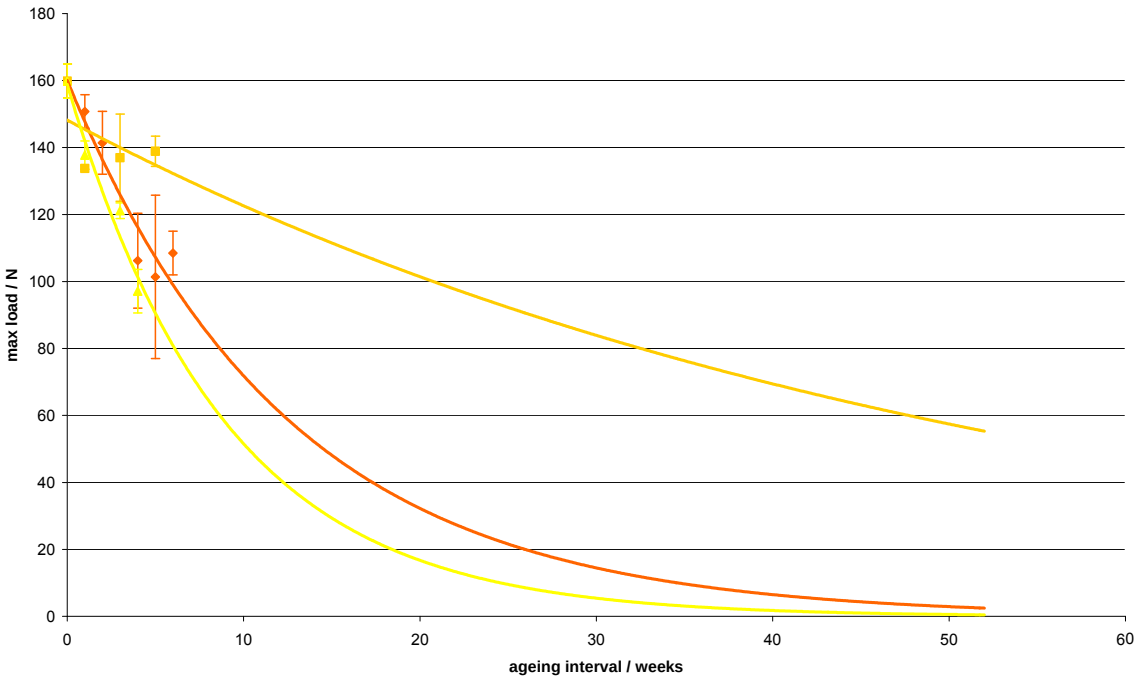

Figure 8.6 – projected tensile strength after ageing at 80°C from kinetics experiments (30% RH: dark orange; 50% RH: orange; 75% RH: yellow)

After ageing for one year the actual remaining tensile strength for the 75% RH aged samples was 10 N and 20 N for both the 30 and 50% RH aged samples. This reveals the ageing at 50% RH caused more deterioration over longer periods than would be predicted by a short term study. The results of the longer-term accelerated ageing experiments demonstrate the benefits of longer periods of ageing as well as a wider range of RH levels. More accurate results could be

obtained by ageing without saturated salt solutions however this would require greater access to RH ageing ovens.

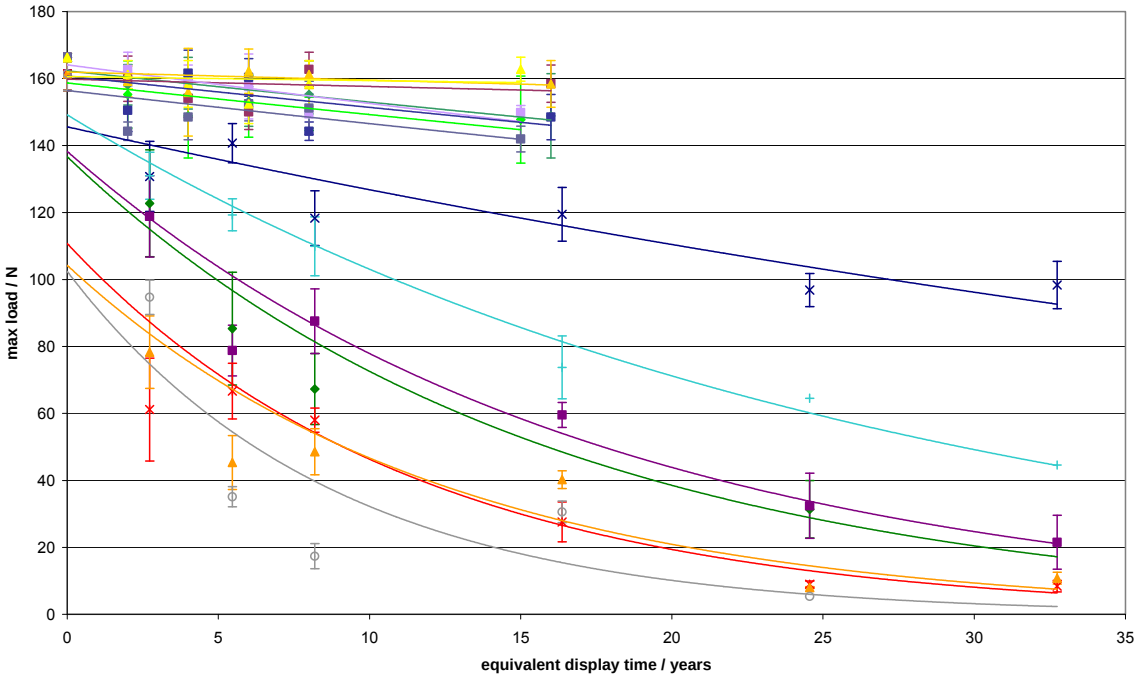

Figure 8.7 – tensile strength results for all accelerated ageing samples

(0% RH: blue x; 30% RH: dark green ♦; 40% RH: aqua +; 50% RH: dark purple ■; 60% RH: red ж; 75% RH: dark orange▲; 100% RH: grey ○; 30L50l: green ♦; 30L200l: bright green ♦; 50L50l: purple ■; 50L200l: light purple ■; 50UV50l: indigo ■; 50UV200l: slate ■; 75L50l: orange ▲; 75L200l: yellow ▲)

Figure 8.7 overlays the tensile strength data from Figures 8.4 and 8.5, with a common equivalent display time on the x-axis. This makes it clear that although UV ageing caused the greatest decrease in the accelerated light ageing samples it is still minor in comparison to the deterioration seen in the thermally aged samples. Based on the effect of high humidity seen in the thermal ageing results, the samples light aged at 75% RH would be expected to be more deteriorated than those aged at lower RH levels. However the 75% RH light aged samples are less

deteriorated than the 30% and 50% RH light aged samples. This is likely to result from the problems maintaining the RH levels in the light ageing chamber.

As the kinetics study was carried out in stages, due to resources, the initial indication had been that the activation energy would be very low and lead to little increase in the rate of silk deterioration. To keep the length of equivalent display time similar shorter interval light ageing was undertaken. However the completed kinetics study gave a greater rate increase than expected, meaning the light accelerated ageing occurs over only half the equivalent display time. However if the light ageing results are extrapolated they still lead to much less deterioration. As thermal ageing at all RH levels led to much greater loss of tensile strength it implies humidity may be much more important for silk deterioration than previously considered.

HPSEC

HPSEC Data Processing

The equipment used for all the HPSEC analysis is the same as described in chapter five. Due to difficulties in processing the HPSEC data for chapter six it became apparent that there were problems with the calibration of samples between batches. Some apparent molecular weight values doubled in magnitude for the same sample, after calibrating the column. This meant there was a large variability between the data points and when determining trendlines for the data the R^2 values were less than 0.5 and in some cases less than 0.1. When the HPSEC data was plotted in the order it was run and the calibration dates marked (red lines in Figure 8.8) it was obvious that some batches had lower molecular weight values when compared with the others (see Figure 8.8).

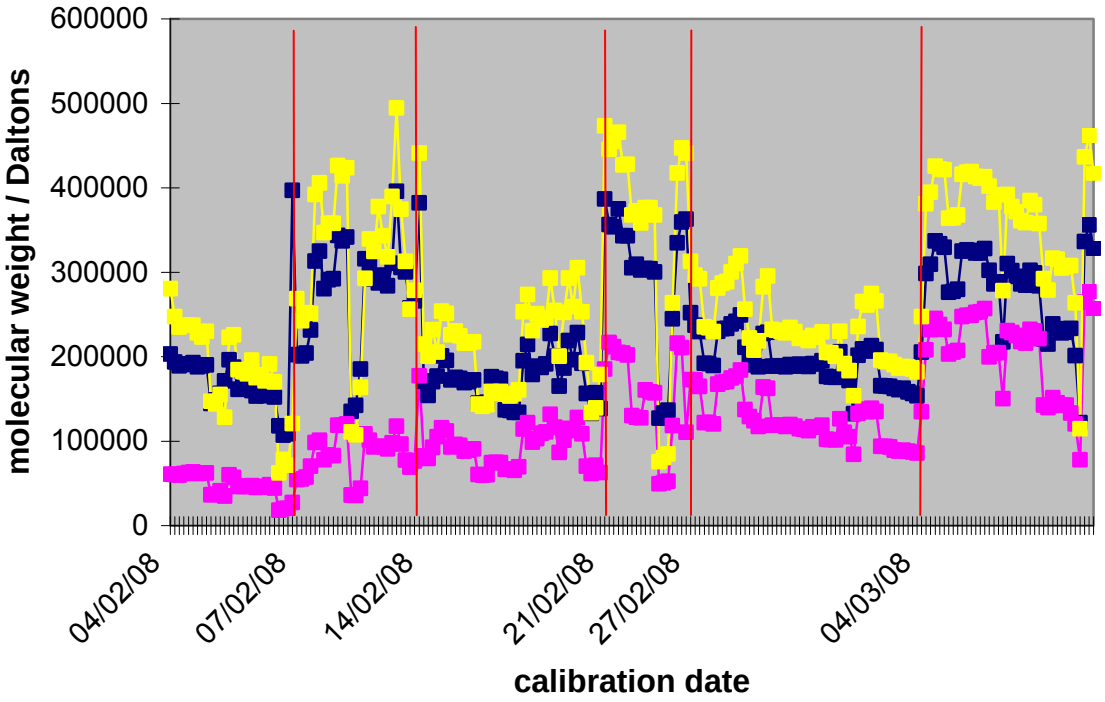

Figure 8.8 – calibration effects in kinetics HPSEC data

(M_w: blue; M_n: pink; M_p: yellow)

As some samples had been run before and after a calibration these were used to attempt to make the various batches comparable. For example in the kinetics experiments samples aged at 60 °C and 30% RH for 2 weeks had an average molecular weight of 324 kDa after two runs before calibration. After the calibration the average of three runs was 165 kDa, a difference of 159 kDa, almost half the value. To try and make the different batches comparable the values were scaled based on the differences between samples run before and after calibration. So for the above example (60 30 2) the average value before calibration was scaled by 1.96 (the ratio between the two sets of averages).

Although scaling the data sets from the different batches gave molecular weights of the correct magnitude and made the results comparable there were still a number of problems when using the data to calculate the activation energy. One difficulty was some trendlines for the molecular weight had increasing slopes with increased

ageing. The tensile testing results for the same samples had shown increasing deterioration with increased ageing so the HPSEC results seemed contradictory. In order to try and make each HPSEC batch between calibrations comparable it was decided to run the same unaged sample at beginning and end of the batch to allow normalisation of the results during the accelerated ageing sample analysis.

When the accelerated ageing samples were processed using this method, it was noted that for the same sample there could still be variations. For example the sample labelled unaged1 was run on four dates between 06/11/2008 and 28/11/2008 and the weight-averaged molecular weight (M_w) values ranged between 122 kDa and 279 kDa. Although generally within the three replicates the values were similar, between the runs there is a bigger variation. Checks on the retention time of the protein standards showed that although the void volume and totally included sample times varied little (between 6 and 24 seconds) changes of around half a minute to each of the standards shifts the average molecular weight of the sample by around 50 kDa.

The effect of the calibration is further complicated by the changes observed in the standards themselves. As described in chapter five the protein standards initially are formed of oligomers, which can also exist as their monomers. Therefore when recalibrating the column special attention must be paid to the retention times of the standards and which order they elute in, to determine the correct molecular weight to include in the calibration file. For example when the chromatograms of each standard are overlaid; if albumin elutes after β amylase, but before alcohol dehydrogenase, then it is most likely to be the trimer with a molecular weight of 198 kDa. However this makes the calibration file an educated guess at best.

To try and overcome the difficulties in the calibration file and the relationship between batches an alternative method of processing the data was sought. As noted in chapter five the lithium thiocyanate (LiSCN) peak provides an internal marker for retention time of a sample. To determine whether it would be possible

to correct the chromatograms using the LiSCN peak, an unaged sample was selected and compared using each method. After each column calibration a new method with the current date and latest calibration was saved. Each of these method files was used to calculate the molecular weight of the unaged sample. This gave M_w values ranging between 66 to 4414 kDa. Some of the methods could be discounted as they were during the development of the HPSEC protocols and so used different parameters in the software. However this still left a wide range of values for the molecular weight of the same sample.

For each method the LiSCN peak was then used to correct the chromatogram and shift the peak positions so LiSCN eluted at 15 minutes. The corrected values of M_w for each method were then calculated, although a relatively wide range (100-700 kDa) was still observed. To overcome the problems between the calibration files and processing the data a reference method file was selected and all samples were then downloaded using this method (silk251108) with the chromatogram corrected using the LiSCN peak as a reference eluting at 15 minutes. This dramatically improved the comparisons between batches however on occasions the peak shift was incorrect. This occurred when a secondary peak was observed on the shoulder of the LiSCN (see Figure 8.9). Unfortunately within the software it was not possible to further correct this problem, as the peak occurred on the shoulder of the LiSCN peak and therefore within the % reference window. Therefore the results were accepted without further amendments.

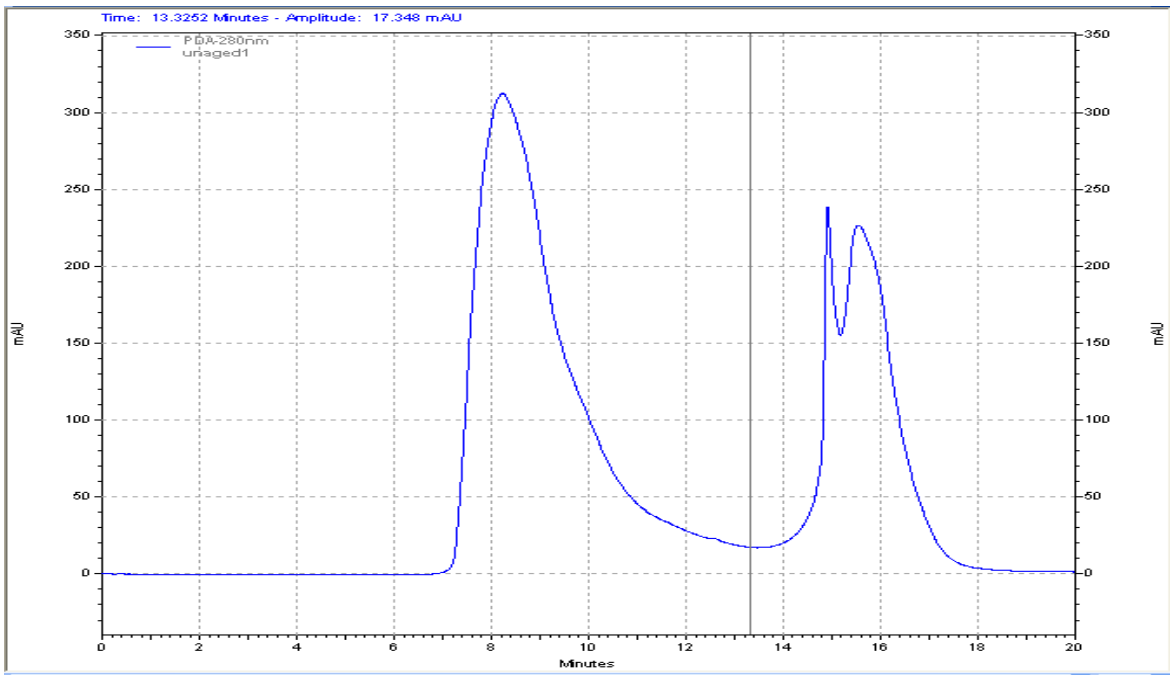

Figure 8.9 – additional peak on shoulder of lithium thiocyanate peak

Despite these corrections a number of problems were still observed in the data. This can be most clearly seen in the run order of the data of the light accelerated ageing samples (Figure 8.10) with a sudden increase in the molecular weight of the sample, without any other changes. This sudden shift was not observed in the tensile testing results implying it relates to a change in the column. A similar jump was seen in the thermal accelerated ageing data results. Figure 8.11 shows the effect this has on the HPSEC results, with an increase from the initial runs (blue and green lines) to the orange line which has a large initial increase. The later runs are all at higher molecular weights (red, burgundy and yellow lines).

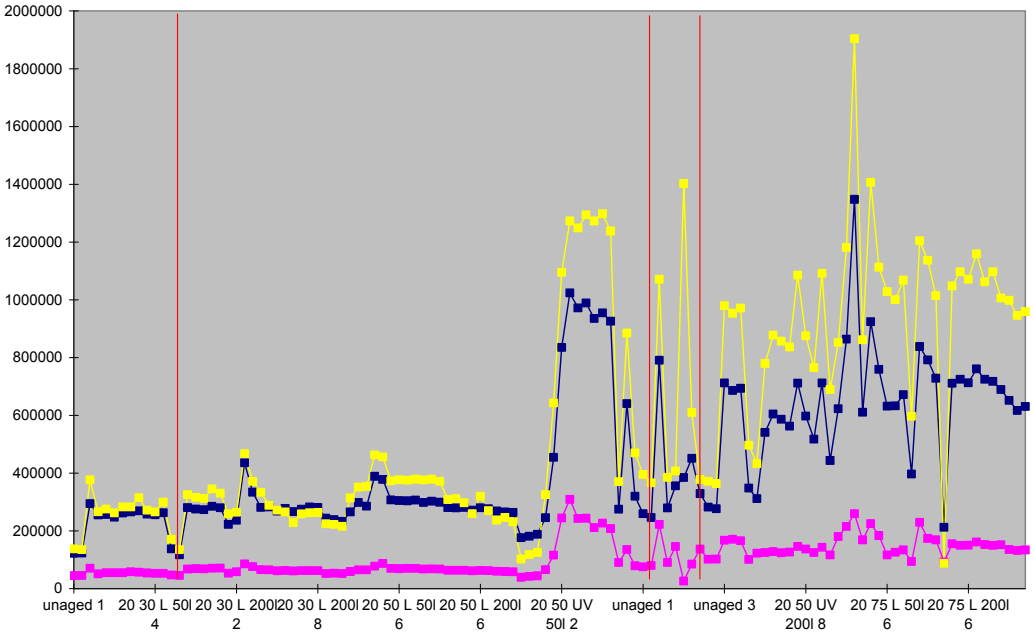

Figure 8.10 – molecular weights of light accelerated aged samples in run order (M_w: blue; M_n: pink; M_p: yellow)

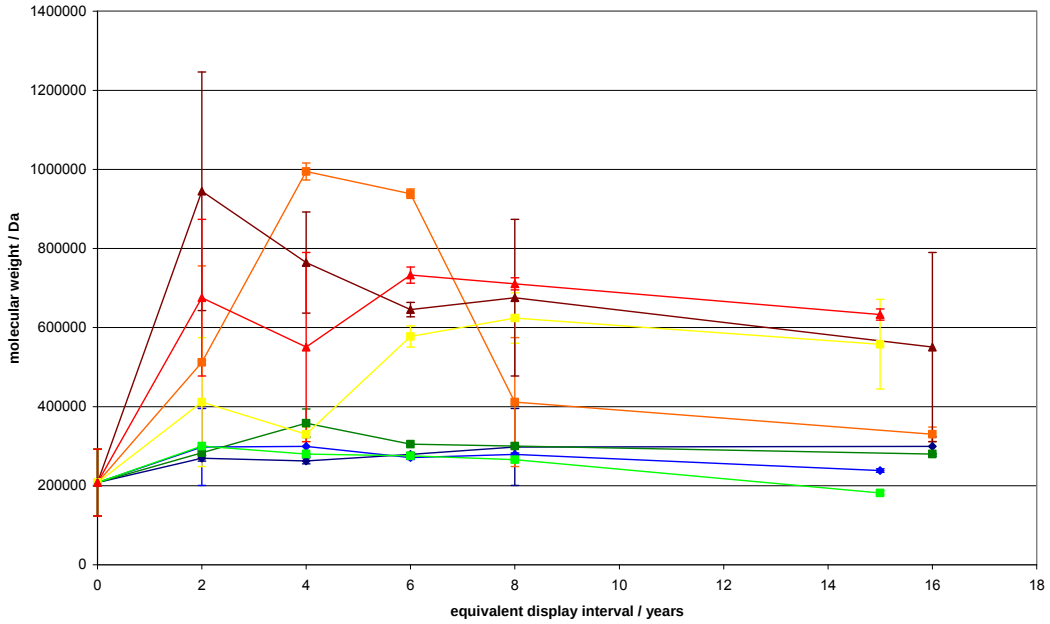

Figure 8.11 – weight-averaged molecular weight of light aged samples

(30L50l: dark blue ♦; 30L200l: blue ♦; 50L50l: dark green ■; 50L200l: bright green ■; 50UV50l: orange ■; 50UV200l: yellow ■; 75L50l: dark red ▲; 75L200l: red ▲)

The data was further corrected using the average of the run before the change and the average of the run afterwards for the same sample to scale the data. The effect on Figure 8.11 can be seen in Figure 8.12 where the HPSEC results are now within a similar range of molecular weight values. Comparison between the data demonstrated there is still some variation which will be discussed in more detail in chapter nine.

In theory the calibration procedure for HPSEC should ensure that batches are comparable with each other. However the work presented here and in chapter five have demonstrated there are a number of problems with both the calibration standards and the software processing of the data. The processes taken to overcome the problems with calibrating, downloading and interpreting the HPSEC results are less than ideal. The large number of processes and scaling effects mean the reported molecular weights are questionable and it is difficult to have confidence in the data reported. However the raw values were so strongly grouped into the batches between calibrations that results could not be compared. In a project of this nature were samples have been analysed over more than two years and the column needs recalibrating approximately once a week then comparison between batches is vital.

HPSEC could be used to compare samples within small batches, for example the Burrell tapestry results reported within chapter five where samples were run over two days. This allows them to be interpreted with confidence that the molecular weights determined from the software are comparable. HPSEC may also be more suited to test deviations from a narrow molecular weight range i.e. if consistently testing new silk to determine poor quality materials. However it is very difficult to see how HPSEC can be used for comparisons of historic materials with widely different molecular weights where there are no references for materials of similar age for comparison. This is particularly true when large datasets are to be used and run over long time periods.

One of the possible causes of the problems observed may be contamination of the column by high salt concentrations. The product literature for the BioSep-SEC-S4000 Columns indicates salt concentrations of 0.5M should not be exceeded.[4] However the concentration of the lithium thiocyanate solution to dissolve the silk is approximately 21.5M. Although only small amounts of the solution are used for each sample injection (20 µl) it is possible repeated exposure to the high salt concentrations is affecting the column performance.

A possible method to overcome this problem would be to dissolve the silk and then dialyse it so it is solubilised in an aqueous solution, as is commonly done for research on silk in other areas, although this has been reported to change the silk conformation.[5] However this would dramatically increase the time to prepare each sample and further increase the expense of running HPSEC for silk molecular weight determinations. Each sample would then have to be run immediately as aqueous solutions of silk gel and solidify after a few days. Generally the expense and reproducibility difficulties of the HPSEC system for analysis of silk are likely to preclude its widespread use within conservation.

The results of the HPSEC analysis are presented below but the difficulties described should be remembered as the interpretation is tentative at best. Generally this technique is of limited use for isolated historic samples as a single molecular weight measurement for a sample gives little information about the condition of an object. Even if sampling across a large object the results are difficult to interpret as the effects of dyeing are known to have an impact of the condition of the sample before ageing occurs,[6] therefore colour will also be important. With increased sample numbers there are increased problems with the data processing and comparison between batches.

One possible development which might make HPSEC results more reliable would be the digitisation of chromatograms. This might allow the chromatograms to be

normalised and interpreted with less influence from the calibration files within the software. This would also improve the use of the HPSEC data for multivariate analysis, as described in chapter eleven. Currently the EZChrom Elite software has been designed to prevent the export of chromatograms into other programmes. This feature is to prevent manipulation of the data and ensure transparency of HPLC analysis for large scale users such as the drug manufacturers.[7] As such the SEC package is an add-on to this more general HPLC package and so has limited capacity.

Another option would be the use of universal standards such as polystyrene. Generally within HPSEC it is preferable to use standards of the same materials as those being analysed i.e. proteins.[8] The problems of protein calibration for HPSEC with particular reference to the protein shape and interaction with the column have been discussed by Oliva *et al*.[9] However due to the changes seen in the standards it might be more appropriate to use standards which although interacting with the column differently give consistent calibrations. This would allow consistent relative molecular weights to be determined and give better comparisons between data sets.

HPSEC Results

After the HPSEC results had been corrected the changes in molecular weight were studied for each set of ageing conditions to determine the extent of silk deterioration caused. There are three measures of molecular weight determined by the software: the weight-averaged molecular weight (M_w), the number-averaged molecular weight (M_n) and the peak molecular weight (M_p). Of these, M_w gives a distribution of the samples' molecular weights and has been previously correlated with elongation. The trends observed in the HPSEC results were the same regardless of the molecular weight measure used to study the silk deterioration, therefore only M_w will be discussed below.

The raw changes in M_w after light ageing are presented in Figure 8.12. There is an initial rise in the molecular weight from the unaged sample (as seen in Figure 8.11), however this sample was run alongside the thermally aged samples and so the processing effects may be responsible. Generally there is little difference between most of the samples after this point (approximately 50 kDa), with small decreases in M_w with increased ageing. The exception to this is the UV aged samples, which show rather erratic changes.

The samples which were exposed to UV radiation at low light levels show a dramatic increase in the molecular weight, approximately doubling between 2 and 4 equivalent display years. However the samples aged at higher light levels and with UV radiation show the opposite trend with an initial decrease in M_w followed by an increase. The reason for these changes is not clear, however the same trend is observed in the uncorrected data (Figure 8.11). This implies that the changes are real and have not been introduced as a result of the data processing methods. The only comparative data indicates exposure to UV radiation leads to a breakdown of the silk chain, observed as a decrease in the M_p values by Tse and Dupont.[10]

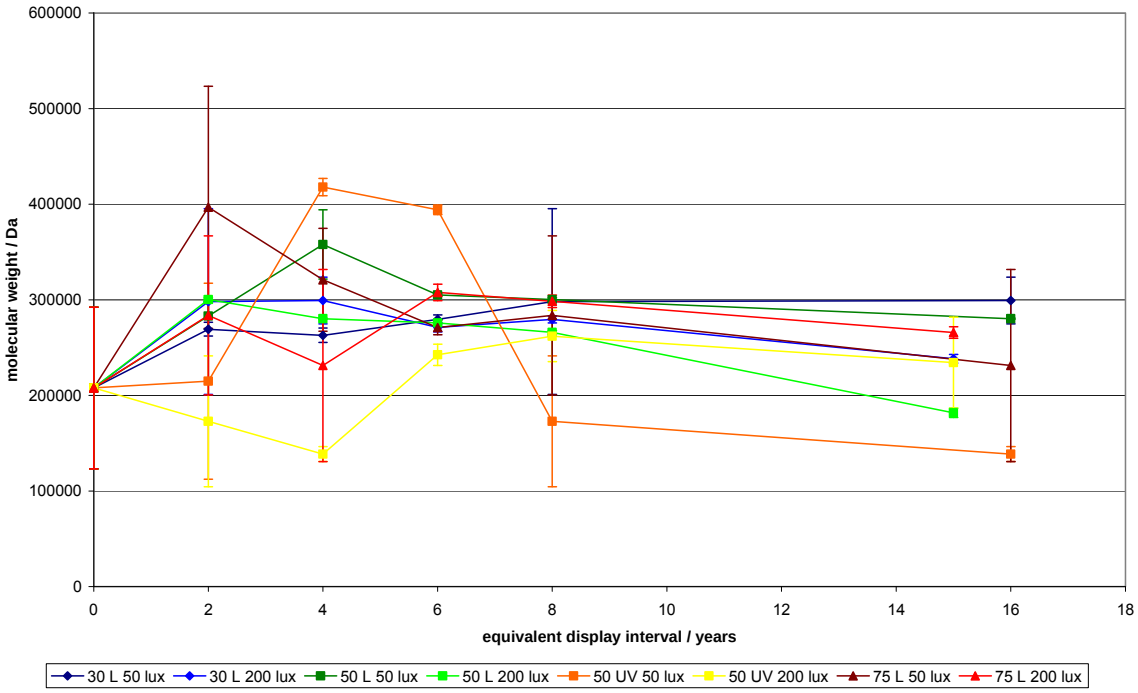

Figure 8.12 – weight-averaged molecular weight results for light aged samples (30L50l: dark blue ♦; 30L200l: blue ♦; 50L50l: dark green ■; 50L200l: bright green ■; 50UV50l: orange ■; 50UV200l: yellow ■; 75L50l: dark red ▲; 75L200l: red ▲)

Similar to the tensile testing results there is more deterioration after UV ageing, especially for the samples aged at 50 lux. For both the 30 and 50% RH aged samples (without UV) there is less deterioration at 50 lux than for samples aged at 200 lux, however this is reversed for the UV aged and 75% RH aged samples. There is no clear reason for this result and further experiments would be required to demonstrate a clear trend. In the case of UV ageing it is likely the very high UV level has accelerated the deterioration. On display this ageing condition is unlikely to occur as at low light levels the proportion of UV radiation is also low.

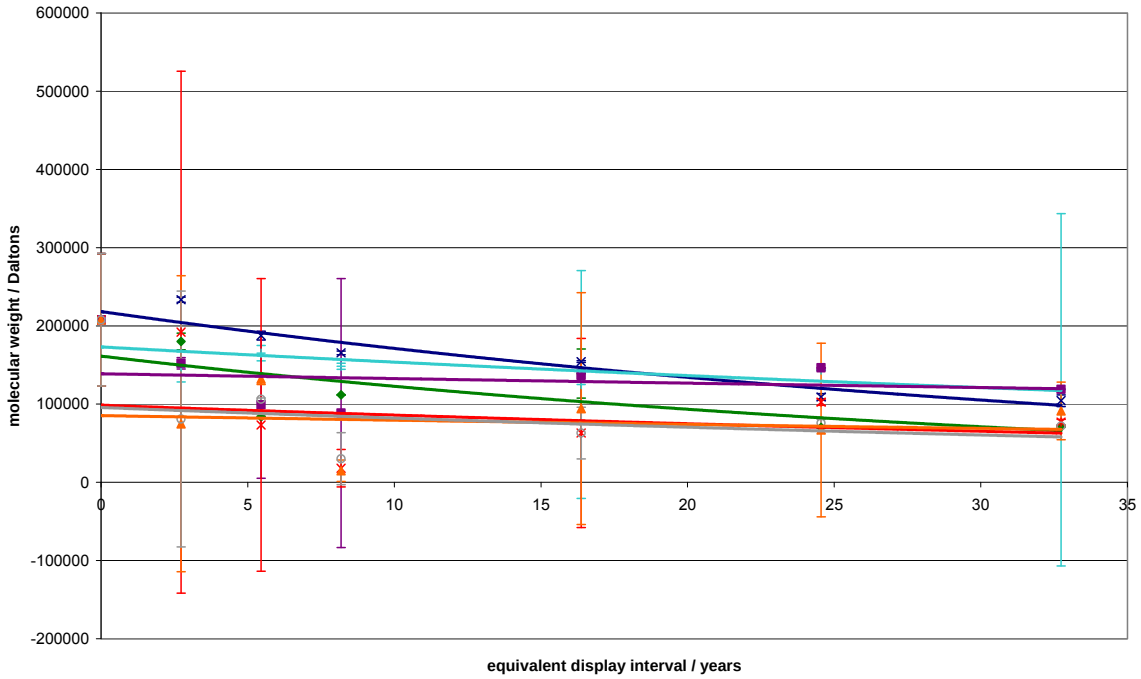

Figure 8.13 – weight-averaged molecular weight results for thermal aged samples (0% RH: blue x; 30% RH: dark green ♦; 40% RH: aqua +; 50% RH: dark purple ■; 60% RH: red ж; 75% RH: dark orange▲; 100% RH: grey ○)

The trends in the HPSEC results for the thermal aged samples (see Figure 8.13) are not as clear as those for the tensile testing results. However there are some similarities, particularly the similar level of deterioration observed for the 60% and 75% RH aged samples. Although for the HPSEC results the 60% and 75% RH aged samples are as deteriorated as the 100% RH aged samples. At early stages in the deterioration there is a larger decrease in M_w with increasing humidity. However as the ageing proceeds the lowest RH level aged samples (0%) show an increase in deterioration compared with the 50% RH aged samples. This may arise from the processing methods as both the 40 and 50% RH samples have been further adjusted to take into account sudden changes in the molecular weights (similar to the effects seen in Figure 8.10).

The increased deterioration of the salt contaminated samples can again be seen in Figure 8.13. Samples aged at 30% RH show a larger decrease in molecular weight than samples aged at 0%, 40% and 50% RH. After a years' ageing at 30% RH the molecular weight is similar to those samples aged at much higher RH levels (60%, 75% and 100% RH). This is similar to the observed changes in the tensile strength of samples aged at 30% RH and further indicates the increased silk deterioration caused by salt contamination.

As can be seen from Figure 8.13 there are significant deviations in the average HPSEC values between the three replicates. The large deviations in the molecular weights, coupled with the intensive processing make it difficult to draw any firm conclusions from the HPSEC data. This is a particular drawback experienced with the HPSEC technique.

Figure 8.14 combines the trends from Figures 8.12 and 8.13. Similar to the tensile testing results the changes after light ageing are noticeably less. However as the light aged samples were analysed using a separate column from the thermal aged results it is difficult to be sure the differences (between 100 and 200 kDa) are real. As discussed in the HPSEC processing section it is difficult to have confidence in the results which limits the conclusions that can be drawn.

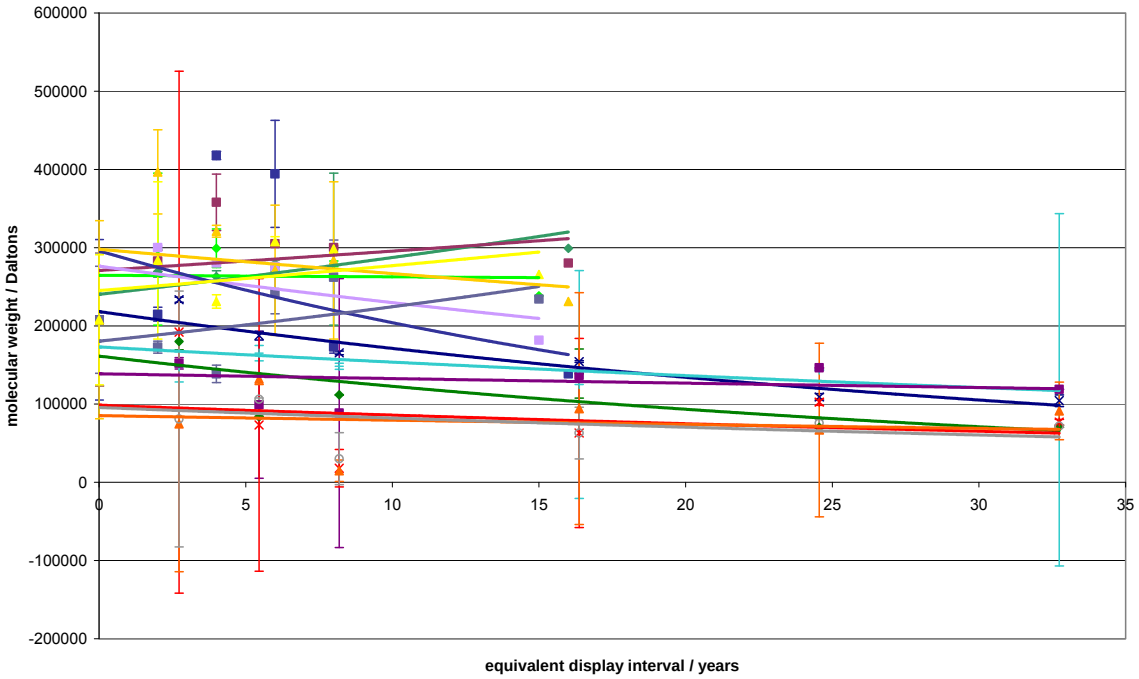

Figure 8.14 – combined light and thermal accelerated ageing HPSEC results

(0% RH: blue x; 30% RH: dark green ♦; 40% RH: aqua +; 50% RH: dark purple ■; 60% RH: red ж; 75% RH: dark orange▲; 100% RH: grey ○; 30L50l: green ♦; 30L200l: bright green ♦; 50L50l: purple ■; 50L200l: light purple ■; 50UV50l: indigo ■; 50UV200l: slate ■; 75L50l: orange ▲; 75L200l: yellow ▲)

Results Correlation

Despite the difficulties, the HPSEC results do seem to confirm a number of the tensile testing results, including the increase in silk deterioration with increased RH during ageing. Both sets of results also indicate that light ageing has caused less damage to the samples than the thermal ageing. Although the inclusion of UV radiation during light ageing does increase the rate of silk deterioration, the damage measured is still less than at low RH levels. The results indicate that both chemical and physical changes are occurring within the samples as a result of ageing. The decrease in the molecular weight of samples indicates the peptide bonds in the silk chains are breaking. This would have an impact on the tensile

properties as the ability of the silk chains to extend and accommodate the increasing load before breaking, is reduced.

Chemical measures of deterioration, such as chromatography, have been reported as being more sensitive than physical testing methods. To determine whether this is true for silk deterioration the tensile strength results were plotted against M_w (see Figure 8.15). This should help identify whether HPSEC is more sensitive to the initial deterioration of silk compared to the physical testing methods.

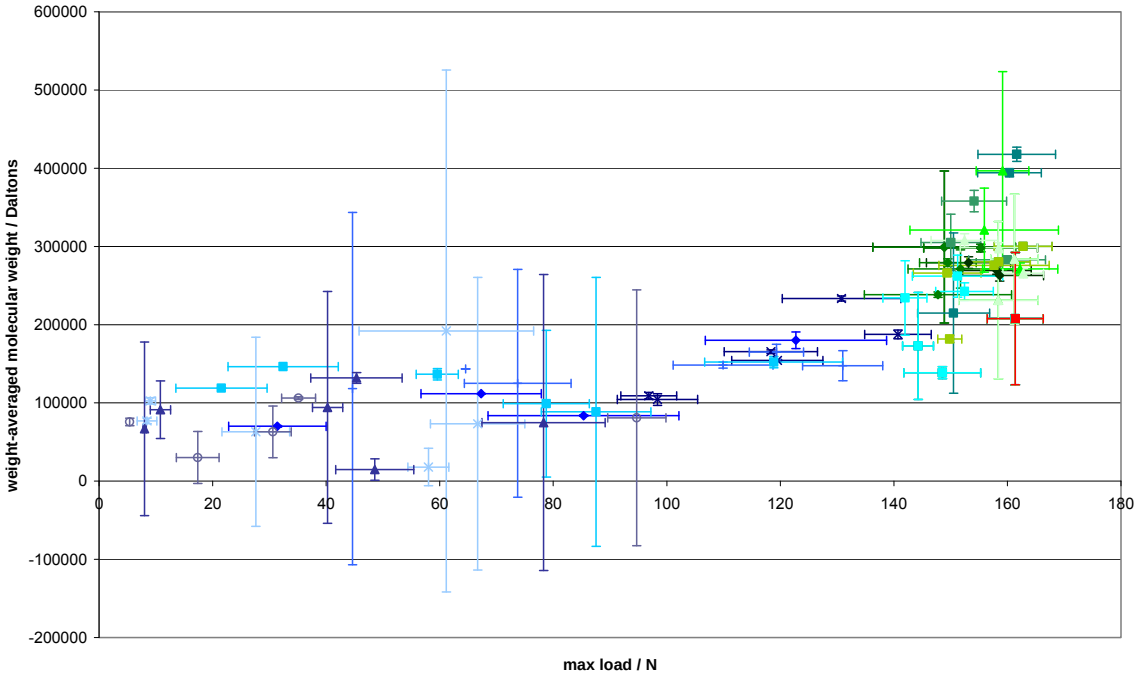

Figure 8.15 – scatter plot of changes in weight-averaged molecular weight with tensile strength (0% RH: dark blue x; 30% RH: blue ♦; 40% RH: mid blue +; 50% RH: light blue ■; 60% RH: pale blue ж; 75% RH: indigo▲; 100% RH: slate ○; 30L50l: dark green ♦; 30L200l: green ♦; 50L50l: mid green ■; 50L200l: olive green ■; 50UV50l: dark aqua ■; 50UV200l: aqua ■; 75L50l: bright green ▲; 75L200l: light green ▲; unaged: red■)

In Figure 8.15 the unaged silk samples are marked by a larger red square. In general the accelerated light aged samples have higher molecular weights but

similar tensile strengths to the unaged samples. In contrast the thermal aged samples show slightly less change in the molecular weight but a much greater shift in tensile strength. This seems to indicate there is a relationship between the tensile strength and molecular weight results. Certainly for the light aged samples there is a change in the molecular weight which is not observed in the tensile strength results. Similar to other studies it seems HPSEC can identify deterioration before tensile testing methods, although as the deterioration proceeds this increased sensitivity is lost.

For the accelerated light ageing samples the increase in molecular weight after ageing could arise from two possibilities. Different HPSEC columns were used to analyse the light and thermally aged samples. The unaged sample included in Figure 8.15 was analysed with the thermally aged samples and so the increase may actually relate to the differences between the columns. The historic micro-samples were also analysed using a different column to the light aged samples and have lower molecular weights. An alternative explanation is that cross-linking between chains occurs during light ageing, which increases the molecular weight of the samples. However if cross-linking occurs a similar increase in the tensile strength may be expected, as seen by Agarwal *et al.*,[11] however there are minimal changes in the tensile strength of samples.

The problems associated with the HPSEC processing means it is difficult to determine deterioration curves for silk at different RH levels. However the curve shown in Figure 8.15 could be used to calculate an approximate tensile strength from the HPSEC results. This could be useful for determining an objects display lifetime and will be explored further in chapter ten.

Rates of Deterioration

As deterioration curves for silk could not be plotted from the raw data an alternative method of studying the rate of silk deterioration was sought. As the tensile

strength gave the most reproducible results of the analytical methods used, this data was used similar to chapter six to determine the rate of silk deterioration. This plots the log of the change in load against time, to calculate the rate of deterioration, k, (see appendix 5). For each set of accelerated ageing conditions k has been determined and is shown in Figure 8.16.

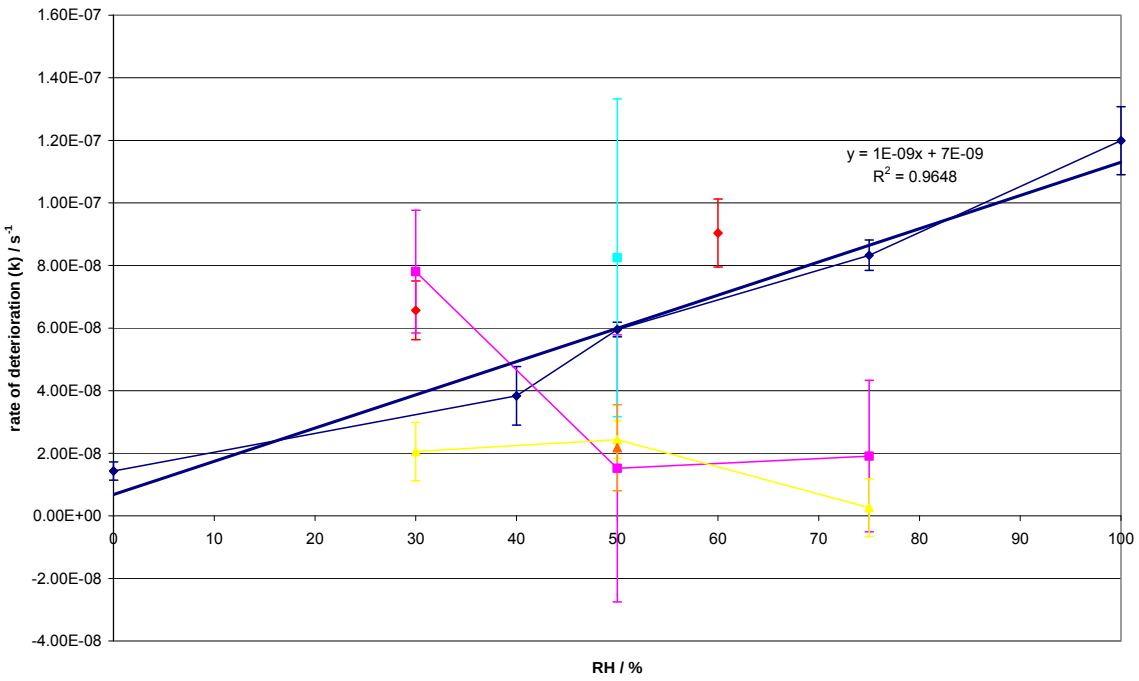

Figure 8.16 – rates of silk deterioration for each accelerated ageing method

(RH ageing: dark blue ♦; RH ageing (salt contaminated): red ♦; 50 lux light ageing: pink ■; 200 lux light ageing: yellow ▲; 50 lux UV ageing: aqua ■; 200 lux UV ageing: orange ▲)

When the salt contaminated samples (30% and 60% RH) are removed from the rest of the thermally accelerated ageing samples there is an approximately linear relationship (seen with the plotted trendline) between the increasing deterioration rates with increasing RH. Although the rate of increase is relatively moderate (an increase of 1.4 times going from 50% to 75% RH) it reveals that higher RH levels lead to greater silk deterioration. The data points at lower RH levels indicate the increase in the deterioration rate may be greater going from 25% to 50% RH. This emphasises the need for further studies focussing on the effect humidity has on the

deterioration rate of silk. The effect of salt contamination can be clearly seen in Figure 8.16 with the red data points noticeably above the other thermally aged samples (blue diamonds).

Generally low RH levels lead to less silk deterioration, seen in both the tensile testing and HPSEC results as well as in the rate of deterioration. Generally within conservation low RH levels are thought to lead to embrittlement of organic materials. Analysis of the low RH aged samples did not show brittle curves in the tensile testing results. However testing was carried out at moderate RH levels and the moisture transport through the silk samples was rapid. To test whether longer term display at low RH levels leads to embrittlement of the silk, tensile tests would have to be performed in dry environments. Unfortunately it is not possible to perform these tests with the equipment available, but they would form interesting further work.

In contrast the rate of deterioration caused by accelerated light ageing is generally much lower. The exception is at 30% RH and 50 lux which is significantly higher than at the higher RH levels also tested at 50 lux. The reason for this difference is unclear as checks showed the samples were not salt contaminated. However Figure 8.16 shows there is little difference in the deterioration caused at 50 or 200 lux during accelerated light ageing. As has already been noted ageing at 50 lux with UV radiation led to increased deterioration of the accelerated light ageing samples. It can also be seen from Figure 8.16 that over the time period required to age these samples the deterioration is greater than in the thermally aged samples at 50% RH and similar to the salt contamination samples.

This highlights one of the problems of the time axis – if the length of ageing is used the UV radiation aged samples are more deteriorated than samples aged using the other ageing methods. However the length of time this equates to on display is actually relatively long. Light (with or without UV radiation included) has commonly been reported as causing more deterioration,[12] however the ageing time periods

are rarely comparative as light ageing takes place under dramatically higher intensity light levels. For these experiments UV ageing led to an increase of 187.5 times ageing at 200 lux and 750 times for ageing at 50 lux, as the light levels are higher above the UV filter. Beneath the filter (ageing without UV) the increase is 105 times for a 200 lux annual light budget and 420 times for 50 lux, slightly lower due to the absorbance of light by the filter. This means the light levels equal a much longer period on display compared with generally quite modest increases in rate using temperature to accelerated reactions. Here a predicted increase from the kinetics experiments of 33 times, ageing at 80 °C compared with natural ageing on display at 20 °C.

Although Figure 8.16 shows low light levels and high UV radiation together lead to increased rates of silk deterioration, as previously mentioned on open display in historic houses it is unlikely this combination would be observed. However this result demonstrates the damaging effects of high UV levels and by association the benefits of reducing UV levels on display.

Conclusions

The accelerated ageing experiments have demonstrated that accelerated light ageing causes little change to the tensile strength of the samples with a slightly bigger loss of extension. A relatively small change was also observed for the HPSEC results of the accelerated light aged samples. Samples light aged at higher RH levels showed less deterioration than those light aged at a low or moderate RH, in contrast to the kinetics experiments. However this may arise from the change in ageing methods between the two sets of experiments. Both the tensile testing and HPSEC results have shown that including UV radiation when light ageing increased the amount of silk deterioration measured.

Greater silk deterioration was measured by both the tensile testing and HPSEC analysis for thermally aged samples. Generally there was an increase in the

deterioration with increasing RH and this was particularly seen in the tensile strength results. For all thermally aged samples the results demonstrate that salt contamination leads to increased deterioration. This was especially observed for samples aged at 30% RH, using magnesium chloride, and at 60% RH using potassium iodide. This may be a result of the salt retaining moisture on the surface of the silk and allowing greater moisture to penetrate the amorphous regions. Samples which had been salt contaminated were brittle which could be seen in the change of the curve in the extension against load plots for the tensile testing analysis.

Problems have been identified in comparing data between calibrations and different columns on the HPSEC, which limits the interpretation of these results. To use the HPSEC results the chromatograms have been corrected using the lithium thiocyanate peak along with some scaling of the data. Possible methods of overcoming these difficulties include the use of universal standards and the digitisation of the chromatograms.

The rates of silk deterioration have been determined from the accelerated ageing experiments. This shows that there is an approximately linear increase in the rate of silk deterioration with increasing humidity levels. Salt contamination of samples further increases the rate of silk degradation. In general the rate of silk deterioration is greater after thermal accelerated ageing than after light accelerated ageing. However combined low light and high UV radiation levels also lead to an increase in the rate of deterioration.

The effect of salt contamination on the samples has a number of implications, the most obvious being to undertake accelerated ageing without using saturated salt solutions in the future. However it also has implications for the display of large scale textiles on walls which might have salt efflorescence or high salt levels in the masonry. It may be necessary to consider the use of barrier layers between textiles and the wall to prevent increased deterioration. This may also be

necessary when higher humidity microclimates have been observed behind tapestries, in order to reduce the rate of silk deterioration.

The effects of high humidities may be the cause of higher than expected deterioration for unfaded samples taken from the reverse of tapestries in the MODHT project. Analysis of the Burrell tapestry samples (chapter five) has already demonstrated that faded and unfaded sections of the same historic thread have similar molecular weights. To study the condition of historic materials further, micro-samples have been analysed using HPSEC. These results are presented in chapter nine and related to the accelerated ageing results presented here.

References

[1] Zou, X., Uesaka, T. and Gurnagul, N. (1996) 'Prediction of Paper Permanence by Accelerated Aging I. Kinetic Analysis of the Aging Process' *Cellulose* **3** 243-267.
[2] Richardson, E. and Garside, P. (2009) 'The Use of Near Infrared Spectroscopy as a Diagnostic Tool for Historic Silk Artefacts' *e-Preservation Science* **6** 68-74.
[3] Lucas, F., Shaw, J. T. B. and Smith, S. G. (1955) 'The Chemical Constitution of Some Silk Fibroins and its Bearing on their Physical Properties' *Journal of the Textile Institute* **46** T440-T452.
[4] BioSep brochure http://www.phenomenex.com/WorkArea/showcontent.aspx?id=8143 accessed 31/07/2009.
[5] Asakura, T., Suita, K., Kameda, T., Afonin, S. and Ulrich, A. S. (2004) 'Structural role of tyrosine in *Bombyx mori* silk fibroin studied by solid-state NMR and molecular mechanics on a model peptide prepared as silk I and II' *Magnetic Resonance in Chemistry* **42** 258-266.
[6] Hallett, K. and Howell, D., (2005), 'Size exclusion chromatography of silk: inferring the textile strength and assessing the condition of historic tapestries' in *ICOM Committee for Conservation 14th Triennial Meeting, The Hague, 12-16th September 2005 Preprints* Verger, I. (ed.) London: James & James Ltd **2** 911-919.

[7] Mitchell, S. personal communication, 23/07/2007.

[8] Goetz, H., Elgass, H. and Huber, L. (1985) 'Determination of Molecular Weight Data in Size-Exclusion Chromatography by Use of Broad-Molecular-Weight-Distributed Standards' *Journal of Chromatography* **349** 357-367.

[9] Oliva, A., Llabrés, M. and Fariña, J. B. (2001) 'Comparative study of protein molecular weights by size-exclusion chromatography and laser-light scattering' *Journal of Pharmaceutical and Biomedical Analysis* **25** 833-841.

[10] Tse, S. and Dupont, A.-L. (2001) 'Measuring Silk Deterioration by High-Performance Size-Exclusion Chromatography, Viscometry, and Electrophoresis' *Historic Textiles, Papers, and Polymers in Museums* Cardamone, J. M. and Baker, M. T. (ed.) ACS Symposium Series **779** Washington DC: American Chemical Society 98-114.

[11] Agarwal, D., Sen, K. and Gulrajani, M. L. (1996) 'Formation of crosslinks in silk by bifunctional reactive dyes: effect on solubility and mechanical properties' *Journal of the Society of Dyers and Colourists* **112** 321-325.

[12] Kim, J.-J. and Wyeth, P. (2009) 'Towards a routine methodology for assessing the condition of historic silk' *e-Preservation* **6** 60-67.

Chapter 9 – Results Comparison for the English Heritage Collection

The chapter presents the results of HPSEC analysis of the English Heritage micro-samples. The results have been related to the objects and their visual condition as assessed during sampling. Comparison of the historic samples' results with published values and the accelerated ageing results are reported. The use of HPSEC to analyse silk in conservation is also discussed, based on the results.

The accelerated ageing results have demonstrated that artificial light ageing causes relatively small changes to the silk samples in comparison to the thermal ageing. Higher humidity levels also accelerated the deterioration to a greater extent than lower humidities. As well as helping to identify the critical causes of silk deterioration, the aim of the accelerated ageing experiments was to create a range of deterioration levels similar to those found in historic collections. Light ageing undertaken for MODHT replicated up to 400 years on display but the samples were not as deteriorated as those from historic materials.[1] Although some historic samples were from tapestries older than 400 years this indicated other deterioration mechanisms could be important for silk degradation.

To determine whether the accelerated ageing created similar levels of deterioration the results were compared with samples from the English Heritage collection. The sample size, number of replicates and destructive nature of tensile testing prevents analysis of historic materials in almost all cases. Therefore HPSEC has been used to compare the accelerated ageing results with the micro-samples taken from the English Heritage collection. Analysis of the English Heritage collection allows the current condition of the silk to be assessed, which could form a benchmark for future comparison. Although the number of micro-samples permitted is still

relatively small (87 samples from over 1000 objects) it may also be possible to look at the condition of a number of objects in more detail and determine if the visual condition assessment matches the analytical results.

Analysis of the English Heritage Silk Collection

Micro-samples taken from objects in the English Heritage collection were analysed using the same HPSEC equipment and parameters discussed in chapter five. Each sample was initially run once before being rerun in duplicate. The results presented are the average of the three runs. Some changes were noted between the initial run and the later reruns, particularly for the samples taken from more recent reproduction silks. Figure 9.1 shows the changes for sample nlran7a, a modern (2002) reproduction silk from Ranger's House. There is an obvious shift in the chromatograms as seen in the lithium thiocyanate (LiSCN) peak which moves from 15 minutes in the first run (blue curve) to 16 minutes in the subsequent reruns (green and aqua curves).

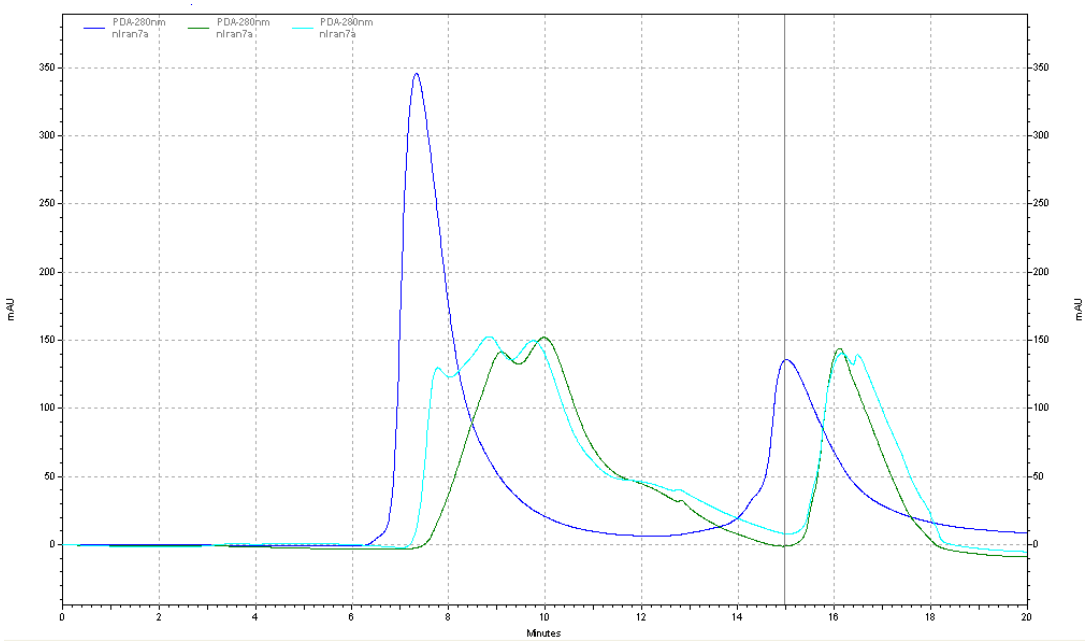

Figure 9.1 – changes to sample nlran7a between initial run (blue) and later reruns (green and aqua)

After correcting the peak movements (by shifting the chromatogram using the LiSCN peak as an internal standard) there is still a substantial difference in the calculated weight-averaged molecular weight (M_w) values between the different runs. The first replicate M_w was ~380 kDa, the second replicate was ~172 kDa and the third replicate was ~89 kDa. Each subsequent replicate leads to an approximate halving of the molecular weight. For the other measures of molecular weight (number-averaged molecular weight (M_n) and peak molecular weight (M_p)) there is a noticeable difference between the first and subsequent runs but not between the duplicate reruns. The change in M_w reflects the significant broadening of the peaks for the rerun samples.

There are a number of reasons why the peak broadening could occur. Analysis of samples in LiSCN over a number of weeks showed no change in the molecular weight (chapter five). However it is possible over longer periods the silk chain is attacked and begins to break into smaller fragments. This would lead to a larger number of smaller chains in the rerun samples than during the initial run. The change in the sample may also have been caused by conformational changes in the silk. In the initial run the silk is likely to have been a long chain and therefore passed quickly through the column. For the rerun samples the silk may have re-formed hydrogen bonds between the chains and may have a more globular conformation. This may lead to the sample interacting more strongly with the column, which would increase the retention time of the silk and change the peak shape.

Although longer incubation in LiSCN is likely to cause further denaturation and some cleavage of the chain, it was not possible as part of this study to determine the exact effect leading to these changes. To eliminate these effects the kinetics and accelerated ageing samples were all run in triplicate. For the older historic materials these changes were not observed (see Figure 9.2). This may arise because the silk chains have already been broken down in to smaller lengths due

to silk deterioration arising whilst on display. However for the smaller historic samples the amount of material was more critical.

For a number of the historic objects the micro-samples taken were very small in size, often no more than a millimetre of thread or just a fine powder. This strongly affected the absorbance recorded by the detector, in milliabsorbance units (mAU). For small samples the peak height was often less than 50 mAU (see Figure 9.2) compared with 350 mAU in Figure 9.1 or over 1000 mAU for unaged silk. This affects the peak area which is then integrated by the software to calculate the molecular weight.

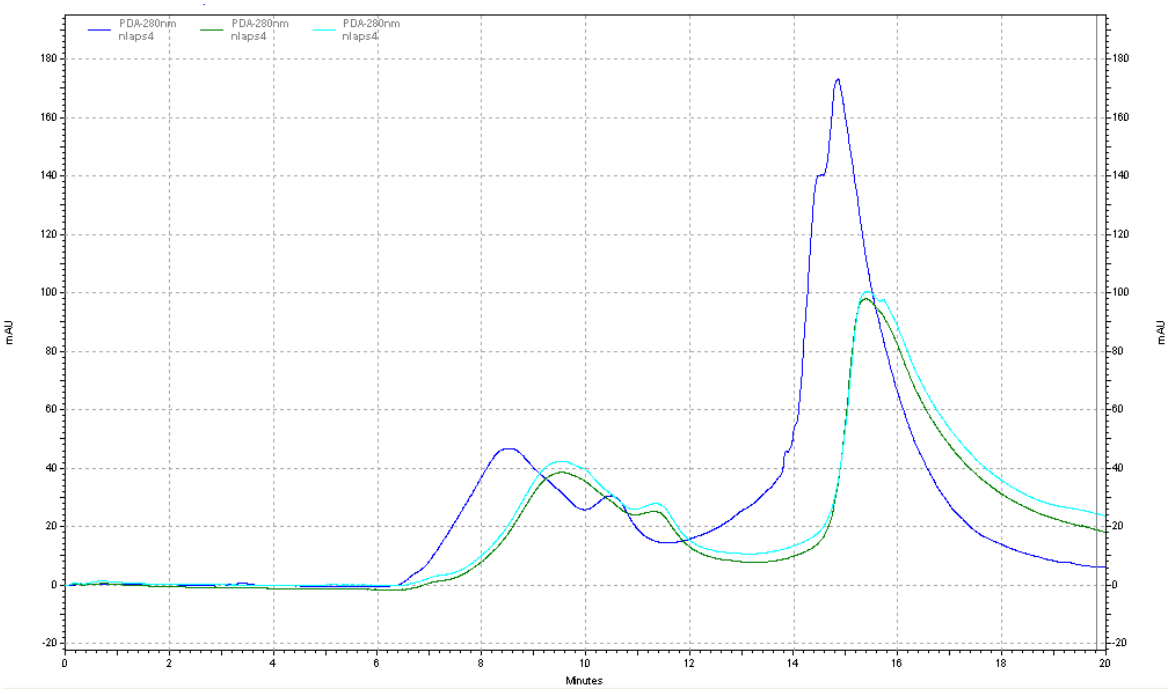

Figure 9.2 – low absorbance for sample nlaps4

For some samples the silk fragment was so small that there was barely a bump in the baseline. Although the points between which to draw the baseline can be selected the software actually positions it and it cannot be manually repositioned by the user. The same is true for the start and finish points for the peak integration, which can be specified but the software determines the peak area.

Although in Figure 9.2 there is still a clear, but small, peak above the baseline in some cases the bump and position of the baseline led to very high molecular weights. For example in Figure 9.3 (sample nlaps1) the calculated M_w was ~707 kDa, however the previous run was ~84 kDa and the final run ~268 kDa. These changes seem to arise primarily from the positioning of the baseline for very small intensity peaks.

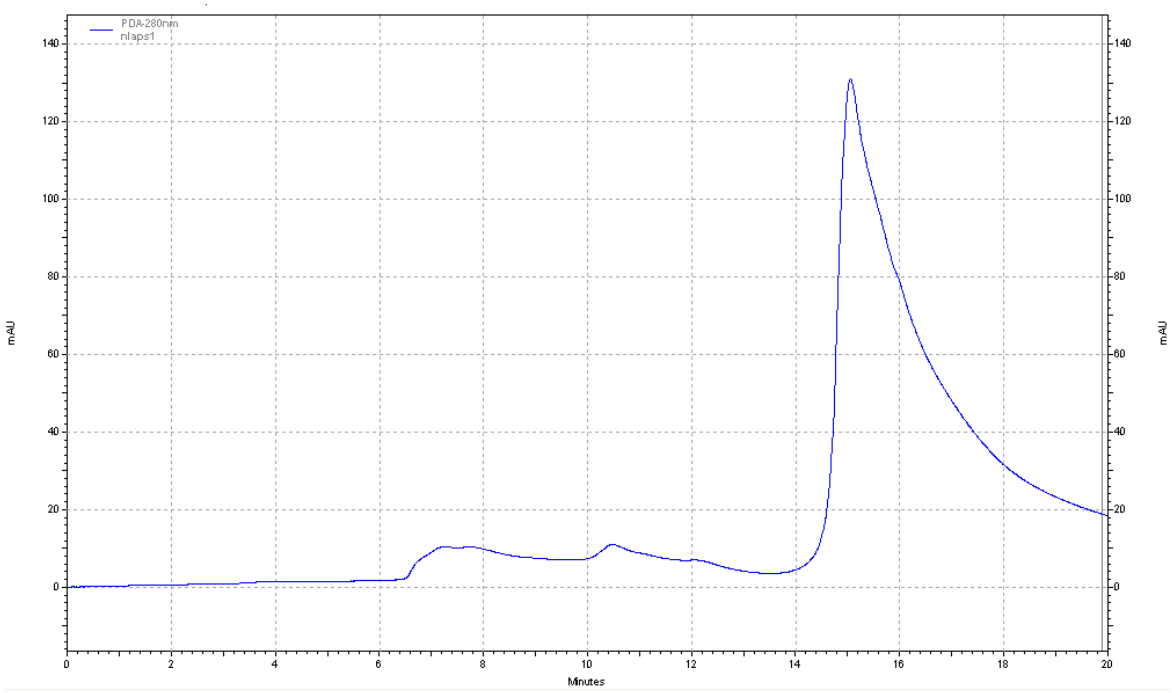

Figure 9.3 – small peak for sample nlaps1

For the kinetics and accelerated ageing samples the large sample size allowed at least 0.6 mg of silk to be used for HPSEC giving concentrated samples and sufficient volume for a number of reruns if recalibration of the column was required. However for the historic micro-samples very few were large enough to be weighed and for those which were, measured around 0.1 mg. Due to the small size these were dissolved in 0.2 ml of LiSCN. Although this allowed HPSEC analysis there was rarely enough sample to allow more than three runs and in one case (nlaps3) the duplicate reruns had no silk peak at all. The English Heritage samples have been downloaded using the same standard method file and corrected for the

LiSCN peak, as described in chapter eight. However there has been no further scaling of the data between batches as it was not possible to compare the same sample before and after calibration.

English Heritage Collection HPSEC Results

The differences between the initial run and later reruns are one of the reasons for the high standard deviations seen in M_w in Figure 9.4. In general the average M_w values for the historic micro-samples are below 250 kDa, although the samples range from 100 kDa to 550 kDa. Despite the variety of display environments there are no clear differences between the properties in Figure 9.4. As has been shown by MODHT dyeing processes have an effect on the condition of the silk before ageing occurs. So the similar silk condition across all the properties, despite differences in age, may be related to previous processing methods, the effects of which are difficult to determine.

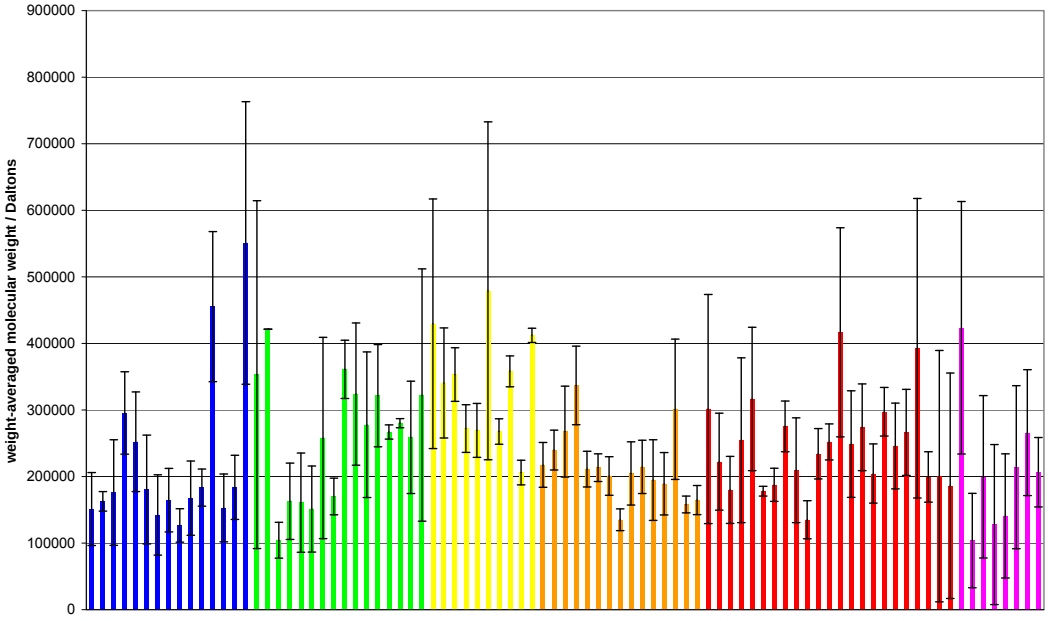

Figure 9.4 – M_w results summary of English Heritage micro-samples
(Audley End House: blue; Apsley House: green; Brodsworth Hall: yellow; Fulford Store: orange; Osborne House: red; Ranger's House: pink)

On average the samples taken from Brodsworth Hall had a higher molecular weight than those from the associated store, Fulford or the other properties. This might be expected comparing the house with its store, as objects in storage are likely to be unsuitable for display due to their fragile condition or previous damage. However Brodsworth Hall would not be expected to have the best condition silks based on their visual appearance. However difficulties when sampling meant some obviously deteriorated silks were not included. For example a very limited number of samples came from wall silk at Brodsworth Hall, as this had been conserved and is now covered by net. This made it very difficult to sample, unless a fibre or thread was protruding out of the net. As a consequence the results for Brodsworth Hall may be slightly skewed towards the better condition objects which had received less invasive or no conservation treatments and so could be sampled for HPSEC analysis.

To determine the impact of previous processing methods on the silk, the HPSEC results were compared with those from the XRF (chapter three). However there was no apparent correlation between the condition measured by HPSEC and the elements identified in the silk. For the samples from Fulford the lowest molecular weight was for a sample identified as containing sulfur (nlful9). However the highest molecular weight was for nlful5 which contained silicon, phosphorus and tin and is likely to be weighted. As neither of the objects have known dates, it is difficult to determine whether the poorer condition of the silk relates to the age of the material or another cause such as its processing. The highest molecular weight sample from Osborne House was also found to contain tin. A number of the weighted samples did not dissolve in LiSCN, but those which did, generally were very friable and powdery. Therefore it seems unlikely that samples identified as containing tin, and in relatively poor condition, should have the highest molecular weight. This may be the result of the metal ion bonding between chains and possibly affecting the conformation of the protein or its interactions with the

column. However as weighted silks were not the main focus of the research this was not investigated further.

For an individual HPSEC result it is difficult to draw conclusions without other data to provide comparisons. For the historic objects this could include taking a number of samples from the same object (such as the Burrell tapestry discussed in chapter five) or from a number of similar objects (e.g. a number of chairs upholstered in the same fabric) to compare the condition between a set of samples. Selecting the same colour thread (for the tapestry) or the same fabric also limits the impact of processing effects, as these are likely to be the same for the same thread or fabric. Within a large collection comparisons are difficult due to the unknown processing methods and their likely impact on the initial condition of the silk before ageing occurs. As well as the effects of different ageing conditions and display environments on the silk condition. However the molecular weight could be used as a benchmark for comparison with subsequent analysis, although this would require further invasive sampling of objects. Alternatively the results could be used to identify the chemical condition of textiles within a collection and prioritise interventive conservation treatments for the most deteriorated objects.

Although the number of objects from which it was possible to take more than one sample was limited, some comparisons were possible. For most artefacts where a number of differently coloured threads could be sampled there was a significant variation between the M_w of the samples. This included a tassel in store at Fulford [90006838] where the red sample (nlful18) was half the molecular weight of the gold sample (nlful17). Although the red samples were not always the lowest molecular weight. The silk skeins [79704568] in the Swiss Cottage Museum at Osborne House had a range of M_w values from 200 kDa for the blue sample to 393 kDa for the red sample. The differences for the variously coloured samples might be expected from the results of MODHT which showed dyeing had an effect on the condition of silk.

In some cases however the colour of the sample seemed to make little difference. Analysis of a cushion [90009023] in store at Fulford showed a relatively narrow range of M_w from 195 kDa to 215 kDa for the pink, cream and gold samples. Similarly sometimes two samples taken from different areas of the same object (and the same coloured panel of silk) had much wider variation. For example, the portiere curtain braid fragments [90007051/53/63/67] from Brodsworth Hall had a difference of ~200 kDa between the lowest and highest M_w samples. Although different curtains of the same design, these can be assumed to have been processed in the same manner, so the large difference must arise from the variety of display environments within Brodsworth Hall. The results further highlights how the unknown history of an object, be it the processing methods used during manufacture, or the varying display conditions, can have an effect but be difficult to determine.

As part of the accelerated ageing experiments it was not possible to study the effects of pollution. However Brodsworth Hall is likely to have had high historic sulfur dioxide (SO_2) levels from nearby industry. The deposition of SO_2 may lead to the formation of sulfurous acid with moisture in the objects and the high humidity levels at this property. As acids are reported to cause damage to silk,[2] this historic pollution may have led to acid deterioration of the collection at Brodsworth Hall. However as seen in Figure 9.4 the M_w values for samples taken from Brodsworth Hall are slightly higher on average, compared to the other properties. This would indicate the historic pollution has been lower than anticipated or had little effect on the condition of the silk artefacts.

Apsley House is situated on a busy roundabout in central London and there are currently high external levels of particulates arising from the traffic. The number of these found inside is minimised by ensuring windows are kept closed and are well sealed. However these particulates are known to be very greasy and difficult to remove from upholstery. There are two ways in which this could lead to increased deterioration. The first being the particulate attracting moisture and enhancing the

moisture content of the silk. As higher humidities (and the presence of salt) have been shown to lead to greater silk deterioration, it is possible this may also enhance the rate of damage. The second possible method would arise from abrasion of the silk when cleaning to remove the particulates. However the M_w results show the silk at Apsley House is also in relatively good condition.

There are some interesting comparisons noted between the HPSEC results and the condition of the objects within the collection. There are eight samples with low M_w (below 150 kDa), which all come from samples identified as in poor condition. This includes silk velvet chair upholstery with missing pile and splits (nlran3) in Figure 9.5. Figure 9.6 shows deteriorated wall silk around a light switch (nlaps4) with exposed wefts revealing the padding material beneath. There were also samples from a highly deteriorated curtain (nlaeh7) and tieback (nlaeh9) in store at Audley End House, as well as seat pads (nlran5 and nlran6), bedspread fringing (nlosb11) and an almost completely disintegrated silk cabinet front (nlful9) at Brodsworth Hall (see Figure 9.7). Although these samples do not come from the oldest artefacts in the collections, in fact most of the samples come from 19th century objects. The poor condition of the silk on these objects may be a result of processing techniques used, rather than the age of the material.

Figure 9.5 – chair seat (nlran3) showing missing silk velvet pile

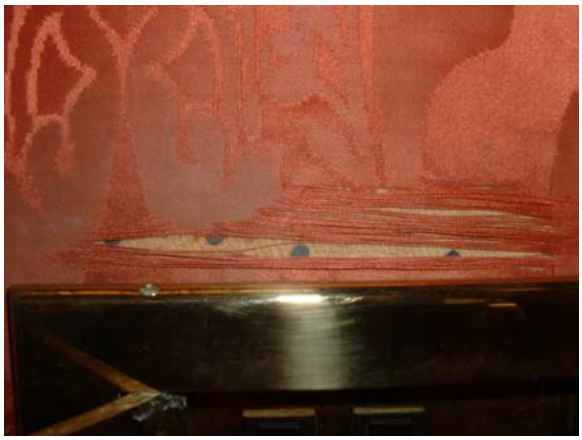

Figure 9.6 – deteriorated wall silk in the Waterloo Gallery at Apsley House

A number of the highest molecular weight samples (M_w greater than 400 kDa) seem to come from samples which visually appeared deteriorated. The most noticeably deteriorated examples were fragments from the portiere curtains (nlbro14 and nlbro18) and shattered wall silk (nlbro2) at Brodsworth Hall, in Figure 9.8. There was also a sample of wall silk from the Waterloo Gallery at Apsley House (nlaps3), which is in stark contrast to the sample, nlaps4, which had one of the lowest molecular weights. For a number of the samples giving exceptionally high M_w the sample size was very small and formed bumps in the baseline. This seems to affect the determination of the peak area and therefore the molecular weight. So although the HPSEC results can highlight some of the most deteriorated samples with low M_w values, there are also samples which were deteriorated but give high M_w values, demonstrating the limited interpretation of the results.

Figure 9.7 – silk fronted cabinet [90006945] at Brodsworth Hall

Figure 9.8 – wall silk in the South Hall at Brodsworth Hall

Figure 9.9 shows the Napoleonic standard which was sampled for the red thread, the area of previous damage where the sample was removed from can be seen at the top right corner. There are a large number of these Napoleonic standards at Apsley House and the condition reports for most of them say they are in poor condition. However this seems to arise from the fading of the standards, as seen in the turned over corner of Figure 9.9, and the heavy tarnishing of the silver

threads. Despite the condition report comments the standards were very difficult to sample due to the good condition of the silk, with the exception of the area of damage shown.

Figure 9.9 – L'Empereur Napoleon au Department de L'Orme tricolor [WM.1654N-1948] from Apsley House

Although it was only possible to take one sample of each colour from the standards, the HPSEC results for these samples all gave M_w results greater than 250 kDa. This shows, in contrast to the reported condition of the object, the silk was actually in good condition, as observed when sampling. This shows an interesting aspect of conservation reports: the object is described as being in poor condition due to fading of the textile, regardless of the actual condition of the substrate. When explaining this research it has often been necessary to highlight the difference in the reactions occurring. Although light is known to cause fading of textiles that does not necessarily mean the silk substrate is also being damaged. In reassessing the causes of silk deterioration, fading reactions have been omitted by using undyed plain silk allowing the changes to the silk to be studied in isolation.

Of the samples with the lowest molecular weights, only one has had major conservation intervention. The matching cabinets at Brodsworth Hall in the library and north corridor have both been conserved and the remaining silk is now held in place by a net layer between the silk and brass grill. The sample from these cabinets (nlful9) was a fragment removed during this conservation process. The curtain and tieback (nlaeh7 and nlaeh9) from Audley End House are kept in storage due to their poor condition. However the other objects with the lowest measured molecular weights are on display and might be suitable for future interventive conservation.

For the samples with high molecular weights some of these samples had been removed during conservation, for example the portiere curtains (nlbro14 and nlbro18) and the removed section of silk from the library fire-screen (nlaeh12). Some other objects had been conserved (nlbro2 from wall silk at Brodsworth Hall) or were in storage due to their poor condition (nlosb14). It is possible the small size of these samples and the associated problems with the processing software mean these have been wrongly assigned high molecular weights. The oldest sample, from a 14th century reliquary bag on display at Ranger's House, had a high molecular weight, although this was also difficult to sample due to the good

condition of the silk. The results indicate that processing techniques used to treat the silks may affect the condition to a greater extent than the date of the object.

Comparison of Results with Published Data

The results from the English Heritage collection have been compared with those published from the MODHT project. As mentioned above the historic samples analysed for MODHT were much more deteriorated than the artificially light aged samples. For the historic samples M_w values in the region of 10 – 40 kDa are reported compared with 40 – 90 kDa for the artificial aged samples. In comparison the English Heritage historic samples are generally between 150 – 250 kDa and the Burrell tapestry samples were around 175 – 225 kDa. There is obviously a large difference in the scale of the results between the analysis performed for this research and that undertaken for MODHT.

There is also an obvious reason for the large difference in the scale of results from the two projects. The calibration for MODHT reports fully dissociated protein standards and so the molecular weights included in the calibration files are significantly lower than those used for this research. As the same sample has not been run on each system it is not possible to determine whether the same molecular weight would be determined regardless of the difference in the calibration files. For example unaged silk had M_w values around ~200 kDa in the thermally aged experiments and this may also be the value found using the MODHT HPSEC system. However if the calibration file is significantly different but the retention time is similar between the two systems then the unaged sample may give M_w values closer to 100 kDa.

A further difference between the two systems is the best fit curves used for the standards' molecular weights, used to determine the calibration. For the system used in this research a quadratic curve was used throughout, however MODHT tended to use a cubic line of best fit. This often gives better R^2 values, indicating a

better fit of the variation of the data, however there are only five data points in the calibration file. For this reason it was recommended by the software engineer that the highest order curve used should be a quadratic equation,[3] unless further data points were included.

The SEC set up calibration file (for the method silk251108) can be seen in Figure 9.10, which shows the quadratic line of best fit through the data points. The value for blue dextran is recorded (see table in Figure 9.10) but this point is not used (empty red square in graph) to determine the molecular weight as the sample is totally excluded by the column. This also shows the overlap between β-amylase (molecular weight of 200 kDa) and albumin (198 kDa) in the graph and with the same retention time in the table. As only five data points are available, to avoid overfitting the data and therefore affecting the calculated molecular weights, quadratic equations were used for the calibration. This is likely to affect how the different software calculates the molecular weight of samples.

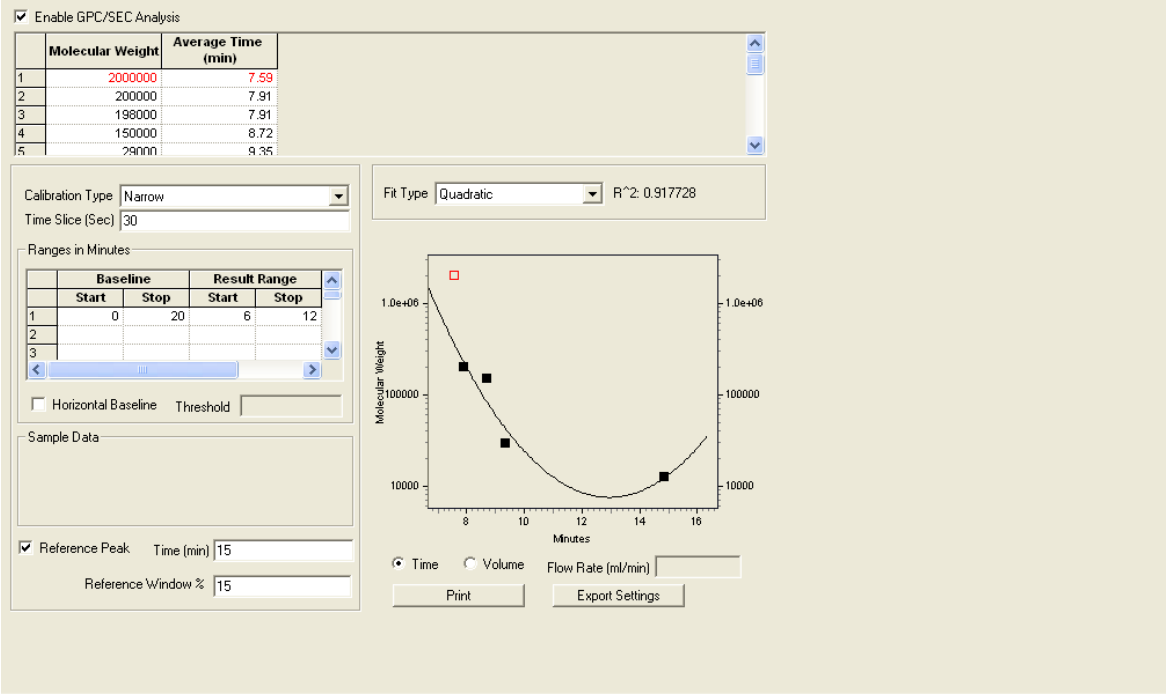

Figure 9.10 – SEC set up calibration

The two HPSEC systems have used the same columns, column oven temperature, detector wavelength and eluents as well as preparing the silk samples using the same method. Therefore the reason why one system would fully dissociate the calibration standards (which also came from the same source), and the other system records the oligomers, is unclear. However the dynamic light scattering (DLS) experiments (chapter five) confirmed globular, undissociated proteins are observed on the HPSEC system used for this research. It is probable that the HPSEC set up is system specific, particularly as both the HPLC and software used for this project came from different manufacturers to those used in the MODHT research.

Comparison of Results with Ageing Experiments

Figure 9.11 compares the HPSEC results for the historic samples (red, orange and yellow) with the light (green) and thermal (blue) accelerated ageing results. The M_w of the majority of the historic samples is between those recorded for the light and thermally aged samples. Generally the light aged samples are ~200 kDa higher in molecular weight than the thermally aged samples. The difference between the samples possibly arises from the use of different columns to analyse the data sets.

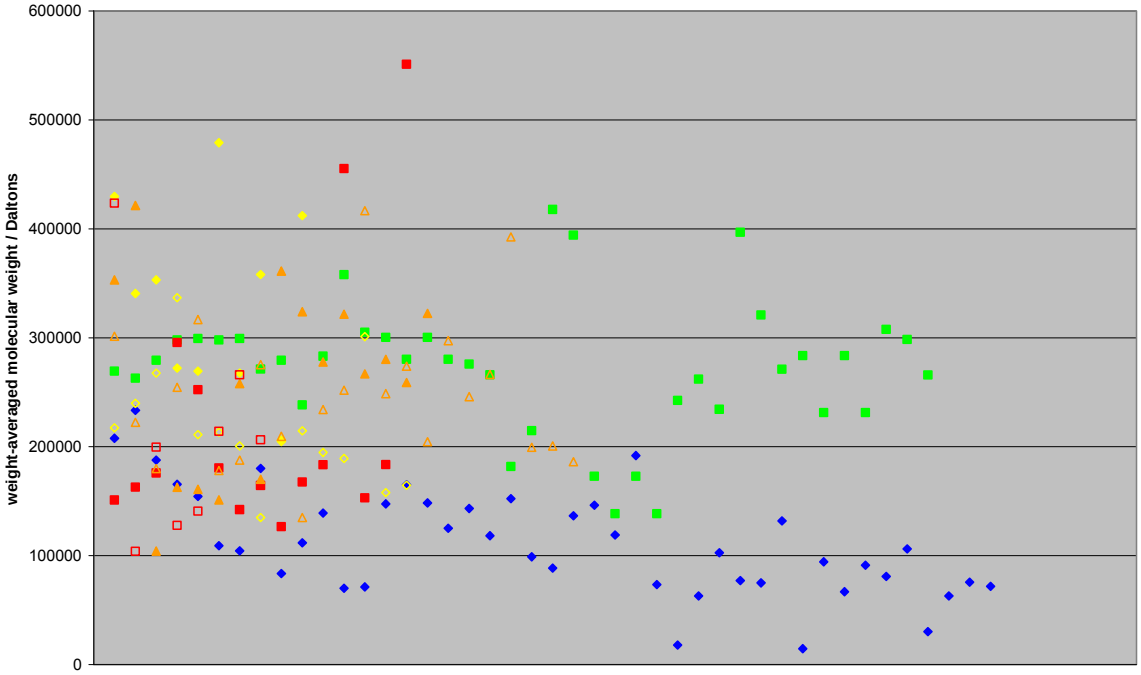

Figure 9.11 – M_w comparison of English Heritage and accelerated ageing samples x axis is number of samples (thermal ageing: blue ♦; light ageing: green ■; Audley End House: red ■; Apsley House: orange ▲; Brodsworth Hall: yellow ♦; Fulford Store: yellow ◊; Osborne House: orange Δ; Ranger's House: red □)

The first column was used to analyse the English Heritage historic samples and those taken from the Burrell tapestry, as well as the initial kinetics experiments. The second column analysed the light accelerated ageing samples with a small number of the rerun English Heritage samples and some kinetics samples aged at 50 °C. The final column was used to analyse the remaining kinetics samples and the thermally aged samples. When the columns are compared there are some differences but the majority of samples fall within the same 100 kDa to 400 kDa range. The only samples that are noticeably outside this are the thermally aged samples, a large number of which are below 100 kDa. However the kinetics samples analysed afterwards are above 100 kDa which implies the columns are similar in performance.

A large number of the thermally aged samples have lower molecular weights than the historic samples. Although there is a possibility this arises from the different columns used to analyse the samples, it is unlikely. Therefore this result implies the thermal accelerated ageing has led to a significant increase in the rate of silk deterioration. Most of the historic silk samples taken from the English Heritage collection are over 100 years old. This suggests the thermal accelerated ageing has led to a far greater increase in the rate than the 33 times predicted by the kinetics study. However to confirm this would require further research in to the kinetics of silk deterioration.

Conclusions

Although HPSEC is a destructive technique, the samples required are very small (< 0.5 mg) in comparison to other techniques. However the smallest micro-samples (< 0.1 mg) gave such small absorbance peaks in the HPSEC detector that the software struggled to place a baseline, which affected the peak area and therefore the calculation of the molecular weight. HPSEC can provide information on the condition of silk, but is probably most useful to compare a number of similar coloured samples from a large object (e.g. tapestries) or to compare sets of objects such as chair upholstery.

As discussed above (and in chapter eight) the HPSEC results are influenced by the equipment set up and performance. There are also limitations when trying to compare large numbers of samples which have been run in different batches as the molecular weight values are often not comparable in scale, despite calibrating the column. The differences in the calibration used for this research, and for MODHT have also been discussed and the changes mean the results cannot be compared. This highlights that the results of HPSEC for silk are system specific.

Analysis of the English Heritage micro-samples has shown these have similar molecular weights to the artificially aged samples. The thermally accelerated

ageing samples had lower molecular weights than the majority of the historic samples which implies the rate of silk deterioration has been increased more than the 33 times suggested from the kinetics study. The results indicate humidity is more important than has previously been thought for silk deterioration reactions. The effect on the English Heritage collection, and other collections' silk artefacts, and methods to reduce the rate of deterioration is discussed further in chapter ten.

References

[1] Hallett, K. and Howell, D., (2005), 'Size exclusion chromatography of silk: inferring the textile strength and assessing the condition of historic tapestries' in *ICOM Committee for Conservation 14th Triennial Meeting, The Hague, 12-16th September 2005 Preprints* Verger, I. (ed.) London: James & James Ltd **2** 911-919.

[2] Harris, M. and Jessup, D. A. (1934) 'The Effect of pH on the Photochemical Decomposition of Silk' *Bureau of Standards Journal of Research* **7** 1179-1184.

[3] Mitchell, S. personal communication, 23/07/2007.

Chapter 10 – Application of Results to Preventive Conservation

The critical factors for silk deterioration, based on the experimental results have been identified and are presented in this chapter. The mitigation of these conditions along with the impact on other artefacts on display in conjunction with silk are discussed. The results have been used to make a number of preventive conservation recommendations. An overview of the use of lifetimes in conservation is presented with the determination of an end point for silk based on the experiments undertaken. The end point has been used to create a silk deterioration curve and isoperms for silk degradation and case study objects are considered to demonstrate how these tools might be used by conservators.

The accelerated ageing results revealed UV radiation increases the silk deterioration caused by light ageing. However in comparison to the thermal ageing the silk is relatively unchanged by light ageing. The thermal ageing experiments demonstrated that increasing humidity levels dramatically increases the rate of silk deterioration. The presence of salt on the silk samples further increased the deterioration seen, particularly for samples aged at 30% RH. These results can be used to make suggestions for improved preventive conservation to increase the longevity of silk on display in historic houses.

As well as optimising the preventive conservation it is also desirable to quantify the magnitude of the improvements that might be possible. An understanding of how much improvement could be achieved, may help justify additional resources to improve the preventive conservation and display environments. By linking the current condition of the silk, and its approximate age, with the accelerated ageing

results it may be possible to determine the size of possible improvements with changes to the display. The limitations of the HPSEC results, as already discussed, may reduce the possibility to predict the condition for the micro-samples. However correlation between the results will be tentatively made to suggest the possible applications of the experimental results presented so far.

Critical Factors for Silk Deterioration

The accelerated ageing results indicate that humidity is more important for silk deterioration than previously thought. Light has generally been identified as the most important factor for silk deterioration.[1,2,3] For preventive conservation in historic houses where silk is displayed this means light levels are controlled to limit exposure to a maximum of 50 lux. This is most commonly done using an annual cumulative exposure, applying the reciprocal principle,[4] as it is difficult to reduce natural light levels to 50 lux. However as well as being difficult to achieve within historic houses, low light levels also make it difficult to view detail and colour differences on objects, particularly for older visitors.[5] Comments from visitors frequently refer to the darkness of the displays and so increasing light levels would also improve the visitor experience.

One of the probable reasons light has been reported as the most deteriorating factor for silk, is the fading of textiles. Light has been shown to cause fading of dyes,[6,7] and so control of light levels is still required. Further research might look at the rate of fading for textiles which have already suffered extensive light exposure and have faded considerably. In these cases any further changes in colour may be negligible with increased light exposure, which might enable increased display light levels if the silk substrate will not be damaged. The accelerated ageing results have shown there is little difference in the rate of silk deterioration between samples aged at 50 lux and those aged at 200 lux. Therefore increases in the display light levels are unlikely to cause a great change to the rate of silk deterioration. The research has shown UV radiation further

increased silk deterioration, which has also been reported in the literature.[8] This highlights the benefits of UV absorbing film currently used on the windows within the historic houses studied.

There are a number of complicating factors which may prevent changes to RH levels from occurring or limit the extent to which it can be applied. Historic house displays nearly always contain mixed materials within the same room, showing the house as it would have been (or is perceived to have been) when lived in. This affects how the display environment can be controlled as there are often a number of materials for which the ideal display environment is different to those of the other objects. Therefore the environmental parameters can be a compromise of all the different objects' specifications. Before any potential changes can be made to the display conditions, it is necessary to consider the impact this would have on the rest of the collection. This is also true of light; however the silk textiles are often identified as the most light-sensitive objects within a display.

Within the rest of the collection items which are thought to be particularly susceptible to low RH levels include wood, especially veneers and marquetry. Within historic houses furniture can form a large part of the collections and changes can be particularly visible as lifting veneers create cracks or missing areas of decoration. However for a large number of materials common to both museum and historic house collections, there has been little research on the optimal environmental conditions for display. Many organic materials are susceptible to mould growth and display below 70% RH is recommended to prevent mould.[9] Therefore very high RH levels are often mitigated, although there is little knowledge on whether mould can reoccur on objects at lower RH levels if previous damage has taken place.

The most comprehensive studies on the effects of humidity have been research on metals.[10,11,12,13] Generally these studies find low RH levels are optimal to prevent corrosion and for some displays (such as individual cases of archaeological iron) it

can be possible to maintain these environments. However the lack of research on the impact of humidity for most materials within collections limits the ability to decide on the best display environment. So although this research has indicated high humidity levels are most damaging for silk, further work would be needed to understand the impact of humidity on other materials. Traditionally the middle RH region from 50% to 65% RH has been suggested as most suitable for the display of organic objects.[14] Interestingly as more organic materials are studied the benefits of lower RH environments is becoming clearer, for discussion see Michalski.[15] Further work is required to understand whether embrittlement at low RH levels occurs for a range of organic materials. However the change in moisture content of silk is reported to be small between 35% and 55% RH,[16] with a rapid decrease below 30% RH. Therefore above 30% RH the embrittlement of silk is unlikely to be a problem.

A further limitation on the reduction of RH levels is the buildings themselves. Within the historic houses studied the temperature is usually used to control the humidity. This is particularly apparent in the winter when the low RH levels lead to low temperatures, as heating further dries out the air. In the summer the RH is usually high but as the temperature is already high, it cannot usually be increased to dry the air. Some properties, such as Ranger's House are using cooling equipment in the summer due to the high temperatures. However lowering the temperature will further increase the RH unless dehumidification also occurs. The use of increased temperatures to reduce the humidity could be problematic as the low activation energy for silk deterioration (determined in chapter six) indicates that the rate of deterioration doubles with a 10 °C increase in temperature. Therefore increases in temperature would increase the deterioration even if the humidity is decreased. This has also been reported for some other organic materials with similar activation energies, such as amorphous polyester, by Michalski.

In some properties the humidity is increased in winter using additional humidifiers or reduced in summer with dehumidifiers. However aesthetically these can look

out of place within historic interiors and are often resisted by curators. There can be further impacts on the building from using humidifiers or dehumidifiers. For example Mecklenburg demonstrated that additional humidification at Smithsonian Institution's Hirshhorn Museum led to moisture condensing in the masonry at low external temperatures.[17] This can have further implications for salt movement and could lead to efflorescence which may further deteriorate textiles on display. Humidity control often requires consultation with buildings managers and engineers to ensure damage is not being created by adding or removing additional moisture.

Monitoring behind tapestries at English Heritage recorded higher humidity microclimates, especially when placed against colder external walls. As higher humidity levels have been shown to accelerate silk deterioration the mitigation of these microclimates is likely to be beneficial to the longevity of the textile. When displaying large scale textiles it may be useful to include thermal buffering layers behind to reduce the temperature difference and therefore minimise the RH levels and variation. Alternatively barrier layers may be considered, these would also prevent salt migration into textiles should salt efflorescence occur. Large textiles could be placed on internal walls, were the temperature difference is likely to be less. However, the positioning of objects within properties is often limited by the size or historic location of an artefact. Therefore the possibility to change the position of an object based on the optimal display environment is decreased.

Preventive Conservation Recommendations

From the research undertaken for this project, the following preventive conservation recommendations can be made:

1. Reduce RH levels (to a minimum of 30%, as less deterioration was observed below 50% RH)
2. Reduce temperature (10 °C decrease doubles lifetime)
3. Remove UV radiation from all light sources

4. Faded silk textiles can be displayed above 50 lux if the dye is unlikely to fade further
5. Mitigate high humidity microclimates behind large scale textiles (such as tapestries)
6. Prevent salt contamination of textiles (for example from efflorescence)

Use of Lifetimes in Conservation

Within collections the age of an object is often known, but its condition and how much longer it can be displayed can be unclear. These details can inform decisions on changes to the display environments and help prioritise interventive conservation treatments. In recent years the use of object lifetimes has become more common within conservation.[18,19,20] The lifetime of an object normally refers to the length of time which it can be displayed for, or used, e.g. documents in archives, or the length of time a coating provides protection to an object. Although given numerical values this is a method of ranking the condition of an object, or performance of a coating, rather than an absolute figure for the lifetime.

Using lifetime values as a guide can provide comparisons between objects to prioritise treatments or between environments to select the most suitable storage or display rooms. This reflects the dual nature of lifetimes, as they are usually predicted from ageing experiments on model materials based on display conditions. Within collections the display environment rather than the object is monitored and this is used to make predictions on the object's lifetime. Often these predictions are based on different materials to those of the objects being studied. For example Climate Notebook® calculates the Time-Weighted Preservation Index (TWPI) based on environmental monitoring data, using the experimentally measured response of cellulose acetate film to different environments.

The benefit of lifetimes is they provide a measure of the deterioration. However the accuracy of the predictions can be reduced as they are often based on the

response of different materials. The lifetime predictions for a variety of materials could be improved by including further data for the environmental effects on deterioration, but research is this area is limited. A further use of this concept is isoperms which are lines of equal permanence at different environmental conditions. Initially developed by Sebera for paper,[21] the change in permanence at different environmental conditions could be compared. Sebera's paper isoperms use an arbitrary value of 1 for the permanence at 21 °C and 50% RH. The plot then shows the increase in the deterioration rate (as a decrease in the permanence) or vice versa with the lines of equal permanence. However isoperms are limited to the effects of temperature and humidity on the lifetime of an object and do not include any data on the effects of light ageing or pollutants.

Sebera's isoperms were plotted from theory as the experimental data required was unavailable. However improvements in the understanding of paper deterioration have led to criticism of the original isoperms.[22] For paper a number of factors including the original source of the cellulose and other additives or contaminants present can also have an effect on the predicted lifetime. Isoperms have also been determined for cellulose acetate, which have been plotted from experimental data. Instead of using a permanence value of 1, these isoperms use the predicted time in years for triacetate film to reach 0.5 acidity at constant conditions[a]. In this case the end point is reached after 50 years at 20 °C and 45% RH.[23] The change in permanence is recorded as the increase in time to reach this end point. For a number of ageing studies on film the end points relate to the end of a useful lifetime, i.e. when the film can no longer be used in a projector. There are a large number of possible measures of deterioration used in these studies, which all give different projected end points.[24] However each measure provides similar comparisons of the effect of conditions on the lifetime of objects.

[a] 0.5 acidity is the point at which triacetate film deterioration becomes autocatalytic and is reported as base acidity mL 0.1N NaOH/g, which is determined by dissolving 1 g of the film in a methylene chloride-ethyl alcohol mixture and titrating the solution with 0.1 N sodium hydroxide with an indicator

For the TWPI the end point for acetate film is used, similar to the acetate isoperms the preservation index (PI) equals 50 years for display at 20 °C and 45% RH. At each data interval for the environmental monitoring the PI is calculated (see Figure 10.1). This is then weighted across the time interval to take into consideration the greater deterioration occurring under higher temperature and higher humidity conditions compared to better display environments. Figure 10.1 shows how seasonal changes in display conditions at Audley End House affect the TWPI values, demonstrating that cooler, drier conditions are preferable (higher TWPI values) as this increases the predicted lifetime for cellulose acetate film. Figure 10.2 shows the simple comparison of each room as a bar chart, with a guide to the ageing rate on the left y axis. This indicates the majority of ground floor rooms at Audley End House have a moderate ageing rate.

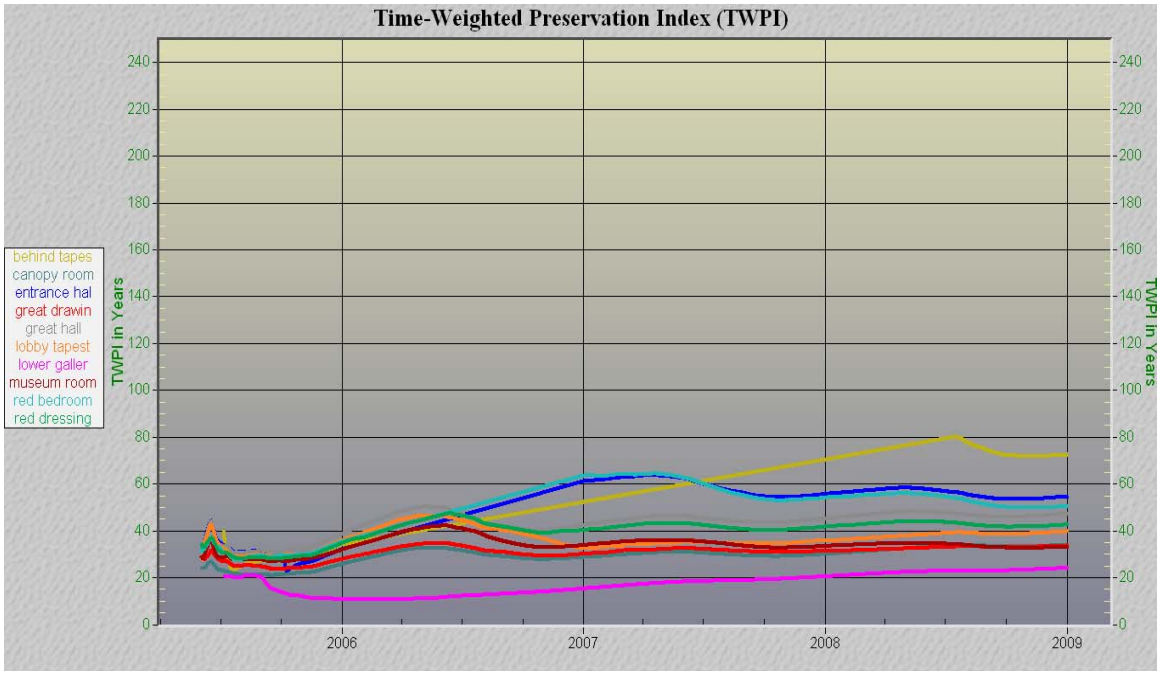

Figure 10.1 – seasonal fluctuations in the TWPI value for ground floor rooms at Audley End House

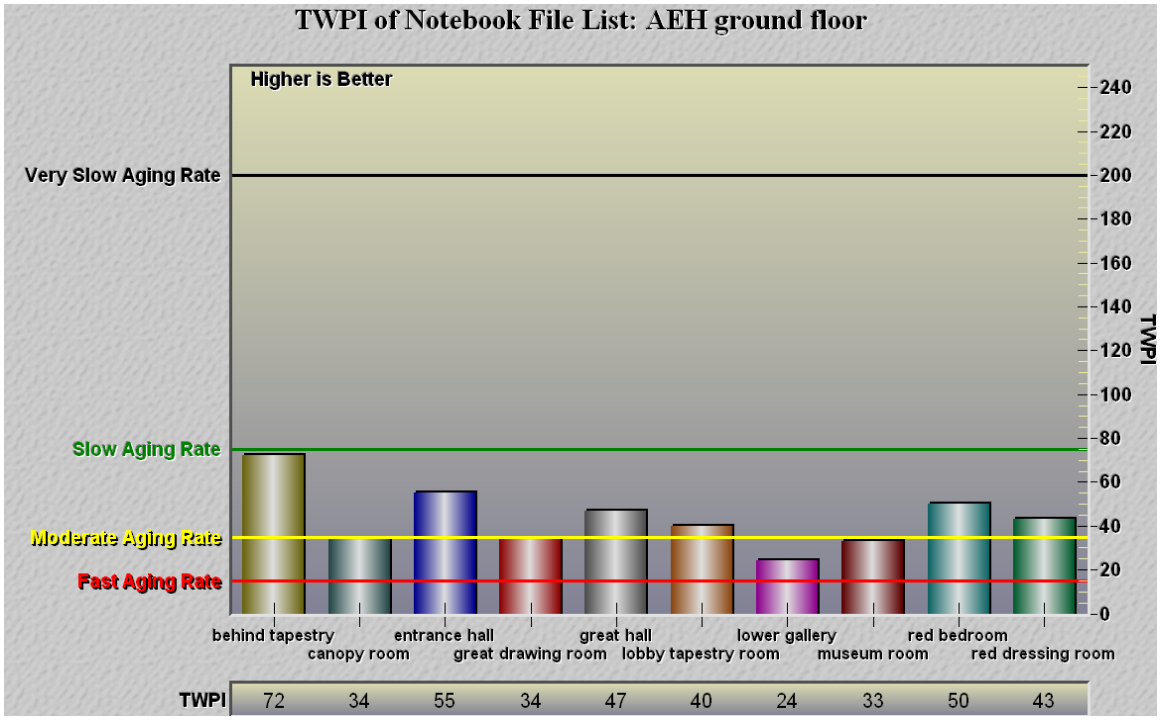

Figure 10.2 – TWPI values for the ground floor rooms at Audley End House

In comparing the display environments in English Heritage (chapter two) the TWPI for each property was determined. Although there was little difference between the properties Brodsworth Hall (TWPI = 50.7) had a marginally higher value than Ranger's House (TWPI = 50.3) with Apsley House (TWPI = 45.4) and Audley End House (TWPI = 45.5) the lowest. The highest TWPI value at Brodsworth Hall matches the slightly higher HPSEC results for the historic micro-samples taken from this property. Similar to the TWPI values there is little difference between the HPSEC results for samples taken from each property.

Although there have not been exact predictions of the end point for silk's display lifetime there are some indications within the literature. For example France suggests "The end of the useful life of a textile usually relates to the loss of mechanical properties associated with its function".[25] For example, the end point for tapestries might occur when it can no longer support its own weight. However the point at which these failures occur were not specified. Recent work on tapestries has indicated a correlation between the elongation of the sample and its

weight-averaged molecular weight (M_w). This indicates the samples had no elongation at approximately 15,000 Daltons.[26] Work by Richardson and Garside used the elastic limit of silk as a measure of damage.[27] These form useful starting points to consider when deciding the end point for the experiments in this research.

Determining the End Point

To calculate a lifetime, and use it as a measure for the possible improvements with changes to the display environment, an end point for silk is required. In reality for objects on display there is likely to be an aesthetic, as well as a condition assessment for the lifetime end point. However the aesthetic impact is difficult to gauge for the accelerated ageing samples as they were plain silk. Although this yellows (as seen in chapter seven) the fading of dyes is likely to influence the perception of objects' display lifetime more than the initial silk deterioration. With further silk deterioration and the appearance of splits in the fabric, the appearance of the substrate silk is likely to become more important. The choice of an end point is also complicated by the type of object. For example a reproduction wall silk, even if over 50 years old, is likely to be removed and replaced if in poor condition. But a silk object, such as a dress of the same period, would be preserved even if the silk was in a poor condition.

The end point was selected using both the accelerated ageing results and the age of the sampled artefacts in the English Heritage collection. To understand the correlation between the accelerated ageing results M_w was plotted against the maximum load (see Figure 10.3). This shows there is little change in the tensile strength of the samples after light ageing (green and aqua data points) but there is an increase in M_w as reported in chapter eight. In comparison the thermally aged samples (blue data points) show a dramatic decrease in tensile strength with decreasing M_w.

An approximate (R^2 = 0.64) logarithmic curve can be fitted through all the data points which bisects the x axis at 30 kDa. However the end point is likely to occur before the tensile strength has completely diminished. Results from MODHT indicated at zero elongation M_w would equal 15 kDa, compared to 30 kDa reported here. However as reported in chapter nine the results from this research and MODHT are not directly comparable due to the difference in calibration files. This means the molecular weight results from MODHT are much lower in scale, as seen for the value at zero elongation.

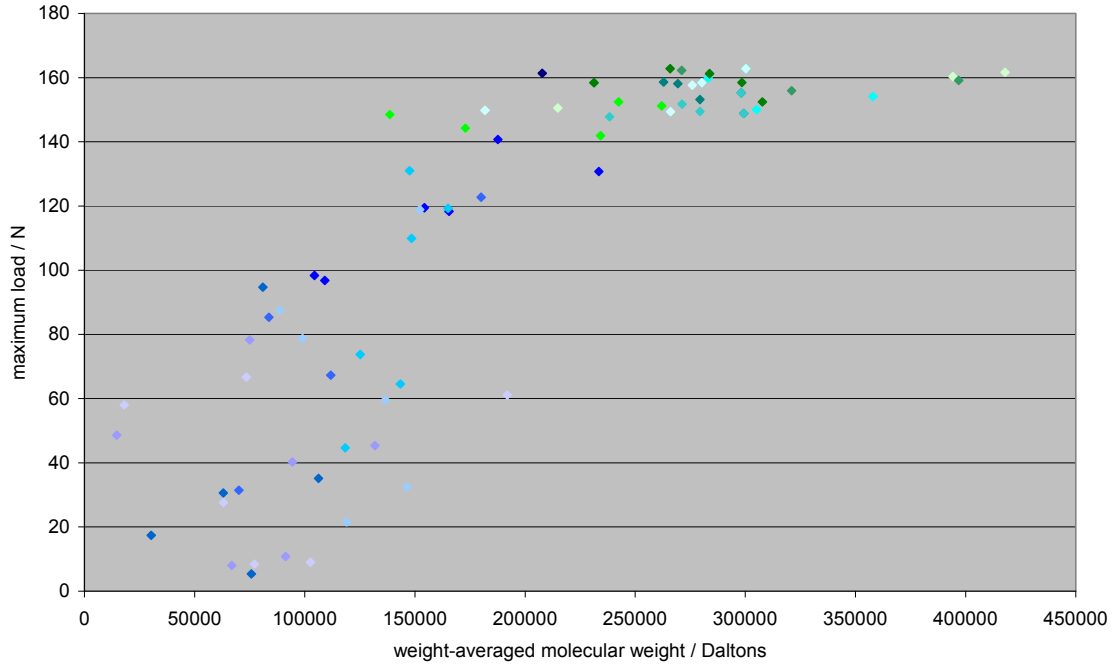

Figure 10.3 – weight-averaged molecular weight and tensile strength results for accelerated ageing samples (unaged: dark blue; 0% RH: blue; 30% RH: mid blue; 40% RH: light blue; 50% RH: pale blue; 60% RH: ice blue; 75% RH: periwinkle blue; 100% RH: cornflower blue; 30L50l: dark aqua; 30L200l: aqua; 50L50l: turquoise; 50L200l: light aqua; 50UV50l: light green; 50UV200l: bright green; 75L50l: mid green; 75L200l: green)

Silk objects are likely to require some strength to remain on display, even if a low strength becomes an indication that interventive conservation treatment is

required. Therefore an end point of 0 N seemed unrealistic. When handling the accelerated ageing samples for analysis, those with tensile strength results below 40 N were often very deteriorated and difficult to test without damaging. Therefore 40 N was selected as the end point; from the approximate curve fitted to the data in Figure 10.3 this gives an M_w of ~50 kDa.

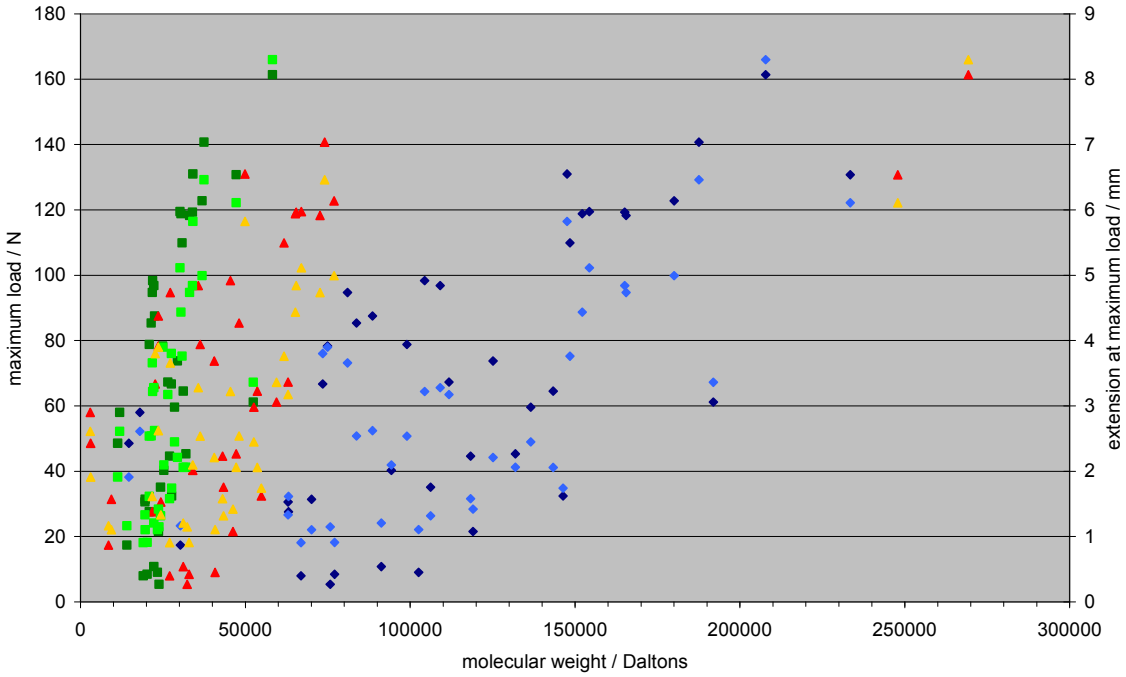

Figure 10.4 – comparison of accelerated ageing HPSEC and tensile testing results (M_w load: dark blue ♦; M_n load: dark green ■; M_p load: red ▲; M_w extension: blue ♦; M_n extension: green ■; M_p extension: orange ▲)

To understand how these end point values related to the other accelerated ageing results, the various measures of molecular weight were plotted against the tensile strength and extension at break values for the thermal ageing samples (see Figure 10.4). It can be seen a tensile strength of 40 N is approximately equal to an extension at break of 2 mm. In comparison at 40 N, M_n is approximately 30 kDa and M_p is around 40 kDa. Having a range of measures as the end point for silk on

display allows research using measures other than M_w and tensile strength to be compared with these results in the future.

From the accelerated ageing experimental results, an end point of 40 N and ~50 kDa had been selected. However how long might a silk on open display last and what condition, or molecular weight, would be expected? To answer this question the age of each historic micro-sample and the HPSEC results were plotted, see Figure 10.5. The accelerated ageing samples and their equivalent display time were also included for comparison. Approximate ages of the micro-samples have been determined based on the object records. The records often state a rather wide date range, for example, second quarter of the 19th century. In order to plot Figure 10.5 a single mid-point was selected for these data ranges, so for the example given the date would be 1837 and the age would be 172 years.

As previously discussed, the M_w of the English Heritage micro-samples have higher values than the majority of the thermally accelerated ageing samples. This can be clearly seen in comparing the blue and green data points for the accelerated ageing samples with the red, orange and yellow points for the historic samples in Figure 10.5. Along with the analytical end point values, it is useful to have an approximate display lifetime of an object. This gives an easily understood measure with which to compare how changes to the display environment might affect the display lifetime of an object, either increasing or decreasing it. This can then be used to make informed decisions about changes to the display conditions.

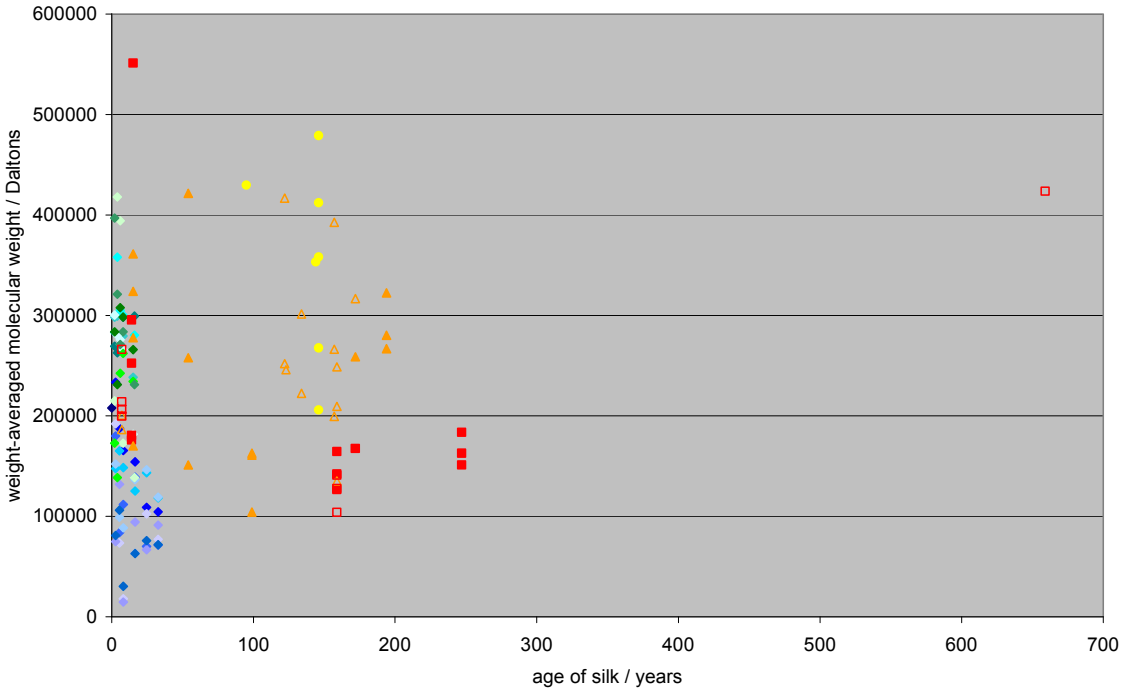

Figure 10.5 – age of English Heritage micro-samples against HPSEC results (unaged: dark blue; 0% RH: blue; 30% RH: mid blue; 40% RH: light blue; 50% RH: pale blue; 60% RH: ice blue; 75% RH: periwinkle blue; 100% RH: cornflower blue; 30L50l: dark aqua; 30L200l: aqua; 50L50l: turquoise; 50L200l: light aqua; 50UV50l: light green; 50UV200l: bright green; 75L50l: mid green; 75L200l: green; Audley End House: red ■; Apsley House: orange ▲; Brodsworth Hall: yellow ♦; Fulford Store: yellow ◊; Osborne House: orange Δ; Ranger's House: red □)

To determine the end point, in terms of display lifetime, the age of the English Heritage collection was used. This value would then be compared with the analytically determined values. With the exception of the reliquary bag from the Wernher Collection at Ranger's House (~650 years), there are no samples beyond 250 years in Figure 10.5. The age of the samples is approximate however despite this Figure 10.5 indicated a suitable end point in terms of display lifetime was 250 years. Although the historic samples, even after 250 years, have higher M_w values than 50 kDa, this value seemed to best relate to the collections age.

This gave three values as measures of the end point for silk on open display. As the majority of experimental results have given exponential decay curves this was used to relate the three values to each other. Figure 10.6 shows the theoretical deterioration curve with an unaged sample having a tensile strength of 160 N and M_w of 200 kDa. At the end point of 250 years the tensile strength has decreased to 40 N and the M_w to 50 kDa. The accelerated ageing results have then been overlaid on this curve (which can be seen in Figure 10.7) using the measured tensile strength values as the y values with the equation shown in Figure 10.6.

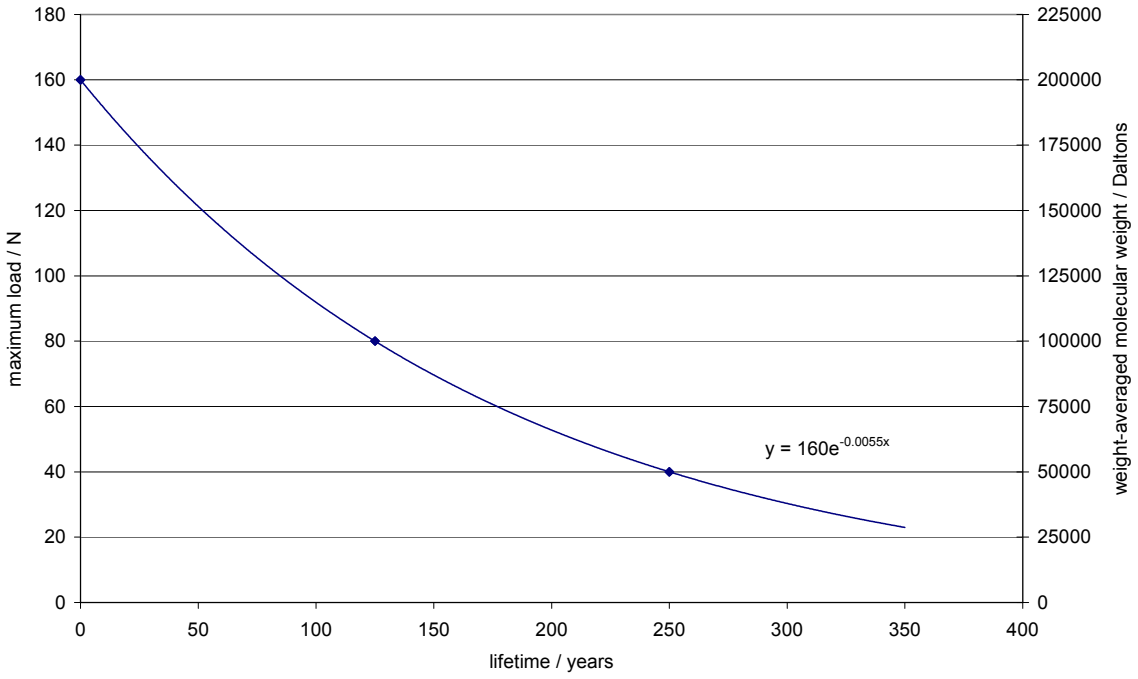

Figure 10.6 – theoretical silk deterioration curve

When the accelerated ageing data is overlaid on the theoretical silk deterioration curve (red data points in Figure 10.7) the light ageing data is clustered around 160 N. However the thermal ageing data points are spread along the deterioration curve, this would indicate the large variation in the deterioration caused during the ageing has led to a wide range of predicted display lifetimes. As the thermal ageing data points are not all located below 50 years display lifetime, Figure 10.7 indicates that the accelerated ageing has led to greater deterioration than the 33

times increase in rate predicted by the kinetics experiments. For the values below 40 N, giving predicted ages greater than 250 years, the samples have been aged at high humidity levels for long time intervals. This demonstrates how damaging high humidity might be, dramatically increasing the predicted display lifetime of the sample.

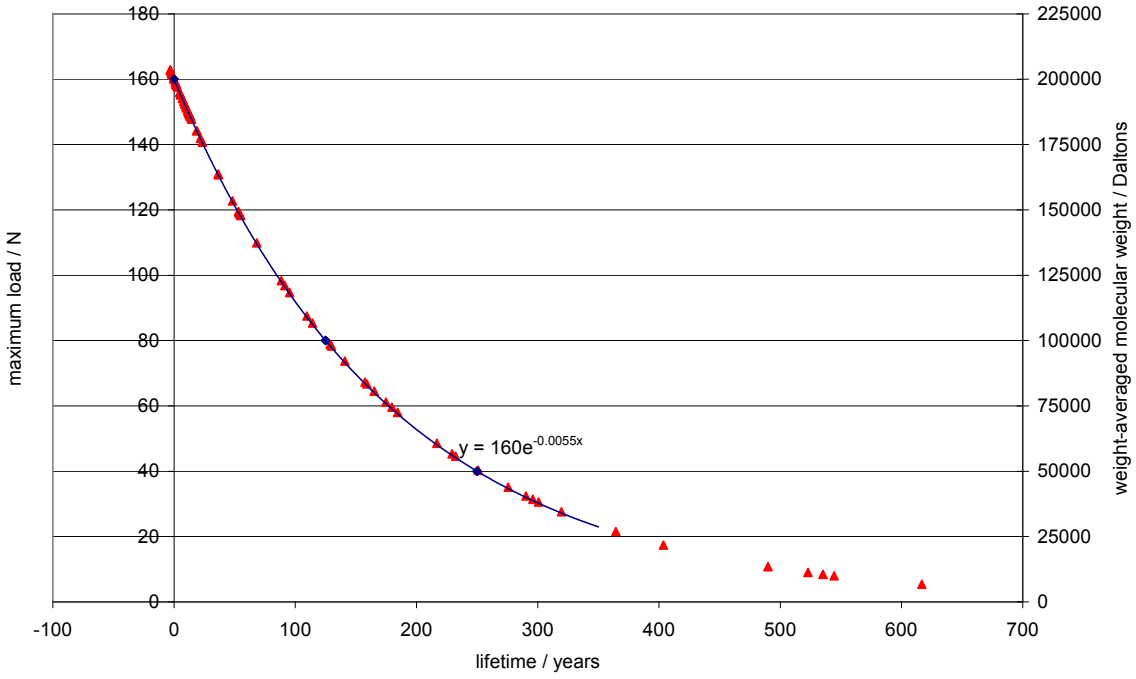

Figure 10.7 – accelerated ageing results overlaid on the silk deterioration curve

Although Figure 10.7 can be used to predict the display lifetime of the accelerated ageing samples, it does not convey how long a sample might be displayed for if the display environment is changed. The silk deterioration curve in Figures 10.6 and 10.7 can be used to map where a sample is in the ageing process and how long it might have remaining. The effect of changes to a sample on the ageing profile cannot be determined from this silk deterioration curve. In order to predict the effect of changing the display environment, the data has been used to plot isoperms for silk deterioration.

Isoperms can be used to plot the effect of changing environmental conditions on the deterioration of a material, here silk. Figure 10.8 plots the isoperms for silk deterioration using the data from the kinetics experiments (E_a = 50 kJ mol^{-1}) and the end point values so at 20 °C and 50% RH, silk will last approximately 250 years. The theoretical curve in Figures 10.6 and 10.7 is roughly approximate to the ageing curve labelled 250 years in Figure 10.8. Figure 10.8 has been plotted similar to Sebera's isoperms for paper using the theoretical equations. This assumes the effect of RH is the same at all temperatures however the data is limited for a full range of RH values at 80 °C only. Therefore Figure 10.8 is a first approximation and the true effect of RH on the rate of silk deterioration would require further investigation. Further experimental work could dramatically improve the understanding of silk deterioration at a wider range of temperature and humidity conditions and better predict the likely deterioration.

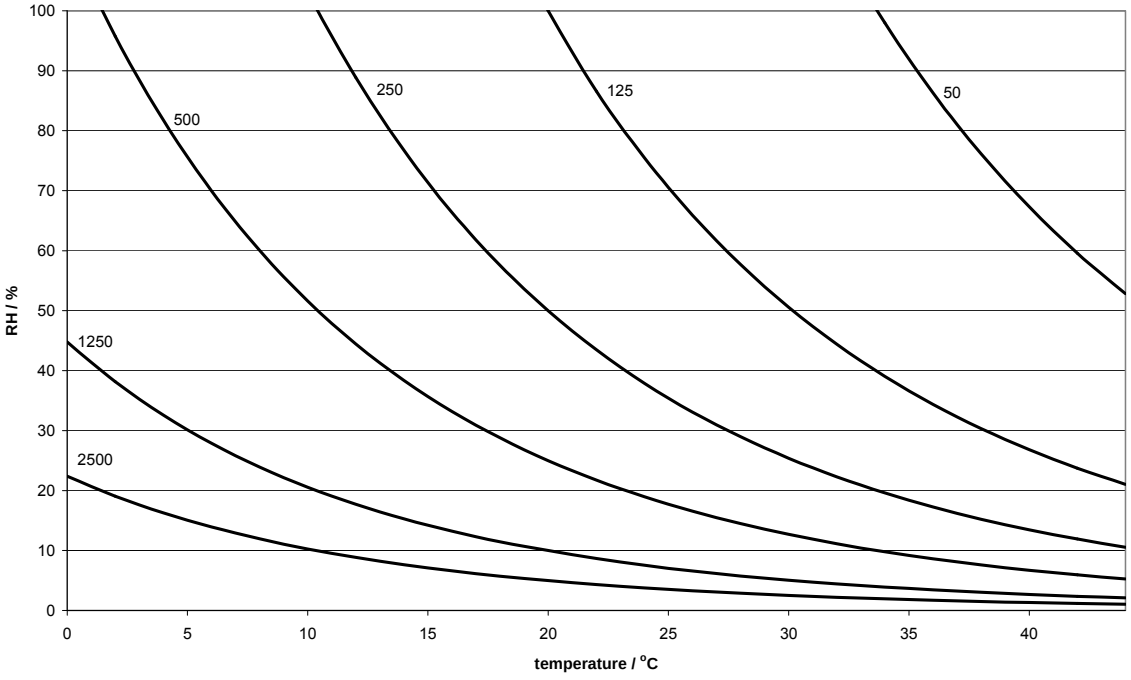

Figure 10.8 – isoperms for silk deterioration (predicted display lifetimes in years, are shown next to each isoperm)

As an example of how Figure 10.8 could be used, at 75% RH and 24 °C, the predicted lifetime for silk is 125 years. If the environmental display conditions are reduced to 50% RH and 20 °C the lifetime increases to 250 years. A further decrease to 35% RH and 15 °C would increase the lifetime to 500 years. This demonstrates a similar principle to the cycling of TWPI values between winter and summer conditions (see Figure 10.1). Higher summer temperatures and humidities are more damaging than low winter RH levels and temperatures.

Case Study Lifetimes

The theoretical silk deterioration curve in Figure 10.6 can be used with analytical results (either tensile strength or M_w) to estimate the display lifetime of the object. This can then be compared with the objects actual age to understand the impact of current display conditions. The effects of changes to the display conditions can be predicted from the isoperms in Figure 10.8 and used to demonstrate the effect on the display lifetime. Although the use of the HPSEC data is limited due to the challenges described in the previous chapters, to demonstrate the use of the isoperms, an object from the English Heritage collection sampled as part of this research has been included as an example.

Figure 10.9 shows the reproduction wall silk from the striped drawing room at Apsley House. This was installed in 1994 and so has been on display for 15 years, if a display lifetime under the current conditions of 250 years is used, this would imply a remaining 235 years on open display. Improvements to the display conditions to double the lifetime would then lead to a possible 470 years on display. The HPSEC results for the red silk from this linen silk weave (nlaps10) had an M_w of 170 kDa. This M_w would indicate approximately 135 N of tensile strength remaining, or from the line of best fit through the experimental data 114 N. This would imply the display lifetime of the sample is somewhere between 31 and 62 years rather than its actual age of 15 years. Staining of the wall silk can be seen in Figure 10.9, which may imply the silk has deteriorated faster than its actual

age would predict. Further work would be required to verify the HPSEC results and the condition of the silk. But the determination of the point at which a sample is on the silk deterioration curve could help inform decisions on display and give a further understanding of the effects of the current display environment.

Figure 10.9 – reproduction wall silk in Striped Drawing Room at Apsley House

The TWPI value for the Striped Drawing Room is 41 years, Apsley House is warmer with less variation (21 ± 4 °C) than most display environments studied during this research, it is also drier (40 ± 15% RH). Generally higher TWPI values are predicted if the temperature and humidity are lower. This is similar to the research presented here, which has indicated higher humidity levels and higher temperatures both lead to increased silk deterioration.

Conclusions

To reduce the rate of silk deterioration the following preventive conservation measures could be applied: reducing RH levels below 50% RH (to a minimum of 30% RH), reducing the temperature, excluding UV radiation from all light sources, mitigating high humidity microclimates behind large scale textiles and preventing salt contamination of silk artefacts. For silk objects, display at 200 lux rather than 50 lux is unlikely to damage the silk and may be appropriate for faded textiles where the dye is not likely to fade further.

From the experimental results a theoretical silk deterioration curve has been plotted which relates the age of the object to its tensile strength and molecular weight. Currently there are some problems with the use of this to predict the condition of the historic micro-samples due to the variability of the HPSEC data. However further work may allow this to more accurately predict the current condition of silk samples from analytical results. The theoretical silk deterioration curve has been further developed to plot isoperms for silk deterioration. This gives an indication of how analytical results can be applied within conservation to give useful tools for conservators. Unfortunately due to the limited data on the effect of RH at a variety of temperatures, this currently does not accurately reflect the impact of RH on silk deterioration. Isoperms are limited as they only include the effects of temperature and RH and the impact of light exposure or pollutants are excluded. Presently this is a limitation of the technique and currently there are few methods within preventive conservation that include both temperature and humidity and light or pollutant effects.

These preventive conservation tools have been developed using experimental results from the analysis of model materials. In order to use the theoretical silk deterioration curve to predict the condition of an object a micro-sample would be required to provide comparative data. However HPSEC is both an invasive and destructive technique, although requiring very small amounts of silk. It would be

preferable to have a means of comparison using a non-invasive and non-destructive technique to provide condition analysis for silk artefacts without sampling. The use of near-infrared (NIR) spectroscopy to provide this data is discussed and a model developed and tested in the next chapters.

References

[1] Tímár-Balázsy, A. and Eastop, D. (1998) 'Fibres' *Chemical Principles of Textile Conservation* Oxford: Butterworth-Heinemann 3-66.

[2] Tucker, P., Kerr, N. and Hersh, S. P. (1980) 'Photochemical Damage of Textiles' *Textiles and Museum Lighting* (The Harpers Ferry Regional Textile Group) December 4 & 5 1980, The Anderson House Museum, National Headquarters of the Society of the Cincinnati, 2118 Massachusetts Ave, NW Washington DC 20008, 23-40.

[3] Vigo, T. L. (1977) 'Preservation of Natural Textile Fibers – Historical Perspectives' in *Preservation of Paper and Textiles of Historic and Artistic Value* Williams, J. C. (ed.) Washington DC: American Chemical Society **164** 189-207.

[4] Thomson, G. (1986) *The Museum Environment* Oxford: Butterworth-Heinemann.

[5] Ashley-Smith, J. (1999) 'Light Entertainment' *Risk Assessment for Object Conservation* Oxford: Butterworth-Heinemann 226-245.

[6] Giles, C. H. and McKay, R. B. (1963) 'The lightfastness of dyes: a review' *Textile Research Journal* **33** 527-577.

[7] Egerton, G. S. (1948) 'Some Aspects of the Photochemical Degradation of Nylon, Silk, and Viscose Rayon' *Textile Research Journal* **18** 659-669.

[8] Tse, S. and Dupont, A.-L. (2001) 'Measuring silk deterioration by high-performance size-exclusion chromatography, viscometry and electrophoresis' in *Historic Textiles, Papers, and Polymers in Museums, ACS Symposium Series 779* Cardamone, J. and Baker, M. (ed.) Washington DC: American Chemical Society 98-114.

[9] Florian, M.-L. (1997) 'Environmental factors in museums and homes which influence germination and vegetative growth of fungi' *Heritage Eaters* London: James & James (Science Publishers) Ltd 125-132.

[10] Thickett, D. and Odlyha, M. (2005) 'Infra-red and Raman Spectroscopy of Iron Corrosion Products' *Proceedings of IRUG6, Florence* Piccollo, M. (ed.) 86-93.

[11] Watkinson, D. and Lewis, M. (2004) 'SS Great Britain iron hull: modelling corrosion to define storage relative humidity' *Preprints of Metal04, Canberra* Ashton, J. (ed.) 88-100.

[12] Scott, D. A. (1990) 'Bronze Disease: A critical review of some chemical problems and the role of relative humidity' *Journal of the American Institute of Conservation* **29** 193-206.

[13] Turgoose, S. (1982) 'Post-excavation Changes in Iron Antiquities' *Studies in Conservation* **22** 85-102.

[14] Staniforth, S. (2006) 'Relative humidity as an agent of deterioration' *The National Trust Manual of Housekeeping* Oxford: Butterworth-Heinemann 102-113.

[15] Michalski, S. (2002) 'Double the life for each five-degree drop, more than double the life for each halving of relative humidity' *ICOM Committee for Conservation 13th Triennial Meeting, Rio de Janeiro, 22-27 September 2002 Preprints* Vontobel, R. (ed.) London: James & James **1** 66-72.

[16] Zhang, X. and Wyeth, P. (2007) 'Moisture Sorption as a Potential Condition Marker for Historic Silks: Noninvasive Determination by Near-Infrared Spectroscopy' *Applied Spectroscopy* **61 (2)** 218-222.

[17] Mecklenburg, M. F. (2007) 'Micro Climates and Moisture Induced Damage to Paintings' *Museum microclimates: contributions to the Copenhagen conference, 19-23 November 2007* Padfield, T. and Borchersen, K. (ed.) Copenhagen: National Museum of Denmark 19-25.

[18] Shashoua, Y. (2003) 'Inhibiting the deterioration of plasticised poly(vinyl chloride) in museum collections' *Conservation Science 2002* London: Archetype Publications 58-64.

[19] Edge, M. (1996) 'Lifetime prediction: fact or fantasy?' *Research techniques in photographic conservation: proceedings of the conference in Copenhagen, 14-19 May 1995* Koch, M. S., Padfield, T., Johnsen, J. S. and Kejser, U. B. (ed.) Copenhagen: Royal Danish Academy of Fine Arts 97-100.

[20] Feller, R. L. (1994) *Accelerated Aging: Photochemical and Thermal Aspects* Research in Conservation Series, Marina del Rey: Getty Conservation Institute.

[21] Sebera, D. K. (1994) 'Isoperms An Environmental Management Tool' http://cool.conservation-us.org/byauth/sebera/isoperm/ accessed 17/10/2009.

[22] Strang, T. and Grattan, D. (2009) 'Temperature and Humidity Considerations for the Preservation of Organic Collections – the Isoperm Revisited' *e-Preservation Science* **6** 68-74.

[23] Reilly, J. M. (1996) 'IPI Storage Guide for Acetate Film' http://www.imagepermanenceinstitute.org/shtml_sub/acetguid.pdf accessed 17/10/2009.

[24] Adelstein, P. Z., Reilly, J. M., Nishimura, D. W., Erbland, C. J. and Bigourdan, J. C. (1995) 'Stability of Cellulose Ester Base Photographic Film: Part V – Recent Findings' *Society of Motion Picture and Television Engineers (SMPTE) Journal* 439-447.

[25] France F. G., (2005) 'Scientific Analysis in the identification of textile materials', in *AHRC Research Centre for Textile Conservation and Textile Studies First Annual Conference – Scientific Analysis of Ancient and Historic Textiles Postprints,* Janaway, R. and Wyeth, P. (ed.) 3 – 11.

[26] Hallett, K. and Howell, D., (2005), 'Size exclusion chromatography of silk: inferring the textile strength and assessing the condition of historic tapestries' in *ICOM Committee for Conservation 14th Triennial Meeting, The Hague, 12-16th September 2005 Preprints* Verger, I. (ed.) London: James & James Ltd **2** 911-919.

[27] Richardson, E. and Garside, P. (2009) 'The Use of Near Infrared Spectroscopy as a Diagnostic Tool for Historic Silk Artefacts' *e-Preservation Science* **6** 68-74.

Chapter 11 – Near-Infrared Spectroscopy and Multivariate Analysis

The principles of near-infrared (NIR) spectroscopy and multivariate analysis (MVA) and their use within conservation are presented. The chapter reports the parameters used and the trial models created to determine if these methods could be applied to the experimental results. NIR spectroscopy has the advantage of being both non-destructive and non-invasive and the potential to predict the condition of silk is discussed. The final MVA model for testing *in situ* is reported and the limitations with regard to the HPSEC data highlighted.

Although the accelerated ageing results can be compared with the samples taken from the English Heritage collection (chapter nine), this is limited to the small number of objects which could be sampled. It would be preferable to compare the laboratory results with objects without requiring samples, then information about more of the collection and its condition could be obtained. One technique which has been proposed for this purpose is near-infrared (NIR) spectroscopy.[1,2]

NIR absorption leads to anharmonic bond vibrations, the largest of which involve the lightest element, hydrogen. Therefore NIR spectra are dominated by X-H absorptions where X is commonly carbon, nitrogen or oxygen. The complexity of the combination and overtone bands of materials in NIR spectroscopy makes it hard to interpret NIR spectra and assign individual peaks to specific chemical interactions, unlike in mid-infrared (MIR) spectroscopy.[3] However similar to MIR spectroscopy, the spectra produced are characteristic and can be used for identification of compounds or materials, as long as there is a suitable reference database.[4]

As described in chapter four, NIR spectroscopy can be used rapidly and non-invasively[5,6] (with a fibre optic probe), which is leading to its increased use in the heritage field.[7] NIR spectroscopy can be used to identify small differences and changes in materials during production or processing, see review by Workman.[8] However the data for each spectrum is relatively large (4001 variables for the work presented here) and in order to compare a large number of spectra, a method of looking at large data sets quickly is required. This can also highlight small changes in the spectra which are subtle enough to be missed by visual observation.

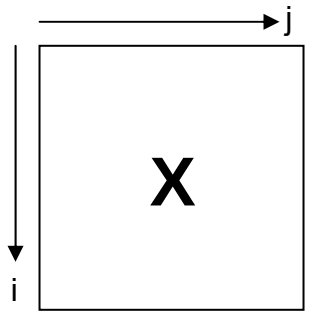

Figure 11.1 – X matrix

With two or three variables the values can be plotted on Cartesian axes and any patterns are visible. As the number of variables increases it becomes more complicated to visualise and therefore to determine any correlations within the results. Multivariate data analysis (MVA) provides a method with which to highlight correlations within large data sets. MVA uses matrix algebra forming an X matrix (see Figure 11.1) of i rows (here the number of spectra) and j columns (spectra variables, here wavenumbers). MVA can demonstrate any changes occurring within the large dataset and the key wavenumbers for the variations. However one of the potential problems of using MVA is an over reliance on the model without actually looking at the NIR spectra or understanding whether the differences modelled are real.

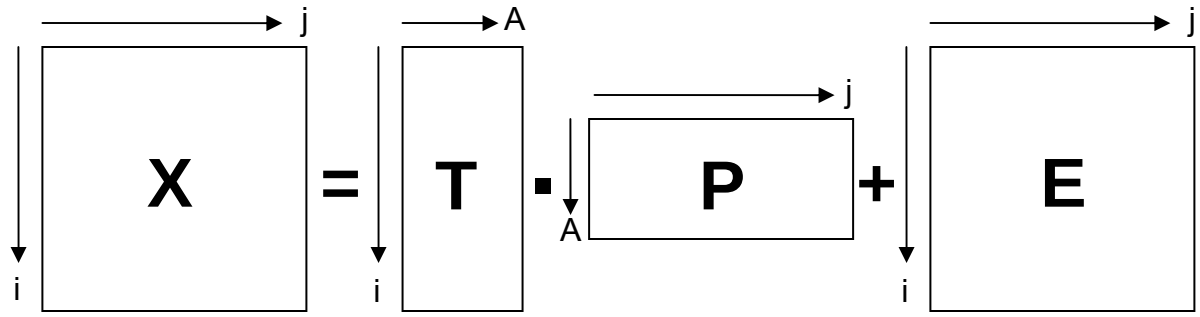

original matrix (X) = Scores (T) . Loadings (P) + error matrix (E)

Figure 11.2 – scores and loadings matrices

In order to see the changes within the data, Principal Component Analysis (PCA) has first been applied. This calculates a new coordinate system to show where correlations are in the data.[9] PCA transforms the X matrix into two smaller matrices the scores & loadings (see Figure 11.2). The scores demonstrate the position of samples along each component of the model and can be used to determine patterns or differences in the samples. The first principal component (PC) is the new axis describing the greatest variance in the data (the red line in Figure 11.3). The second PC is orthogonal to the first and describes the next largest amount of variance, this continues until all the data has been modelled.

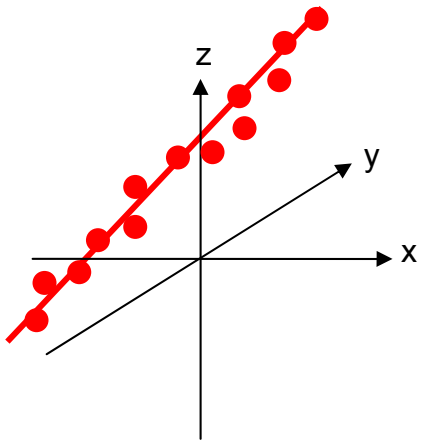

Figure 11.3 – plot of the first principal component (red line) in Cartesian space

The loadings demonstrate how much each variable contributes to the components of the model, so if the loading is small for the 1st PC, it is not accounted for by that PC. These represent the cosine of the angle of the new PC from the original axes so closer the PC is to original axis, the greater the contribution, e.g. θ = 0, cosθ = 1, or the reverse θ = 180, cosθ = -1. If the PC is at right angles then the variable has no effect (θ = 90, cosθ = 0). The loadings plots for NIR spectra can be used to highlight the wavelengths of particular interest (see Figure 11.4) and determine if noise rather than spectral information is being modelled.

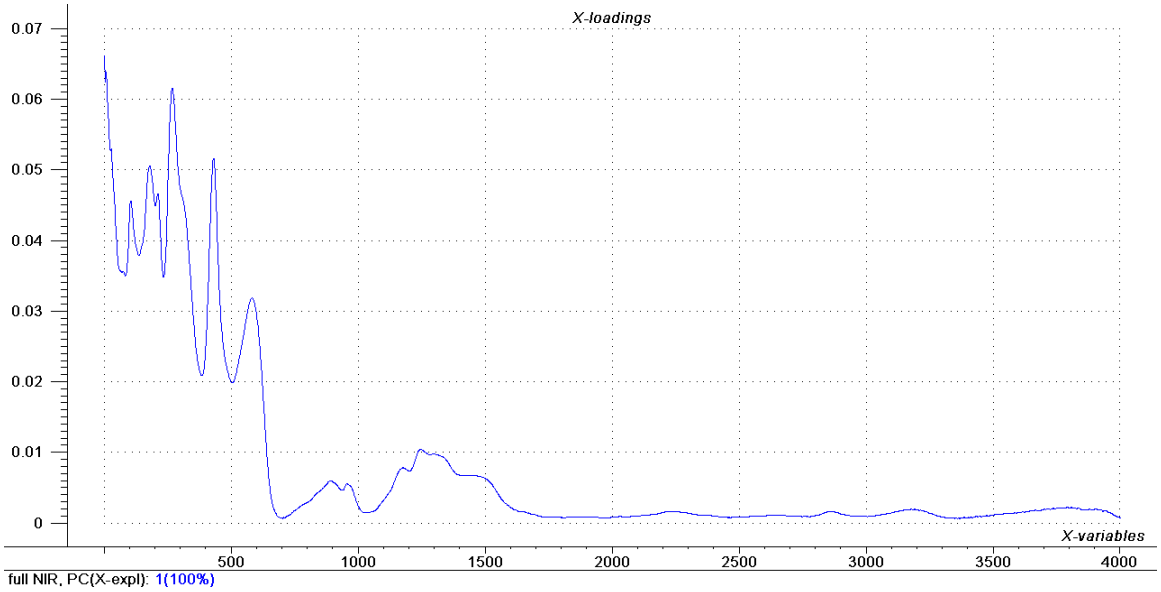

Figure 11.4 – loadings plot for kinetics samples (note for loadings plots the X-variables are the x column numbers rather than the spectral wavenumbers)

PCA is also important to identify any possible outliers within the data set, as these can skew the PCs and effect how successfully the model describes the data. Whether a sample is an outlier or an extreme sample needs special consideration. If an extreme sample is omitted as an outlier this effects how future samples with similar properties are modelled and whether they are accurately predicted or not.

Partial Least Squares (PLS) Regression relates a y variable to variations in the x variables and can be used to predict the y variables based on measured values of x. For example when a spectroscopic technique (NIR) is to be used instead of a more time consuming or invasive lab analysis (or in case of *in situ* study where samples cannot be taken). A key feature of PLS is the common scores matrix to both the x and y matrices. However PLS predictions will not be accurate if the experimental data used is inadequate,[10] for example if there are too few samples or the calibration samples used are unrepresentative of the predictive ones. There are two methods; PLS1 models a single y variable, whereas PLS2 can model several simultaneously. PLS2 models can be quicker to calculate however the estimates are often worse than those from individual PLS1 models.

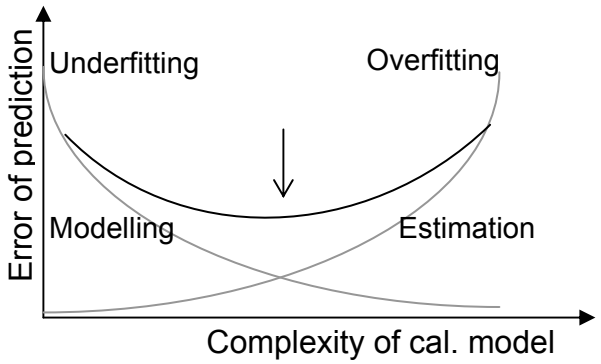

Figure 11.5 – prediction error curve (redrawn from Esbensen[11])

There are two measures of the error in the regression model. The first is the RMSEC (root mean square error of calibration) which is a measure of the average difference between the predicted and measured response values at the calibration stage. Similarly the RMSEP (root mean square error of prediction) is calculated at the prediction (or validation) stage. The prediction error has two parts, the modelling error which generally decreases with increasing components and the error in the regression parameters which increases with additional components. There is normally a minimum error which occurs at the optimum number of PCs

(see Figure 11.5). This ensures the model best fits the data but without over modelling the noise. When using the models to make predictions one less PC was used to avoid overfitting, i.e. if the optimum number of PCs was three, two PCs were used for prediction. Comparison of the predicted results showed this gave more accurate predicted values.

The use of MVA allows the NIR spectral variables to be compared alongside results from tensile testing and HPSEC analysis. For textiles, previous studies have used MVA for textile identification[12] and to build predictive models relating data from destructive analytical techniques with methods of non-invasive analysis.[13] This provides a possible way of relating research results to actual objects without having to sample the objects but by using a non-invasive technique such as NIR spectroscopy. To study whether it may be feasible to build a suitable model which compares the analytical results already discussed (chapters eight to ten) with actual objects, a trial was undertaken.

The trial used data from the kinetics study (chapter six) to determine whether this approach may be possible. Following the trial the data from the accelerated ageing results (chapter eight) was used to build predictive models for real objects based on their NIR spectra (see *in situ* study in chapter twelve). In order to build the models each sample from either the kinetics or accelerated ageing experiments was analysed using NIR spectroscopy prior to HPSEC sampling and tensile testing. The NIR spectroscopy data collection parameters and the trial models are discussed below.

Experimental Details

A number of tests were performed to determine the optimum parameters for collecting NIR spectra. This included selecting the number of scans used to acquire each spectrum (4, 32, 64 and 256), the position and orientation angle of the probe on the silk strip, the number of layers and the positioning of reflecting

aluminium foil behind the sample. Increasing the scan number from 4 to 32 dramatically reduces the noise in the 9000-12000 cm^{-1} region (see Figure 11.6). With a further increase to 64 scans there is a slight improvement in the noise around 4000 cm^{-1}. However above 64 scans made no improvement from 64 scans but substantially increased the collection time, therefore 64 scans will be used to acquire NIR spectra.

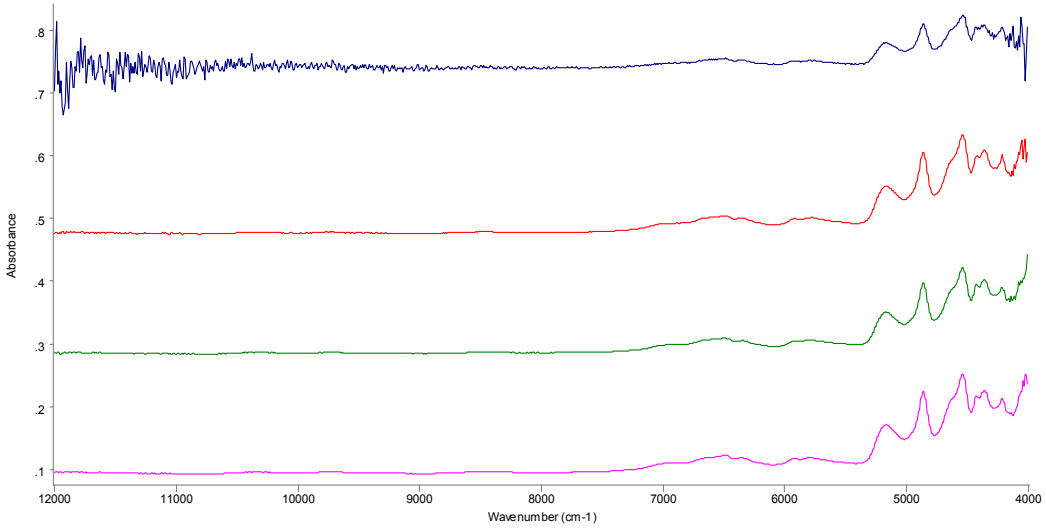

Figure 11.6 – effect of increasing scan numbers for silk test samples
(4 scans: blue; 32 scans: red; 64 scans: green; 256 scans: pink)

Placing reflecting aluminium foil behind the sample had little effect on the spectrum, except at very low scan numbers. The position of the probe on the sample made no noticeable difference, although the orientation angle affected the intensity of a number of peaks. To ensure consistent results all spectra were recorded with the probe oriented parallel to the warp direction. Increasing the number of layers gave a slight improvement in the signal to noise to ratio (see Figure 11.7). However this work was preparation for the *in situ* study (chapter twelve) where for most samples it would not be possible to record the spectra of more than one layer, hence a single layer was used throughout.

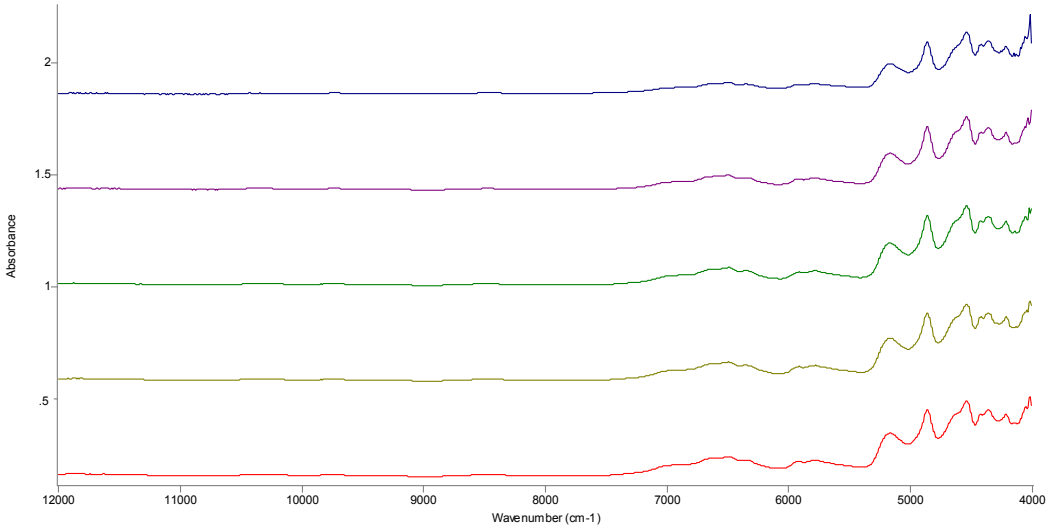

Figure 11.7 – effect of additional layers of silk on NIR spectrum

(1 layer: blue; 2 layers: purple; 3 layers: green; 4 layers: gold; 5 layers: red)

NIR spectra have been collected using a Perkin Elmer Spectrum One Fourier-transform near infrared spectrometer (FT-NIR) with an Axiom fibre optic probe scanning between 4000-12000 cm^{-1} with a resolution of 8 cm^{-1} and a scan accumulation of 64. The background reference was Spectralon® . All data was collected in absorbance at 22 ± 2 °C and 52 ± 5% RH. Baseline corrections and spectra averaging were carried out in Thermo Galactic Grams AI version 8. Additional spectral pre-processing and MVA analysis was performed with Camo Technologies Inc. The Unscrambler® version 9.7 software.

For each trial PCA was performed first to identify any clustering within samples and possible separation of data sets (e.g. between light and thermally aged samples). This highlighted the important variables (wavenumbers) and allowed the effect of spectral transformations to be studied along with the identification and removal of outliers. Models were built using the full cross validation method, which removes each sample one at a time and fits it to the model as a new sample. This method measures the difference between the actual and projected values. After

performing PCA, the tensile testing and HPSEC results were compared with the models using PLS.

A number of spectral pre-processing methods were trialled to determine the effect on the data and the optimal processing methods to build the predictive model. The methods examined were mean-centring, multiplicative scatter correction (MSC), standard normal variate (SNV) and Norris gap function with both the first and second derivative spectra and varying gap sizes. The processing and impact of each method on the data is discussed further below.

Mean-centring transforms the data by subtracting the average of the column from each value in that column. This makes all the results interpretable in terms of variation around the mean and centres the data round the origin. Generally this is pre-selected as standard when building models in the Unscrambler software; however in all models this was unselected unless testing the effect of mean-centring on the model. In the PCA models mean-centring had little effect on the scores plots beyond centring them however the effect on the PLS1 models was substantial and are discussed further within each of the data sets.

Multiplicative Scatter Correction (MSC) was developed to remove the amplification and offsetting effects caused by light scattering from uneven sample surfaces (which often arise from particles of differing sizes but here the textile weave structure). Applying MSC prevents light scattering rather than the chemical signals, being modelled. MSC compares each individual spectrum with an average spectrum. When applied to the PCA models MSC led to a diagonal trend in the scores plots.

Standard Normal Variate (SNV) transformation is similar to MSC in that it removes scatter effects from spectral data. However the spectrum is transformed using only data from that spectrum and not an average of the spectral data set. This row

transformation centres each spectrum on zero. For the PCA models built SNV processing led to an arc in the scores plot.

Derivative spectra are commonly used to increase the resolution, revealing hidden information such as closely overlapping peaks and reducing baseline effects. However this also amplifies noise within the spectra and so smoothing methods such as SNV can then subsequently be applied. The Norris-gap function is a gap-segment transformation, where the segment equals one. Two segments are separated by a gap (the gap size can be selected in the software) and the average of each segment is calculated. The difference between the two averages is then used to replace the original x value. For each dataset both the first and second derivative spectra with gap windows of 1, 5, 11, 15 and 19 were selected along with the effect of additionally using the SNV transformation. Increasing the gap window has the effect of smoothing the spectra, however at large gap windows there is an increased risk that small peaks can be lost with the data smoothing.[14]

Kinetics Model

For the initial trial, spectra from each of the three replicates from the kinetics experiments (chapter six) were analysed with the NIR spectrometer and tensile tester, then averaged in The Unscrambler software to be compared. PCA of the NIR spectra highlighted a number of samples were outliers (for example 8050D2, 8050D4 and 8050D6 in Figure 11.8). Further investigation identified a number of the individual samples, which had been averaged, contained salt contamination. The effect of salt contamination can be seen in the NIR spectra (see Figure 11.9) as an increased absorbance and spikier peaks at 5060, 5160 and 6900 cm^{-1}. In order to understand the problem the individual spectra rather than the averaged replicate spectra were used to build the PCA model. This highlighted individual samples within the replicates that were salt contaminated (see Figure 11.10). For example sample 8050D4i is an extreme outlier in Figure 11.10 and the NIR spectra indicated salt contamination was present in Figure 11.9.

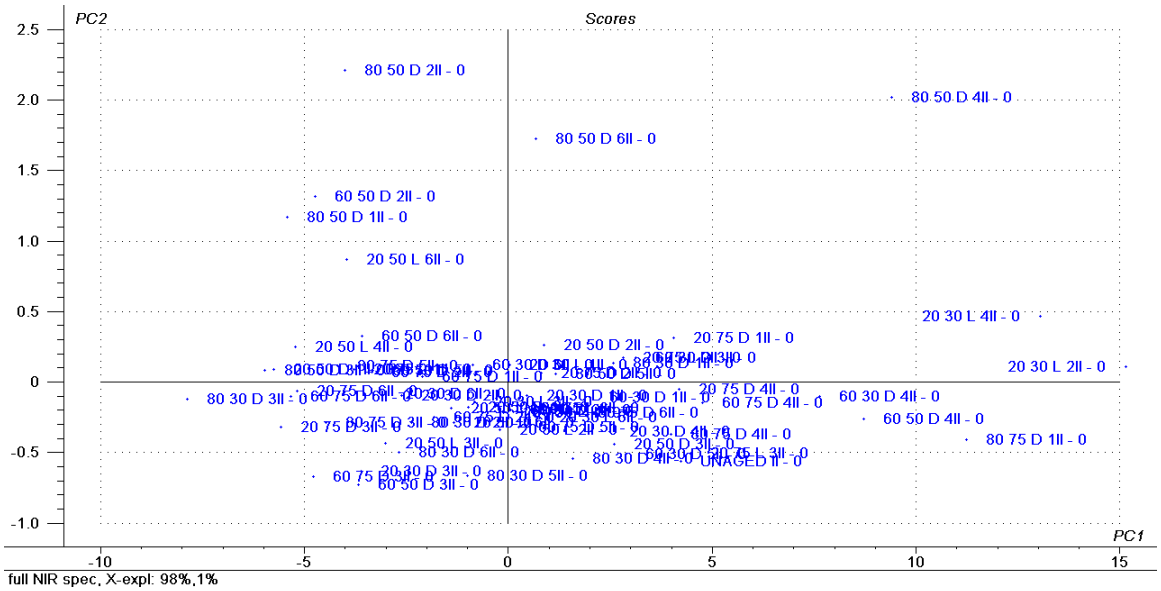

Figure 11.8 – scores plot of preliminary PCA model (averaged NIR spectra)

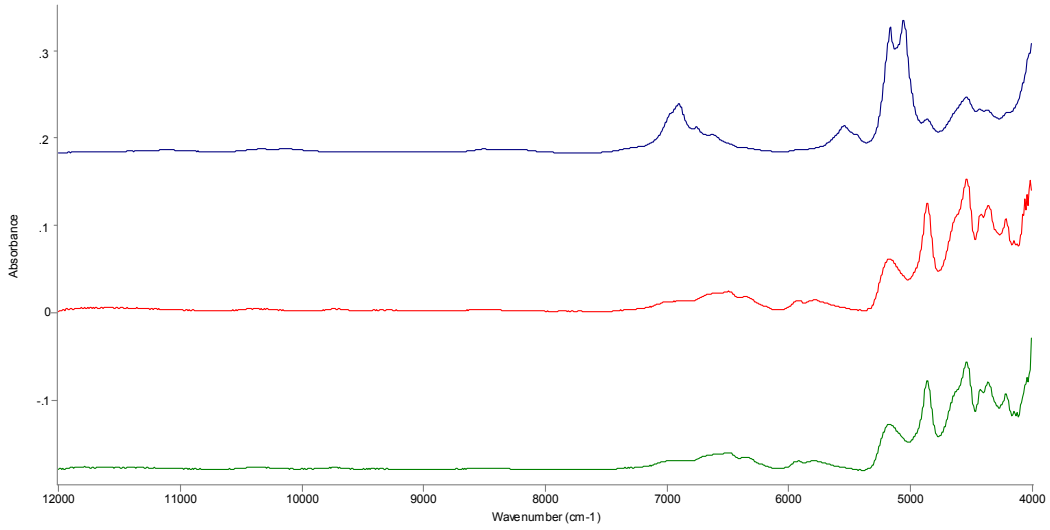

Figure 11.9 – NIR spectra showing salt contamination of the first replicate from sample 8050D4 (blue trace) the second and third replicate are shown for comparison (red and green traces)

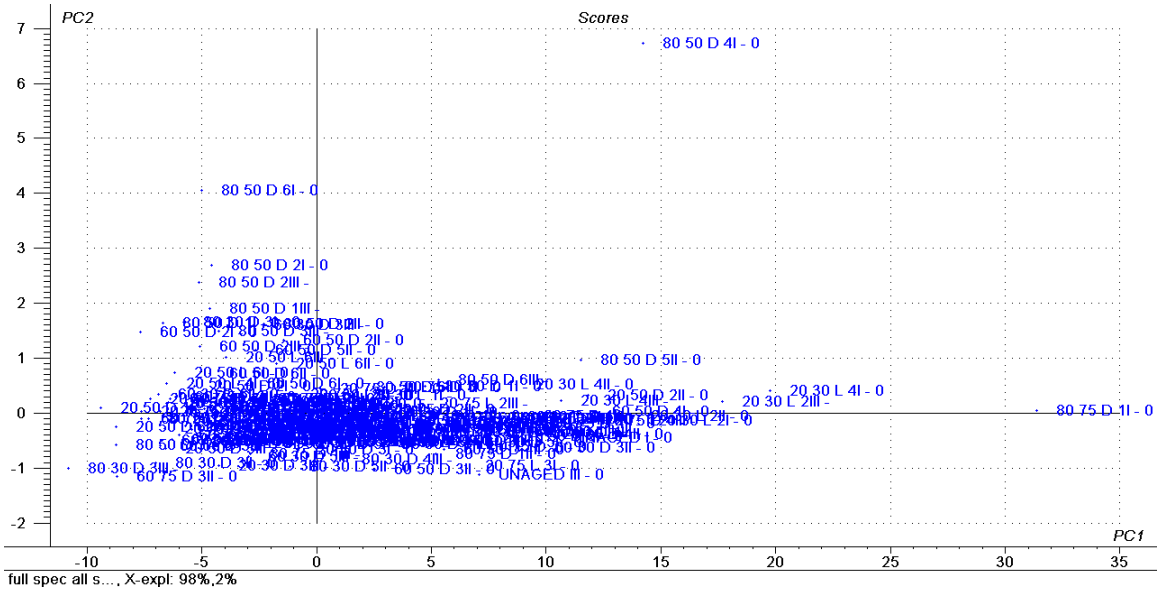

Figure 11.10 – scores plot of PCA model using individual spectra

Due to the salt contamination of some samples, each individual replicate was re-evaluated. This included reanalysis of the NIR spectra and tensile testing data along with a visual check for the presence of salt. Samples found to contain salt were then removed from the data set. The remaining spectra were averaged using GRAMS and the modelling repeated. Although this reduces the size of the data set (105 samples compared with the initial 363 spectra), it also prevents the model highlighting differences arising from the salt contamination rather than silk deterioration. The averaging of the non-contaminated samples avoids over estimation of how accurately the model predicts samples. As the full cross validation method was used, if three replicate measurements exist then the comparison may be overly optimistic, using averaged spectra removes this problem. The tensile testing data has been averaged in the same way as the NIR spectra, i.e. if replicate ii was salt contaminated the average of replicates i and iii has been used in both sets of data. The replicate averages determined after removing the salt contaminated samples have been used in all work reported in previous chapters. HPSEC samples are averages of three repeated runs of a sample taken from replicate i and so have been processed differently.

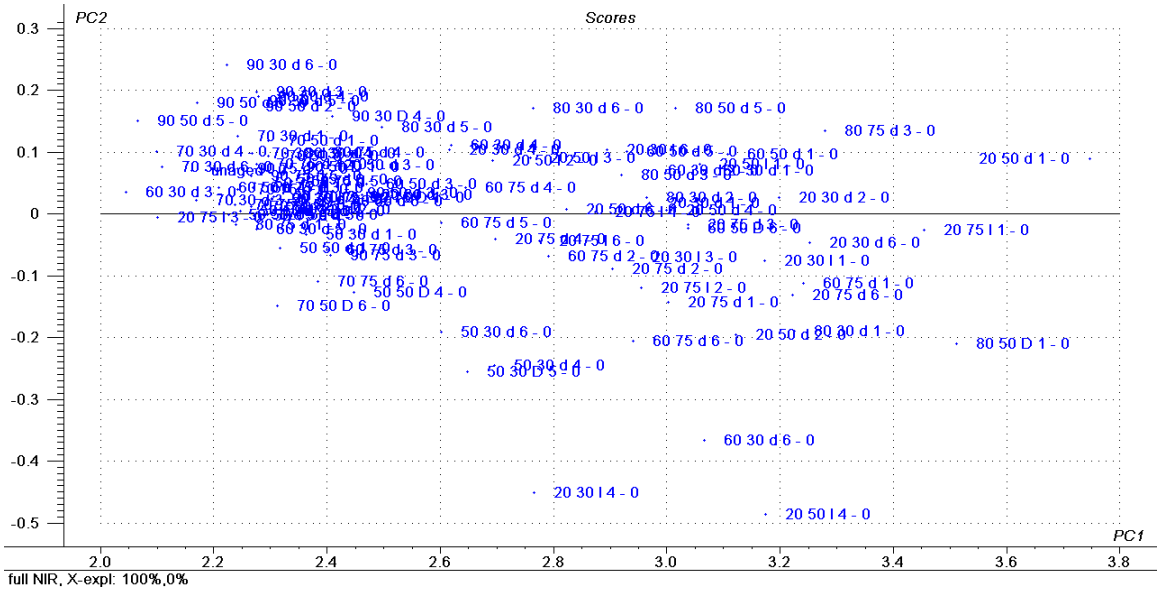

Figure 11.11 – PCA scores plot after removing salt contaminated samples

PCA models were run with the new data to study the effects of spectral pre-processing. All models used full cross validation, with weights set to 1.0, and no centring of the data. Initially 10 PCs were used to build each model, however in each case the PC at which the variance formed a plateau was noted and the model rerun with this lower value. This increased the speed of processing and avoided modelling noise. Some samples still appeared as possible outliers, notably 2030L4, 2050L4 and 6030D6 (see lower PC2 values in Figure 11.11) and further analysis indicates these may have small amounts of salt contamination but have been included as it is not as apparent as with the samples which have already been removed.

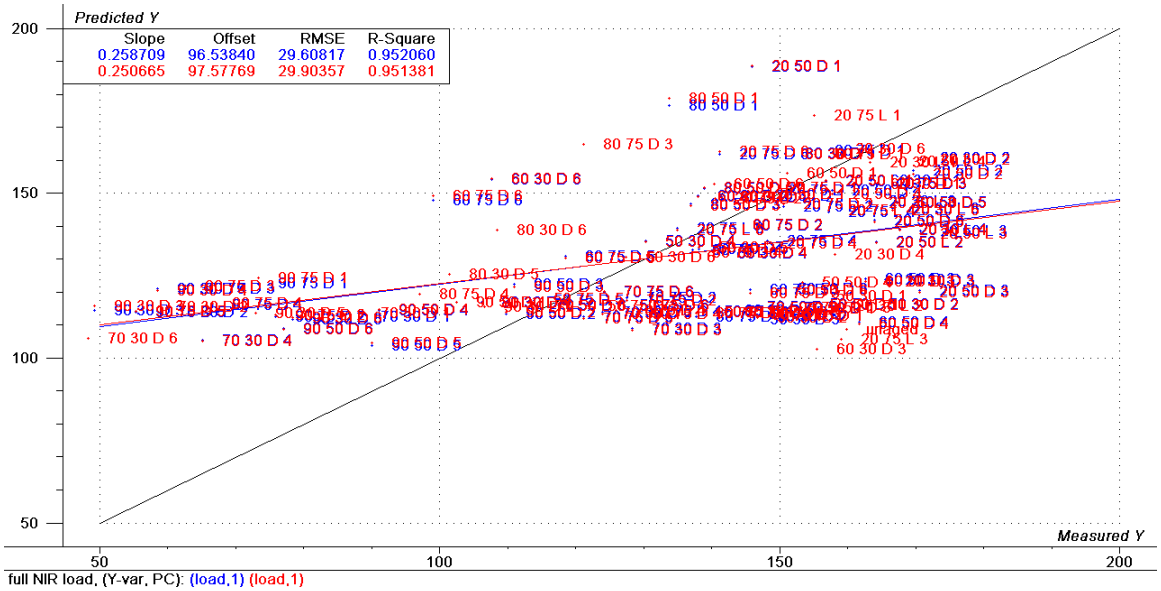

Figure 11.12 – predicted (red) vs. measured (blue) plot for initial PLS-regression model (the regression lines for both sample sets are also shown)

PLS1 regression between the NIR spectra (before pre-processing) and the tensile testing data were used to determine the initial errors in models. A decrease in the RMSE values was used to measure the improvement arising from a spectral pre-processing method. The initial RMSE values for both calibration and prediction were around 30 for load data (see Figure 11.12) and 2 for extension data. Mean-centring the spectra caused a large increase in the RMSE values for both load and extension data. Possibly because mean-centring the spectra introduced a broad peak between 10000 and 12000 cm^{-1} (between 3500 and 4000 x-variables in Figure 11.13). Reducing the NIR spectrum wavenumbers included in the model can remove this region. However there was also an increase in variance with increasing PC's. MSC showed a slight improvement in the RMSE values but this was greater when SNV was used.

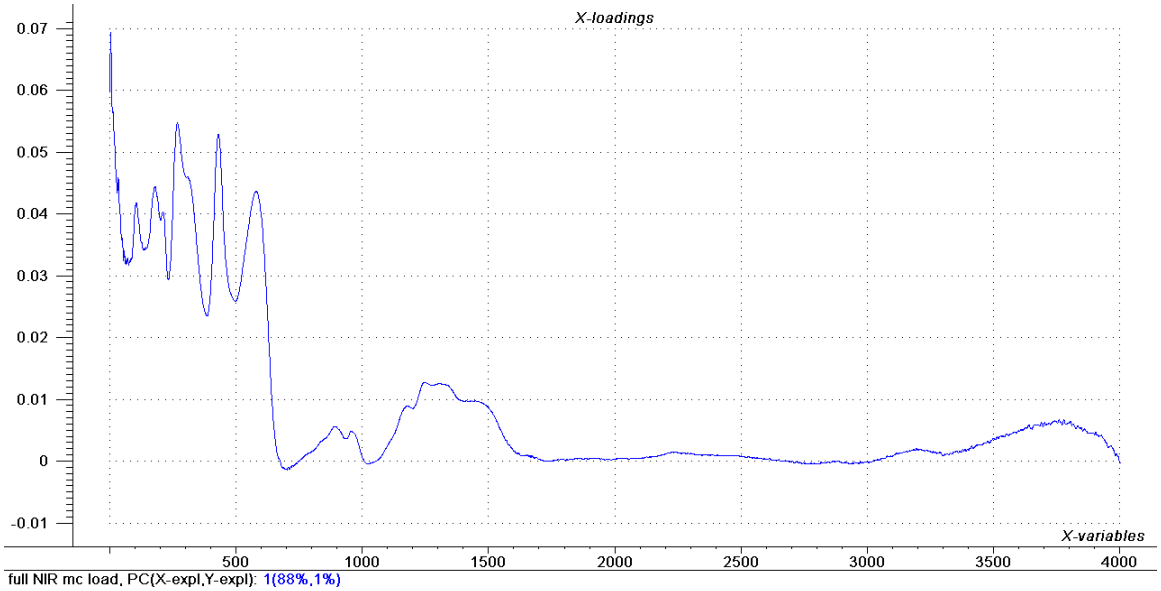

Figure 11.13 – loadings plot for mean-centred NIR data using full spectrum

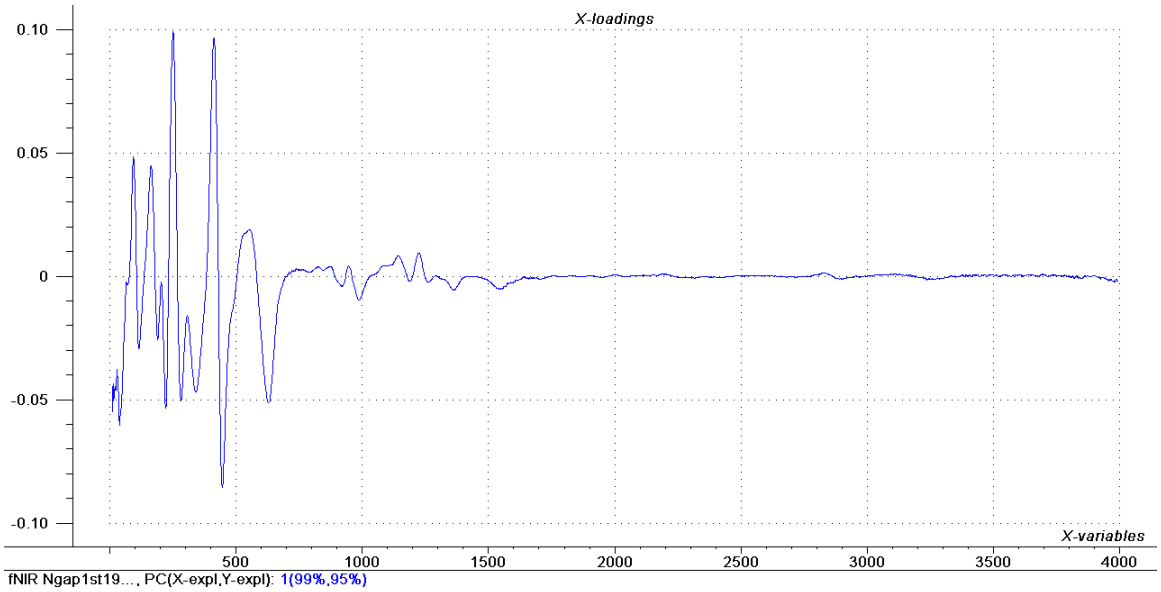

Figure 11.14 – loadings plot showing first derivative spectrum

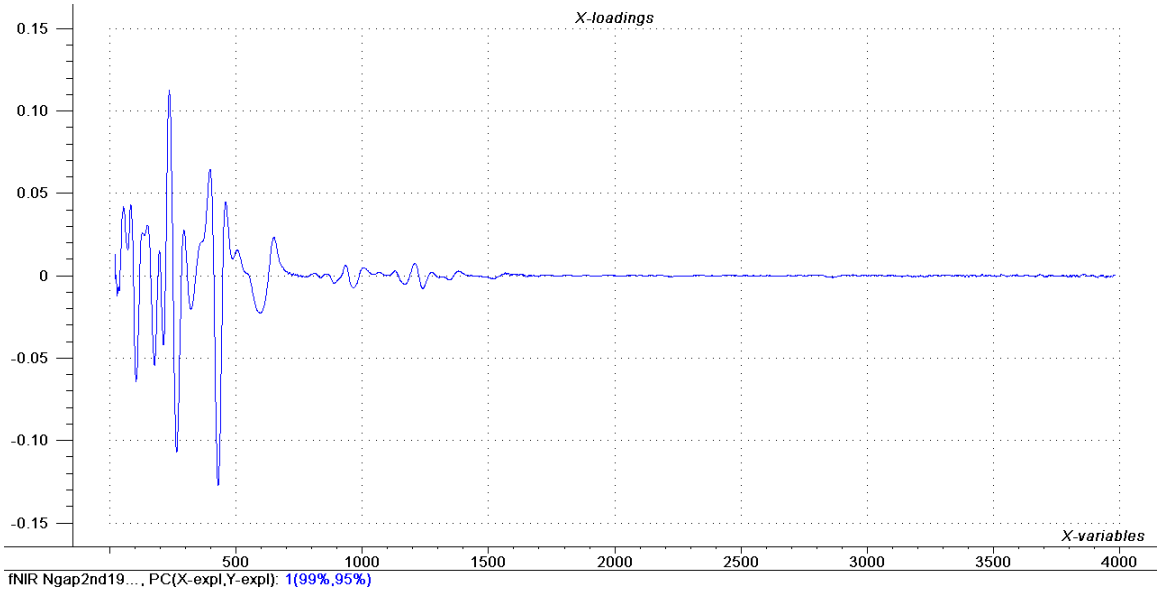

Figure 11.15 – loadings plot showing second derivative spectrum

Results after transforming the spectra with the Norris gap function show that increasing the gap window decreases the RMSE values for spectra processed with the 1st derivative. When the 2nd derivative was used RMSE values tended to be higher, although with increasing gap window these decreased and the RMSEP and RMSEC values merged. This is unsurprising as increasing the gap size has the effect of smoothing the spectra and therefore will decrease the amount of noise modelled. Smoothing methods are often used in combination, for example the Norris gap derivatives with a SNV transformation.

To test whether this would be suitable, spectra were first processed using SNV and then with the Norris gap function for both the 1st and 2nd derivative, in each case with a gap window of 19 (see Figures 11.14 and 11.15). Both showed decreased RMSE values, however using the 2nd derivative after SNV gave much lower RMSE values (20 compared with 30 for the unprocessed spectra) (Figure 11.16). A further reduction occurred when the spectral region was limited to 4400-5400 cm^{-1} (see Figure 11.17). In Figure 11.15 this relates to x-variables between 200 and 700 as outside this region the spectra contained few peaks and is mostly noise. Including noise can lead to models which poorly describe the deterioration.

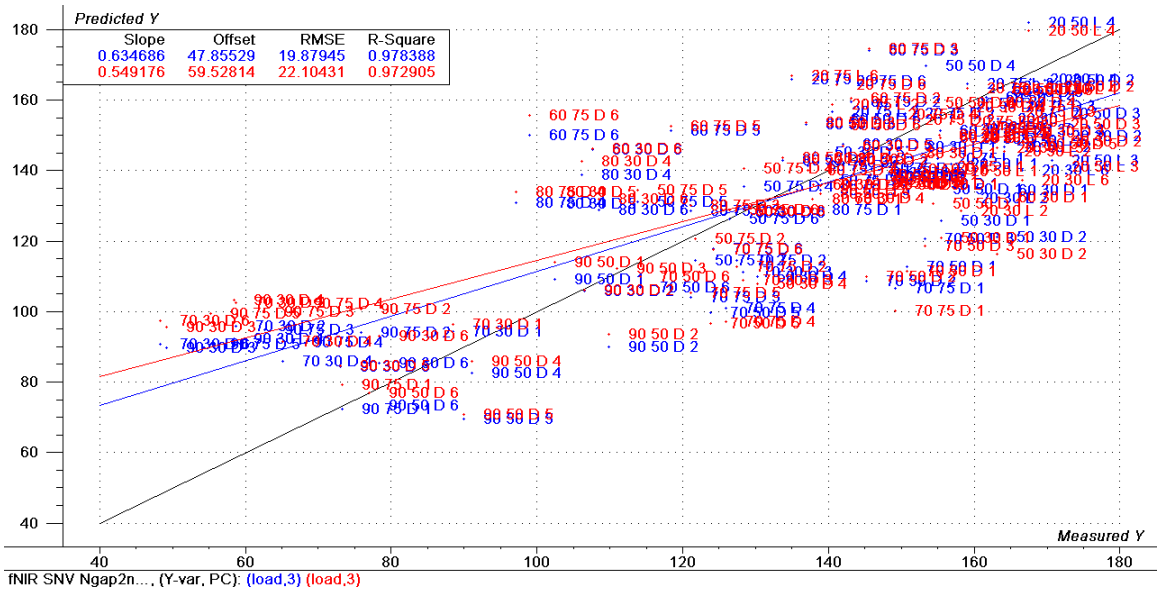

Figure 11.16 – predicted vs. measured plot for model after spectral pre-processing using SNV and 2nd derivative with gap window of 19

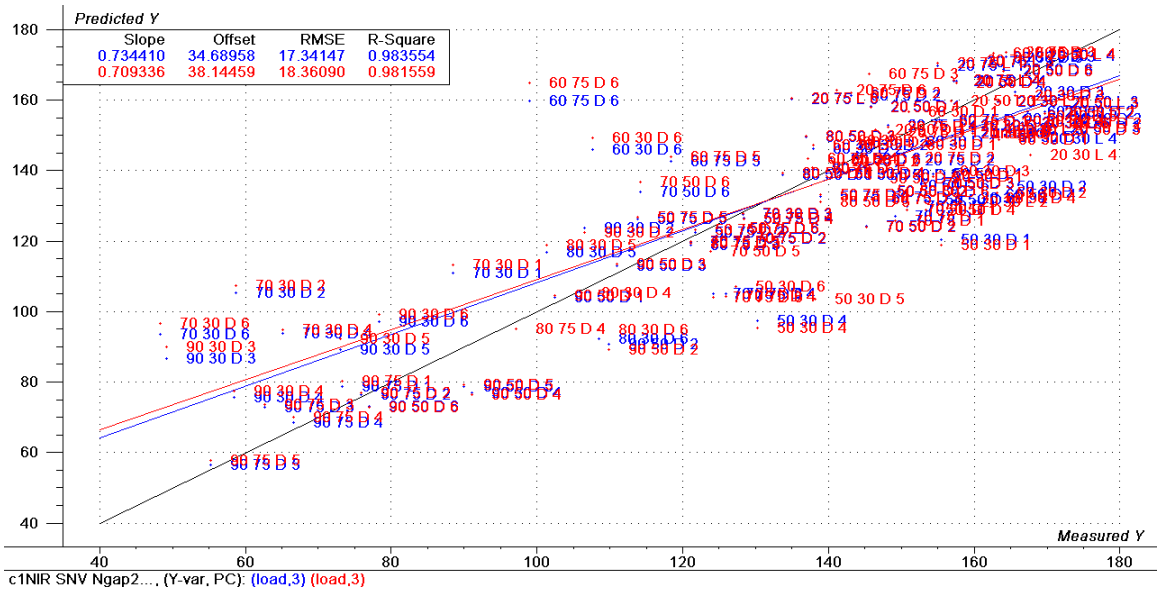

Figure 11.17 – predicted vs. measured plot for model used in Figure 11.16 but after pre-processing and limiting the spectral region

As the NIR spectra had already been pre-processed (above) these could be compared using PLS1 regression with the HPSEC data. In the first instance all

three measures of molecular weight (M_w, M_n and M_p) were used individually against the NIR spectra. However in all three cases the patterns were similar, therefore only weight-averaged molecular weight (M_w) was used for later models. This demonstrated similar patterns to the tensile testing trial models with the lowest RMSE values obtained using a reduced spectral region (4400-5400 cm^{-1}) and SNV followed by a 2nd derivative Norris gap transformation with a gap window of 19. Figure 11.18 demonstrates that the predicted values cover a limited range (~200-270 kDa) compared with the measured values (100-350 kDa). This indicates that for HPSEC the model predictions are insufficiently precise.

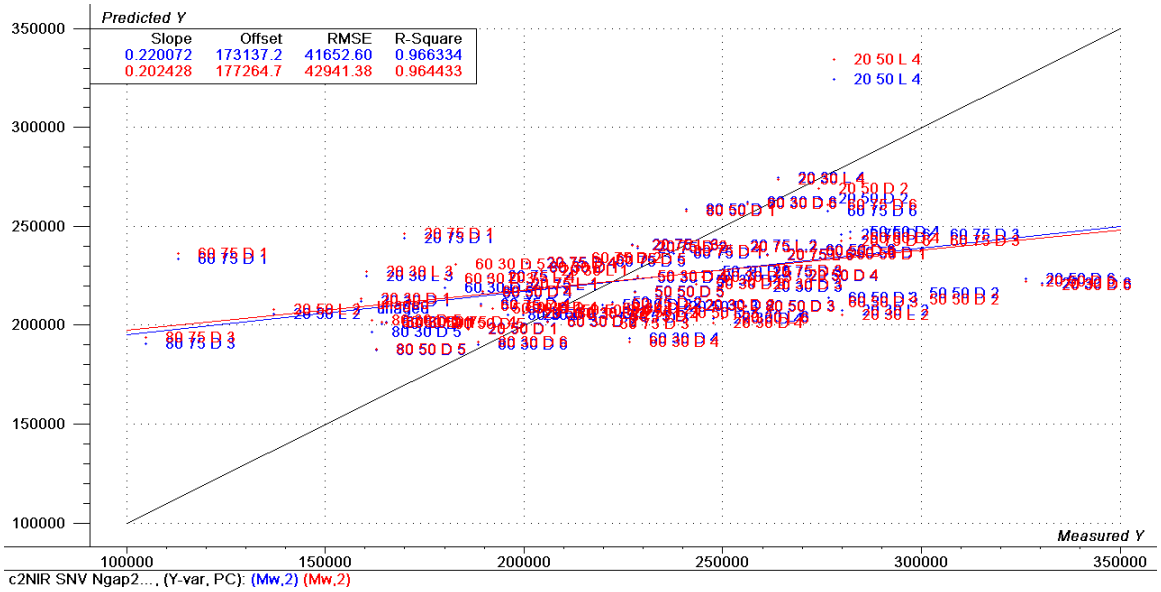

Figure 11.18 – predicted vs. measured plot for molecular weight data

As the models for both the tensile testing and HPSEC results used the same spectral pre-processing a PLS2 regression model was created using both M_w and load as the y variables. Although the RMSEC remained the same as in the model using just M_w, the RMSEP increased causing a shift in the predicted values, seen as a separation of the red (predicted) from the blue (calibration) points in Figure 11.19, which is most noticeable at the lowest measured molecular weight values (~100 kDa) of the model. Therefore the separate models will be used to predict tensile testing and molecular weight results. The initial HPSEC models are poor at

predicting the molecular weight of the calibration samples and therefore unlikely to be suitable for further development.

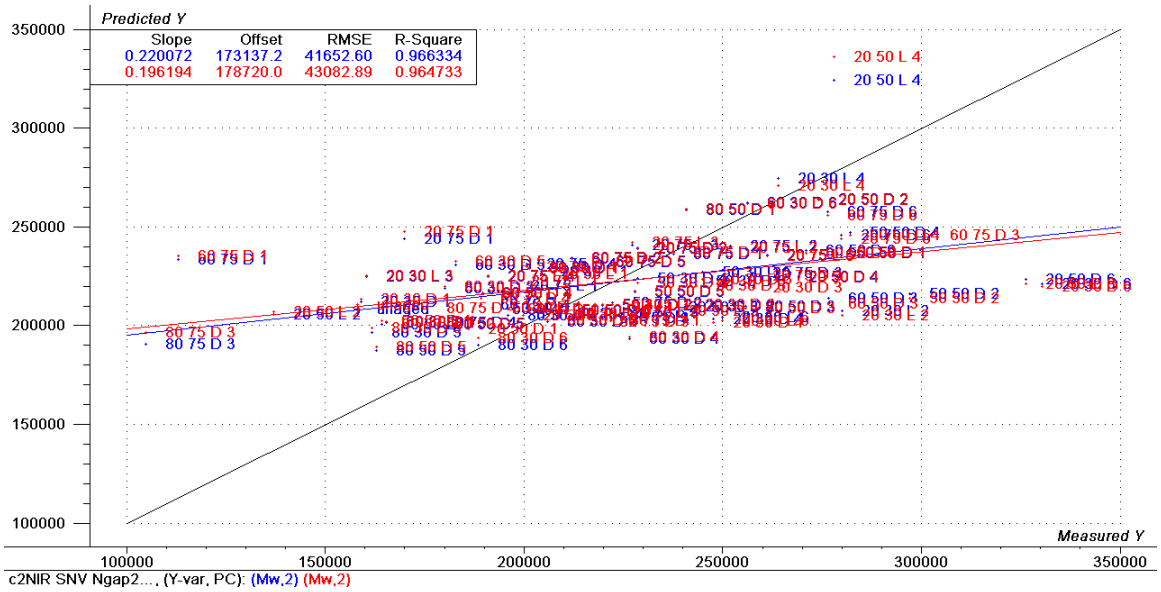

Figure 11.19 – predicted vs. measured plot for PLS2 model for molecular weight and tensile strength data

A simple test was undertaken to evaluate whether it was likely to be possible to determine the tensile testing values from the NIR spectra. Five samples from the accelerated ageing results were selected at random and their NIR spectra used to predict the tensile strength results, which had already been measured. From the five selected test samples two samples had been light aged and three heat aged. The two light aged samples predicted values were lower than the measured values (see Table 11.1). This is likely to arise from the limited number of light aged samples included in the kinetics ageing, meaning these samples are not adequately represented by the model.

Two of the three heat aged samples were predicted within the standard deviation of the tensile testing results. The predicted tensile strength for the lowest measured test sample (75D3) was higher than the standard deviation of the measured value, but had a high deviation in the model. The deviation (quoted as

the ± value in tables 11.1 and 11.2) is calculated by Unscrambler using the model error, sample leverage and residual X-variance. Large deviations indicate the predicted sample is different to the calibration samples. For 75D3 the deviation is large in comparison to the predicted value and this is probably due to the much greater deterioration seen in this sample compared to the samples aged during the kinetics experiments.

Sample ID	Measured Maximum Load / N	Kinetics Model Prediction
50UV50I2	150.5 ± 6	142.9 ± 16
75L200I15	162.8 ± 4	143.2 ± 17
0D3	118.3 ± 8	112.6 ± 18
40D2	119.3 ± 5	119.5 ± 17
75D3	48.6 ± 7	64.7 ± 37

Table 11.1 – comparison of kinetics model predictions and measured results

As a larger amount of light ageing was undertaken for the accelerated ageing these samples were used to build a PCA model to determine whether they could be separated from the heat aged samples. Although there was some separation (see Figure 11.20) with 30% RH light aged grouping in the positive PC1 and PC2 quadrant and UV aged samples in the negative PC1 and PC2 quadrant, clear groups were not formed suggesting there are not large differences based on the ageing method used. However the predicted values in Table 11.1 indicate it should be possible to use NIR spectroscopy to non-invasively determine the condition of the silk. Therefore models using the accelerated ageing data were also produced.

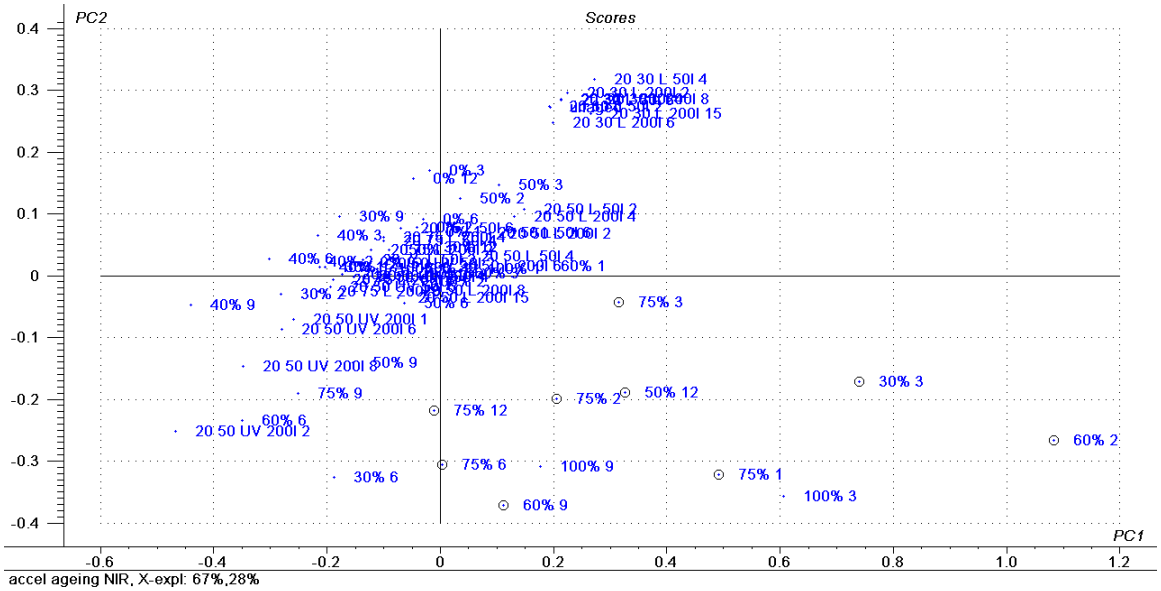

Figure 11.20 – scores plot for initial PCA model of accelerated ageing samples

Accelerated Ageing Model

NIR spectra were recorded for each of the six replicates for each accelerated ageing condition and then averaged in Grams. As with the kinetics model, each model had no data centring, weights were set to 1 and full cross validation was used. The initial PCA highlighted some samples had salt contamination, these were: 30D3, 50D12, 60D2, 60D9, 75D1, 75D2, 75D3 and 75D6 (circled in Figure 11.20). This was verified by comparison of the unprocessed NIR spectra with unaged silk and NIR spectra of the salts used for the saturated salt solutions.

Work focussed on the use of tensile strength measurements which had shown greater reproducibility in the laboratory analysis. In the kinetics model the HPSEC samples were poorly predicted by the models and so these were looked at in less detail. The NIR spectra were processed as in the kinetics model and PLS1 regression models built with the tensile testing data. The initial PLS1 model, with no spectral pre-processing, gave an RMSEC value of 28.5 and an RMSEP of 32.3

(see Figure 11.21) using the maximum load results and an RMSEC of 1.53 and an RMSEP of 1.73 for the extension at maximum load results.

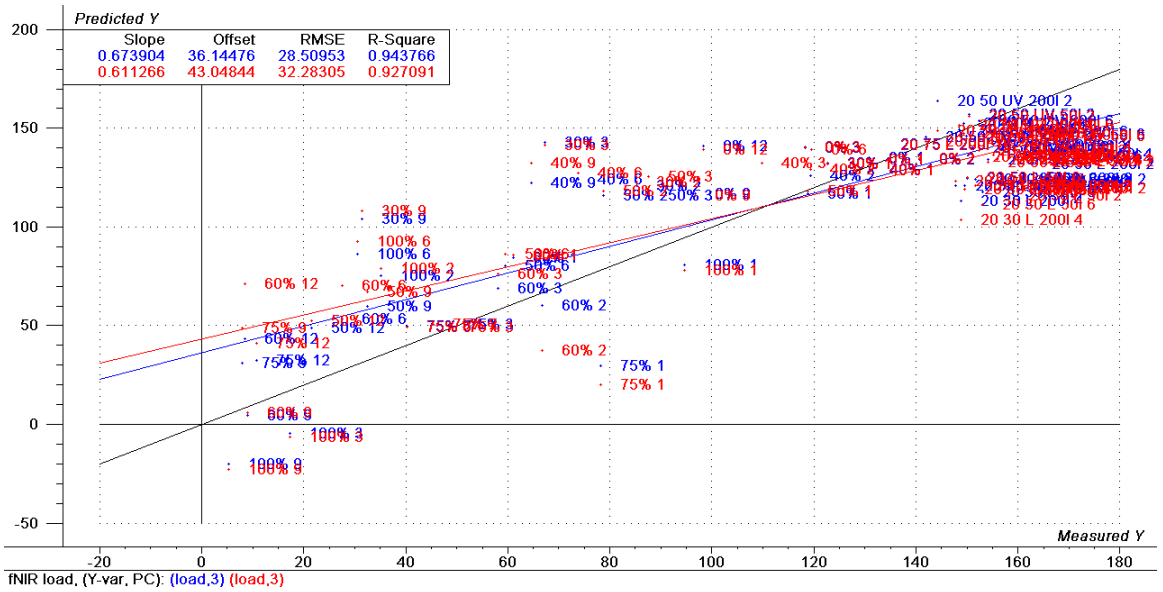

Figure 11.21 – initial predicted vs. measured plot

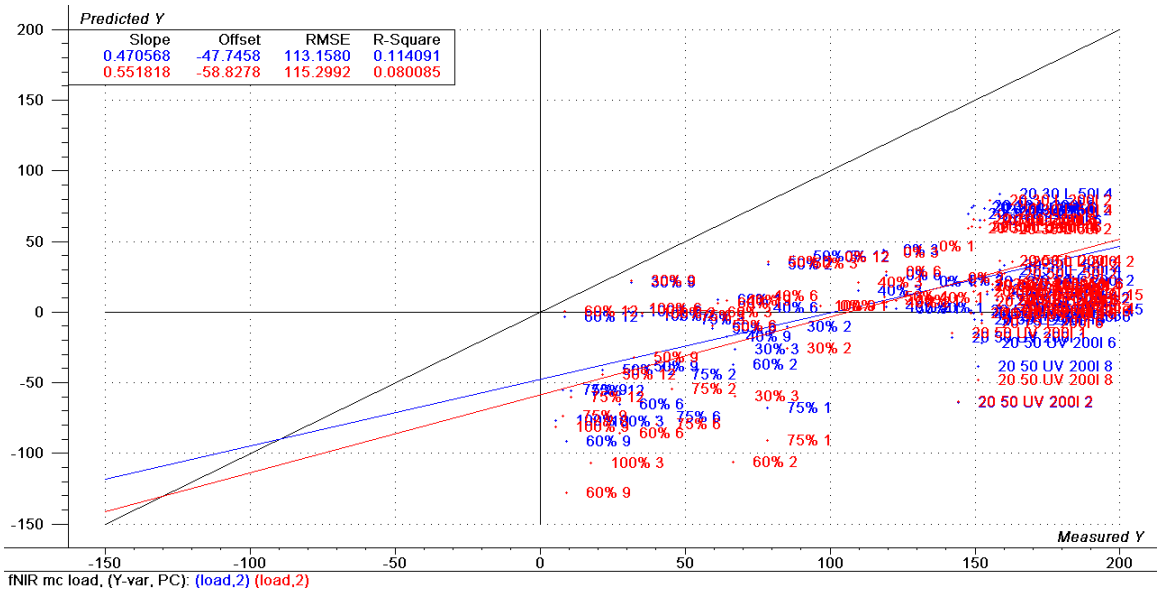

Figure 11.22 – effect of mean-centring on predicted vs. measured plot

The use of mean-centring increased the RMSEC to 113 and the RMSEP to 115 (see Figure 11.22) with rising variance after two PCs. Although as Figure 11.22

shows mean-centring further highlights the separation of light aged samples as discussed above. MSC and SNV made little improvement to either RMSE value (<0.5). Again the derivative spectra were calculated with the lowest RMSE values for a gap window of 19 for both the first and second derivative.

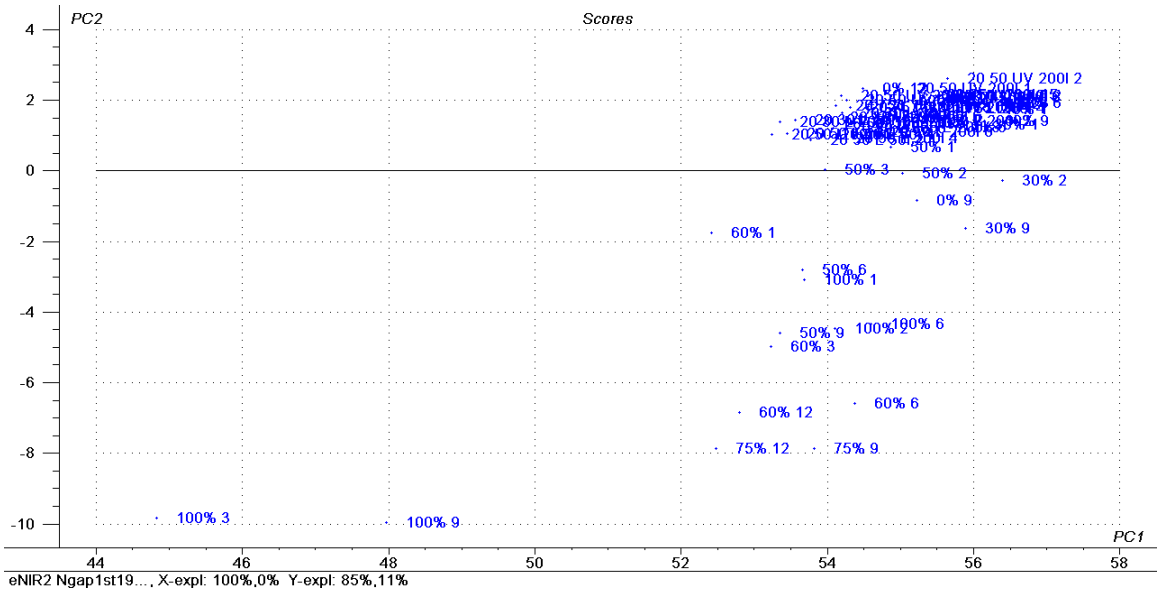

Figure 11.23 – scores plot of final model

The lowest RMSE values were observed by transforming the spectra using the 1st derivative Norris gap function with a gap window of 19 followed by SNV transformation. In the kinetics test model SNV was applied before the derivative spectra was calculated, however applying the transformation after the derivative removes the noise introduced during the processing. The samples found to be salt contaminated in the PCA were also removed. There are still two outliers seen in Figure 11.23 (100D3 and 100D9) but these are known to be real samples and therefore were included in the model. After reducing the spectral region to 4100-5100cm^{-1} (see Figure 11.24) to ensure noise is not being modelled an RMSEC of 18.0 and RMSEP of 19.9 with 3PCs was obtained. This was also applied to the HPSEC results and similarly gave the best model after Norris gap 1st derivative with a gap window of 19 and SNV transformation.

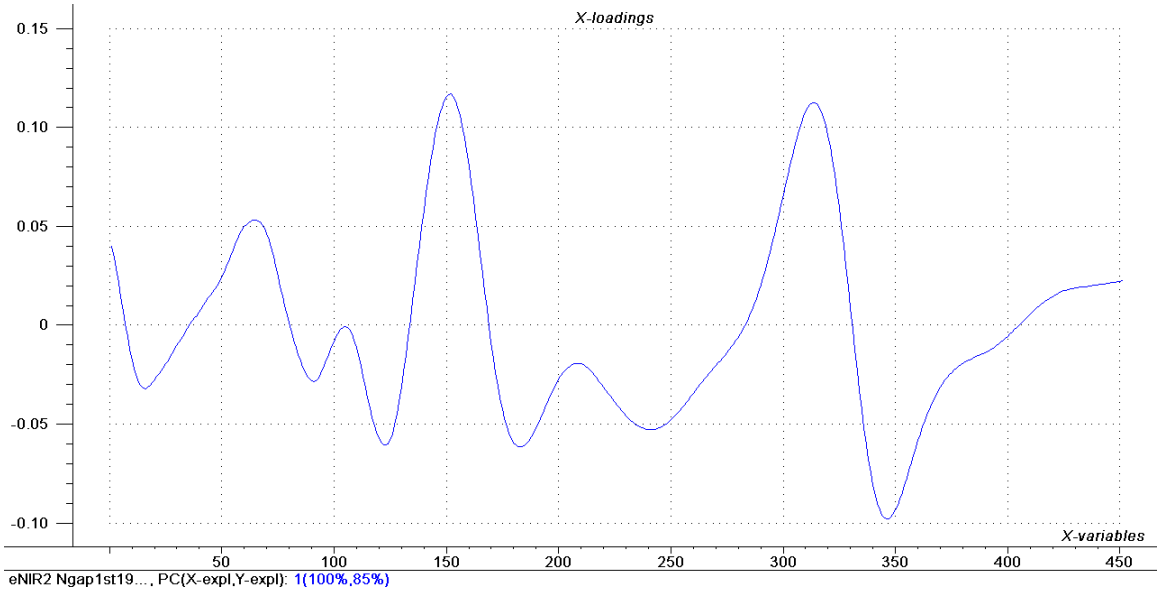

Figure 11.24 – loadings plot of final model

The final PLS1 regression model used 3 PCs with a limited spectral region (4100-5100cm^{-1}) after pre-processing the spectra using the Norris gap function (1st derivative with a gap window of 19) followed by SNV transformation. The first PC of the model explained 100% of the x-variance and 85% of the y-variance. This means the first PC describes most of the variance in the data, with higher PCs contributing little to the model. The loadings plot (Figure 11.24) shows the significant peaks contributing to model are at 4500 cm^{-1} (x-variable 150), 4824 cm^{-1} (x-variable 315) and 4890 cm^{-1} (x-variable 345). Mo has identified a number of peaks for silk in NIR spectra including 4530 cm^{-1} (combination of the amide A and amide III) and 4860 cm^{-1} (combination of the amide A and amide II).[15] These peaks are seen in the unprocessed and second derivative spectra and associated loadings. However in the first derivative spectra (and Figure 11.24) these peaks occur at zero and the significant loadings are at the turning points for the combinations identified by Mo.

Testing the Accelerated Ageing Model

To test the calibration model a validation set using the kinetics samples was built. Although the RMSE values were still relatively low (RMSEC 19.14 and RMSEP 23.75) there are definite differences between the two sets of data as seen in Figure 11.25. The differences are also reflected in that for each set of samples the minimum RMSE values were obtained with different spectral pre-processing to build the individual models. Although the samples were cut from the same batch of silk, this may reflect the longer and more extreme ageing experienced by the accelerated ageing samples compared to the kinetics samples.

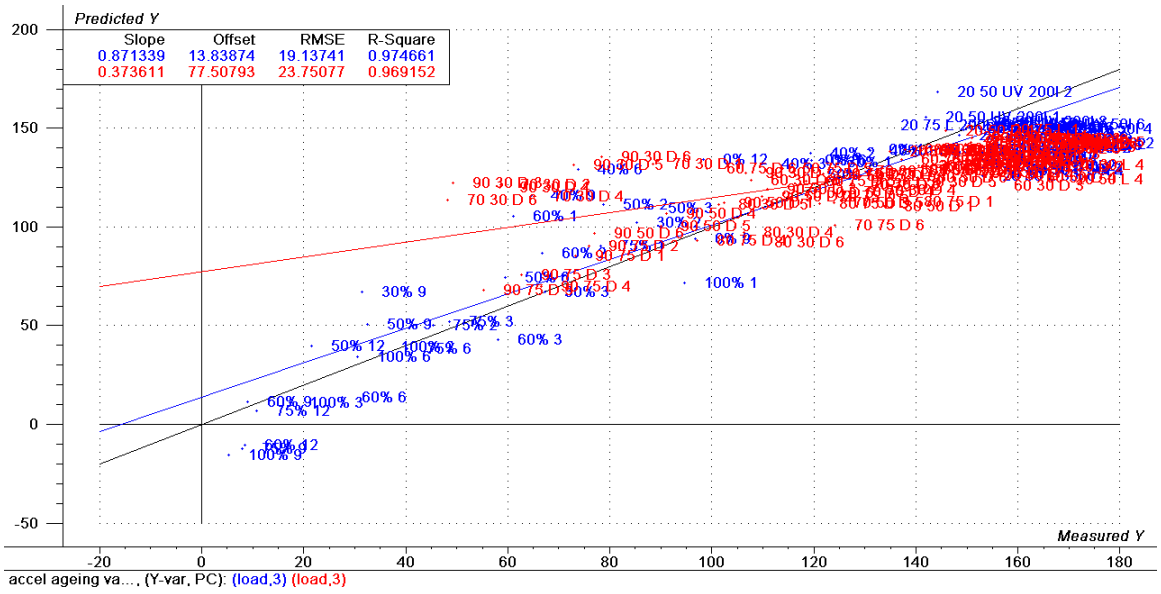

Figure 11.25 – predicted vs. measured plot for validation set model

To determine which model was most suited for the *in situ* study, the initial cross validation model and the validation set model were used to predict the tensile strength of five kinetics samples. These are compared in Table 11.2.

Sample ID	Measured Maximum Load / N	Cross Validation Model Prediction	Validation Set Model Prediction
2030D4	158.2 ± 10	140.3 ± 28	136.0 ± 29
2050L2	164.2 ± 13	142.7 ± 28	135.2 ± 30
5075D2	121.8 ± 20	132.1 ± 17	116.5 ± 21
8030D2	141.4 ± 9	141.2 ± 29	131.5 ± 32
8075D4	97.1 ± 7	89.5 ± 26	114.7 ± 34

Table 11.2 – comparison of accelerated ageing model predictions and measured results

Using the validation set model the predicted values have a narrower range (maximum difference of 20 compared with almost 70 in the measured data) and are not ranked in the correct order. However the cross validation model, which uses the accelerated ageing samples to predict the kinetics samples, gives closer values to the measured results. These are ranked in the correct order although the predicted values for 20 °C samples are slightly lower than those for the heat aged samples. However the model is sufficiently close to the actual values to demonstrate potential for use *in situ*.

For the HPSEC results similar predictions were attempted using the same five samples in Table 11.2. However the ability of the model to predict the weight-averaged molecular weight was less successful. The measured values varied from around 200 to 750 kDa, whereas the predicted values are between 180 and 280 kDa. This is similar to the problems observed in the kinetics model. The model also fails to predict the samples in the correct order and so the highest measured molecular weight is not the highest predicted value. For both the kinetics and accelerated ageing models this problem is probably related to the difficulties experienced when processing the HPSEC data (see chapter eight). Therefore the molecular weight models were deemed unsuitable for further prediction using the *in situ* spectra. This limits the comparison of the HPSEC results from micro-samples

(chapter nine) to the *in situ* study (chapter twelve); however the results of such a comparison are unlikely to be meaningful.

Conclusions

It has been possible to build a predictive model to determine the tensile strength of silk samples from their NIR spectra using MVA. The predicted values, although not the exact measured values are similar, and within the deviation of the model. Importantly the predicted values are ranked in the correct order, so the lowest measured tensile strength is also the lowest predicted value. This may be important to compare the relative values of the *in situ* predictions.

One possibility to overcome the problems with the HPSEC software would be to digitise the raw chromatograms to import into the MVA software for further analysis. This would circumnavigate the need to use the molecular weight values (M_w, M_n or M_p) calculated by software. As it is not possible to export the raw chromatograms from the HPSEC software and there was insufficient time to pursue digitisation this may be suitable for further development of the existing data. It may also be possible to incorporate the information recorded at all wavelengths by the HPSEC software rather than just at 280 nm, which has been used to process the data. This may highlight other changes occurring within the samples not seen in the chromatograms at the selected detection wavelength.

The ageing of samples without using saturated salt solutions is likely to provide more reliable data for models leading to more accurate predictions. One weakness of the model is that it has been built using samples of aged modern silk of the same weave structure. The model could be made more realistic for *in situ* use by testing whether other parameters such as the weave structure or silk mixed with other materials in the weave e.g. silk warp and linen weft has an effect. The reference set could also include coloured and weighted silk to reflect the textiles

common to collections. If necessary these other materials could be included within the model to enhance the ability to predict silk deterioration *in situ*.

References

[1] Zhang, X. and Wyeth, P. (2007) 'Moisture Sorption as a Potential Condition Marker for Historic Silks: Noninvasive Determination by Near-Infrared Spectroscopy' *Applied Spectroscopy* **61(2)** 218-222.

[2] Kim, J.-J. and Wyeth, P. (2009) 'Towards a routine methodology for assessing the condition of historic silk' *e-Preservation* **6** 60-67.

[3] Richardson, E., Martin, G., Wyeth, P. and Zhang, X. (2008) 'State of the art: non-invasive interrogation of textiles in museum collections' *Microchimica Acta* **162** 303-312.

[4] Kawano, S. (2002) 'Sampling and Sample Presentation' in *Near-Infrared Spectroscopy Principles, Instruments, Applications* Siesler, H. W., Ozaki, Y., Kawata, S. and Heise, H. M. (ed.) Weinheim: Wiley-VCH 115-124.

[5] Bokobza, L. (2002) 'Origin of Near-Infrared Absorption Bands' in *Near-Infrared Spectroscopy Principles, Instruments, Applications* Siesler, H. W., Ozaki, Y., Kawata, S. and Heise, H. M. (ed.) Weinheim: Wiley-VCH 11-41.

[6] Zhou, Y., Xu, H. R. and Ying, Y. B. (2008) 'NIR Analysis of Textile Raw Material' *Spectroscopy and Spectral Analysis* **28 (12)** 2804-2807.

[7] http://www.science4heritage.org/survenir/ accessed 05/10/2009.

[8] Workman, J. (1993) 'A review of process near infrared spectroscopy: 1980-1994' *Journal of Near Infrared Spectroscopy* **1** 221-245.

[9] Esbensen, K. H. (2002) 'Principal Component Analysis (PCA) - Introduction' *Multivariate Data Analysis in Practice* 5th Edition Oslo: CAMO Process AS 29.

[10] Brereton, R. G. (2003) 'Calibration' *Chemometrics Data Analysis for the Laboratory and Chemical Plant* Chichester: Wiley 271-338.

[11] Esbensen, K. H. (2002) 'Validation: Mandatory Performance Testing' *Multivariate Data Analysis in Practice* 5th Edition Oslo: CAMO Process AS 160.

[12] Cleve, E., Bach, E. and Schollmeyer, E. (2000) 'Using chemometric methods and NIR spectrophotometry in the textile industry' *Analytica Chimica Acta* **420** 163-167.

[13] Richardson, E. and Garside, P. (2009) 'The Use of Near Infrared Spectroscopy as a Diagnostic Tool for Historic Silk Artefacts' *e-Preservation Science* **6** 68-74.

[14] Brereton, R. G. (2003) 'Signal Processing' *Chemometrics Data Analysis for the Laboratory and Chemical Plant* Chichester: Wiley 119-182.

[15] Mo, C.-L., Wu, P.-Y., Chen, X. and Shao, Z,-Z, (2006) 'Near-Infrared Characterization on the Secondary Structure of Regenerated *Bombyx mori* Silk Fibroin' *Applied Spectroscopy* **60** 1438-1441.

Chapter 12 – *In Situ* Case Study

The selection of Brodsworth Hall and its collection for the *in situ* case study are presented along with the characterisation of the property's silk collection. The *in situ* case study has been used to determine the potential of the NIR / MVA model to predict the condition of silk non-invasively. The chapter presents the results and discusses the limitations of the model with regard to its use on artefacts compared with model samples. Preventive measures to prolong the lifetime of silks at Brodsworth Hall are also discussed.

The aim of the case study was to characterise the collection of silks in one English Heritage property. The collection in the selected property was used to apply the results from the research undertaken, for example the X-ray Fluorescence Spectroscopy (XRF) and High Performance Size Exclusion Chromatography (HPSEC) analysis of the micro-samples. The accelerated ageing experiments have indicated high humidity is important for silk deterioration and the case study tests whether changes to this may be possible and the impact this might have of the rest of the collection. The idea of using a display lifetime as a measure of the condition and how the current display conditions affect this has been discussed in chapter ten. The case study will determine whether it is possible to determine these from near-infrared (NIR) spectra and the possible improvements expected with alterations to the environmental conditions.

As discussed in chapter three, XRF analysis can identify the presence of metallic elements in textiles and has been shown to be applicable for *in situ* use. As weighted silks are thought to have an inherent deterioration mechanism due to the metallic elements present, their identification is of particular interest to conservators, curators and collection managers. Knowing how many of these textiles are in the collection, their location and condition can help prioritise conservation treatments and improve display and storage conditions. A further aim

of the study was to identify these textiles, as the possible number of samples will always be limited and *in situ* analysis allows a much greater number of objects to be analysed.

NIR spectroscopy can be used to look at changes in materials such as the moisture content of silk.[1] Fluctuations in humidity in the room lead to changes in the amount of moisture in the silk. However the moisture content has been reported as a possible means of monitoring the condition of the silk materials within collections, which would enable regular checks of silk collections to be made without sampling objects. Chapter eleven has demonstrated that NIR spectroscopy, in conjunction with multivariate analysis (MVA) can predict the tensile strength of a test sample from its NIR spectrum. As NIR spectroscopy is a non-invasive and non-destructive method, it would provide a way of determining the condition of the collection without removing samples. This type of condition monitoring would improve both our understanding of the collection and how we can care for it; therefore a trial was undertaken to determine the feasibility of using this method within historic houses.

Selection of Property

Surveys of each of the properties (see chapter two) had raised a number of questions including whether the poor condition of black silks relates to the dyeing methods and the identification of materials used to make velvets. Each of the properties contains different materials and there are different questions associated with each, so the choice of which to study in more depth was not obvious. The majority of the collection, and the questions, related to three properties (Audley End House, Brodsworth Hall and Osborne House) hence it made sense to choose one of these. However the majority of the collection at Osborne House belongs to the Royal Collection rather than being part of the English Heritage collection so this was excluded.

The collection at Audley End House, although covering a wider range of dates, is more limited in terms of the range of objects and physical access to them. At Brodsworth Hall a number of the textiles date from the original furnishing of the property by Lapworths around 1863. However there are some later replacement wall silk in the South Hall from circa 1914. Although the range of dates is quite limited the variety of objects is much wider. At Brodsworth Hall (and the stored collection at Fulford) silk can be found in soft furnishings, banners, upholstery and costume. Within these objects there were a large number of velvet textiles as well as possible weighted materials. The condition of the silk is also very variable including very friable, powdery silks and heavily split silk as well as a mix of faded and unfaded silks in the drawing room. This presented a greater opportunity for the NIR spectroscopy trial and so Brodsworth Hall (see Figure 12.1) was selected for the *in situ* case study.

Specific questions to be answered at Brodsworth Hall included how many of the velvets were silk? Does the visual condition of faded and / or split silks match the predicted condition from NIR spectroscopy and MVA? Are weighted silks present in the collection and if so, how many? Do these weighted materials separate from unweighted silks in MVA models? What is the composition of the metal threads in the Brodsworth Hall collection? The study aimed to answer these questions.

Figure 12.1 – Brodsworth Hall

There are two further advantages to Brodsworth Hall. The NIR spectrometer can be moved around on a trolley for *in situ* analysis but is still quite large and cumbersome so the lift at Brodsworth Hall to move equipment upstairs was advantageous. Generally access to the collection at Brodsworth Hall on both the visitor route and stores is good which allowed for a large number of objects to be analysed. The display at Brodsworth Hall also has the greatest possibility to make changes to the environmental controls. The majority of the silk collection is displayed downstairs or in storage, whereas the most vulnerable of the veneered wooden materials are upstairs. Therefore modification of RH levels, if thought appropriate, may be possible without adversely affecting the rest of the collection on display at this property.

Brodsworth Hall Collection

From the initial search of the object database at English Heritage (HOMS) around 300 items for Brodsworth Hall were listed as containing silk. This included a large number of curtain tiebacks and tassels, as well as lampshades, prize ribbons, banners, tablecloths, bed covers, as well as the more obvious upholstery and

costume items. During the collections survey of Brodsworth Hall eighteen samples were removed for XRF and HPSEC analysis, and nineteen from objects in the associated stored collection at Fulford. However in some cases identification of whether the sample was silk was required first, this was particularly true for the velvet materials.

Samples nlful10 and nlful11 were both taken from a velvet chair [90003210] at Fulford. Attenuated Total Reflectance (ATR) analysis showed these samples were wool and both the EDS and XRF analysis identified sulfur, probably from the wool, although it could potentially also come from the purple dye or pollutant contamination. A number of other sampled velvets were also identified as wool using ATR analysis (nlbro3 shell chair (Figure 12.2) [90009569] and nlbro8 picture shelf under the painting of The Lawrence (Figure 12.3)). ATR analysis (see appendix 6) identified two samples as cotton; in both cases these seemed to be the weft fibres, as they were taken from very deteriorated silk upholstery (nlbro6 ottoman [90009624] and nlbro13 side ottoman [9003612]).

Figure 12.2 – shell chair [90009569] at Brodsworth Hall

Figure 12.3 – picture shelf in Dining Room at Brodsworth Hall

After ATR analysis thirty one samples of the thirty seven micro-samples removed were identified as silk and therefore suitable for HPSEC analysis. However, a number of the historic samples failed to dissolve in the lithium thiocyanate solution required to solubilise silk before HPSEC analysis. In total only twenty five samples could be analysed by HPSEC. In general the samples which did not dissolve were those in which tin had been identified during EDS or XRF analysis (nlful3, nlbro9, nlbro10, nlbro12). This was not surprising as the HPSEC method is reported to be unsuitable for weighted silk samples.[2]

However there were some discrepancies where tin was identified but the sample still dissolved (nlful1, nlful2, nlful5, nlful9). The reason for this difference is unclear but could relate to the processing techniques by which the tin was introduced. However the condition of the silk may be more important as the samples which dissolved were very friable and powdery whereas those that remained insoluble were in good condition. It is possible, in the cases where the samples dissolved, that the silk actually formed a clear dispersion of the powdery sample, although the HPSEC results (chapter nine) indicate molecular weights similar to other samples which fully dissolved.

Tin had been identified in a number of the micro-samples, most of which formed part of the costume collection. Iron was also identified in two black tassels. Although removing the micro-samples helped identify wool and silk velvets and the presence of metallic elements, this limited the number of samples for HPSEC analysis. The HPSEC results show samples taken from objects on display (rather than objects in storage) had slightly higher weight-averaged molecular weights (M_w). This may reflect that the condition of objects in storage generally precludes their display. However there were no clear trends observed in the HPSEC results when compared to the visual condition of the textiles. It was hoped the NIR spectra could be correlated with the HPSEC analysis of accelerated aged samples to produce a model for the *in situ* condition of textiles. This could then be

compared with the analysis of the micro-samples, however as the model predictions were not satisfactory (see chapter eleven) this did not take place.

Brodsworth Hall Visit

The *in situ* visit to Brodsworth Hall took place over the 22nd and 23rd July 2008. NIR spectroscopy was carried out in the following rooms, the environmental conditions during the visit are given in brackets: South Hall (20 ± 1 °C, 63 ± 7% RH), Billiard Room (20 ± 1 °C, 68 ± 4% RH), Drawing Room (21 ± 0.5 °C, 68 ± 1% RH), Library (20 ± 1.5 °C, 58 ± 8% RH), North Hall ground floor (21 ± 1 °C, 60 ± 10% RH), Store (20.5 ± 1.5 °C, 63.5 ± 4.5% RH), Bedroom 8 (21 ± 1.5 °C, 61 ± 4% RH) and the Bedroom Corridor (21 ± 1 °C, 63 ± 3% RH). XRF analysis was carried out in the same rooms and at Fulford store on the 21st July 2008. Objects for analysis were selected prior to the visit based on the initial collections survey findings and results from analysis of the historic samples. The selection includes some displayed and stored costume items, velvets which could not be sampled but required identification, and silk upholstery and wall linings.

Figure 12.4 – NIR spectrometer *in situ* at Brodsworth Hall

NIR spectra were acquired using the same equipment (see Figure 12.4) and parameters as given in chapter eleven. XRF spectra were acquired using the same equipment and parameters as given in chapter three.

Previous Silk Condition Studies

Deuterium exchange studies on silk have demonstrated rapid exchange of the OH combination band at 5170 cm^{-1} arising from water. The intensity of this band, measured via NIR spectroscopy, was then used to derive moisture sorption profiles for unaged and aged silks. The moisture sorption profile is shown to change with ageing, with differences observed depending on the ageing method. A linear correlation is reported between the moisture content and intensity at 5170 cm^{-1} and

it is further suggested this parameter could be used as a condition marker for historic silks. A similar observation has been reported for linen[3].

The NIR spectral sorbed moisture parameter, I(5170) is shown to decline after ageing; with thermal ageing causing the most pronounced effect compared with sunlight ageing[4]. This is suggested to arise from changes to the intercrystalline amorphous regions of the silk fibroin upon ageing. The moisture parameter has been correlated with residual strength measurements and shows a good correlation[5], although the amount of data scatter is also dependent on the ageing method. However this parameter has not been used in this study as this peak was found to be affected by peaks arising from salt contamination at similar wavenumbers. The model used in chapter eleven limited the spectral region to 4100-5100 cm^{-1}, excluding this wavenumber.

Further correlations between tensile testing data and NIR spectra have been found by Richardson and Garside[6]. This demonstrates the use of NIR spectroscopy in combination with multivariate analysis to highlight areas of stress within silk artefacts. Although a preliminary study it is proposed that NIR spectroscopy could be used to analyse textiles on display that are at risk of physical stresses, such as hanging banners or costume on mannequins. This demonstrates that NIR spectroscopy has the potential to be used to monitor both the chemical and physical condition of silk as long as a suitable reference set was available.

Similar to the work by Richardson and Garside, the model in chapter eleven has used NIR spectroscopy to predict the tensile strength of test samples. By analysing objects *in situ* it is hoped to be able to demonstrate the potential of the model to predict the condition of the collection, using its tensile strength.

Analysis Results

XRF

Three sofas (one in the South Hall [90009615] and two in the Drawing Room [90008973 and 90008974]) were analysed with XRF in various positions, all of which identified tin, sometimes at trace levels (see Appendix 7). This suggests either some of the upholstery has been weighted or that tin was used as the mordant for these dyes. In modern reproduction upholstery fabrics weighted silk is not used[7] and tin has been reported as a mordant for red dyes[8] so it may be that it arises from a mordant rather than weighting. The absorbance recorded *in situ* at Brodsworth Hall gives greater Sn/Rh ratio values (>1) compared with the model samples (>0.4) used in chapter three, therefore it has not been possible to compare the values to determine if silk is definitely weighted. The sofa analysed in the South Hall also contained iron at trace levels, possibly due to also sampling an internal structure, as with crimson silk upholstery iron is unlikely to be a mordant or weighting agent due to the brown staining it causes.[9]

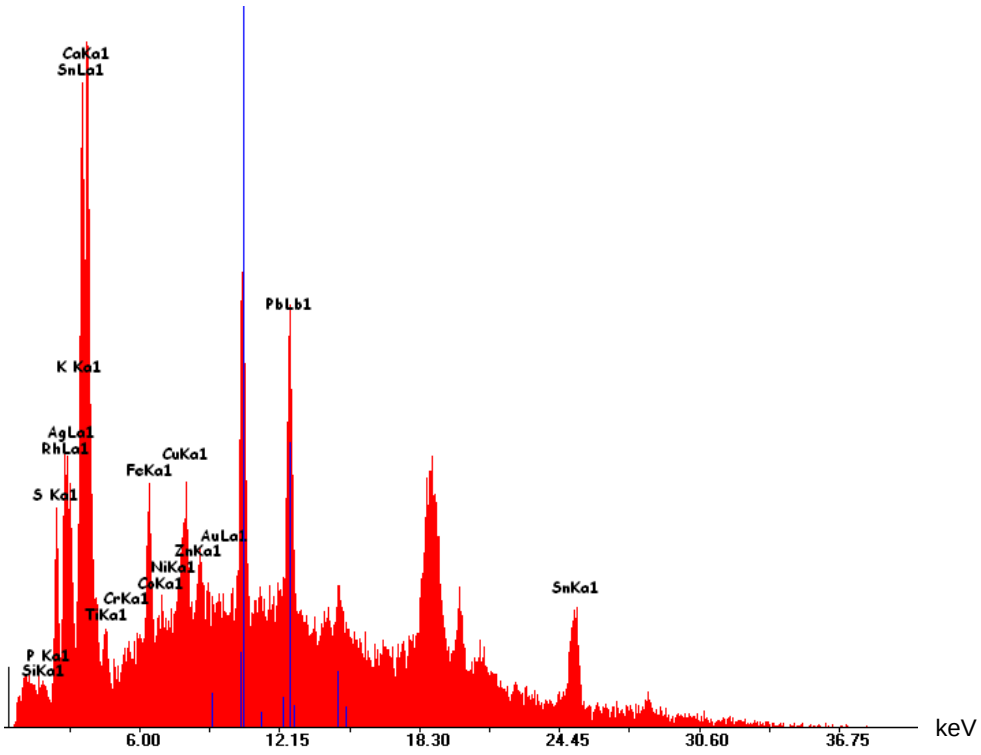

Figure 12.5 – XRF spectrum of Drawing Room sofa behind exit door (the software autoscales the maximum peak to 90% intensity)

For the sofa behind the exit door in the Drawing Room lead was also identified (see Figure 12.5) at trace levels, as well as the tin reported for the other sofas. Although other elements are labelled in the spectrum, when the element to rhodium peak area ratio is calculated the only other element present is sulfur at trace levels. Lead was used as a weighting agent; however this was the only sofa where lead was identified, so it may arise from another source such as dust. Lead was also identified in the wall silk in this area. Further lead was identified in the wall silk in the South Hall. As these panels are fixed it is not possible to determine what is beneath, but this may arise from lead paint on the underlying wall. However identifying the source of lead may be important due to the health and safety implications of lead dust.[10] The majority of panels of wall silk contained no metallic elements, although sulfur was observed in some areas.

Figure 12.6 – cummerbund set from Brodsworth Hall

Figure 12.7 – prize ribbon [90015011] from Brodsworth Hall

Metal threads can provide additional information on the status of objects, for example if threads on the cummerbund set (Figure 12.6) were gold or gilt it would imply greater expense than the brass threads identified. The *in situ* XRF facilitated identification of a large number of the metal threads within the Brodsworth Hall collection. Copper and zinc were identified in a number of objects, including metal threads on objects in store and the metal grille front on the cabinet in the north corridor [90009706]. One of these objects is a prize ribbon (see Figure 12.7), XRF analysis identified brass threads along with tin, silicon and phosphorus, in the silk ribbon indicating it is made from weighted silk. Results from objects at the Fulford store only identified iron on the black tassels [90006837 and 90006838].

NIR Identification

NIR spectroscopy can also be used for identification of materials as long as there is a sufficient database for the comparison of spectra. The identifications presented were done by Emma Richardson using the database compiled as part of her PhD studies, full results are listed in appendix 8. This confirmed that both the black and cream parasol displayed on the chaise in Bedroom Eight were made of silk as was the prize ribbon in Figure 12.7. The velvets on both the jockey chair and carpet beneath (see Figure 12.8) were both identified as wool velvet. This *in*

situ NIR spectroscopy and ATR on micro-samples from the collection identified most of the velvets as having a wool pile, although silk velvet was found noticeably on the picture frames in Bedroom Eight.

Figure 12.8 – velvets in the Billiard Room at Brodsworth Hall including jockey scales [90009340]

As there is a sampling depth of approximately 1 mm with the NIR spectrometer it was possible to identify both the padding beneath the upholstery as well as the upper layer. For all the Drawing Room, South Hall and Top Corridor sofas and ottomans which were analysed the upholstery (& if tested the gimp) were identified as silk, with a cellulosic layer over the padding material (Figures 12.9 and 12.10). Similarly the Drawing Room walls are silk lined with a cellulosic lining, in this case the replacement cotton wall panels directly opposite the windows were not tested.

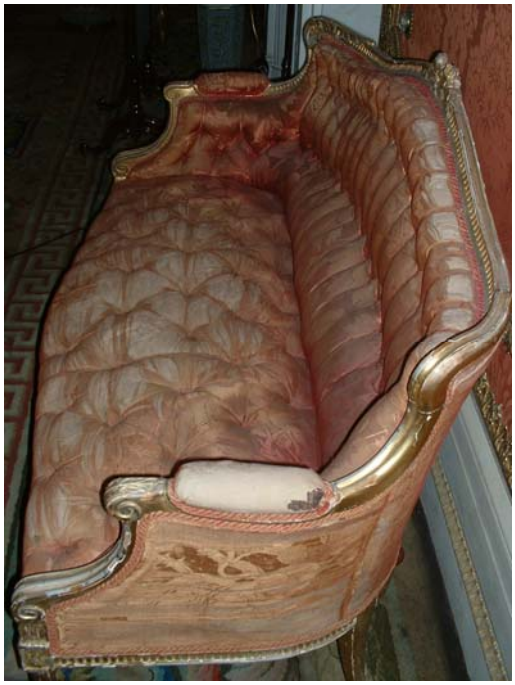

Figure 12.9 – sofa [90008973] with darker silk inside arm rest (back) and missing upholstery on rest and back (front)

Figure 12.10 – remaining crimson silk around button in upholstery, with exposed wefts at front

The difference between the spectra for the silk wall lining and the cellulosic padding layer can be seen in Figure 12.11. In this case the materials are clearly distinguishable, however sometimes further processing can be required to highlight the spectral differences for example, whether a material is wool, silk or nylon.

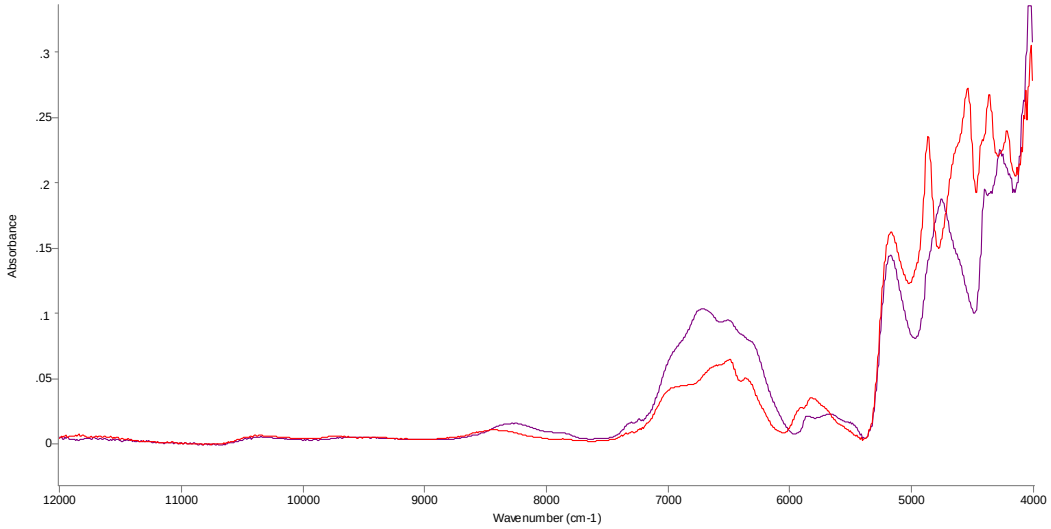

Figure 12.11 – NIR spectra of silk upholstery (red) and padding (purple)

NIR Comparison with MVA Model

The above section demonstrated it was possible to identify materials on display at Brodsworth Hall using NIR spectroscopy. However it was also hoped to use the NIR spectra to provide information on the tensile strength of the materials on display. The spectra acquired *in situ* from Brodsworth Hall were compared with the final model (PLS1-regression using NIR spectra limited to 4100-5100 cm^{-1} after spectral pre-processing using Norris gap 1^{st} derivative with gap window of 19 and then SNV transformation) from the MVA work (see chapter eleven).

As already mentioned the NIR spectrometer samples to a depth of 1 mm, although this can be useful for identification, it is likely to be problematic for prediction purposes, as the model has been built using the pure silk from the accelerated ageing samples. To overcome the potential that the spectra will contain more than silk and therefore the accuracy of the predictions be affected, the selected spectra were those which were clearly identifiable as silk with no further processing (such as subtractions) required. Although subtraction of padding materials can leave a spectrum which can be identified as silk, for comparison with the model these

spectra may be less suitable due to comparison with the model silk samples. These spectra, although obviously silk may still contain information from materials underneath, such as padding materials, which may still affect the predictions made by the model. However a larger number of samples, without further processing were preferable. This limited the number of spectra to thirty nine from a possible seventy five recorded *in situ* at Brodsworth Hall.

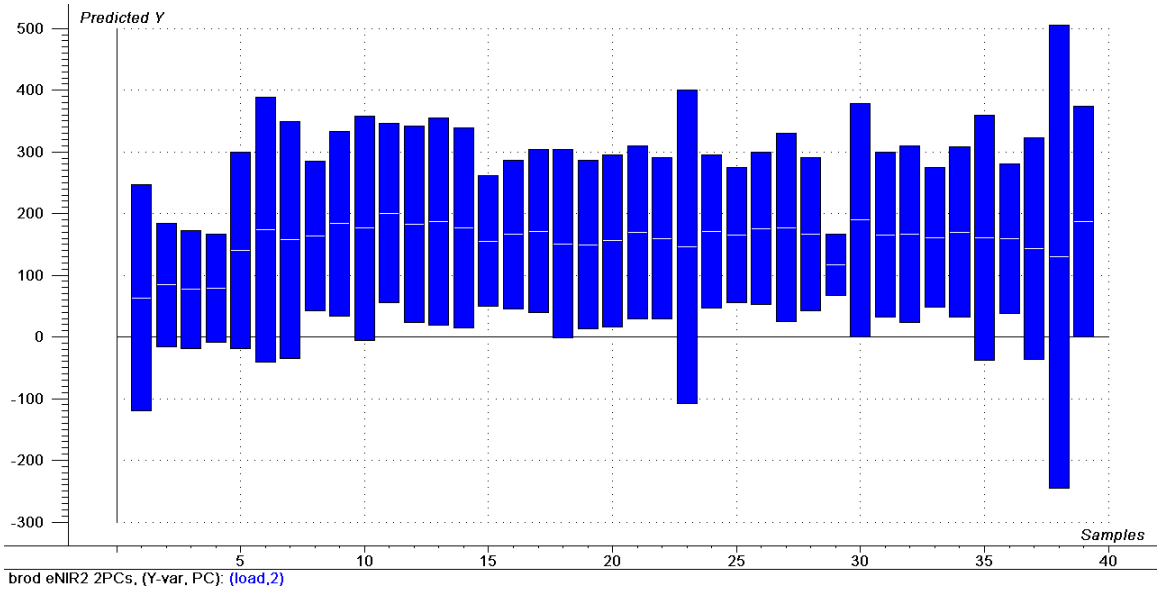

Figure 12.12 – predicted tensile strength (white line) of *in situ* NIR spectra with the deviation shown as a blue bar

The thirty nine NIR spectra collected from the objects have been used to predict the tensile strength from the model, using two principle components (see Figure 12.12). The predicted tensile strengths range from 63 N to 201 N, with a large deviation (the blue bars above and below the predicted value in Figure 12.12). Generally a large deviation indicates the predicted samples are substantially different to the calibration samples and that the predicted values are likely to be imprecise. Reinforcing this view is the fact that the unaged silk used in the accelerated ageing experiments had a tensile strength of ~160 N and approximately 60% of the spectra give predictions above this value. Therefore the model predictions are too high for silk that has been, in most cases, on display for

over 100 years. However these results can be used as a relative measure of the silks' tensile strength in terms of its condition.

To determine whether there was an underlying cause for the high predicted values of tensile strength the effect of colour and metallic elements identified using XRF was determined. As can be seen in Figure 12.13 dark colours give a rising baseline in the NIR spectra. However the model samples between 4100-5100 cm^{-1} and so this area should have little impact. To test this theory the raw, uncorrected NIR spectra were used in the model to predict the tensile strength. The predicted values were very similar with the greatest difference being 5 N, well within the deviation of the models. This indicated that the colour of the material analysed had little effect on the predicted values.

Figure 12.13 – rising baseline in NIR spectrum due to black colour of material

Metallic elements, in weighted silk or used as mordants, may also affect the NIR spectra recorded *in situ*. To determine whether metallic elements impact on the predicted tensile strength, the elements identified by the XRF were recorded next to the predicted values. No correlation could be observed between the presence of any particular element and the predicted tensile strength. In the NIR spectra there

are increases in the peak intensity at 5180 and 6970 cm^{-1}, in the weighted samples (see Figure 12.14). However as discussed above the model uses a limited spectral range and so these changes are unlikely to affect the predicted values.

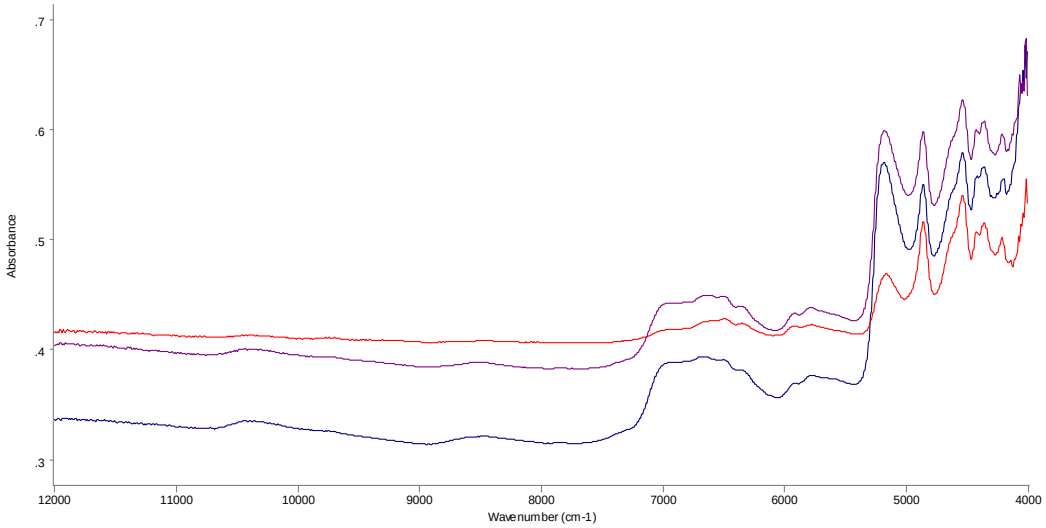

Figure 12.14 – effect of inorganic elements on NIR spectra
(unaged silk: red; weighted samples: blue and purple)

To further test the effect of metallic elements a PCA model of the thirty-nine NIR spectra from Brodsworth Hall was built (see Figure 12.15). There is a slight separation of some of the weighted samples (circled in Figure 12.15) even when using the limited spectral range, which indicates weighting may still have a slight effect on the predicted tensile strength values. However there is not a clear separation of weighted from unweighted materials, so NIR spectroscopy could not be used to identify weighted silks without further work to build suitable models. Extension of the spectral range above 7000 cm^{-1} to include the broad peak around this value in Figure 12.14 could also be beneficial for models to identify weighted silks.

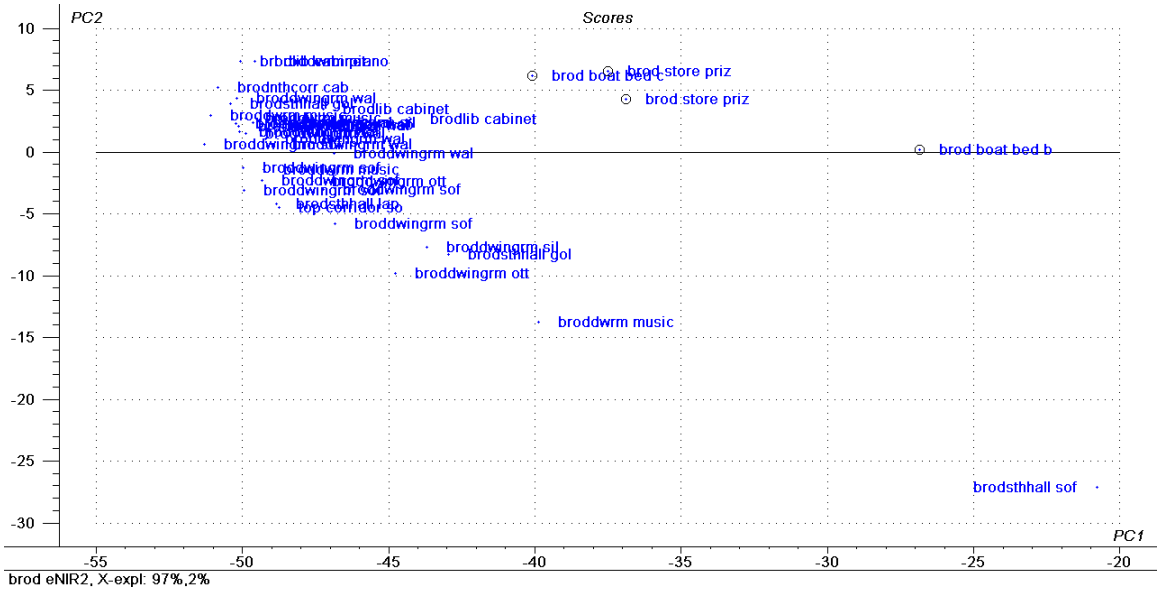

Figure 12.15 – scores plot of *in situ* NIR spectra from Brodsworth Hall

Although the predicted values of tensile strength are too high, the reasons for this do not seem to simply relate to the colour or processing of the silk. As a result the predicted tensile strength cannot be used as exact values however it is possible to rank the samples against each other. As discussed in chapter ten there are many measures of lifetimes for materials, although these are not exact values they provide a means to compare different display environments. Therefore although it is not possible to give an actual remaining strength the values could instead be used to scale the condition of objects.

When the predicted tensile strength values are ranked in order, it can be seen that the lowest predicted values are for objects where the silk was visibly shattered and in poor condition, for example the parasol silk and ribbon fragments. There are some further trends; samples described as shattered had lower predicted strength than those described as good or very good condition. Interestingly faded samples generally give higher predicted values than the unfaded areas. For example the wall next to the exit door in the Drawing Room, the faded area prediction was 170 N, whereas the unfaded area was 160 N, although as the deviation in the model is large these are tentative observations at best. However it demonstrates the model

could be used to compare the condition of samples and rank those which are in the poorest condition and prioritise treatments. With further work to build a more comprehensive model it may be possible to make improved predictions of the silks' condition.

Possible Condition Analysis Results

Three objects have been taken as examples to demonstrate how these results might relate to those presented in chapters' eight to ten. The cream parasol gave a relatively low tensile strength prediction (~84 N) which would indicate the object is around 120 years old using the silk deterioration curve in chapter ten. The curve would also indicate the molecular weight is approximately 105 kDa, although the sample from this object (nlbro9) did not dissolve in lithium thiocyanate and so the HPSEC data cannot be compared. The approximate age is roughly correct however this object has one of the lowest predicted tensile strengths from the model.

The curtain braid from the portiere curtains had a predicted tensile strength of 143 N, which would give an age of approximately 20 years and molecular weight of 180 kDa from the silk deterioration curve. Analysis of fragments from these curtains [90007051/53/63/67] gave a wide range of molecular weights (268 kDa to 479 kDa) which are much higher than the predicted molecular weight, although the object is much older than the suggested age. This highlights the problems with both the HPSEC results and the predicted tensile strength values. This is further demonstrated by the predicted tensile strength of the library cabinet silk front [90006945] which was 190 N. This is 30 N above the value for unaged silk and so values for the condition cannot be predicted.

Currently the silk deterioration curve cannot be used with the predicted tensile strength values as these are too high. However with further analysis of collections and an expanded reference set the model, and therefore its predictions, could be

improved. One of the problems of trying to correlate the age of an object with its condition is the unknown previous display and treatments of the object. Conservation treatments or poor display and storage conditions could affect both the condition of the object and the analytical determination of molecular weight, for example consolidants may affect the solubility of silk. Therefore predictions of future display lifetimes will always be limited by these unknown previous histories.

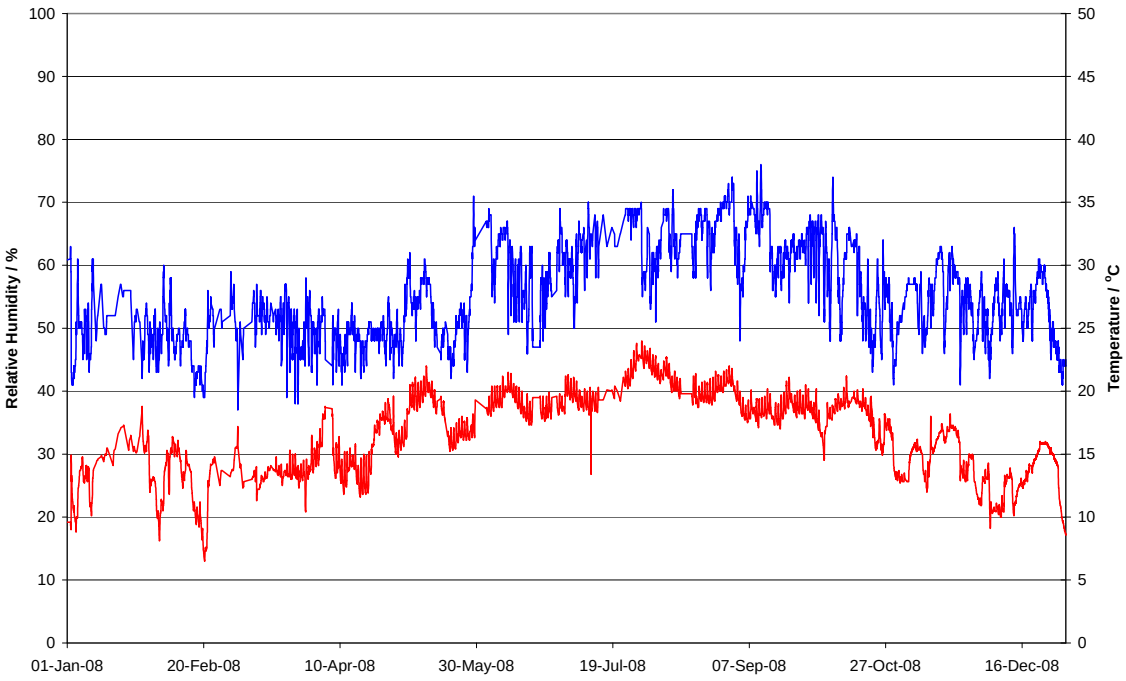

Figure 12.16 – environmental monitoring data for the Drawing Room at Brodsworth Hall in 2008 (RH: blue; temperature: red)

Potential Preventive Conservation Measures

Changes to the environment at Brodsworth Hall are likely to impact on the other objects on display. Figure 12.16 shows the environmental monitoring data for the Drawing Room at Brodsworth Hall during 2008, one of the rooms with a large amount of silk. It can be seen that the humidity is relatively high, particularly between May and October when it can reach almost 70% RH. There are two possible methods to reduce the humidity. One would be to increase the

temperature, however as shown by the kinetics reactions this would also increase the rate of deterioration. For example, when the room is at 21 °C and 70% RH, to decrease the RH to 50% would require a temperature increase of 5.5 °C. This would increase the rate of deterioration by approximately 1.4 times, which is equivalent to the decrease in deterioration rate caused by reducing the RH, as reported by other authors.[11] The other method would be the use of dehumidification however this could impact on other objects within the room such as the piano, as well as affecting the aesthetics of the room.

Dehumidifiers can either be manually emptied or plumbed into a drain. The first requires careful checks to ensure the tank is not full and also when emptying to prevent spillages onto wooden floors or carpets which can create staining. The second requires a suitable drainage point being available and a discrete position which is still effective for dehumidifying the room. For these reasons dehumidifiers are rarely used in display rooms at English Heritage and tend to be more suitable for storage rooms. Analysis of the data from Brodsworth Hall indicates that the low temperatures are more beneficial, than the deterioration from the higher humidities (higher TWPI values are calculated for this property) and so changes may be unnecessary.

Conclusions

The *in situ* XRF analysis has allowed identification of materials which could not be sampled or underlying materials to be highlighted for example the presence of lead. The *in situ* XRF also enabled the identification of a large number of metal threads within the Brodsworth Hall collection with the majority made from brass.

The *in situ* NIR spectroscopy has found most of the velvets on display at Brodsworth Hall have a wool pile. The study also provided identification of the padding materials which could not be sampled. Both sets of results aid the curators' interpretation of the collection and its status based on the materials used.

However the predictive model using the NIR spectra gave tensile strength values which were too high for objects on display for over 100 years.

The reason for the models inaccurate predictions probably relates to the contamination of the spectra by underlying materials such as padding. There may also be an effect from changes to the weave structure, mixed materials used in the weave, for example ATR identified cotton wefts in some of the silk sofa upholstery, and previous treatments including nylon netting. However the model can be used to rank condition of objects which matched the observed visual condition of objects during the property survey. It may also be possible to use the predicted values as benchmarks with which to compare later predictions from further NIR analysis.

To improve the predictions from the model, a greater variety of silks including different weave structures and mixed fibre weaves as well as treated textiles could give more accurate predictions of the silks' tensile strength as a measure of its condition. The model could also be further developed to enable the identification of weighted silks, which is not currently possible.

References

[1] Zhang, X. and Wyeth, P. (2007) 'Moisture Sorption as a Potential Condition Marker for Historic Silks: Noninvasive Determination by Near-Infrared Spectroscopy' *Applied Spectroscopy* **61(2)** 218-222.

[2] Tse, S. and Dupont, A.-L. (2001) 'Measuring Silk Deterioration by High-Performance Size-Exclusion Chromatography, Viscometry, and Electrophoresis' *Historic Textiles, Papers, and Polymers in Museums* Cardamone, J. M. and Baker, M. T. (ed.) ACS Symposium Series **779** Washington DC: American Chemical Society 98-114.

[3] Wyeth, P. (2005) 'Signatures of ageing: correlations with behaviour' *Scientific Analysis of Ancient and Historic Textiles AHRC Research Centre for Textile*

Conservation and Textile Studies First Annual Conference 13-15 July 2004Postprints Janaway, R. and Wyeth, P. (ed.) 137-142.

[4] Kim, J.-J. and Wyeth, P. (2009) 'Towards a routine methodology for assessing the condition of historic silk' *e-Preservation* **6** 60-67.

[5] Richardson, E., Martin, G., Wyeth, P. and Zhang, X. (2008) 'State of the art: non-invasive interrogation of textiles in museum collections' *Microchimica Acta* **162** 303-312.

[6] Richardson, E. and Garside, P. (2009) 'The Use of Near Infrared Spectroscopy as a Diagnostic Tool for Historic Silk Artefacts' *e-Preservation Science* **6** 68-74.

[7] Humphries, R. personal communication, 12/10/2007.

[8] Hacke, M., Hallett, K., Peggie, D., Quye, A. and Vanden Berghe, I. (2009) 'Model Tapestries' *'Wrought in Gold and Silk' Preserving the Art of Historic Tapestries* Quye, A., Hallett, K. and Herrero Carretero, C. (ed.) Edinburgh: National Museums Scotland Enterprises Ltd – Publishing 54-73.

[9] Hacke, M. (2008) 'Weighted silk: history, analysis and conservation' *Reviews in Conservation* **9** 3-15.

[10] http://www.sigmaaldrich.com/MSDS/MSDS/DisplayMSDSPage.do accessed 05/10/2009.

[11] Michalski, S. (2002) 'Double the life for each five-degree drop, more than double the life for each halving of relative humidity' *ICOM Committee for Conservation 13th Triennial Meeting, Rio de Janeiro, 22-27 September 2002 Preprints* Vontobel, R. (ed.) London: James & James **1** 66-72.

Conclusions

1. The English Heritage collection includes over 1000 objects with silk from which a sub-set of 100 objects were selected and micro-samples taken to provide information on the condition of the silk. Elemental analysis of the micro-samples identified the presence of tin in around 10% of the samples indicating the original objects may be made of weighted silk. A large number of silver and brass metal threads were also identified as decoration on the silk textiles. Within the English Heritage collection there are a large number of velvet objects and identification of silk velvets was particularly difficult when in a poor condition. Determination of the condition of the historic silk samples using HPSEC demonstrated the accelerated ageing experiments caused similar levels of deterioration to objects which have been naturally aged. Generally light aged samples had slightly higher molecular weights than the historic materials whereas the thermally aged samples were generally lower. However processing of the results from the historic samples was affected by the very small size of some samples, which meant the HPSEC software struggled to place a baseline and integrate the peak area.

2. HPSEC has been used to analyse the historic micro-samples from the English Heritage collection and the accelerated ageing samples. Although initial HPSEC method development provided repeatable chromatograms and molecular weights for unaged samples, problems between different runs, methods and calibrations have occurred. Dynamic light scattering (DLS) has confirmed the calibration standards are not denatured under the HPSEC operating conditions used, as seen in the chromatograms. This means the HPSEC results give higher molecular weights than reported for samples analysed during MODHT. To overcome the problems data was corrected using the lithium thiocyanate peak and a standard method file; however some normalisation of the data using samples run before and after calibration was still required. HPSEC is best suited to the analysis of a small number samples which can be run as a group,

3. Sampling of the same thread from both the front and back of the Dudley Armorial tapestry from the Burrell Collection has been possible. The samples taken from the front of the tapestry were faded in comparison to the same thread on the reverse of the tapestry. However HPSEC analysis of the small number of yellow threads taken from the tapestry demonstrated that the condition of the silk is similar regardless of the level of fading. This is a strong indication from historic materials that light is not the sole cause of deterioration for silk textiles, although this is a separate reaction to the fading which has occurred.

4. The kinetics experiments have indicated the activation energy is approximately 50 kJ mol^{-1} for silk deterioration. This indicates an increase in the rate of reaction of 33 times when ageing at 80 °C, compared to a room temperature of 20 °C (taken from the average temperature at the English Heritage properties studied). However the limited number of samples and small range of RH levels tested could be expanded to improve the accuracy of this prediction. Similarly improved analysis of the samples, using more sensitive techniques may also increase the accuracy and reduce the errors in this calculation.

5. Longer term accelerated ageing experiments have been used to study silk deterioration, using light and thermal ageing at a range of RH levels. The experimental conditions led to some unexpected deterioration including loss of material for samples in contact with the metal shelf in the humidity oven. The rate of silk deterioration was also accelerated for samples which were contaminated by the saturated salt solutions used to create the RH environment,

6. Accelerated ageing experiments on model materials have suggested the following preventive conservation measures would increase the lifetime of silk on open display in historic houses: reducing the RH below 50% (to a minimum of 30% RH), lower temperatures and exclusion of UV radiation. Environmental monitoring behind tapestries has identified the formation of high RH microclimates. As high RH particularly increases the rate of silk deterioration, mitigation of these microclimates would be beneficial for the longevity of textiles. Methods to ensure textiles are not contaminated by salt, i.e. the use of barrier layers if hung on walls with salt efflorescence would also increase the display lifetime of the textiles. As there is little difference between the condition of samples after light ageing at 50 lux or 200 lux, it may be possible to increase display light levels if the dyes are unlikely to fade any further.

7. The experimental results have been used to plot a theoretical silk deterioration curve, which relates the age of samples, taken from the age of the historic materials, to the molecular weight and tensile strength, taken from the

8. The applicability of near-infrared (NIR) spectroscopy to predict the tensile strength of model samples has been demonstrated with the use of a suitable multivariate analysis (MVA) model. However due to the problems with the HPSEC data, an accurate prediction of the molecular weight of samples was not possible. The MVA model enables the accelerated ageing results obtained using destructive analytical techniques to be compared with a non-invasive and non-destructive method (NIR). The model was used to predict the tensile strength of objects on display at Brodsworth Hall. Although the magnitude of the tensile strength exceeds that for samples which have been on display for over 100 years, the samples condition could be ranked using the predictions. Therefore the results could be used to prioritise interventive conservation treatments or highlight where preventive conservation could be improved. NIR spectroscopy was also used to identify some materials which could not be sampled, particularly velvets.

Further Work

1. Although analysis identified the presence of elements within textiles, it was more difficult to determine the process that introduced the identified elements, i.e. mordanting or weighting. Calibration of the XRF with textile standards could improve the quantification of elements in silk and provide a means of determining the previous processing a textile has undergone. This would be useful for conservators and provide a simple way to identify materials which may be likely to rapidly deteriorate, for example heavily weighted or bleached silks.

2. The accelerated ageing of samples has indicated that decreasing the RH causes less deterioration. However low RH levels are generally reported to lead to embrittlement for a range of organic materials. Analysis of textiles was carried out in the middle RH region so samples aged in low RH environments had equilibrated to the higher RH. It may be of interest to analyse materials at a range of RH levels both before and after ageing to determine if embrittlement has occurred. This would also confirm whether low RH environments (below 30% RH) may be appropriate for the display of textiles or if it would lead to embrittlement and desiccation of the textile.

3. A number of difficulties have affected the HPSEC results. The data could be reinterpreted by digitising the chromatograms and calculating the peak area independently, or importing the raw chromatogram into the MVA software. This would also improve the possibility of the MVA model to predict the molecular weight of samples from NIR spectra. The MVA software would also be able to analyse the full wavelength region collected during HPSEC analysis rather than just the discrete channel at 280 nm. This may highlight other changes occurring which are not currently observed. Another possibility would be to calibrate the HPSEC using alternative standards, such as polystyrene, which although different to protein standards would not be expected to dissociate and therefore give greater confidence in the calibration files.

4. Accelerated ageing experiments used a plain weave, modern silk as an exemplar for the materials within the English Heritage collection. However it is possible the critical deterioration factors and activation energies vary for weighted silks and mixed material weave structures. For example silk velvets often show complete loss of pile for areas exposed to light compared to protected areas, so light deterioration might be more important for these textiles than the plain weave silk tested. The inclusion of other materials would also improve the ability of the MVA models to predict the condition of silk for real objects from the NIR spectra. The prediction of the model could also be improved by acquiring *in situ* spectra without sampling the materials behind, for example padding materials on upholstered furniture. Although this would be quite difficult, reflecting aluminium foil could be gently placed behind the silk where splits are present in the upper silk layer.

5. A large number of the accelerated ageing samples were affected by salt contamination during the experiments. This affects the analysis and interpretation of the data as seen in the MVA models. Although ageing in the humidity oven also caused unexpected loss of areas in contact with the metal shelf, it may be possible to age the samples in the humidity oven using a different experimental set up and prevent contamination of the silk. This would further improve the understanding of the RH effect on silk deterioration as well as the predictions from the MVA model.

Bibliography

Adelstein, P. Z. (1981) 'Stability of Processed Polyester Base Photographic Films' *Journal of Applied Photographic Engineering* **7 (6)** 160-167.

Adelstein, P. Z., Reilly, J. M., Nishimura, D. W. and Erbland, C. J. (1992) 'Stability of Cellulose Ester Base Photographic Film: Part 1 – Laboratory Testing Procedures' *Society of Motion Picture and Television Engineers (SMPTE) Journal* 336-346.

Adelstein, P. Z., Reilly, J. M., Nishimura, D. W. and Erbland, C. J. (1992) 'Stability of Cellulose Ester Base Photographic Film: Part 2 – Practical Storage Considerations' *Society of Motion Picture and Television Engineers (SMPTE) Journal* 347-353.

Adelstein, P. Z., Reilly, J. M., Nishimura, D. W. and Erbland, C. J. (1995) 'Stability of Cellulose Ester Base Photographic Film: Part 3 – Measurement of Film Degradation' *Society of Motion Picture and Television Engineers (SMPTE) Journal* **104** 281-291.

Adelstein, P. Z., Reilly, J. M., Nishimura, D. W. and Erbland, C. J. (1995) 'Stability of Cellulose Ester Base Photographic Film: Part 4 – Behavior of Nitrate Base Film' *Society of Motion Picture and Television Engineers (SMPTE) Journal* **104** 359-369.

Adelstein, P. Z., Reilly, J. M., Nishimura, D. W., Erbland, C. J. and Bigourdan, J. L. (1995) 'Stability of Cellulose Ester Base Photographic Film: Part 5 – Recent Findings' *Society of Motion Picture and Television Engineers (SMPTE) Journal* 439-447.

Agarwal, D., Sen, K. and Gulrajani, M. L. (1996) 'Formation of crosslinks in silk by bifunctional reactive dyes: effect on solubility and mechanical properties' *Journal of the Society of Dyers and Colourists* **112** 321-325.

Ambrose, E. J. and Elliott, A. (1951) 'Infra-red Spectra and Structure of Fibrous Proteins' *Proceedings of the Royal Society of London. Series A Mathematical and Physical Sciences* **206 (1085)** 206-219.

Anon. (1985) *Identification of Textile Materials* 7th Edition Manchester: The Textile

Institute.

Asakura, T., Iwadate, M., Demura, M. and Williamson, M. P. (1999) 'Structural analysis of silk with ^{13}C NMR chemical shift contour plots' *International Journal of Biological Macromolecules* **24** 167-171.

Asakura, T., Nakazawa, Y., Ohnishi, E. and Moro, F. (2005) 'Evidence from ^{13}C solid-state NMR spectroscopy for a lamella structure in an alanine-glycine copolypeptide: A model for the crystalline domain of *Bombyx mori* silk fiber' *Protein Science* **14** 2654-2657.

Asakura, T., Okonogi, M., Nakazawa, Y. and Yamauchi, K. (2006) 'Structural Analysis of Alanine Tripeptide with Antiparallel and Parallel β-Sheet Structures in Relation to the Analysis of Mixed β-Sheet Structures in *Samia cynthia ricini* Silk Protein Fiber Using Solid State NMR Spectroscopy' *Journal of the American Chemical Society* **128** 6231-6238.

Asakura, T., Suita, K., Kameda, T., Afonin, S. and Ulrich, A. S. (2004) 'Structural role of tyrosine in *Bombyx mori* silk fibroin studied by solid-state NMR and molecular mechanics on a model peptide prepared as silk I and II' *Magnetic Resonance in Chemistry* **42** 258-266.

Ashley-Smith, J. (1999) *Risk Assessment for Object Conservation* Oxford: Butterworth-Heinemann.

Asquith, R. S., Otterburn, M. S. and Sinclair, W. J. (1974) 'Isopeptide Crosslinks – Their Occurrence and Importance in Protein Structure' *Angewandte Chemie International Edition* **13(8)** 514-520.

Balasundaram, D., Selvisabhanayakam, and Mathivanan, V. (2009) 'Studies on Comparative Feed Efficacy of MR2 Variety Mulberry Leaves and MR2 Treated with Vitamin B-6 on *Bombyx mori* (L.) in Relation to Cocoon Weight and Silk Traits' *Journal of Experimental Zoology India* **12 (1)** 187-190.

Ballard, M., Koestler, R. J. and Indicator, N. (1986) 'Weighted Silks Observed Using Energy Dispersive X-ray Spectrometry' *Scanning Electron Microscopy* **2** 499-506.

Ballard, M., Koestler, R. J., Blair, C. and Indicator, N. (1989) 'Historical Silk Flags Studied by Scanning Electron Microscopy – Energy Dispersive X-ray

Spectrometry', in *Archaeological Chemistry IV*, Advances in Chemistry Series No 220 Washington DC: American Chemical Society 419-428.

Ballard, M., Koestler, R. J., Blair, C. Santamaria, C. and Indicator N (1989) 'Historic Silk Flags from Harrisburg' in *Historic Textile and Paper Materials II, Conservation and Characterisation*, Developed from a Symposium by the Cellulose Paper and Textile Division at the 196th National Meeting of the American Chemical Society Washington DC: American Chemical Society 134-142.

Ballard, M., Koestler, R. J. and Indicator, N. (1990) 'Recent results concerning the degradation of historic silk flags' *ICOM Committee for Conservation 9th Triennial Meeting Dresden, Germany, 26-31 August 1990 Preprints* Paris: ICOM Committee for Conservation 277-282.

Bamford, C. H. and Dewar, M. J. S. (1949) 'Photosensitisation and Tendering by Vat Dyes' *Journal of the Society of Dyers and Colourists* **65** 674-681.

Beaven, G. H. and Holiday, E. R. (1952) 'Ultraviolet Absorption Spectra of Proteins and Amino Acids' *Advances in Protein Chemistry* **7** 319-386.

Becker, M. A. and Tuross, N. (1992) 'Novel Approaches for Assessing the Preservation of Historic Silks: A Case Study of the First Ladies' Gowns' *Materials Research Society Bulletin* **17** 39-44.

Becker, M. A., Hersh, S. P. and Tucker, P. A. (1987) 'The Influence of Tin Weighting Agents on Silk Degradation Part 1 Inorganic Weighting and Mordanting Agents in Some Historic Silk Fabrics of the 18th and 19th Centuries' *ICOM Committee for Conservation 8th Triennial Meeting, Sydney, Australia, 6-11th September 1987, Preprints* Marina del Ray, C.A.: Getty Conservation Institute **1** 339-344.

Becker, M. A., Hersh, S. P. and Tucker, P. A. (1989) 'The Stabilization of Silk to Light and Heat' *Historic Textile and Paper Materials II – Conservation and Characterization* Zeronian, S. H. and Needles, H. L. (ed.) Advances in Chemistry Series No. 410 Washington DC: American Chemical Society 94-107.

Becker, M. A., Magoshi, Y., Sakai, T. and Tuross, N. C. (1997) 'Chemical and

Physical Properties of Old Silk Fabrics' *Studies in Conservation* **42** 27-37.

Becker, M. A., Willman, P. and Tuross, N. C. (1995) 'The U.S. First Ladies Gowns: A Biochemical Study of Silk Preservation' *Journal of the American Institute of Conservation* **34** 141-152.

Bergmann, W. (1939) 'Facts and Theories Concerning the Formation of Natural Silk' *Textile Research* **9** 329-342.

Bergmann, W. (1940) 'Relations Between the Food and Silk of Silkworms' *Textile Research* **10** 462-475.

Beste, L. F. and Hoffman, R. M. (1950) 'A qualitative study of resilience' *Textile Research Journal*, **20 (7)** 441-453.

BioSep brochure http://www.phenomenex.com/WorkArea/showcontent.aspx?id=8143 accessed 31/07/2009.

Bloustine, J., Berejnov, V. and Fraden, S. (2003) 'Measurements of Protein-Protein Interactions by Size Exclusion Chromatography' *Biophysical Journal* **85** 2619-2623.

Bokobza, L. (2002) 'Origin of Near-Infrared Absorption Bands' in *Near-Infrared Spectroscopy Principles, Instruments, Applications* Siesler, H. W., Ozaki, Y., Kawata, S. and Heise, H. M. (ed.) Weinheim: Wiley-VCH 11-41.

Bora, M. N., Baruah, G. C. and Talukdar, C. L. (1993) 'Investigation on the Thermodynamical Properties of Some Natural Silk Fibres with Various Physical Methods' *Thermochimica Acta* **218** 425-434.

Borsacchi, S., Cappellozza, S., Catalano, D., Geppi, M. and Ierardi, V. (2006) 'Solid State NMR Investigation of the Molecular Dynamics of Cocoon Silks Produced by Different *Bombyx mori* (Lepidoptera) Strains' *Biomacromolecules* **7** 1266-1273.

Boulet-Audet, M., Lefèvre, T., Buffeteau, T. and Pézolet, M. (2008) 'Attenuated Total Reflection Infrared Spectroscopy: An Efficient Technique to Quantitatively Determine the Orientation and Conformation of Proteins in Single Silk Fibers' *Applied Spectroscopy* **62 (9)** 956-962.

Breese, R. R. and Goodyear, G. E. (1986) 'Fractography of Historic Silk Fibers' in

Historic Textile and Paper Materials Conservation and Characterization Needles, H. L. and Zeronian, S. H. (ed.) American Chemical Series 212 Washington: American Chemical Society 95-109.

Brereton, R. G. (2003) *Chemometrics Data Analysis for the Laboratory and Chemical Plant* Chichester: Wiley.

Bresee, R. R. and Telthorst, L. A. (1982) 'Energy dispersive X-ray fluorescence and neutron activation analysis of historic silk textiles' CCI Unpublished Technical report.

Brill, T. B. (1980) *Light, Its Interaction with Art and Antiquities* New York: Plenum Press.

Brooks, M. M., O'Connor, S. and McDonnell, J. G. (1996) 'The Application of Low-energy X-radiography in the Examination and Investigation of Degraded Historic Silk Textiles: Preliminary Report', *ICOM Committee for Conservation 11th Triennial Meeting Edinburgh, Scotland, 1-6 September 1996 Preprints* London: James and James (Science Publishers) **2** 670-679.

BS EN 20139:1992 ISO 139:1973 Textiles – Standard Atmospheres for Conditioning and Testing.

BS EN ISO 13934-1:1999 Textiles. Textile properties of fabrics. Determination of maximum force and elongation at maximum force using the strip method.

Bühner, M. and Sund, H. (1969) 'Yeast Alcohol Dehydrogenase: - SH Groups, Disulfide Groups, Quaternary Structure, and Reactivation by Reductive Cleavage of Disulfide Groups' *European Journal of Biochemistry* **11** 73-79.

Cai, Z. and Qiu, Y. (2003) 'Using an Aqueous Epoxide in Bombyx mori Silk Fabric Finishing' *Textile Research Journal* **73(1)** 42-46.

Cai, Z., Jiang, G. and Qiu, Y. (2004) 'Chemical Modification of Bombyx Mori Silk with Epoxide EPSIB' *Journal of Applied Polymer Science* **91** 3579-3586.

Cai, Z., Jiang, G. and Yang, S. (2001) 'Chemical finishing of silk fabric' *Coloration Technology* **117** 161-165.

Carboni, P. (1952) *Silk, Biology, Chemistry and Technology* Walter, K. (transl.) London: Chapman and Hall.

Carlene, P. W. (1944) 'The Moisture Relations of Textiles. A Survey of the

Literature' *Journal of the Society of Dyers and Colourists* **60** 232-237.

Carr, C. M. (2006) 'Monitoring of Damage to Historic Tapestries (MODHT) EVK4-2001-00048 Final Report'.

Chen, X., Shao, Z., Marinkovic, N. S., Miller, L. M., Zhou, P. and Chance, M. R. (2001) 'Conformation transition kinetics of regenerated *Bombyx mori* silk fibroin membrane monitored by time-resolved FTIR microscopy' *Biophysical Chemistry* **89** 25-34.

Cheung, H.-Y., Lau, K.-T., Zhao, Y.-Q. and Lu, J. (2008) 'Tensile Properties of Different Silkworm Silk Fibers' *Advanced Materials Research* **47-50** 1213-1216.

Chevillard, M., Couble, P. and Prudhomme, J.-C. (1986) 'Complete Nucleotide Sequence of the Gene Encoding the *Bombyx mori* Silk protein P25 and Predicted Amino Acid Sequence of the Protein' *Nucleic Acids Research* **14 (15)** 6341-6342.

Ciferri, O., Becker, M. E. and de Rossi, E. (2003) 'Characterization of Bacteria Isolated from Naturally Aged Silk Fibroin' *Art, Biology, and Conservation: Biodeterioration of Works of Art The Metropolitan Museum of Art, New York* Koestler, R. J., Koestler, V. H., Charola, A. E. and Nieto-Fernandez, F. E. (ed.) New Haven: Yale University Press 191-207.

Cleve, E., Bach, E. and Schollmeyer, E. (2000) 'Using chemometric methods and NIR spectrophotometry in the textile industry' *Analytica Chimica Acta* **420** 163-167.

Collections Conservation Research Plan, Internal English Heritage report (2006)

Couble, P., Chevillard, M., Moine, A., Ravel-Chapuis, P. and Prudhomme, J.-C. (1985) 'Structural Organization of the P_{25} gene of *Bombyx mori* and Comparative analysis of it 5' flanking DNA with that of the Fibroin Gene' *Nucleic Acids Research* **13 (5)** 1801-1814.

Cowie, J. M. G. (1997) *Polymers: Chemistry and Physics of Modern Materials 2nd Edition* London: Chapman and Hall.

Crick, F. H. C. and Kendrew, J. C. (1957) 'X-ray Analysis and Protein Structure' *Advances in Protein Chemistry* **12** 133-214.

Crighton, J. S., (1993), 'Silk: a Study of its Degradation and Conservation' in *Conservation Science in the UK* Tennent, N. H. (ed.) 96-98.

D'Olier, A. A. and Mack, P. B. (1936) 'The Effect of Darkroom Storage on Unweighted and Tin Weighted Silk – Paper III' *Rayon and Melliand Textile Monthly* **17** 102.

Dai, C.-A., Kramer, E. J., Washiyama, J. and Hui, C.-Y. (1996) 'Fracture Toughness of Polymer Interface Reinforced With Diblock Copolymer: Effect of Homopolymer Molecular Weight' *Macromolecules* **29 (23)** 7536-7543.

Daniels, V. and Leese, M. (1995) 'The Degradation of Silk by Verdigris' *Restaurator* **16** 45-63.

Das, S. (2008) 'Structure, Property, and Relaxation Behaviour of Mulberry (*Bombyx mori*) and Tasar (*Antheraea Mylita*) Silk' *Journal of Natural Fibers* **5 (3)** 218-226.

Denny, M. W. (1980) 'Silks – their Properties and Functions', in *The Mechanical Properties of Biological Materials* (*Symposia of the Society for Experimental Biology*) **34** Vincent J. F. V. and Currey, D. J. (eds.) New York: Cambridge University Press 247-272.

Dicko, C., Vollrath, F. and Kenney, J. M. (2004) 'Spider Silk Protein Refolding Is Controlled by Changing pH' *Biomacromolecules* **5** 704-710.

Ding, H. Z. and Wang, Z. D. (2007) 'Time-temperature superposition method for predicting the permanence of paper by extrapolating accelerated ageing data to ambient conditions' *Cellulose* **14** 171-181.

Drummy, L. F., Farmer, B. L. and Naik, R. R. (2007) 'Correlation of the β-sheet crystal size in silk fibers with the protein amino acid sequence' *Soft Matter* **3** 877-882.

Drummy, L. F., Phillips, D. M., Stone, M. O., Farmer B. L. and Naik, R. R. (2005) 'Thermally Induced α-Helix to β-Sheet Transition in Regenerated Silk Fibers and Films' *Biomacromolecules* **6** 3328-3333.

Durasevic, V., Machnowski, W. and Kotlinska, A. (2008) 'Dyeing Behaviour of Differently Degummed Silk Fibers' *4th International Textile Clothing and Design Conference Book of Proceedings 5-8th October 2008 Dubrovnik,*

Croatia Dragcevic, Z. (ed.) 341-346.

Dussubieux, L. and Ballard, M. W. (2005) 'Using ICP-MS to Detect Inorganic Elements in Organic Materials: A New Tool to Identify Mordants of Dyes on Ancient Textiles' *Materials Issues in Art and Archaeology VII* Materials Research Society Symposium Proceedings **852** Warrendale PA: Materials Research Society 291-296.

Dussubieux, L., Naedel, D., Cunningham, R., Alden, H. and Ballard, M. W. (2005) 'Accuracy, Precision and Investigation: mordant analysis on Antique Textiles by Various Methods' *ICOM Committee for Conservation 14th Triennial Meeting, The Hague, 12-16th September 2005 Preprints* Verger, I. (ed.) London: James & James Ltd **2** 898-903.

Earland, C. and Robins, S. P. (1973) 'A Study of the Cystine Residues in Bombyx mori and Other Silks' *International Journal of Peptide and Protein Research* **5** 327-335.

Earland, C. and Stell, J. G. P. (1957) 'The Reaction of Silk Fibroin with Oxidizing Agents' *Biochimica et Biophysica Acta* **23** 97-102.

Earland, C. and Stell, J. G. P. (1966) 'Formation of New Crosslinkages in Proteins by Oxidation of the Tyrosine Residues with Potassium Nitrosyldisulphonate' *Polymer* **7** 549- 556

Earland, C., Stell, J. G. P. and Wiseman, A. (1960) 'The Oxidative Insolublization of Proteins' *Journal of the Textile Institute* **51** T817-T827.

Edge, M. (1996) 'Lifetime prediction: fact or fantasy?' *Research techniques in photographic conservation: proceedings of the conference in Copenhagen, 14-19 May 1995* Koch, M. S., Padfield, T., Johnsen, J. S. and Kejser, U. B. (ed.) Copenhagen: Royal Danish Academy of Fine Arts 97-100.

Edwards, H. G. M and Farwell, D. W. (2005) 'Raman Spectroscopic Studies of Silk' *Journal of Raman Spectroscopy* **26** 901-909.

Egerton, G. S. (1948) 'Some Aspects of the Photochemical Degradation of Nylon, Silk, and Viscose Rayon' *Textile Research Journal* **18** 659-669.

Egerton, G. S. (1948) 'The Action of Light on Viscose Rayon, Silk and Nylon, Undyed and Dyed with Some Vat Dyes' *Journal of the Textile Institute* **39**

T293-T304.

Elliott, A. and Malcolm, B. R. (1956) 'Infrared Studies of Polypeptides Related to Silk' *Transactions of the Faraday Society* **52** 528-536.

Emsley, A. M. and Stevens, G. C. (1994) 'Kinetics and mechanisms of the low-temperature degradation of cellulose' *Cellulose* **1(1)** 26-56.

Emsley, A. M., Ali, M. and Heywood, R. J. (2000) 'A size exclusion chromatography study of cellulose degradation' *Polymer* **41** 8513-8521.

Erhardt, D. and Mecklenburg, M. F., (1995), Accelerated VS Natural Aging: Effect of Aging Conditions on the Aging Process of Cellulose, *Materials Issues in Art and Archaeology IV* Vandiver, P. B., Druzik, J. R., Madrid, G., Luis, J., Freestone, I. C. and Wheeler, G. S. (ed.) Warrendale P. A.: Materials Research Society **352**, 247 – 270.

Esbensen, K. H. (2002) *Multivariate Data Analysis in Practice* 5th Edition Oslo: CAMO Process AS.

Feller, R. L. (1994) *Accelerated Aging: Photochemical and Thermal Aspects* Research in Conservation Series, Marina del Rey: Getty Conservation Institute.

Fikioris, M. (1981) 'Textile Conservation for Period Room Settings in Museums and Historic Houses' in *Preservation of Paper and Textiles of Historic and Artistic Value II* Williams, J. C. (ed.) Washington DC: American Chemical Society **193** 253-274.

Florian, M.-L. (1997) 'Environmental factors in museums and homes which influence germination and vegetative growth of fungi' *Heritage Eaters* London: James & James (Science Publishers) Ltd 125-132.

France F. G., (2005) 'Scientific Analysis in the identification of textile materials', in *AHRC Research Centre for Textile Conservation and Textile Studies First Annual Conference – Scientific Analysis of Ancient and Historic Textiles Postprints,* Janaway, R. and Wyeth, P. (ed.) London: Archetype, 3–11.

Fraser, R. D. B., MacRae, T. P. (1973) *Conformation in Fibrous Proteins* New York and London: Academic Press.

French, D. and Edsall, J. T. (1945) 'The Reactions of Formaldehyde with Amino

Acids and Proteins' *Advances in Protein Chemistry* **2** 277-335.

Fry, C., Xavier-Rowe, A., Halahan, J. and Dinsmore, J. (2007) 'What's Causing the Damage! The Use of a Combined Solution-Based Risk Assessment and Condition Audit' *Preprints of Museum Microclimates Conference The National Museum Denmark 19-23 November 2007* 107-114.

Funding Agreement Between the Department for Culture, Media and Sport (DCMS), Department for Communities and Local Government (DCLG), Department for Environment, Food and Rural Affairs (DEFRA) and English Heritage 2005/6-2007/8. http://www.culture.gov.uk/NR/rdonlyres/67B548CA-A01C-4FFD-9243-D95208A129CC/0/EHFundingAgreement06_08.pdf accessed 30/07/2007.

Gage, L. P. and Manning, R. F. (1980) 'Internal Structure of the Silk Fibroin Gene of *Bombyx mori*' *The Journal of Biological Chemistry* **255 (19)** 9444-9450.

Gamo, T., Inokuchi, T. and Laufer, H. (1977) 'Polypeptides of Fibroin and Sericin Secreted from the Different Sections of the Silk Gland in *Bombyx mori*' *Insect Biochemistry* **7** 285-295.

Gardiner, J., Carlson, J., Eaton, L. and Duffy, K. (2000) '"That fabric seems extremely bright": non-destructive characterization of nineteenth century mineral dyes via XRF analysis' *Conservation Combinations: Preprints North American Textile Conservation Conference 2000, Asheville, North Carolina, March 29-31 2000.* Asheville, N.C.: Biltmore House 100-115.

Garside, P. and Brooks, M. M. (2006) 'Probing the Microstructure of Protein and Polyamide Fibres' in *The Future of the 20th Century. Postprints of the AHRC Research Centre for Textile Conservation and Textile Studies Second Annual Conference July 2005*, Rogerson, C. and Garside, P. (ed.) London: Archetype 67-71.

Garside, P. and Wyeth, P. (2002) 'Characterization of silk deterioration' *Strengthening the Bond: Science and Textiles. Preprints of the North American Textile Conservation Conference April 2002* Whelan, V.J. (ed.) Philadelphia, PA: North American Textile Conservation Conference 55-60.

Garside, P. and Wyeth, P., (2006) 'Textiles' in *Conservation Science Heritage*

Materials, Cambridge: The Royal Society for Chemistry, 56-91.

Garside, P., Lahlil, S. and Wyeth, P. (2005) 'Characterization of Historic Silk by Polarized Attenuated Total Reflectance Fourier Transform Infrared Spectroscopy for Informed Conservation' *Applied Spectroscopy* **59 (10)** 90-95.

Georgakoudi, I., Tsai, I., Greiner, C., Wong, C., DeFelice, J. and Kaplan, D. (2007) 'Intrinsic fluorescence changes associated with the conformational state of silk fibroin in biomaterial matrices' *Optics Express* **15 (3)** 1043-1053.

Ghosh, A. and Das, S. (2008) 'Tensile and Twist Failure of Mulberry and Tasar Silk' *Journal of the Textile Institute* **99 (2)** 165-168.

Giles, C. H. and McKay, R. B. (1963) 'The lightfastness of dyes: a review' *Textile Research Journal* **33** 527-577.

Gillen, K. T. and Clough, R. L. (1989) 'Time-Temperature-Dose Rate Superposition: A Methodology for Extrapolating Accelerated Radiation Aging Data to Low Dose Rate Conditions' *Polymer Degradation and Stability* **24** 137-168.

Glišović, A. and Salditt, T. (2007) 'Temperature dependent structure of spider silk by X-ray diffraction' *Applied Physics A: Materials Science and Processing* **87** 63-69.

Goetz, H., Elgass, H. and Huber, L. (1985) 'Determination of Molecular Weight Data in Size-Exclusion Chromatography by Use of Broad-Molecular-Weight-Distributed Standards' *Journal of Chromatography* **349** 357-367.

Goto, Y., Tsukada, M. and Minoura, N. (1990) 'Molecular Cleavage of Silk Fibroin by an Aqueous Solution of Lithium Thiocyanate' *Journal of Sericultural Science of Japan* **59 (6)** 402-409.

Greenspan, L. (1977) 'Humidity Fixed Points of Binary Saturated Aqueous Solutions' *Journal of Research of the National Bureau of Standards – A. Physics and Chemistry* **81A (1)** 89 – 96.

Grieff, S., Kutzke, H., Riekel, C., Wyeth, P. and Lahlil, S., (2005) 'Surveying silk fibre degradation by crystallinity determination: a study on the Tang dynasty silk treasure from Famen Temple, China', in *AHRC Research Centre for*

Textile Conservation and Textile Studies First Annual Conference –Scientific Analysis of Ancient and Historic Textiles Postprints Janaway, R. and Wyeth, P. (ed.) London: Archetype 38–43.

Guan, J. P. and Chen, G. Q. (2008) 'Flame resistant modification of silk fabric with vinyl phosphate' *Fibers and Polymers* **9 (4)** 438-443.

Guan, J., Yang, C. Q. and Chen, G. (2009) 'Formaldehyde-free flame retardant finishing of silk using a hydroxyl-functional organophosphorus oligomer' *Polymer Degradation and Stability* **94** 450-455.

Gulrajani, M. L., Sethi, S., Gupta, S. (1992), 'Some studies in degumming of silk with organic acids' *Journal of the Society of Dyers and Colourists* **108 (2)** 79-86.

Ha, S.-W., Gracz, H. S., Tonelli, A. E. and Hudson, S. M. (2005) 'Structural Study of Irregular Amino Acid Sequences in the Heavy Chain of *Bombyx mori* Silk Fibroin' *Biomacromolecules* **6** 2563-2569.

Hacke, A.-M., Carr, C. M. and Brown, A. (2004) 'Characterisation of metal threads in Renaissance tapestries' *Metal 04* Canberra: National Museum of Australia 415-426.

Hacke, M. (2008) 'Weighted silk: history, analysis and conservation' *Reviews in Conservation* **9** 3-15.

Hakimi, O., Knight, D. P., Knight, M. M., Grahn, M. F. and Vadgama, P. (2006) 'Ultrastructure of Insect and Spider Cocoon Silks' *Bimacromolecules* **7** 2901-2908.

Hallett, K. and Howell, D. (2005) 'Size exclusion chromatography as a tool for monitoring silk degradation in historic tapestries', in *AHRC Research Centre for Textile Conservation and Textile Studies First Annual Conference – Scientific Analysis of Ancient and Historic Textiles Postprints,* Janaway, R. and Wyeth, P. (ed.) London: Archetype 143–150.

Hallett, K. and Howell, D. (2005) 'Size exclusion chromatography of silk: inferring the textile strength and assessing the condition of historic tapestries' in *ICOM Committee for Conservation 14th Triennial Meeting Preprints, The Hague, 12-16th September 2005 Preprints* **2** 911-919.

Hallett, K. personal communication, 05/04/2007.

Halvorson, B. G. and Kerr, N. (1994) 'Effect of Light on the Properties of Silk Fabrics Coated with Parylene-C' *Studies in Conservation* **39** 45-56.

Hansen, E. F. and Ginell, W. S. (1989) 'The Conservation of Silk with Parylene-C' *Historic Textile and Paper Materials II – Conservation and Characterization* Zeronian, S. H. and Needles, H. L. (ed.) American Chemical Series 410 Washington D.C.: American Chemical Society 108-133.

Hansen, E. F. and Sobel, H., (1994), 'Effect of the Environment on the Degradation of Silk: A Review', in *The Textile Specialty Group Postprints of Papers Delivered at the Textile Subgroup Session, American Institute for Conservation 20th Annual Meeting, Buffalo, New York, 1992*, Washington DC: American Institute for Conservation, 114-130.

Harris, M. (1934) 'The Photochemical Decomposition of Silk' *American Dyestuff Reporter Proceedings of the American Association of Textile Chemists and Colorists* **403-405** 215-217.

Harris, M. and Jessup, D. A. (1934) 'The Effect of pH on the Photochemical Decomposition of Silk' *Bureau of Standards Journal of Research* **7** 1179-1184.

Hearle, J. W. S., Lomas, B. and Cooke, W. D. (1998) 'Single Fibre Failure' in *Atlas of Fibre Fracture and Damage to Textiles* 2nd Edition Cambridge: Woodhead Publishing Ltd 13-24.

Hermes, A. C., Davies, R. J., Grieff, S., Kutzke, H., Wyeth, P. and Riekel, C. (2006) 'Characterization of Decay of Ancient Chinese Silk Fabrics by Microbeam Synchrotron Radiation Diffraction' *Biomacromolecules* **7** 777-783.

Hersh, S. P., Hutchins, J. K., Kerr, N. and Tucker, P.A. (1980) 'Prevailing Opinion in the U.S.A. on the Desirable Qualities of Fabric Consolidants' *Proceedings of International Conference on the Conservation and Restoration of Textiles, Milan, Italy* 96-103.

Hirabayashi, K. (1981) 'The deterioration and preservation of silk fabrics' *Kobunkazai no kagaku* **26** 24-34.

Hirabayashi, K., Takei, M. and Kondo, M. (1984) 'Deterioration mechanism of silk

fabrics' *Archaeology and Natural Science* **17** 61-72.

Holmes, F. H. and Smith, S. I. (1952) 'Sedimentation and Diffusion of Soluble Fibroin' *Nature* **169 (4292)** 193.

Honda, H. (1979) 'Storage of silk fabrics in the environment without oxygen' *Sen-i Seihin Shohi kagaku* **20 (4)** 135-140.

Horan, R. L., Antle, K., Collette, A. L., Wang, Y., Huang, J., Moreau, J. E., Volloch, V., Kaplan, D. L. and Altman, G. H. (2005) 'In vitro degradation of silk fibroin' *Biomaterials* **26** 3385-3393.

Hossain, K. S., Ochi, A., Ooyama, E., Magoshi, J. and Nemoto, N. (2003) 'Dynamic Light Scattering of Native Silk Fibroin Solution Extracted from Different Parts of the Middle Division of the Silk Gland of the *Bombyx mori* Silkworm' *Biomacromolecules* **4** 350-359.

Howell, D. (1992) 'Silk Degradation Studies' in *Silk: Harpers Ferry Regional Textile Group, 11th Symposium*, Washington DC: Harpers Ferry Regional Textile Group 11-12.

Howell, D. (1996) 'Some Mechanical Effects of Inappropriate Humidity on Textiles' *ICOM Committee for Conservation 11th Triennial Meeting Edinburgh, Scotland, 1-6 September 1996 Preprints* London: James and James **2** 692-698.

Howitt, F. O. (1955) 'Silk Fibroin as a Fibrous Protein' *Textile Research Journal* **25** 242-246.

http://www.dow.com/PublishedLiterature/dh_0032/0901b803800322bb.pdf?filepath=glycerine/pdfs/noreg/115-00677.pdf&fromPage=GetDoc accessed 03/08/2009.

http://www.english-heritage.org.uk/server/show/conWebDoc.166 accessed 30/07/2007.

http://www.geciasia.com/apo/resources/library/lighting/prod_catalogues/downloads/Fluorescent.pdf accessed 03/08/2009.

http://www.phenomenex.com/products/brands/view.aspx?id=9705 accessed 31/07/2009.

http://www.science4heritage.org/survenir/ accessed 05/10/2009.

http://www.sigmaaldrich.com/MSDS/MSDS/DisplayMSDSPage.do accessed 05/10/2009.

http://www.tate.org.uk/collections/borrowing/care-and-treatment.shtm accessed 27/07/2009.

Hu, B.-W., Zhou, P., Noda, I. and Ruan, Q.-X. (2006) 'Generalized Two-Dimensional Correlation Analysis of NMR and Raman Spectra for Structural Evolution Characterizations of Silk Fibroin' *Journal of Physical Chemistry B* **110** 18046-18051.

Hu, W., Yanagi, Y., Arai, M., Hirabayashi, K. and Yoshitake, N. (1987) 'Effect of humidity on the degradation of silk' *Journal of Sericultural Science of Japan* **52 (2**) 127-130.

Hu, X., Kaplan, D. and Cebe, P. (2006) 'Determining Beta-Sheet Crystallinity in Fibrous Proteins by Thermal Analysis and Infrared Spectroscopy' *Macromolecules* **39** 6161-6170.

Humphries, R. personal communication, 12/10/2007.

Hutton, E. A. and Gartside, J. (1949) 'The Moisture Regain of Silk. Adsorption and Desorption of Water by Silk at 25 °C' *Journal of the Textile Institute* **40** T161- T169.

Iida, H. (1972) *Sen-i Kako*, **24** 165, 267.

Iizuka, E. (1985) 'Silk Thread – Mechanism of Spinning and its Mechanical Properties' *Journal of Applied Polymer Science: Applied Polymer Symposium.* **41** 173-185.

Indicator, N., Koestler, R. J. and Sheryll, R. (1985) 'The Detection of Mordants by Energy Dispersive X-Ray Spectrometry Part I. Dyed Woolen Textile Fibers' *Journal of the American Institute of Conservation* **24** 104-109.

Inoue, S., Tanaka, K., Arisaka, F., Kimura, S., Ohtomo, K. and Mizuno, S. (2000) 'Silk Fibroin of *Bombyx mori* Is Secreted, Assembling a High Molecular Mass Elementary Unit Consisting of H-chain, L-chain, and P25, with a 6:6:1 Molar Ratio' *Journal of Biological Chemistry* **275 (51)** 40517-40528.

Inoue, S.-I., Magoshi, J., Tanaka, T., Magoshi, Y. and Becker, M. (2000) 'Atomic Force Microscopy: *Bombyx mori* Silk Fibroin Molecules and Their Higher

Order Structure' *Journal of Polymer Science Part B: Polymer Physics* **38 (11)** 1436-1439.

Jiang, P., Liu, H., Wang, C., Wu, L., Huang, J. and Guo, C. (2006) 'Tensile behaviour and morphology of differently degummed silkworm (*Bombyx mori*) cocoon silk fibres' *Materials Letters* **60** 919-925.

Jirousek, C. A. (1998) 'The End of the Silk Road: Implications of the Decline of Turkish Sericulture' *Textile History* **29 (2)** 201-225.

Kafatos, F. C. and Williams, C. M. (1964) 'Enzymatic Mechanism for the Escape of Certain Moths from Their Cocoons' *Science* **146 (3643)** 538-540.

Kaszuba, M., McKnight, D., Connah, M. T., McNeil-Watson, F. K. and Nobbmann, U. (2008) 'Measuring Sub Nanometre Sizes Using Dynamic Light Scattering' *Journal of Nanoparticle Research* **10** 823-829.

Kawahara, Y. (1993) 'Analysis of the void structure of silk fibers by tin weighting' *Sen'i Gakkaishi* **49 (12)** 621-627.

Kawahara, Y., Furuta, H., Shioya, M., Kikutani, T. and Takaku, A. (1994) 'Analysis of structure and swelling behavior of silk fibers treated with a mixture of glyoxal and urethane resins' *Sen'i Gakkaishi* **50 (11)** 505-509.

Kawahara, Y., Shioya, M., Kikutani, T. and Takaku, A. (1994) 'Analysis of swelling behavior of silk fibers by small angle x-ray scattering' *Sen'i Gakkaishi* **50 (5)** 199-207.

Kennedy, C. J., Von Lerber, K. and Wess, T. J. (2005) 'Measuring Crystallinity of Laser Cleaned Silk by X-ray Diffraction' *e-Preservation Science* **2** 31-37.

Kerr, N. (1992) 'Understanding the Behaviour of Silk: Structure-Property Relationships' in *Silk: Harpers Ferry Regional Textile Group, 11th Symposium*, Washington DC: Harpers Ferry Regional Textile Group 5-9.

Keyserlingk, M. (1990) 'The Use of Adhesives in Textile Conservation' *ICOM Committee for Conservation 9th Triennial Meeting Dresden, Germany, 26-31 August 1990 Preprints* Paris: ICOM Committee for Conservation **1** 307-312.

Khan, M. M. R., Gotoh, Y., Miura, M., Morikawa, H. and Nagura, M. (2006) 'Influence of an Iodine Treatment on the Structure and Physical Properties of *Bombyx mori* Silk Fibroin Fiber' *Journal of Polymer Science: Part B:*

Polymer Physics **44** 3418-3426.

Kim, J.-J. and Wyeth, P. (2009) 'Towards a routine methodology for assessing the condition of historic silk' *e-Preservation* **6** 60-67.

Kim, J.-J., Zhang, X. and Wyeth, P. (2008) 'The Inherent Acidic Characteristics of Aged Silk' *e-Preservation Science* **5** 41-46.

Kim, K. J., Southon, J., Imamura, M. and Sparks, R. (2008) 'Development of Sample Pretreatment of Silk for Radiocarbon Dating' *Radiocarbon* **50 (1)** 131-138.

Koch, P.-A. (1963) *Microscopic and Chemical Testing of Textiles*, London: Chapman and Hall.

Koestler, R. J., Indicator, N. and Sheryll, R. (1985) 'The Detection of Metallic Mordants by Energy Dispersive X-Ray Spectrometry Part II. Historical Silk Textiles' *Journal of the American Institute of Conservation* **24** 110-115.

Koestler, R. J., Sheryll, R. and Indicator, N. (1985) 'Identification of Dyeing Mordants and Related Substances on Textile Fibers: A Preliminary Study Using Energy Dispersive X-ray Spectrometry' *Studies in Conservation* **30** 58-62.

Korenberg, C. (2007) 'The effect of ultraviolet-filtered light on the mechanical strength of fabrics' *The British Museum Technical Research Bulletin* **1** 23-27.

Krasnov, I., Diddens, I., Hauptmann, N., Helms, G., Ogurreck, M., Seydel, T., Funari, S. S. and Müller, M. (2008) 'Mechanical Properties of Silk: Interplay of Deformation on Macroscopic and Molecular Length Scales' *Physical Review Letters* **100 (4)** 048104-1-048104-4.

Kratky, O. (1956) 'An X-ray Investigation of Silk Fibroin' *Transactions of the Faraday Society* **52** 558-570.

Kuruppillai, R. V., Hersh, S. P. and Tucker, P. A. (1985) 'Degradation of Silk by Heat and Light' *AIC Preprints of Papers Presented at the 13th Annual Meeting Washington DC 22-26th May 1985* Washington, DC: American Institute for Conservation of Historical and Artistic Works 157.

Lefèvre, T., Rousseau, M.-E. and Pézolet, M. (2006) 'Orientation-Insensitive

Spectra for Raman Microspectroscopy' *Applied Spectroscopy* **60 (8)** 841-846.

Lefèvre, T., Rousseau, M.-E. and Pézolet, M. (2007) 'Protein Secondary Structure and Orientation in Silk as Revealed by Raman Spectromicroscopy' *Biophysical Journal* **92** 2885-2895.

Leksophee, T., Supansomboon, S. and Sombatsompop, N. (2004) 'Effects of Crosslinking Agents, Dyeing Temperature, and pH on Mechanical Performance and Whiteness of Silk Fabric' *Journal of Applied Polymer Science* **91** 1000-1007.

Li, G., Zhou, P., Shao, Z., Xie, X., Chen, X., Wang, H., Chunyu, L. and Yu, T. (2001) 'The Natural Silk Spinning Process – A Nucleation-Dependent Aggregation Mechanism?' *European Journal of Biochemistry* **268** 6600-6606.

Li, Y., Yuen, C. W. M., Hu, J. Y. and Cheng, Y. F. (2006) 'Analysis of the Structural Characteristics of Nanoscale Silk Particles' *Journal of Applied Polymer Science* **100** 268-274.

Liu, J., Shao, J. and Zheng, J. (2004) 'Radiation Grafting/Crosslinking of Silk Using Electron-Beam Irradiation' *Journal of Applied Polymer Science* **91** 2028-2034.

Lloyd, H., Lithgow, K., Brimblecombe, P., Yoon, Y. H., Frame, K. and Knight, B. (2002) 'The effects of visitor activity on dust in historic collections' *The Conservator* **26** 72-84.

Lotz, B., Gonthier-Vassal, A., Brack, A. and Magoshi, J. (1982) 'Twisted Single Crystals of *Bombyx mori* Silk Fibroin and Related Model Polypeptides with β-Structure – A Correlation with the Twist of the Beta-Sheets in Globular Proteins' *Journal of Molecular Biology* **156** 345-357.

Lower, E. S. (1988) 'Silk: its Properties and Main End-Uses' *Textile Month* August 1988 9-14.

Lucas, F. (1966) 'Cystine Content of Silk Fibroin (*Bombyx mori*)' *Nature* **210 (5039)** 952-953.

Lucas, F. and Rudall, K. M. (1968) 'Extracellular Fibrous Proteins: The Silks' in

Comprehensive Biochemistry Florkin, M. and Stotz, H. (ed.) **26B** Amsterdam: Elsevier Publishing 475-558.

Lucas, F., Shaw, J. T. B. and Smith S. G. (1955) 'The Chemical Constitution of Some Silk Fibroins and its Bearing on their Physical Properties' *Journal of the Textile Institute*, **46** T440-T452.

Lucas, F., Shaw, J. T. B. and Smith, S. G. (1957) 'The Amino Acid Sequence in a Fraction of the Fibroin of *Bombyx mori*' *Biochemical Journal* **66** 468-479.

Lucas, F., Shaw, J. T. B. and Smith, S. G. (1958) 'The Silk Fibroins' *Advances in Protein Chemistry* **13** 107-242.

Lucas, F., Shaw, J. T. B. and Smith, S. G. (1960) 'Comparative Studies of Fibroins I The Amino Acid Composition of Various Fibroins and its Significance in Relation to their Crystal Structure and Taxonomy' *Journal of Molecular Biology* **2** 339-349.

Lucas, F., Shaw, J. T. B. and Smith, S. G. (1962) 'Some Amino Acid Sequences in the Amorphous Fraction of the Fibroin of *Bombyx mori*' *Biochemical Journal* **83** 164-171.

Magoshi, J. and Magoshi, Y. (1975) 'Physical Properties and Structure of Silk. II. Dynamic Mechanical and Dielectric Properties of Silk Fibroin' *Journal of Polymer Science: Polymer Physics Edition* **13** 1347-1351.

Magoshi, J. and Nakamura, S. (1975) 'Studies on Physical Properties and Structure of Silk. Glass Transition and Crystallization of Silk Fibroin' *Journal of Applied Polymer Science* **19** 1013-1015.

Magoshi, J., Magoshi, Y. and Nakamura, S. (1977) 'Physical Properties and Structure of Silk. III. The Glass Transition and Conformational Changes of Tussah Silk Fibroin' *Journal of Applied Polymer Science* **21** 2405-2407.

Magoshi, J., Magoshi, Y. and Nakamura, S. (1981) 'Physical Properties and Structure of Silk. VII. Crystallization of Amorphous Silk Fibroin Induced by Immersion in Methanol' *Journal of Polymer Science: Polymer Physics Edition* **19** 185-186.

Magoshi, J., Magoshi, Y. and Nakamura, S. (1985) 'Crystallization, Liquid Crystal, and Fiber Formation of Silk Fibroin' *Journal of Applied Polymer Science:*

Applied Polymer Symposium **41** 187-204.

Magoshi, J., Magoshi, Y. and Nakamura, S. (1985) 'Physical properties and structure of silk: 10. The mechanism of fibre formation from liquid silk of silkworm *Bombyx mori*' *Polymer Communications* **26** 309-311.

Magoshi, J., Magoshi, Y., Nakamura, S., Kasai, N. and Kakudo, M. (1977) 'Physical properties and structure of silk. V. Thermal Behavior of Silk Fibroin in the Random-Coil Conformation' *Journal of Polymer Science: Polymer Physics Edition* **15** 1675-1683.

Magoshi, J., Mizuide, M., Magoshi, Y., Takahashi, K., Kubo, M. and Nakamura, S. (1979) 'Physical Properties and Structure of Silk. VI. Conformational Changes in Silk Fibroin Induced by Immersion in Water at 2 to 130°C' *Journal of Polymer Science: Polymer Physics Edition* **17** 515-520.

Mandal, B. B. and Kundu, S. C. (2008) 'A Novel Method for Dissolution and Stabilization of Non-Mulberry Silk Gland Protein Fibroin Using Anionic Surfactant Sodium Dodecyl Sulfate' *Biotechnology and Bioengineering* **99 (6)** 1482-1489.

Manisankar, G., Ujjal, M. and Aniruddha, M. (2008) 'Effect Of Environmental Factors (Temperature and Humidity) on Spinning Worms of Silkworm (*Bombyx mori* L.)' *Research Journal of Chemistry and Environment* **12 (4)** 12-18.

Marsh, R. E., Corey, R. B. and Pauling, L. (1955) 'An Investigation of the Structure of Silk Fibroin' *Biochimicia et Biophysica Acta* **16** 1-34.

Marsh, R. E., Corey, R. B. and Pauling, L. (1955) 'The Crystal Structure of Silk Fibroin' *Acta Crystallographica* **8** 62.

Marsh, R. E., Corey, R. B. and Pauling, L. (1955) 'The Structure of Tussah Silk Fibroin' *Acta Crystallographica* **8** 710-715.

Masschelein-Kleiner, L. and Maes, L. R. J. (1978) 'Ancient Dyeing Techniques in Eastern Mediterranean Regions' *ICOM Committee for Conservation 5th Triennial Meeting, Zagreb, 1-8 October 1978 Preprints* Paris: ICOM 78/9/83.

Matsumoto, A., Kim, H. J., Tsai, I. Y., Wang, X., Cebe, P. and Kaplan, D. L. (2007) 'Silk' *Handbook of Fiber Chemistry 3rd Edition* Lewin, M. (ed.) London:

Taylor and Francis 383-405.

McCaffrey, L. M. (1992) 'Some Theory behind Silk Degradation and Stabilization' in *Silk: Harpers Ferry Regional Textile Group, 11th Symposium*, Washington DC: Harpers Ferry Regional Textile Group 15-21.

Mecklenburg, M. F. (2007) 'Micro Climates and Moisture Induced Damage to Paintings' *Museum microclimates: contributions to the Copenhagen conference, 19-23 November 2007* Padfield, T. and Borchersen, K. (ed.) Copenhagen: National Museum of Denmark 19-25.

Mercer, E. H. (1954) 'Studies on the Soluble Proteins of the Silk Gland of the Silkworm, *Bombyx mori*' *Textile Research Journal* **24** 135-145.

Meredith, R. (1945) 'The Tensile Behaviour of Raw Cotton and Other Textile Fibres' *Journal of the Textile Institute* **36** T107-T123.

Merritt, J. L. (1992) 'Silk: History, Cultivation and Processing' in *Silk: Harpers Ferry Regional Textile Group, 11th Symposium*, Washington DC: Harpers Ferry Regional Textile Group 1-3.

Meyer, K. H. and Mark, H. (1928) *Chemische Berichte* **61** 1932.

Michalski, S. (2002) 'Double the life for each five-degree drop, more than double the life for each halving of relative humidity' *ICOM Committee for Conservation 13th Triennial Meeting, Rio de Janeiro, 22-27 September 2002 Preprints* Vontobel, R. (ed.) London: James & James **1** 66-72.

Miller, J. E. (1986) 'A Comparative Analysis of Degradation in Naturally Aged and Experimentally Degraded Silk' PhD Dissertation (Kansas State University)

Miller, J. E. and Reagan, B. M. (1989) 'Degradation in Weighted and Unweighted Historic Silks', *Journal of the American Institute of Conservation* **28** 97-115.

Miller, L. D., Putthanarat, S., Eby, R. K. and Adams, W. W. (1999) 'Investigation of the nanofibrillar morphology in silk fibers by small angle X-ray scattering and atomic force microscopy' *International Journal of Biological Macromolecules* **24** 159-165.

Millington, K. R., Maurdev, G. and Jones, M. J. (2007) 'Thermal chemiluminescence of fibrous proteins' *Polymer Degradation and Stability* **92** 1504-1512.

Minoura, N., Tsukada, M. and Nagura, M. (1990) 'Physico-chemical properties of silk fibroin membrane as a biomaterial' *Biomaterials* **11 (6)** 430-434.

Mitchell, S. personal communication, 23/07/2007.

Miyazawa, M. and Sonoyama, M. (1998) 'Second derivative near infrared studies on the structural characterisation of proteins' *Journal of Near Infrared Spectroscopy* **6** A253-A257.

Mo, C., Wu, P., Chen, X. and Shao, Z.-Z. (2006) 'Near-Infrared Characterization on the Secondary Structure of Regenerated *Bombyx mori* Silk Fibroin' *Applied Spectroscopy* **60(12)** 1438-1441.

Monti, P., Freddi, G., Bertoluzza, A., Kasai, N. and Tsukada, M. (1998) 'Raman Spectroscopic Studies of Silk Fibroin from *Bombyx mori*' *Journal of Raman Spectroscopy'* **29** 297-304.

Monti, P., Taddei, P. Freddi, G., Asakura, T. and Tsukada, M. (2001) 'Raman spectroscopic characterization of *Bombyx mori* silk fibroin: Raman spectrum of Silk I' *Journal of Raman Spectroscopy* **32** 103-107.

Mosher, H. H. (1932) 'Usual Degumming Methods Prove Harmful to Silk-Wool Unions' *Textile World* (Nov.) 86-87.

Mossotti, R., Innocenti, R., Zoccola, M., Anghileri, A. and Freddi, G. (2006) 'The degumming of silk fabrics: a preliminary near infrared spectroscopy study' *Journal of Near Infrared Spectroscopy* **14 (3)** 201-208.

Nakamura, S., Saegusa, Y., Yamaguchi, Y., Magoshi, J. and Kamiyama, S. (1986) 'Physical Properties and Structures of Silk. XI. Glass Transition Temperature of Wild Silk Fibroins' *Journal of Applied Polymer Science* **31** 955-956.

Needles, H. L., Cassman, V. and Collins, M. J. (1986) 'Mordanted, Natural-Dyed Wool and Silk Fabrics' *Historic Textile and Paper Materials Conservation and Characterization* Needles, H. L. and Zeronian, S. H. (ed.) **212** Washington DC: American Chemical Society 199-210.

Nishi, H. (1979) 'The relations between yellowing of silk and aromatic amino acids' *Nippon snashi-gaku zasshi* **48** 164-170.

Nishimura, D. personal communication, 28/03/2008.

O'Connor, S. and Maher, J. (2007) 'Assessing the Risks of X-Radiography to Textiles' in *X-Radiography of Textiles, Dress and Related Objects* O'Connor, S and Brooks, M. M. (ed.) Oxford: Butterworth-Heinemann 91-95.

O'Connor, S. personal communication, 06/03/2008.

Odegaard, N., Smith, D. R., Boyer, L. V. and Anderson, J. (2006) 'Use of handheld XRF for the study of pesticide residues on museum objects' *Collection Forum* **20** 42-48.

Odlyha, M., Theodorakopoulos, C. and Campana, R., (n.d.), 'Damage Assessment of Tapestries by Infrared Spectroscopy (ATR-FTIR)' MODHT poster.

Odlyha, M., Wang, Q., Foster, G. M., de Groot, J., Horton, M. and Bozec, L., (2005) 'Monitoring of damage to historic tapestries: the application of dynamic mechanical thermal analysis to model and historic tapestries', in *AHRC Research Centre for Textile Conservation and Textile Studies First Annual Conference – Scientific Analysis of Ancient and Historic Textiles Postprints* Janaway, R. and Wyeth, P. (ed.) London: Archetype 126–134.

Odlyha, M., Wang, Q., Foster, G. M., de Groot, J., Horton, M. and Bozec, L. (2005) 'Thermal analysis of Model and Historic Tapestries' *Journal of Thermal Analysis and Calorimetry* **82** 627-636.

Okamoto S. and Kikuchi M. (1958) 'The decomposition of silk fibroin by sunlight. V, On the discrystallization of the crystalline parts of silk by light' *Journal of Sericultural Science of Japan* **27** 367-373.

Okamoto, S. and Kimura, T. (1953) *Journal of the Society of Textile and Cellulose Industry Japan.* **9** 284.

Oliva, A., Llabrés, M. and Fariña, J. B. (2001) 'Comparative study of protein molecular weights by size-exclusion chromatography and laser-light scattering' *Journal of Pharmaceutical and Biomedical Analysis* **25** 833-841.

Otterburn, M. S. (1977) 'The Chemistry and Reactivity of Silk' in *The Chemistry of Natural Fibres* Asquith, R.S. (ed.), New York: John Wiley and Sons, Inc., 53-80.

Pace, C. N. (1986) 'Determination and Analysis of Urea and Guanidine Hydrochloride Denaturation Curves' *Methods in Enzymology* **131** 266-280.

Palmer, A. (2006) ‘’A bomb in the collection’: researching and exhibiting early 20th-century fashion’ in *The Future of the 20th Century. Postprints of the AHRC Research Centre for Textile Conservation and Textile Studies Second Annual Conference July 2005* Rogerson, C. and Garside, P. (ed.) London: Archetype, 41-47.

Pascoe, M. W. (1980) ‘Science and Ethics in Textile Conservation’ in *Proceedings of the International Conference on the Conservation and Restoration of Textiles, Milan, Italy* 104-106.

Preghenella, M., Pezzotti, G. and Migliaresi, C. (2007) ‘Comparative Raman spectroscopic analysis of orientation in fibers and regenerated films of *Bombyx mori* silk fibroin’ *Journal of Raman Spectroscopy* **38 (5)** 522-536.

Putthanarat, S., Stribeck, N., Fossey, S. A., Eby, R. K. and Adams, W. W. (2000) ‘Investigation of the nanofibrils of silk fibers’ *Polymer* **41** 7735-7747.

Quye, A., Hallett, K. and Herrero Carretero, C. (2009) *’Wrought in Gold and Silk’ Preserving the Art of Historic Tapestries* Edinburgh: National Museums Scotland Enterprises Ltd – Publishing.

Ram, A. T., Masaryk-Morris, S., Kopperi, D. and Bauer, R. W. (1992) ‘Simulated Aging of Processed Cellulose Triacetate Motion Picture Films’ *Journal of Imaging Science and Technology* **36(1)** 21-28.

Ramjeesingh, M., Huan, L.-J., Garami, E. and Bear, C. E. (1999) ‘Novel method for evaluation of the oligomeric structure of membrane proteins’ *Biochemical Journal* **342** 119-123.

Reilly, J. M. (1996) ‘IPI Storage Guide for Acetate Film’ http://www.imagepermanenceinstitute.org/shtml_sub/acetguid.pdf accessed 17/10/2009.

Riboud, K. (1977) ‘A Closer View of Early Chinese Silks’ in *Studies in Textile History*, Veronika Gervers ed., Toronto: Royal Ontario Museum 252-280.

Rice, J. W. (1968) ‘Principles of Textile Conservation Science No. IX How Humidity may affect Rug, Tapestry, and Other Textile Collections’ *Textile Museum Journal* **2 (3)** 53-56.

Richards, H. R. (1984) ‘Thermal Degradation of Fabrics and Yarns Part 1: Fabrics’

Journal of the Textile Institute **1** 28-36.

Richardson, E. and Garside, P. (2009) 'The Use of Near Infrared Spectroscopy as a Diagnostic Tool for Historic Silk Artefacts' *e-Preservation Science* **6** 68-74.

Richardson, E., Martin, G., Wyeth, P. and Zhang, X. (2008) 'State of the art: non-invasive interrogation of textiles in museum collections' *Microchimica Acta* **162** 303-312.

Roberson, D. D. (1981) 'Permanence / Durability and Preservation Research at the Barrow Laboratory' *Preservation of Paper and Textiles of Historic and Artistic Value II* Advances in Chemistry Series 193 Washington D.C.: American Chemical Society 45-55.

Roberts, N. M. and Mack, P. B. (1936) 'A Study of the Effects of Light and Air on Unweighted and Tin Weighted Silk – Paper II' *Rayon and Melliand Textile Monthly* 49-51.

Robson, A., Woodhouse, J. M. and Zaidi, Z. H. (1970) 'Cystine in Silk Fibroin, Bombyx mori' *International Journal of Protein Research* **2** 181-189.

Robson, R. M. (1998) 'SILK Composition, Structure, and Properties', in, *Handbook of Fiber Chemistry*, International Fiber Science and Technology Series /15 Second Edition Lewin, M. and Pearce, E. M. (ed.) New York: Marcel Dekker 415 – 463.

Robson, R. M. (1999) 'Microvoids in *Bombyx mori* silk. An electron microscope study' *International Journal of Biological Macromolecules* **24** 145-150.

Ross, J. E., Johnson, R. L. and Edgar, R. (1936) 'Degradation of Weighted Silk Fibroin by Acid and Alkali' *Textile Research Journal* **6** 207-216.

Rössle, M., Panine, P., Urban, V. S. and Riekel, C. (2004) 'Structural Evolution of Regenerated Silk Fibroin Under Shear: Combined Wide- and Small-Angle X-ray Scattering Experiments Using Synchrotron Radiation' *Biopolymers* **74 (4)** 316-327.

Rutherford, H. A. and Harris, M. (1941) 'Photochemical Reactions in Silk' *American Dyestuff Reporter* **14** 345-346 and 363-364.

Sasaki, T. and Noda, H. (1973) 'Studies on Silk Fibroin of *Bombyx mori* Directly Extracted from the Silk Gland I. Molecular Weight Determination in

Guanidine Hydrochloride or Urea Solutions' *Biochimica et Biophysica Acta* **310** 76-90.

Sasaki, T. and Noda, H. (1973) 'Studies on Silk Fibroin of *Bombyx mori* Directly Extracted from the Silk Gland II. Effect of Reduction of Disulfide Bonds and Subunit Structure' *Biochimica et Biophysica Acta* **310** 91-103.

Sato, M. and Sasaki, Y., (2005) 'Studies on ancient Japanese silk fibres using FTIR microscopy', in *AHRC Research Centre for Textile Conservation and Textile Studies First Annual Conference – Scientific Analysis of Ancient and Historic Textiles Postprints,* Janaway, R. and Wyeth, P. (ed.) London: Archetype 44–47.

Saunders, D. and Kirby, Jo (1996) 'Light-Induced Damage: Investigating the Reciprocity Principle' *ICOM Committee for Conservation, 11th Triennial Meeting, Edinburgh, Scotland 1-6 September 1996 Preprints* Bridgland, J. (ed.) London: James and James Ltd 87-90.

Saville, B. P. (2003) *Physical Testing of Textiles* Cambridge: Woodhead Publishing.

Schnabel, E. (1958) *Annalen der Chemie* **615** 173.

Schnabel, E. and Zahn, H. (1958) *Annalen der Chemie* **614** 141.

Schoeser, M. (2007) *Silk* New Haven, C.T.: Yale University Press.

Schroeder, W. A. and Kay, L. M. (1955) 'The Amino Acid Composition of *Bombyx mori* Silk Fibroin and of Tussah Silk Fibroin' *Journal of the American Chemical Society* **77** 3908-3913.

Scott, D. A. (1990) 'Bronze Disease: A critical review of some chemical problems and the role of relative humidity' *Journal of the American Institute of Conservation* **29** 193-206.

Scott, W. M. (1931) 'The Weighting of Silk I-IV' *American Dyestuff Reporter* **20** 517-518, 539-540, 543, 557-562, 591-594, 621-622.

Scott, W. M. (1934) 'Recent Developments in the Chemistry of Silk and of Silk Processing I-V' *American Dyestuff Reporter* **23** 217-221, 253-254, 283-284, 330-332, 339-340, 363-364.

Scott, W. M. (1935) 'Developments During 1934 in the Chemistry of Silk and Silk

Processing' *American Dyestuff Reporter* **24** 443-450.

Sebera, D. K. (1994) 'Isoperms An Environmental Management Tool' http://cool.conservation-us.org/byauth/sebera/isoperm/ accessed 17/10/2009.

Seeley, N. J. (1997) 'Textiles on Open Display: The Conservation Issues' In *Textiles in Trust* Marko, K. (ed.) London: Archetype 8-13.

Sen, K., Babu K, M. (2004) 'Studies on Indian Silk. I. Macrocharacterization and Analysis of Amino Acid Composition' *Journal of Applied Polymer Science* **92(2)** 1080-1097.

Sen, K., Babu K, M. (2004) 'Studies on Indian Silk. II. Structure-Property Correlations' *Journal of Applied Polymer Science* **92(2)** 1098-1115.

Sen, K., Babu K, M. (2004) 'Studies on Indian Silk. III. Effect of Structure on Dyeing Behavior' *Journal of Applied Polymer Science* **92(2)** 1116-1123.

Setoyama, K. (1982) 'Effect of water on the heat yellowing of silk fabrics and the changes in amino acid composition in silk fibroin by heated sealed tubes' *Journal of Sericultural Science of Japan* **51** 365-369.

Seydel, T., Kölln, K., Krasnov, I., Diddens, I., Hauptmann, N., Helms, G., Ogurreck, M., Kang, S.-G. Koza, M. M. and Müller, M. (2007) 'Silkworm Silk under Tensile Strain Investigated by Synchrotron X-ray Diffraction and Neutron Spectroscopy' *Macromolecules* **40** 1035-1042.

Shao, J. Z., Zheng, J. H., Liu, J. Q. and Carr, C. M. (2004) 'FT-Raman and FT-IR spectroscopic studies of silk fibroin' *Quality Textiles for Quality Life 83rd Textile Institute World Conference 23-27th May 2004, Shanghai, PR China* 427-431.

Shao, J., Zheng, J., Liu, J., Carr, C. M. (2005) 'Fourier Transform Raman and Fourier Transform Infrared Spectroscopy Studies of Silk Fibroin' *Journal of Applied Polymer Science* **96** 1999-2004.

Shashoua, Y. (2003) 'Inhibiting the deterioration of plasticised poly(vinyl chloride) in museum collections' *Conservation Science 2002* London: Archetype Publications 58-64.

Shaw, J. T. B. (1964) 'Fractionation of the Fibroin of *Bombyx mori* with Trypsin'

Biochemical Journal **93** 45–54.

Shaw, J. T. B. (1964) 'Fractionation of the Fibroin of *Bombyx mori* with Alkali' *Biochemical Journal* **93** 54-61.

Shaw, J. T. B. and Smith, S. G. (1961) 'Comparative Studies of Fibroins IV The Composition and Structure of Chemically Resistant Fractions from Some Silk Fibroins' *Biochimica et Biophysica Acta* **52** 305-318.

Siesler, H. W., Ozaki, Y., Kawata, S. and Heise, H. M. (2002) *Near-Infrared Spectroscopy Principles, Instruments, Applications* Weinheim: Wiley-VCH.

Sinohara, H. and Asano, Y. (1967) 'Carbohydrate Content of Fibroin and Sericin of the Silkworm, *Bombyx mori*' *The Journal of Biochemistry* **62(1)** 129-130.

Sirichaisit, J., Brookes, V. L., Young, R. J. and Vollrath, F. (2003) 'Analysis of Structure/Property Relationships in Silkworm (*Bombyx mori*) and Spider Dragline (*Nephila edulis*) Silks Using Raman Spectroscopy' *Biomacromolecules* **4** 387-394.

Sitch, D. A. and Smith, S. G. (1957) 'The Oxidation of Silk Fibroin by Hydrogen Peroxide and by Peracetic Acid' *Journal of the Textile Institute* **48** T341-T355.

Skelton, M. (1995) 'Use of Qualitative Nondestructive X-Ray Fluorescence Analysis in the Characterization of Chinese or Western Provenance for 18th-Century Painted/Printed Silk' *The Conservation of 18th-Century Painted Silk Dress*, Paulozik, C. and Flakerly, S. (ed.) New York: Metropolitan Museum of Art 6-15.

Sonoyama, M. and Nakano, T. (2000) 'Infrared Rheo-Optics of *Bombyx mori* Fibroin Film by Dynamic Step-Scan FT-IR Spectroscopy Combined with Digital Signal Processing' *Applied Spectroscopy* **54 (7)** 968-973.

Sprague, K. (1975) 'The *Bombyx mori* Silk Proteins: Characterization of Large Polypeptides' *Biochemistry* **14 (5)** 925-931.

Srinivasan, R. and Jakes, K. A. (1997) 'Examination of Silk Fibers from a Deep Ocean Site: SEM, EDS, & DSC' *Material Research Society Symposium Proceedings* Washington D.C.: Materials Research Society **462** 375-380.

Stephens, M. (1997) 'The humidification of textiles : a literature review of the

effects of moisture on textile fibres and an investigation of the effects of three humidification techniques on the tensile properties of naturally aged and new silk, wool and linen' Student report (PG Diploma in Textile Conservation) University of London, Textile Conservation Centre in affiliation with the Courtauld Institute of Art

Stewart, F. H. C. (1966) 'Poly-L-Alanylglycyl-L-Alanylglycyl-L-Serylglycine: A Synthetic Model of *Bombyx mori* Silk Fibroin' *Australian Journal of Chemistry* **19** 489-501.

Strang, T. and Grattan, D. (2009) 'Temperature and Humidity Considerations for the Preservation of Organic Collections – the Isoperm Revisited' *e-Preservation Science* **6** 68-74.

Stuart, B. H. (2007) *Analytical Techniques in Materials Conservation* Chichester: John Wiley & Sons, Ltd.

Sung, N. Y., Byun, E. B., Kwon, S. K., Kim, J. H., Song, B. S., Choi, J. I., Kim, J. K., Yoon, Y., Byun, M. W., Kim, M. R., Yook, H. S. and Lee, J.W. (2009) 'Effect of Gamma Irradiation on the Structural and Physiological Properties of Silk Fibroin' *Food Science and Biotechnology* **18(1)** 228-233.

Suzuki, E. (1967) 'A quantitative study of the amide vibrations in the infra-red spectrum of silk fibroin' *Spectrochimica Acta* **23A** 2303-2308.

Sykes, P. (1984) *Textile Conservation Group Newsletter*, 10 May 1984, **6 (5).**

Szostak-Kotowa, J. (2004) 'Biodeterioration of textiles' *International Biodeterioration and Biodegradation* **53** 165-170.

Taddei, P., Asakura, T., Yao, J. and Monti, P. (2004) 'Raman Study of Poly(Alanine-Glycine)-Based Peptides Containing Tyrosine, Valine, and Serine as Model for the Semicrystalline Domains of *Bombyx mori* Silk Fibroin' *Biopolymers* **75** 314-324.

Takahashi, Y., Gehoh, M. and Yuzuriha, K. (1991) 'Crystal Structure of Silk (*Bombyx mori*)' *Journal of Polymer Science: Part B: Polymer Physics* **29** 889-891.

Takahashi, Y., Gehoh, M. and Yuzuriha, K. (1999) 'Structure Refinement and Diffuse Streak Scattering of Silk (*Bombyx mori*)' *International Journal of*

Biological Macromolecules **24** 127-138.

Takei, F., Kikuchi, Y., Kikuchi, A., Mizuno, S. and Shimura, K. (1987) 'Further Evidence for Importance of the Subunit Combination of Silk Fibroin in Its Efficient Secretion from the Posterior Silk Gland Cells' *The Journal of Cell Biology* **105** 175-180.

Tanaka, K., Inoue, S. and Mizuno, S. (1999) 'Hydrophobic interactions of P25, containing Asn-linked oligosaccharide chains, with the H-L complex of silk fibroin produced by *Bombyx mori*' *Insect Biochemistry and Molecular Biology* **29** 269-276.

Tanaka, K., Kajiyama, N., Ishikura, K., Waga, S., Kikuchi, A., Ohtomo, K., Takagi, T. and Mizuno, S. (1999) 'Determination of the site of disulfide linkage between heavy and light chains of silk fibroin produced by *Bombyx mori*' *Biochimica et Biophysica Acta* **1432** 92-103.

Tanaka, K., Mori, K. and Mizuno, S. (1993) 'Immunological Identification of the Major Disulfide-Linked Light Component of Silk Fibroin' *Journal of Biochemistry* **114** 1-4.

Tanford, C. (1964) 'Isothermal Unfolding of Globular Proteins in Aqueous Urea Solutions' *Journal of the American Chemical Society* **86** 2050-2059.

Tashiro, Y., Otsuki, E. and Shimadzu, T. (1972) 'Sedimentation Analyses of Native Silk Fibroin in Urea and Guanidine·HCl' *Biochimica et Biophysica Acta* **257** 198-209.

Taylor, J. (2005) 'An Integrated Approach to Risk Assessments and Condition Surveys' *Journal of the American Institute for Conservation* **44** 127-141.

Tazima, Y. (1984) 'Silkworm moths' *Evolution of Domesticated Animals* London: Longman 416-424.

Teramoto, H. and Miyazawa, M. (2005) 'Molecular Orientation Behaviour of Silk Sericin Film as Revealed by ATR Infrared Spectroscopy' *Biomacromolecules* **6** 2049-2057.

The International Silkworm Genome Consortium (2008) 'The genome of a lepidopteran model insect, the silkworm *Bombyx mori*' *Insect Biochemistry and Molecular Biology* **38** 1036-1045.

The National Trust (2006) *The National Trust Manual of Housekeeping* Oxford: Butterworth-Heinemann.

Thickett, D. and Odlyha, M. (2005) 'Infra-red and Raman Spectroscopy of Iron Corrosion Products' *Proceedings of IRUG6, Florence* Piccollo, M. (ed.) 86-93.

Thomson, G. (1986) *The Museum Environment* Oxford: Butterworth-Heinemann.

Tímár-Balázsy, A. and Eastop, D. (1998) *Chemical Principles of Textile Conservation* Oxford: Butterworth-Heinemann.

Tonini, C., (1978) 'Atomic Absorption Spectrophotometry in the Textile Chemistry Laboratory' *Tinctoria* **75** 160-162.

Trathnigg, B. (2000) 'Size-exclusion Chromatography of Polymers' in *Encyclopedia of Analytical Chemistry* Meyers, R. A. (ed.) Chichester: Wiley 8008-8034.

Trotman, S. R. (1936) 'The Determination of Damage in Silk' *Journal of the Society of Chemical Industry (Transactions)* **55** 325T-327T.

Trotman, S. R. and Bell, H. S. (1935) 'The Determination of Damage in Silk' *Journal of the Society of Chemical Industry (Transactions)* **54** 141T-142T.

Tse, S. and Dupont, A.-L. (2001) 'Measuring silk deterioration by high-performance size-exclusion chromatography, viscometry and electrophoresis' in *Historic Textiles, Papers, and Polymers in Museums, ACS Symposium Series 779* Cardamone, J. and Baker, M. (ed.) Washington DC: American Chemical Society 98-114.

Tsuboi, Y., Ikejiri, T., Shiga, S., Yamada, K. and Itaya, A. (2001) 'Light can transform the secondary structure of silk protein' *Applied Physics A: Materials Science and Processing* **73** 637-640.

Tsukada, M. and Hirabayashi, K. (1980) 'Change of Silk Fibroin Structure by Ultraviolet Radiation' *Journal of Polymer Science: Polymer Letters Edition* **18** 507-511.

Tsukada, M., Nagura, M., Ishikawa, H. and Shiozaki, H. (1991) 'Structural Characteristics of Silk Fibers Treated with Epoxides' *Journal of Applied Polymer Science* **43** 643-649.

Tucker, P., Kerr, N. and Hersh, S. P. (1980) 'Photochemical Damage of Textiles'

Textiles and Museum Lighting (The Harpers Ferry Regional Textile Group) December 4 & 5 1980, The Anderson House Museum, National Headquarters of the Society of the Cincinnati, 2118 Massachusetts Ave, NW Washington DC 20008, 23-40.

Turgoose, S. (1982) 'Post-excavation Changes in Iron Antiquities' *Studies in Conservation* **22** 85-102.

Turner, A. J. (1920) 'The Influence of Atmospheric Exposure on the Properties of Textiles' *Journal of the Society of Dyers and Colourists* **36** 165-173.

Tweedie, A. S. (1938) 'A Study of the Viscosity Method for the Determination of Damage in Silk' *Canadian Journal of Research* **16B** 134-150.

U.S. Environmental Protection Agency (EPA) methods 282.1 Tin (Atomic Absorption, Direct Aspiration) and 282.2 Tin (Atomic Absorption, Furnace Technique) http://www.caslab.com/EPA-Methods/?term_search=&page=4 accessed 28/07/2009.

Vigo, T. L. (1977) 'Preservation of Natural Textile Fibers – Historical Perspectives' in *Preservation of Paper and Textiles of Historic and Artistic Value* Williams, J. C. (ed.) Washington DC: American Chemical Society **164** 189-207.

Wakui, M., Yatagai, M., Kohara, N., Sano, C., Ikuno, H., Magoshi, Y. and Saito, M. (2001) 'ICP-AES and X-ray fluorescence determination of mordants on fabric dyed with natural dyes' *Bunkazai Hozon Shufuku Gakkai shi: kobunkazai no kagaku* **45** 12-26.

Warwicker, J. O. (1954) 'The Crystal Structure of Silk Fibroin' *Acta Crystallographica* **7** 565-573.

Warwicker, J. O. (1956) 'The Crystal Structure of Silk Fibroins' *Transactions of the Faraday Society* **52** 554-557.

Warwicker, J. O. (1960) 'An X-ray Study of the Sorption of Water by the Silk Fibroin of *Bombyx mori*' *Journal of the Textile Institute* **57** T289-T292.

Warwicker J. O. (1960) 'Comparative Studies of Fibroins II. The Crystal Structures of Various Fibroins' *Journal of Molecular Biology* **2** 350-362.

Watkinson, D. and Lewis, M. (2004) 'SS Great Britain iron hull: modelling corrosion to define storage relative humidity' *Preprints of Metal04, Canberra* Ashton,

J. (ed.) 88-100.

Willcox, P. J., Gido, S. P., Muller, W. and Kaplan, D. L. (1996) 'Evidence of a Cholesteric Liquid Crystalline Phase in Natural Silk Spinning Processes' *Macromolecules* **29** 5106-5110.

Williams, E. T. and Indicator, N. (1986) 'Detection of Metallic Mordants on Textiles by Particle-Induced X-Ray Emission' *Scanning Electron Microscopy* **3** 847-850.

Wolfgang, W. G. (1970) 'Silk' *Encyclopedia of Polymer Science and Technology* Mark, H. and Gaylord, N. (ed.) **12** New York: John Wiley & Sons, Inc, 578-585.

Wong Po Foo, C., Bini, E., Hensman, J., Knight, D. P., Lewis, R. V. and Kaplan, D. L. (2006) 'Role of pH and charge on silk protein assembly in insects and spiders' *Applied Physics A Materials Science & Processing* **82** 223-233.

Workman, J. (1993) 'A review of process near infrared spectroscopy: 1980-1994' *Journal of Near Infrared Spectroscopy* **1** 221-245.

Wyeth, P., (2005) 'Signatures of ageing: correlations with behaviour', in *AHRC Research Centre for Textile Conservation and Textile Studies First Annual Conference – Scientific Analysis of Ancient and Historic Textiles Postprints* Janaway, R. and Wyeth, P. (ed.) London: Archetype 137–142.

Xavier-Rowe, A., Fry, C. and Stanley, B. (2008) ' Power to Prioritize: Applying Risk and Condition Information to the Management of Dispersed Collections' *Conservation and Access Contributions to the London Congress 15-19 September 2008* Saunders, D., Townsend, J. H. and Woodcock, S. (ed.) London: The International Institute for Conservation of Historic and Artistic Works 186-191.

Xiaojun, P. Jitao, W. and Jie, S. (1993) 'Silk finishing with Epoxides' *Journal of the Society of Dyers and Colourists* **109 (4)** 159-163.

Yamada, H., Nakao, H., Takasu, Y. and Tsubouchi, K. (2001) 'Preparation of undegraded native molecular fibroin solution from silkworm cocoons' *Materials Science and Engineering C* **14** 41-46.

Yamaguchi, K., Kikuchi, Y., Takagi, T., Kikuchi, A., Oyama, F., Shimura, K. and

Mizuno, S. (1989) 'Primary Structure of the Silk Fibroin Light Chain Determined by cDNA Sequencing and Peptide Analysis' *Journal of Molecular Biology* **210** 127-139.

Yamauchi, K., Imada, T. and Asakura, T. (2005) 'Use of Microcoil Probehead for Determination of the Structure of Oriented Silk Fibers by Solid-State NMR' *Journal of Physical Chemistry B* **109** 17689-17692.

Yamazaki, M. (2003) 'Shattered Silk' MA Dissertation (Textile Conservation Centre).

Yanagi, Y., Kondo, Y. and Hirabayashi, K. (2000) 'Deterioration of Silk Fabrics and Their Crystallinity' *Textile Research Journal* **70 (10)** 871-875.

Yanagi, Y., Hu, W. and Hirabayashi, K. (1986) 'Warp breaking of old silk fabrics made in the Edo period' *Kobunkazai no kagaku* **31** 51-54.

Yang, Y. and Li, S. (1993) 'Silk Fabric Non-formaldehyde Crease-resistant Finishing Using Citric Acid' *Journal of the Textile Institute* **84 (4)** 638-644.

Yonemura, N. and Sehnal, F. (2006) 'The Design of Silk Fiber Composition in Moths Has Been Conserved for More Than 150 Million Years' *Journal of Molecular Evolution* **63** 42-53.

Yoshida, Z. and Kato, M. (1955) *Journal of the Chemical Society of Japan.* **58** 274, 667.

Yumusak, C. and Alekberov, V. (2008) 'The Effects of Electrical Discharge on the Mechanical Properties of *Bombyx mori* Silk Fibroin' *Fibers and Polymers* **9 (1)** 15-20.

Zahn, H. and Krasowski, A. (2005) 'Silk' In *Ullmann's Encyclopedia of Industrial Chemistry* Weinheim: Wiley-VCH GmbH & Co. 1-14.

Zbilut, J. P., Scheibel, T., Huemmerich, D., Webber, C. L., Colafranceschi, M. and Giuliani, A. (2006) 'Statistical approaches for investigating silk properties' *Applied Physics A: Materials Science & Processing* **82** 243-251.

Zeronian, S. H., Alger, K. W., Ellison, M. S. and Al-Khayatt, S. M. (1986) 'Studying the Cause and Type of Fiber Damage in Textile Materials by Scanning Electron Microscopy' in *Historic Textile and Paper Materials Conservation and Characterization* Needles, H. L. and Zeronian, S. H. (ed.) American

Chemical Series 212 Washington DC: American Chemical Society 77-94.

Zhang, H., Magoshi, J., Becker, M., Chen, J. Y. and Matsunaga, R. (2002) 'Thermal Properties of *Bombyx mori* Silk Fibers' *Journal of Applied Polymer Science* **86 (8)** 1817-1820.

Zhang, X. and Wyeth, P. (2007) 'Moisture Sorption as a Potential Condition Marker for Historic Silks: Noninvasive Determination by Near-Infrared Spectroscopy' *Applied Spectroscopy* **61(2)** 218-222.

Zhao, H.-P., Feng, X.-Q., Yu, S.-W., Cui, W.-Z. and Zou, F.-Z. (2005) 'Mechanical Properties of Silkworm Cocoons' *Polymer* **46** 9192-9201.

Zheng, S., Li, G., Yao, W. and Yu, T. (1989) 'Raman Spectroscopic Investigation of the Denaturation Process of Silk Fibroin' *Applied Spectroscopy* **43 (7)** 1269-1272.

Zhou, C. Z., Confalonieri, F., Medina, N., Zivanovic, Y., Esnault, C., Yang, T., Jacquet, M., Janin, J., Duguet, M., Perasso, R., Li, Z.-G. (2000) 'Fine organization of *Bombyx mori* fibroin heavy chain' *Nucleic Acids Research* **28** 2413-2419.

Zhou, C.-Z., Confalonieri, F., Jacquet, M., Perasso, R., Li, Z.-G., Janin, J. (2001) 'Silk Fibroin: Structural Implications of a Remarkable Amino Acid Sequence' *Proteins: Structure, Function, and Genetics* **44** 119-122.

Zhou, L., Chen, X., Shao, Z., Huang, Y. and Knight, D. P. (2005) 'Effect of Metallic Ions on Silk Formation in the Mulberry Silkworm, *Bombyx mori*' *Journal of Physical Chemistry B.* **109** 16937-16945.

Zhou, P., Xie, X., Knight, D. P., Zong, X.-H., Deng, F. and Yao, W.-H. (2004) 'Effects of pH and Calcium Ions on the Conformational Transitions in Silk Fibroin Using 2D Raman Correlation Spectroscopy and 13C Solid-State NMR' *Biochemistry* **43** 11302-11311.

Zhou, Y., Xu, H. R. and Ying, Y. B. (2008) 'NIR Analysis of Textile Raw Material' *Spectroscopy and Spectral Analysis* **28 (12)** 2804-2807.

Zong, X.-H., Zhou, P., Shao, Z.-Z., Chen, S.-M., Chen, X., Hu, B.-W., Deng, F. and Yao, W.-H. (2004) 'Effect of pH and Copper (II) on the Conformation Transitions of Silk Fibroin Based on EPR, NMR, and Raman Spectroscopy'

Biochemistry **43** 11932-11941.

Zou, X., Uesaka, T. and Gurnagul, N. (1996) 'Prediction of paper permanence by accelerated aging I. Kinetic analysis of the aging process' *Cellulose* **3** 243-267.

Zuber, H., (1961), *Kolloid-Zeitschrift* **179** 100.

Zuber, H., Ziegler, K. and Zahn, H. (1957) *Zeitschrift für Naturforschung* **126** 734.